Bulletin
of
The Geological Society of America

VOLUME 70 July 1959 NUMBER 7

CONTENTS

	Pages
Geology and gravimetry of the Mustang Hill laccolith, Uvalde County, Texas. By Robert Greenwood and Vance M. Lynch	807–826
Granitization, migmatization, and fusion in the northern Entiat Mountains, Washington. By Dwight F. Crowder	827–878
Contact metamorphism of magnesian limestones at Crestmore, California. By C. Wayne Burnham	879–920
Short Notes	
Leached, clay-enriched zones in post-Sangamonian drift in southwestern Ohio and southeastern Indiana. By Ansel M. Gooding, James Thorp, and Erling Gamble	921–926
Leached, clay-enriched zones in post-Sangamonian drift in southwestern Ohio and southeastern Indiana: a reply. By Richard P. Goldthwait	927–928
Gravity anomalies off the west coast of North America. 1. Seamount Jasper. By J. C. Harrison and W. C. Brisbin	929–934
Lower Precambrian rocks of the Timiskaming region, Quebec and Ontario, Canada. By W. G. Q. Johnston	935–938
Have the sediments of the Cobalt series near the south end of Lake Timiskaming been deformed into mountains? By M. E. Wilson	939–940
Paleozoic and Mesozoic fossils in a thick stratigraphic section in the eastern Sierra Nevada, California. By C. Dean Rinehart, Donald C. Ross, and N. King Huber	941–946
Minimum age of the Lower Devonian slate near Jackman, Maine. By P. M. Hurley, A. J. Boucot, A. L. Albee, Henry Faul, W. H. Pinson, H. W. Fairbairn	947–950

Subscription $15.00 per year.
Printing Office: Mt. Royal & Guilford Aves., Baltimore 2, Md.
Communications for publications should be addressed to The Geological Society of America, Dr. H. R. Aldrich, Secretary, 419 West 117 Street, New York, N. Y.
Please give notice of change of address 4 weeks in advance. Claims for nonreceipt of the Bulletin of a given month must be sent to the Secretary of the Society before the end of the second succeeding month.

Second-class Postage paid at Baltimore, Md.
Accepted for mailing at special rate of postage provided for in Section 1103
Act of October 3, 1917, authorized on July 8, 1918.

PAPERS IN PRESS FOR FORTHCOMING ISSUES

ORIGIN OF THE ULTRAMAFIC COMPLEX AT UNION BAY, SOUTHEASTERN ALASKA. By John C. Ruckmick and James A. Noble

GEOLOGIC EVOLUTION OF THE BEARTOOTH MOUNTAINS, MONTANA AND WYOMING. PART 3. GARDNER LAKE AREA, WYOMING. By Rae L. Harris, Jr.

GRAVITY TECTONICS IN THE NAUKLUFT MOUNTAINS OF SOUTH WEST AFRICA. By Hermann Korn and Henno Martin (Translated by John G. Dennis)

GEOCHEMICAL TABLE OF THE ELEMENTS FOR 1959. By Jack Green

HISTORY OF IMURUK LAKE, SEWARD PENINSULA, ALASKA. By David M. Hopkins

THRUST FAULTING IN SINKING VALLEY, BLAIR AND HUNTINGDON COUNTIES, PENNSYLVANIA. By N. N. Moebs and R. B. Hoy

TURBIDITES IN FLYSCH OF THE POLISH CARPATHIAN MOUNTAINS. By S. Dzulynski, M. Ksiazkiewicz, and Ph. H. Kuenen

FUSED-QUARTZ EXTENSOMETER FOR SECULAR, TIDAL, AND SEISMIC STRAINS. By Hugo Benioff

IGNEOUS ROCKS AND CONSTITUENT HORNBLENDES OF THE HENRY MOUNTAINS, UTAH. By Celeste G. Engel

STRATIGRAPHIC-SEDIMENTARY SIGNIFICANCE OF CONTEMPORARY CLIMATE AND RELIEF IN FOUR REGIONS OF THE ANDES MOUNTAINS. By H. F. Garner

PRECAMBRIAN ROCKS OF THE HALL VALLEY AREA, FRONT RANGE, COLORADO. By Ernest E. Wahlstrom and Ok Joon Kim

105
8818

BULLETIN OF GEOLOGICAL SOCIETY OF AMERICA
VOL. 70, PP. 807–826, 9 FIGS. JULY 1959

GEOLOGY AND GRAVIMETRY OF THE MUSTANG HILL LACCOLITH, UVALDE COUNTY, TEXAS

ROBERT GREENWOOD AND VANCE M. LYNCH

ABSTRACT

Mustang Hill is one of about 90 small intrusions in Cretaceous sediments paralleling the Balcones fault zone of central Texas. Igneous activity in the province extends from earliest Cenomanian to Maestrichtian and includes some extrusive rocks. Faulting probably overlaps this period but is mainly later.

The Mustang Hill intrusion, 1½ miles in diameter, is an analcitic basalt with 27 per cent olivine, resembling mafic members of alkaline basalt suites from Scotland and Australia. Presence of distinctively diopsidic clinopyroxene, with absence of orthopyroxene and pigeonite, is confirmed as characteristic of this nonorogenic magma type. Limestone flags (Eagle Ford formation) in the concordant floor of the intrusion dip 3°–10° centripetally and have been locally crumpled by the basalt in small-scale *décollements* over more massive limestone. Broader folding is related to subsidence beneath and around the intrusion.

Field relations and geophysical findings justify the name laccolith for this quasi-concordant mass. A detailed gravity survey reveals an asymmetrical maximum over the intrusion with 2.2 milligals of Bouguer anomaly relief. The highest point on the anomaly is in the southwest portion of the exposed igneous rock, whence the anomaly drops off sharply to the southwest, but has a relatively gentle gradient change to the northeast. The general shape of the anomaly suggests that the high point is associated with an igneous feeder, and the gentle gradient to the northeast is probably associated with a tabular body tapering away from the feeder.

CONTENTS

TEXT

	Page
Introduction	807
Geography	808
Stratigraphy	810
Petrology	812
Basalt	812
Pegmatoid veins	815
General petrology of the intrusion	816
Nomenclature	817
Contact metamorphism	819
Hydrothermal alteration	820
Structure	821
Regional structure	821
Structure in and around the intrusion	821
Gravimetry	822
Introduction	822
Methods	822
Results	822
Interpretation	823
Conclusions	823
References cited	824

ILLUSTRATIONS

Figure	Page
1. Igneous rocks along the Balcones fault zone of central Texas	808
2. Mustang Hill laccolith	809
3. Variation of mode in Basalt no. 118	810
4. Variation in olivine composition, Mustang Hill	810
5. Topographic map, Mustang Hill	811
6. Bouguer gravity map, Mustang Hill	817
7. Residual-gravity map, Mustang Hill	818
8. Isopach map of igneous material, based on refined gravity data	819
9. Cross sections: geological interpretation compared with unrefined geophysical interpretation	820

TABLES

Table	Page
1. Chemical analyses of Mustang Hill and related rocks	812
2. Volumetric modal analyses of Mustang Hill and related rocks	813
3. Chemical analyses of clinopyroxene, Mustang Hill and related rocks	814

INTRODUCTION

Igneous rocks associated with the Balcones fault zone are known in Texas from Kinney County on the west to Travis County on the east, with the greatest variety and concentration in Uvalde County (Fig. 1). Most of them are plugs of nepheline basalt and related ultra-

mafic types, with a few phonolites and olivine basalts.[1]

Lenticular bodies of fragmental igneous material in the same province represent submarine mud flows or pyroclastic rocks (Smiser and Wintermann, 1935; Greenwood, 1956). All occur in Cretaceous sediments.

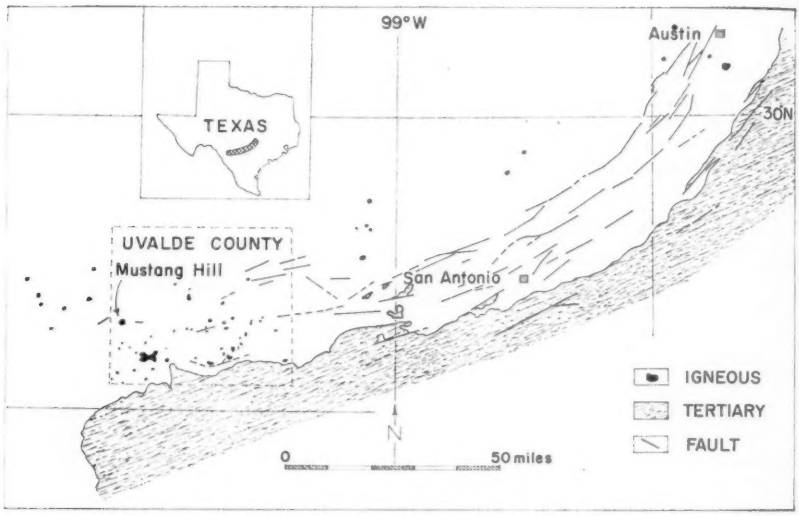

FIGURE 1.—IGNEOUS ROCKS ALONG THE BALCONES FAULT ZONE OF CENTRAL TEXAS

Following the early work of Hill (1890), Vaughan (1900), and others, Lonsdale (1927) published a regional study of this petrographic province, referring to Mustang Hill as the "Mustang Waterhole" intrusion (p. 22, 75). The Pilot Knob focus, near Austin, has received particular attention (Durham, 1949) and has been the subject of a geophysical investigation (Romberg and Barnes, 1954).

Mustang Hill was chosen for study largely because it is better exposed than other intrusions of this petrographic province, and because the structural evidence for a shallow floor clearly invited geophysical investigation.

Sayre (1936) mapped Uvalde County on a reconnaissance scale. The classic report on the Uvalde quadrangle by Vaughan (1900) does not include Mustang Hill but does provide a valuable introduction to the general geology.

Geological mapping on aerial photographs was undertaken by Greenwood in 1955, as part of a research program at the University of Houston, financed by the General Crude Oil Company of Houston. This grant also paid for thin sections and for two silicate analyses by the University of Minnesota laboratory. Acknowledgment is made to the Shell Development Company for two X-ray diffraction runs and the use of a Frantz magnetic separator.

The geophysical study was made by Lynch in partial fulfillment of requirements for the degree of Master of Science at the University of Houston. The advice and assistance of Mr. Fred Romberg, and a critical reading of the manuscript by Mr. Louis C. Pakiser, Jr., are gratefully acknowledged. The gravity meters were generously loaned by the Tidelands Exploration Company of Houston and the Texas Instruments Company.

Mr. R. H. Harris, Jr., of Uvalde, kindly gave permission for these investigations to be made on his ranch.

GEOGRAPHY

Mustang Hill is 4 miles north of Cline, a railroad station on U. S. Highway 90, west of Uvalde, Texas. It is 105 miles west of San Antonio. The area is of low to moderate relief; local elevations range from 1000 to 1250 feet.

[1] Rock names in this paper conform to the usage of Johannsen (1939).

FIGURE 2.—MUSTANG HILL LACCOLITH

It lies within the northern margin of the Gulf Coastal Plain physiographic province, a few miles south of the dissected scarp of the Edwards Plateau, and is included in the Turkey Mountain quadrangle. The topography shown on Figure 5 was surveyed by Lynch in connection with the gravimetric work.

The semiarid climate and sparse, rocky soil are favorable to thornbush and some grass. In the area of Figure 2, exposures are better than elsewhere, because of erosion of gullies trending northward to the West Nueces River. These obsequent streams dissect a broad surface of low relief, which slopes gently southward with the regional drainage.

Stratigraphy

The Mustang Hill intrusion lies in Cretaceous marine sediments. The stratigraphic units shown in Figure 2 are generally recognized in Texas (Sellards *et al.*, 1932, p. 271), with local modifications as here described. A local columnar section was recently published by Hazzard *et al.* (1956, p. 61). The Georgetown, Grayson, and Buda formations make up the Washita group of the Comanche series, separated by regional unconformity from the overlying Eagle Ford and Austin chalk formations of the Gulf series.

GEORGETOWN LIMESTONE: Limited exposures

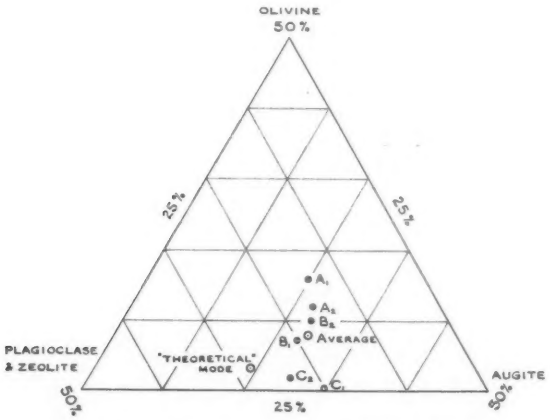

FIGURE 3.—VARIATION OF MODE IN BASALT NO. 118

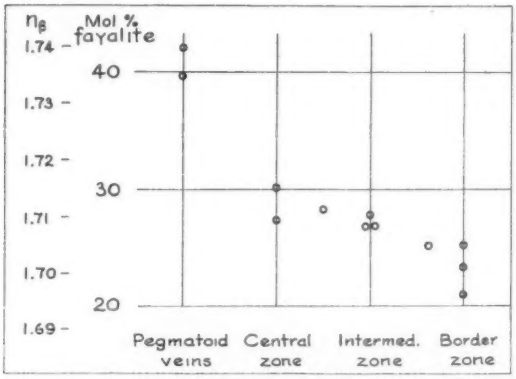

FIGURE 4.—VARIATION IN OLIVINE COMPOSITION, MUSTANG HILL

of the upper Georgetown are found in the West Nueces River. It is a hard, thick-bedded white crystalline limestone, with strong vertical jointing. The Georgetown is late Albian in age (Sellards *et al.*, 1932, p. 385).

forms soft bluffs protected by the overlying Buda limestone.

Locally intercalated in the Grayson formation east of Mustang Hill are submarine volcanic mudflows of ultramafic rock, the earliest

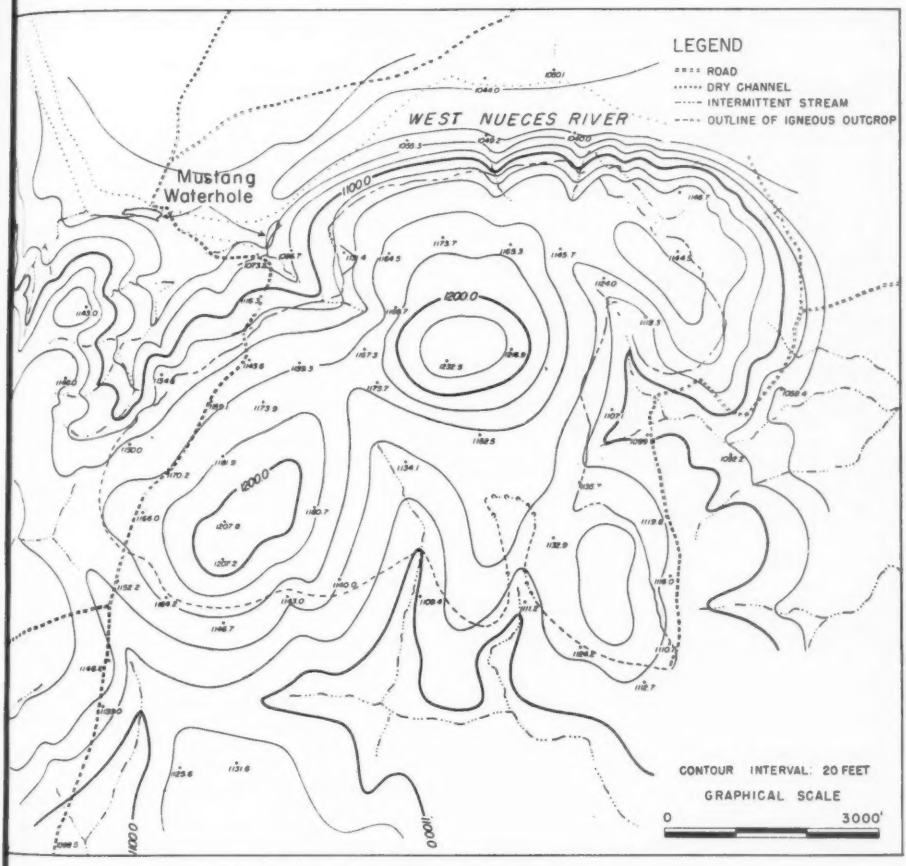

FIGURE 5.—TOPOGRAPHIC MAP, MUSTANG HILL

GRAYSON SHALE: The thickness of this formation, along the south bank of the West Nueces River, is estimated between 100 and 150 feet. The basal member is an argillaceous limestone, locally named the West Prong lentil (Greenwood, 1956, p. 169). Diagnostic ammonites (*Turrilites brazosensis*) place its age near the Albian-Cenomanian transition. Above the limestone is the typical Grayson lithology of blue-gray claystone with thin limy ledges of the oyster *Exogyra arietina* Roemer. The claystone

manifestations of igneous activity in the region (Greenwood, 1956).

BUDA LIMESTONE: Thick-bedded, brittle, dense porcellanous limestone 80–90 feet thick constitutes the Buda formation here. No diagnostic fossils were collected, but the formation is elsewhere considered early Cenomanian (Sellards *et al.*, 1932, p. 400). The top of the Buda forms an easily recognized shelf, a useful structure contour in field mapping.

EAGLE FORD FORMATION: Nearly all the ex-

posed border of the laccolith is intrusive into the Eagle Ford beds. After a hiatus caused by gentle uplift, making

"the beachy girdle of the ocean
too wide for Neptune's hips"
(Shakespeare, W., 1600, Act III, Sc. 1)

mapped because the transition to the overlying Austin chalk is gradual.

Petrology

Basalt

The Mustang Hill intrusion, except for minor pegmatoid veins near the core, is an olivine basalt. The rock is massive and homogeneous, with brownish olivine phenocrysts (about 1 mm) in a fresh, nearly black, fine to aphanitic matrix of plagioclase and pyroxene. The name basalt is used without implication of extrusive origin.

Table 1.—Chemical Analyses of Mustang Hill and Related Rocks

	1	2	3	4	5	6
SiO_2	44.89	44.18	45.11	39.92	44.37	46.26
Al_2O_3	10.36	10.67	12.44	8.60	12.74	13.36
Cr_2O_3	0.15	n.d.	0.10	0.14	n.d.	n.d.
Fe_2O_3	1.80	0.97	2.67	4.40	2.15	2.34
FeO	10.15	10.03	9.36	8.00	9.42	10.53
MnO	0.16	n.d.	0.22	0.24	0.18	0.12
TiO_2	1.96	1.30	2.34	2.70	2.19	1.78
MgO	15.96	17.77	11.56	20.17	14.71	8.87
CaO	10.46	9.75	10.61	10.68	9.30	9.18
Na_2O	2.04	2.37	3.05	1.91	3.00	3.27
K_2O	0.67	1.23	1.01	1.03	1.41	1.23
H_2O+	0.74	0.97	0.78	1.45	0.20	2.08
H_2O-	0.15		0.16	0.43	0.05	0.15
P_2O_5	0.30	0.38	0.51	0.51	0.71	0.42
Total	99.79	99.62	99.92	100.18	100.14**	99.10*

* Includes 0.31 listed as CO_2 0.06, "etc." 0.25

** Sic

1. Basalt No. 118, intermediate zone of Mustang Hill (R2175 Univ. of Minnesota Rock Analysis Laboratory)
2. Kylite of Benbeoch, Scotland (Johannsen, 1939, vol. IV, Table 83, No. 4)
3. Plagioclase basalt, Pinto Mtn., Uvalde Co. (Clarke, 1900, p. 61, anal. B)
4. Nepheline basalt, Black Mtn., Uvalde Co. (Clarke, 1900, p. 63, anal. I)
5. Chrysophyric hyalobasanite, Pribilof Is. (Barth, 1956, Table 6, anal. No. 8)
6. Analcite-olivine dolerite, SE. Australia (David, 1950, Table 27, anal. No. 9)

Eagle Ford strata were laid down near the end of Cenomanian time and on into the Turonian. No angular disparity with the Buda is seen, but a regional unconformity is recognized (Sellards *et al.*, 1932, p. 401).

In western Uvalde County two facies of the Eagle Ford meet (Sellards *et al.*, 1932, p. 431). On the northeast side of Mustang Hill the basal beds are thin-bedded dense gray limestone, interbedded with black, gray, and salmon-colored silty shale, having a strong petroleum smell when freshly broken. To the south and west, thin- to medium-bedded yellowish-brown crystalline limestone flags directly overlie the Buda. Upper beds consist of limestone flags throughout. The Eagle Ford here is probably 200 feet thick, but the upper contact was not

Average material from Locality 118 (Fig. 2) was selected for detailed study. This rock was analyzed (Table 1), and three thin sections (118 A, B, C) were cut from chips taken within a few inches of each other, and corresponding to the analyzed material. Using the Chayes point counter, two independent traverses of 850 points each were run on each of the three thin sections. The averages of these modal analyses appear in Table 2.

To assess the adequacy of the grain count, the

three major constituents, olivine, augite, and plagioclase plus zeolite, were recalculated to 100 per cent and plotted on a triangular diagram (Fig. 3). This diagram shows that the variation between two counts on the same section is consistently less than the variation between two sections cut from the same rock specimen. This further demonstrates the fact that, even in a fine-grained megascopically homogeneous rock such as this, the accuracy of precision micrometry is largely illusory. Accurate modal analyses can best be attempted by the crushing, splitting, and separation of bulk samples.

Figure 3 also shows that variations in the mode of this rock are caused largely by variations in amount of olivine. The "theoretical mode" calculated from chemical analyses and optical data, is plotted for comparison. It suggests that an alkaline mesostasis went undetected in the Rosiwal analyses.

The petrography of specimen 118 will be described, and other parts of the intrusion will be mentioned insofar as they differ from it. The fabric is holocrystalline porphyritic with olivine phenocrysts, locally with augite and plagioclase phenocrysts, and the groundmass is fine-grained. Textural evidence indicates that the order of crystallization is olivine, apatite-augite, plagioclase-hornblende, biotite-magnetite, analcite, and lastly zeolite.

OLIVINE: The olivine occurs as phenocrysts 0.5–2.0 mm (average 1 mm), equant subhedral and quite fresh except for traces of serpentinization along minute fractures. Phenocrysts commonly occur in clots of several individuals. Refractive indices indicate 27 mol per cent fayalite, on the basis of Kennedy's chart (1947, p. 567). Opaque equant inclusions of 0.01 mm, possibly a spinel mineral, are common in the olivine. Compositional zoning in individual crystals is not revealed by gross measurements, and no detailed investigation was undertaken.

AUGITE: Augite is typically confined to groundmass, as prisms 0.2 mm in length, although phenocrysts seriate up to 0.7 mm were seen in one section. It is purplish pink, and the cores of phenocrysts are paler than the rims and groundmass. Faint pleochroism occurs as follows: X = purplish pink, Y = orange brown, Z = gray. Refractive indices, determined in sodium light to an accuracy of ±.0005, are α1.689, β1.699, γ1.722. Concentric oscillatory zoning is best seen in sections of phenocrysts perpendicular to an optic axis. The extinction angle Z ∧ C is 46°, and 2V is 55° (about Z), as measured by the method of Fairbairn and Podolsky (1951).

Clusters of augite crystals are euhedral against plagioclase in this rock, in contrast to the diabasic

TABLE 2.—VOLUMETRIC MODAL ANALYSES OF MUSTANG HILL AND RELATED ROCKS

	117	85	115	118	112	T.M.	1	2	3*
Olivine	3.2	22.2	32.4	26.80	20.0	24.8	37.8	29.5	29.0
Augite	28.6	33.6	35.5	34.16	39.8	33.2	25.1	27.6	23.0
Plagioclase	44.0	40.1	25.6	29.20	31.2	30.4	26.8	33.1	23.0
Iron ore	5.6	2.33	3.0	3.05	5.4	3.0	2.1	4.4	4.0 (inc.
Hornblende	1.0	0.25	0.5	1.56	1.0	2.0	—	—	apatite)
Biotite	0.4	0.3	1.2	2.52	1.4	2.0	2.0	1.8	
Nepheline	—	—	—	—	—	1.5	3.8	2.3	
Apatite	1.4	0.1	0.5	0.25	0.2	0.6	0.6	0.7	
Zeolite	14.8	1.1	1.3	2.41	1.0	2.4	—	—	
Analcite	1.0	—	—	0.05	—	0.1	1.8	0.6	

* Includes 23% nephelinic glass.

117 Pegmatoid veins, Mustang Hill

85 Central zone, Mustang Hill

115 Central zone, Mustang Hill

118 Intermediate zone (anal. 1, Table 1), Mustang Hill; Average of 3 thin sections, 5307 points counted

112 Outer zone, Mustang Hill

T.M. "Theoretical mode" of Specimen 118, calculated from chemical analysis of rock (Table 1) and of augite (No. 1, Table 3), and optical data

1 Kylite, Benbeoch, Scotland (*See* Table 1, No. 2) (Johannsen, 1939, v. IV, p. 225)

2 Kylite of Benbraniachan, Scotland (Johannsen, 1939, v. IV, p. 225)

3 Chrysophyric hyalobasanite, Pribilof Is. (*See* Table 1, No. 5) (Barth, 1956, p. 127, Sample 8)

texture of a normal basalt. Most of the augite probably crystallized before plagioclase, as would be expected from the mafic character of the bulk composition, to judge from the diopside-anorthite-forsterite diagram of Osborne and Tait (1952, Fig. 5). $(Mg, Fe^2, Mn)_{.970}(Al, Cr, Fe^3)_{.056}Ti_{.057}(Si, Al)_{2.00}O_{5.974}OH_{.26}$, which may be abbreviated to $W_{1.00}(X,Y)_{1.083}Z_2O_6$ as suggested by Hess (1949, p. 624), where W represents cations in eight-fold co-ordination, X and Y in six-fold, and Z in four-fold. The

TABLE 3. CHEMICAL ANALYSES OF CLINOPYROXENES, MUSTANG HILL AND RELATED ROCKS

	1	2	3	4	5	6	7	8
SiO_2	49.24	45.23	49.23	49.20	49.85	46.66	51.48	47.86
Al_2O_3	4.61	7.73	2.01	3.33	3.75	5.76	2.87	6.17
Cr_2O_3	0.40	n.d.	n.d.	n.d.	n.d.	n.d.	n.d.	0.02
Fe_2O_3	0.68	2.95	2.87	1.85	2.55	1.84	0.70	2.44
FeO	6.00	4.07	3.53	5.30	6.09	7.22	6.26	5.07
MnO	0.10	0.07	0.09	0.18	0.19	0.13	0.18	0.14
TiO_2	2.05	4.28	2.25	1.83	1.37	3.21	1.16	1.67
MgO	14.18	12.25	14.69	15.03	14.38	12.18	14.35	13.87
CaO	22.06	23.37	24.23	23.33	21.76	22.21	22.04	21.54
Na_2O	0.55	0.47	0.46	0.40	0.42	0.81	0.54	0.72
K_2O	0.04	0.12	0.15	tr	tr	0.10	0.16	0.13
H_2O+	0.20	0.37	0.38	—	—	0.14	0.13	0.11
H_2O-	0.00		—	0.03	0.01	0.01	0.13	0.03
NiO	n.d.	0.05	n.d.	n.d.	n.d.	n.d.	n.d.	n.d.
Total	100.11	100.96	99.89	100.48	100.37	100.27	100.00	99.77
n_α	1.689		1.695	1.697	1.698	1.702*		1.693
n_β	1.699		1.701	1.707	1.706	1.706*		1.698
n_γ	1.722		1.721	1.722	1.720	1.728*		1.720
$2V_x$	55°		60°	48°	50°	44–52°	42°	48°
Z_c	46°		46°			42–45		45°

* mean values

1. From Mustang Hill no. 118. Associated with plagioclase $An_{.50}$ and olivine Fa_{28} (R2257, Univ. of Minnesota Rock Analysis Laboratory)
2. From nepheline basalt of Black Mtn., Uvalde Co. (Table 1, no. 4) (Clarke, 1900, analysis K)
3. From nepheline peridotite, Uganda (Sahama, 1952, p. 466)
4. From picrite with olivine Fa_{21}, Shiant Isles, Scotland (Murray, 1954, Table 1, pyroxene no. 1)
5. From picrodolerite with olivine Fa_{29}, Shiant Isles, Scotland (Murray, 1954, Table 1, pyroxene no. 20)
6. Pyroxene B-1, with olivine Fa_{25}, lower level of teschenite, Australia (Wilkinson, 1957, Table 2, analysis II)
7. From lower part of Skaergaard intrusion, Greenland (Muir, 1951, Table II, analysis 5)
8. From camptonite dike no. 4271, Skaergaard intrusion, Greenland (Vincent, 1953, Table II)

Augite was separated from specimen 118 by grinding to 100–200 mesh, removing olivine and iron ores with the Frantz isodynamic separator, and centrifuging the nonmagnetic fraction in methylene iodide. After repeated cleaning and recycling, 6.5 g of augite was obtained for analysis, and a grain section of this material showed less than 0.1 per cent impurities. An analysis of this augite appears as No. 1 in Table 3, along with analyses of similar clinopyroxenes. All are from mafic magmas, and all but Nos. 7 and 8 have alkalic affinities. Calculation yields the structural formula $Ca_{.875}(Na,K)_{.042}$-

0.20 per cent of H_2O+ in the analysis has been calculated as hydroxyl, in the absence of visible inclusions or hydrated alteration products in the augite.

Computation of the augite as $Ca_{47}Mg_{42}Fe_{11}$ shows it to be more calcic than the typical pyroxene of mafic magmas depicted by Hess (1949, Pl. 1). On Hess' diagram an augite of the above composition would have a β index of 1.687 and a 2V of 56°. The higher indices of the Mustang Hill augite are attributable to TiO_2 (Murray, 1954, p. 24) and correspond well with the observed increase of 0.004

in β for each 1 per cent of TiO_2 in synthetic diopside (Segnit, 1953, p. 222). Furthermore, the 2V in synthetic diopside increases 4½° for each 1 per cent of TiO_2 (E. R. Segnit, personal communication). All the titanaugites cited by Hess are from the Duluth gabbro and related tholeiitic (plateau basalt) rock types.

Paralleling detailed work on pyroxenes of gabbros and ferrogabbros typified by the Skaergaard intrusion (Muir, 1951) and the pyroxenes of picrite basalts (Muir and Tilley, 1957), attention has lately been given to the pyroxenes of mafic rocks of alkaline affinities (Murray, 1954; Wilkinson, 1956a; Barth, 1956, p. 126). The distinctively calcic character of such pyroxenes has been well explained by Kennedy (1933) and Wilkinson (1956a). As a result of the subsilicic character of the magma abundant olivine crystallizes early and does not react to form orthopyroxene. The ratio of Ca to MgFe available for pyroxene crystallization is therefore high, favoring diopside rather than pigeonite or even normal augite.

In contrast to the diversity of pyroxene composition in tholeiitic basalts, there is little change during differentiation in the pyroxene of alkaline mafic magmas, aside from a gradual increase in the Fe/Mg ratio. At Mustang Hill, color zoning suggests enrichment in titanium during crystallization. The pyroxenes of these alkalic rocks are not alkalic Table 3, analyses 1, 2, 4, 5). The sodium is reserved for the latest felsic minerals.

PLAGIOCLASE: No detailed study of the plagioclase was attempted. It overlaps augite in crystallization, but is chiefly later, in aggregates of 0.1- to 0.5 mm laths with albite twinning; the laths are roughly tangential to clumps of mafic minerals. A few plagioclase crystals range up to 1 mm in length. Refractive indices and extinction angles on albite twins indicate a composition of An_{70} in the cores of the larger crystals and An_{40} in the rims. Calculation from the chemical analysis suggests a gross plagioclase composition of An_{50}, roughly confirming the optical estimation. Minute amounts of clear, untwinned, low-relief material are seen along grain boundaries and sporadically replace individual twin lamelae in the plagioclase. This material may be orthoclase or late-magmatic albite distinct from the normal sequence of plagioclase crystallization. Clusters of zeolites cut the plagioclase, and occasional thin crosscutting rivulets of a low-index pinkish isotropic mineral are probably sodalite.

ORES: Recalculation of the chemical analysis of the rock suggests that the opaque constituents contain roughly equal amounts of magnetite and intergrown ilmenite. They appear in thin section as equant skeletal bodies 0.2 to 0.4 mm across, poikilitically including augite and plagioclase, and having sufficient regularity of outline to suggest that they are single crystals formed relatively late in the sequence. There is a notable absence of fine-grained opaque minerals, or "magnetite dust".

BIOTITE AND AMPHIBOLE: Biotite is evenly disseminated through the groundmass as shreds and flakes about 0.1 mm in size. It is strongly pleochroic from deep reddish brown to nearly colorless, rarely green to colorless. The amphibole is of very similar aspect and color, with nearly parallel extinction (positive elongation), and in the absence of diagnostic cleavage traces the two minerals look alike. Amphiboles from similar rocks have been called barkevikite, but the term is poorly defined, and typical sodic amphiboles of small extinction angle have negative elongation.

Both biotite and amphibole are apparently of normal magmatic paragenesis, rather than late reaction products.

ZEOLITE: Radiating 0.2-mm clusters of a fibrous zeolite replace the plagioclase and are concentrated in interstitial nests, apparently as a deuteric product. They show parallel extinction, low birefringence, and mean index near 1.508. Most fibers show positive elongation, a few negative elongation. Similar material, although of lower refractive index, is abundant in the pegmatoid veins and is discussed in more detail in the section on Pegmatoid Veins.

APATITE: Apatite occurs sparsely as short (about 0.1 mm) hexagonal crystals contemporaneous with augite.

ANALCITE: Analcite is rare in thin section but appears in grain immersions as clear equant isotropic grains, 0.05 to 0.10 mm in size, free from intergrowths. The refractive index of 1.502 is high for analcite, but X-ray diffraction clearly shows the analcite pattern in the felsic fraction of the rock. Paragenesis of analcite is discussed in the next section.

Pegmatoid Veins

Coarse-grained dikelike bodies of irregular width occur in an area about 200 feet wide in the central knob of Mustang Hill. They grade into normal basalt over a distance of 2-3 cms. Their texture is crudely diabasic, with laths of plagioclase and augite 3–10 mm in length subparallel to the walls of the vein. Microscopically, the mineralogy is similar to that of the surrounding basalt, but plagioclase is dominant, olivine a minor constituent, and zeolite and analcite are relatively abundant (Table 2). Such veins, representing a hydrous residuum of the magma, are recognized in the crinanite of the Shiant Isles (Turner and Verhoogen, 1951, p. 156).

The olivine is notably more fayalitic (Fa_{40-42}) than in the surrounding basalt (Fig. 4). Much of it is interstitial to plagioclase and augite, in a manner which suggests formation late in the sequence. According to Turner and Verhoogen (1951, p. 107), melts rich in $FeSiO_3$ may yield pyroxene which later reacts to form olivine. The olivine here, however, is present not as a reaction rim but as independent

crystals. The more nearly euhedral olivine crystals are abnormally elongated, a feature noted elsewhere in the gabbroic parts of basic alkaline rocks by Wilkinson (1956b, p. 446) and others.

Plagioclase is strongly zoned from labradorite to sodic andesine, and the purplish titanaugite shows oscillatory zoning; its average indices are close to the augite of the basalt. Ilmenite-magnetite occurs as skeletal crystals 1 mm in size. Apatite is correspondingly coarse, and amphibole and biotite are minor.

Clusters of fibrous zeolite, up to 2 mm in size, abundantly replace the plagioclase and fill fractures n the rock. They resemble the zeolite of the basalt, except for a slightly lower mean index (near 1.503). An X-ray powder photograph of the lightest fraction separable from this rock showed lines referable to natrolite and analcite. The relatively high indices and occasional negative elongation are in conflict with the published properties of natrolite, and this zeolite may be gonnardite, which has a very similar powder pattern (Meixner, 1956).

Analcite, identified from the X-ray work, occurs as clear equant grains, 0.1 to 0.5 mm in size, having an index of 1.492, which is less than the analcite from the basalt. Analcite in these rocks appears on textural evidence to be late magmatic (Lonsdale, 1940, p. 1597–1600) rather than deuteric. It does not replace plagioclase. Thin irregular rivulets of pinkish material replacing plagioclase have the optical properties of noselite or sodalite. No such mineral was recognized in the X-ray powder photograph, probably because of the small percentage in the sample.

Little is known about the equilibrium relations between nepheline and analcite in magmas. An obvious deduction is that analcite is favored by high H_2O pressure in the system. We are limited in this direction, however, by the almost complete freshness of the olivine, indicating that the serpentine field was scarcely attained. According to Friedman (1951, p. 29) "analcite and olivine can coexist in the temperature range 500°–600°C at considerable H_2O pressure", but more data are needed. According to a recent study of the system Na_2O–Al_2O_3–SiO_2–H_2O, nepheline is unstable below 460°C. in the presence of excess water at high pressure, and analcite is unstable above 525°C. (Sand *et al.*, 1957, p. 177–78) so that 525°C. would seem to be an upper limit for the late magmatic history of this rock. Certain alkaline mafic lavas recently described from the Pribilof Islands (Barth, 1956) show chemical and mineralogical similarities to Mustang Hill (Tables 1, 2). What is described as "nephelinic glass" in the Pribilof lavas would probably have given rise to analcite in an intrusive environment.

General Petrology of the Intrusion

In the field, grain size decreases from the center toward the contact, and three concentric zones have been arbitrarily drawn. The central zone is bounded by a gentle scarp, reflecting the somewhat greater resistance to erosion of the coarser-grained rock. A smaller area around the southwest knob of the hill is also assigned to this zone. The central zone is characterized by the presence of seriate phenocrysts of augite and plagioclase. In the intermediate zone, which constitutes the bulk of the intrusive, augite and plagioclase phenocrysts are rare or absent except in the inner part of the zone. The outer, or contact, zone is not clearly demarcated from the intermediate zone, but for a distance of a few hundred feet horizontally from the intrusive contact the groundmass of the basalt is aphanitic. An isolated intrusion 2600 feet in length, 3 miles S. 60°E. of Mustang Hill, is identical with the contact zone of Mustang Hill and occurs at a comparable stratigraphic horizon.

Olivine occurs as a single generation of phenocrysts of comparable size and abundance throughout all zones; however, the observed increase in the Fe/Mg ratio with distance from the lower contact (Fig. 4) argues against a simple intratelluric crystallization of olivine before emplacement of the intrusive. The variation in olivine composition is less marked than that observed elsewhere by Wilkinson (1956b, p. 448) but follows a similar trend. Typical modes of the three zones are shown in Table 2. No clear-cut zones of magmatic differentiation are apparent. Turkey Mountain, in Kinney County northwest of Mustang Hill, is suggested for future studies of differentiation, such as have been carried out in Australia by Wilkinson (1958).

The observed mode of the type specimen 118 (Table 2) was checked by calculating a "theoretical mode" from the chemical analyses of the rock and the augite, using an olivine composition estimated from optical data, and arbitrarily assigning 0.34 per cent MnO to the olivine. Such a calculation yields an excess of Na and Al over the Si available for forming plagioclase. Varying the amount of analcite and zeolite cannot significantly reduce the discrepancy. Assumption of 1.5 per cent of theoretical nepheline satisfactorily resolves the difficulties, but no nepheline was found either in thin section or in X-ray diffraction records. Possibly there is a cryptocrystalline alkaline mesostasis, not apparent in this section.

Among other rocks in the Uvalde area which have been analyzed, the basalt of Pinto Mountain (Table 1, no. 3) resembles Mustang Hill most closely, although the analysis suggests a

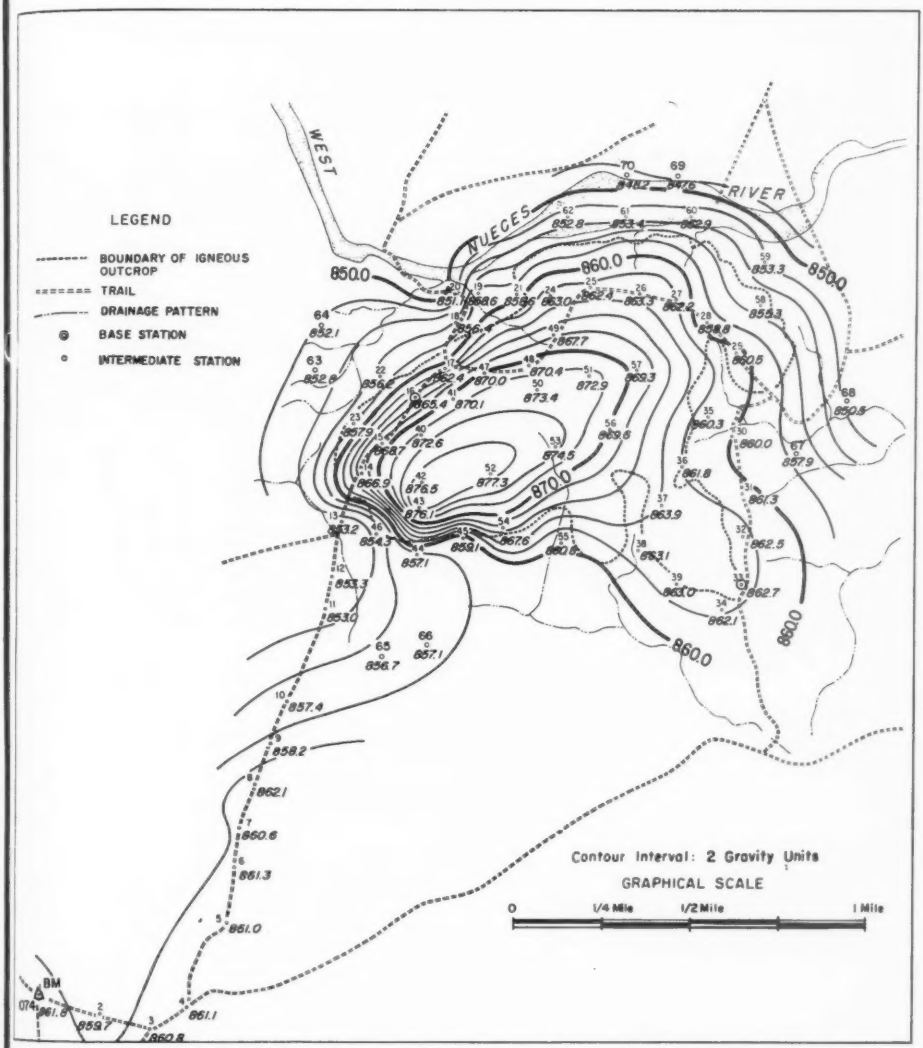

FIGURE 6.—BOUGUER GRAVITY MAP, MUSTANG HILL

more felsic rock. Pinto Mountain, about 24 miles northwest of Mustang Hill, is one of several apparently concordant intrusions in the Eagle Ford formation; Turkey Mountain is the thickest. Detailed petrographic work might reveal significant relationships among these bodies.

Nomenclature

Analcitic olivine basalt is an adequate name for the rock of Mustang Hill. Its closest relative appears to be kylite (Johannsen, 1939, v. IV, p. 226), a Scottish olivine theralite containing modal nepheline in excess of analcite. Accordinto to Johannsen, the presence of nepheline distinguishes theralite, whereas analcite characterizes crinanite and teschenite. However, the teschenites and crinanites he cites are consistently more leucocratic than the Mustang Hill basalt. The type kylite is described by Tyrrell (1912, p. 121) from the sill of Benbeoch near Dalmellington, Ayrshire, Scotland, as a

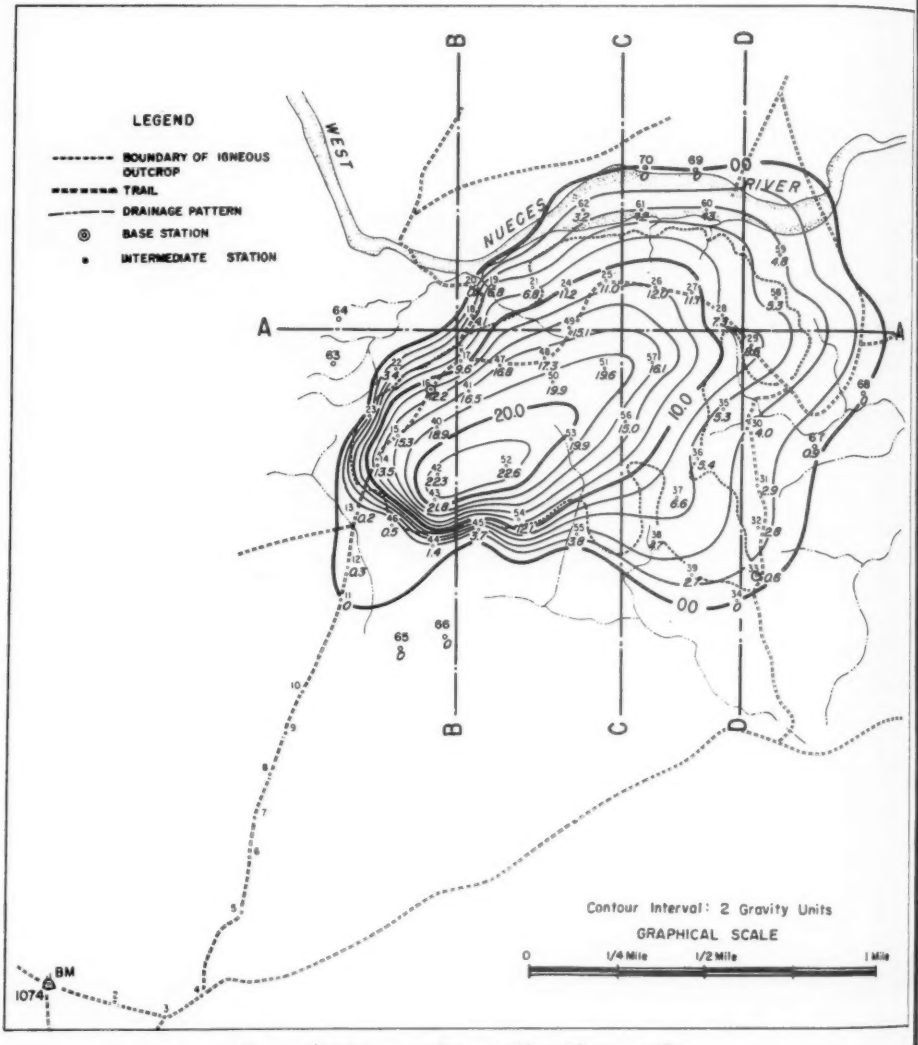

FIGURE 7.—RESIDUAL-GRAVITY MAP, MUSTANG HILL

rather fine-grained olivine-titanaugite-labradorite rock in which the mafic minerals have a "pseudoporphyritic aspect". The plagioclase is zoned from "Ab_4An_5 to Ab_5An_3" and rimmed by a trace of orthoclase. There is skeletal ilmenite, scraps of reddish biotite, and a little clear analcite and apatite. "Decomposed nepheline" occurs in the groundmass. Related masses contain traces of barkevikite (Tyrrell, 1912, p. 128). An analysis of the type kylite is reproduced in Table 1, and its mode in Table 2. The mode of a related, but unanalyzed kylite from the neighboring Benbraneachan sill is also given in Table 2, and this more closely compares with the mode of the Mustang Hill rock, except that this kylite contains nepheline.

Field relations of the kylites and related rocks are discussed in the concluding section of this paper.

Contact Metamorphism

At many points around the margin of the Mustang Hill intrusion, except the poorly exposed south and southwest sides, effects of contact metamorphism are visible in the flaggy limestone and siltstone of the Eagle Ford formation. These effects are limited to a zone about 20 feet thick, measured perpendicular to the extrapolated intrusive contact at that point. This refers to the lower contact of the intrusive; the roof has been entirely eroded. Intensity of metamorphism varies greatly from place to place.

In metamorphism the siltstones are darkened, thoroughly indurated, and apparently silicified to a porcellanous texture; their original laminations are enhanced by an intensification of color contrast. The grain size of the quartz has increased from the original 0.01 mm or less, of the clastic grains, to about 0.025 mm in the recrystallized intergrowth. The sporadic calcite, originally associated with microfossils, is recrystallized into 0.10-mm aggregates of sharp rhombohedral crystals.

The flaggy limestones are also indurated, their laminations accentuated in grayish green, although detailed impressions of *Inoceramus* are preserved. In thin section, calcite of 0.05- to 0.10-mm grain makes up most of the rock; bedding laminae are emphasized by bands of slightly coarser grain. Rounded single crystals

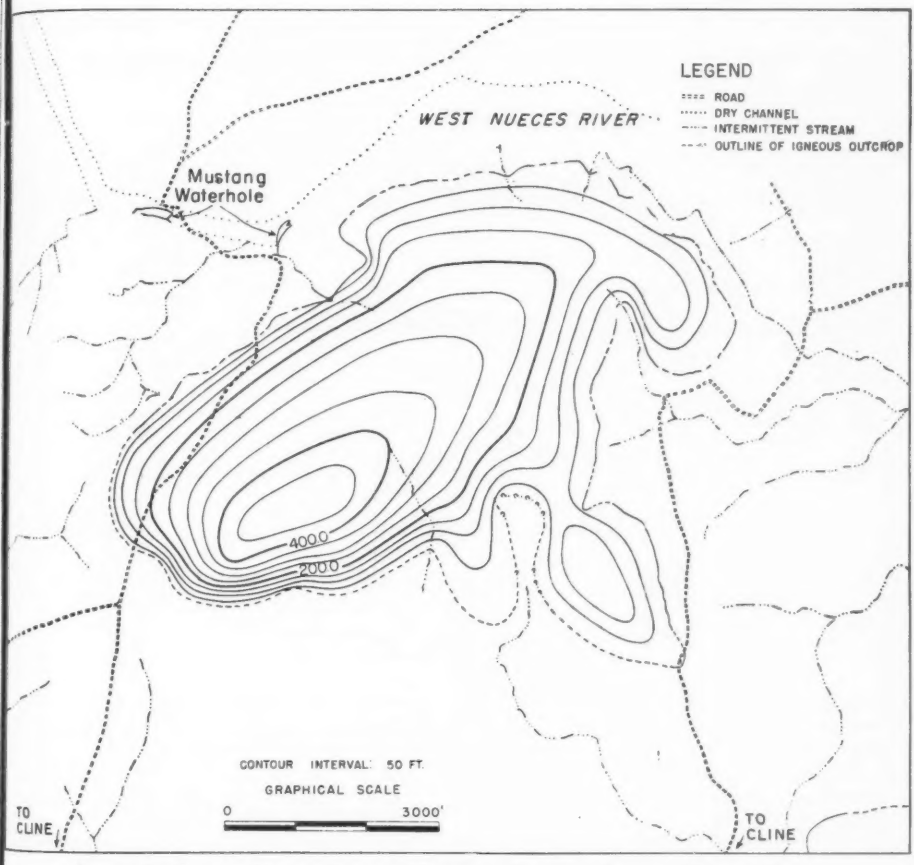

FIGURE 8.—ISOPACH MAP OF IGNEOUS MATERIAL, BASED ON REFINED GRAVITY DATA

of calcite, 0.2 mm in size, are probably recrystallized Foraminifera. The microlaminae of the bedding bend around them. Rectangular sharp-walled aggregates of cross-fiber calcite, lying

Beneath the small outlier of basalt on the northeast side of Mustang Hill (Fig. 2), Eagle Ford siltstone shows no metamorphism, and less than 5 feet below the basalt it has a strong

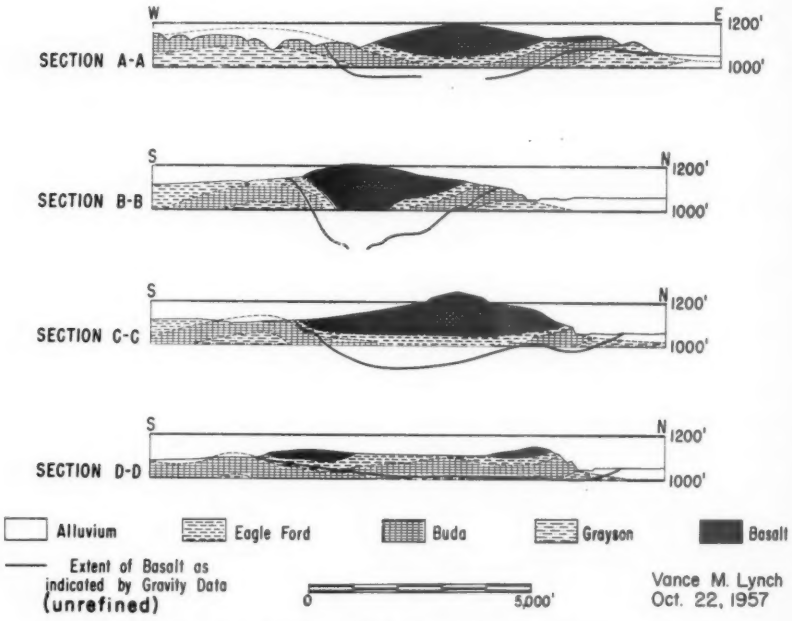

FIGURE 9.—CROSS SECTIONS: GEOLOGICAL INTERPRETATION COMPARED WITH UNREFINED GEOPHYSICAL INTERPRETATION

subparallel to the bedding, represent fragments of *Inoceramus*. In some specimens, lenticles of chert have been partially recrystallized to 0.10-mm grain size. The pale-green bands in the metamorphosed limestone remain unaccounted for; possibly they are traces of chlorite formed from clay minerals. No calc-silicate minerals or other evidences of high temperature were found in the sediments. By mathematical consideration of the temperatures to be expected around tabular mafic intrusions, it has been suggested that an intrusive about 100 feet thick would raise the country rock, 15 feet from the contact, to 550°C. for 12 years (Jaeger, 1957, p. 315). It is unlikely that such temperatures could be maintained in rocks such as the Eagle Ford beds without the formation of forsterite around 560°C, or of tremolite around 320°C, under 1000 feet of cover (Bowen, 1940, Fig. 14). Probably Jaeger's assumption of an 1100°–800°C. range for the crystallization of the intrusive is too high.

petroleum smell. If the petroleum antedates the intrustion, as seems likely, it demonstrates the limited nature of the metamorphism.

Around the summit of Mustang Hill itself, chips of pinkish flinty shale are sparsely distributed. Unless these have been artificially transported, they must represent fragments of the metamorphosed roof of the intrusion, preserved by their superior resistance to weathering.

Hydrothermal Alteration

The basalt is free of visible hydrothermal alteration, except at one locality, where the road crosses the intrusive on the northwest side (Fig. 2). The rock there is earthy gray green and crumbly; it has relict igneous texture similar to the fresh basalt into which it grades. The original olivine is altered almost completely to aggregates of pale-green montmorillonoids, believed to be nontronite or saponite by analogy

with material from a near-by area (Greenwood, 1956, p. 171). The pyroxene is bleached to very pale-green augite, and clinozoisite (?) needles are developed between pyroxene and plagioclase. Plates and spindles of ilmenite-magnetite abound in the groundmass and are presumably largely derived from the original dark minerals. In contrast, the plagioclase is remarkably fresh, and no more than a trace of zeolite was seen.

The major changes here have been the hydration of olivine and the abstraction of Fe and Ti from the dark minerals. The alteration differs markedly from the late-magmatic changes, in which Na was added. It is impossible to say whether the water was magmatic in origin or was derived from the intruded sediments.

Structure

Regional Structure

The Cretaceous sediments shown in Figure 2 have a regional dip of 0° to 5°S. An easily followed structural contour is the Buda–Eagle Ford contact, everywhere sharp and readily followed on the ground. Immediately southeast of Mustang Hill is a gentle anticline, its axis N. 80° W., exposing a core of Buda limestone flanked on north and south by Eagle Ford beds. In part of this structure the brittle Buda is thoroughly fractured and recemented with coarse calcite. The fold is shown on the cross sections B, C, and D (Fig. 9). Gentle folding on a smaller scale is seen a mile to the east on the same axis, and traces of basalt are encountered in that direction. Consistent northward dips are not typical of the region, and here they are believed to be genetically connected with the intrusion of Mustang Hill. SectionA-A of Figure 9 also shows a gentle anticline west of Mustang Hill. Locations of all cross sections appear on Figure 7.

Minor faulting occurs in a rather consistent pattern. Steep faults cut the Cretaceous sediments in a northeasterly direction within a few miles of Mustang Hill; three have their apparent downward movement on the southeast, and one on the northwest. The faults are clean fractures with little or no brecciation, and movement may have been no more than a few tens of feet. None of these faults cuts Mustang Hill itself, but one bounds a minor basaltic intrusion 3 miles to the southeast, where field relations suggest that faulting postdates intrusion. These faults represent, on a much diminished scale, the westward prolongation of the Balcones fault zone (Sellards and Baker, 1934, p. 60–62).

Structure In and Around The Intrusion

The igneous mass of Mustang Hill stands as a broad elevation of gentle slope, except for local steepening around the central knob and the cliff cut by the West Nueces River (Fig. 5). The intrusion is roughly equidimensional in plan, 1–1½ miles across, and is best exposed on the north and east sides where the local relief and dissection are greatest. The contact can be established to within 50 feet along much of its length, and the base of the igneous rock is with the lower 30 feet of the Eagle Ford formation, except on the northeast lobe where it truncates the basal Eagle Ford and invades the upper Buda. At several localities near the igneous contact the flaggy limestone and siltstone of the Eagle Ford are thrown into folds of 20- to 40-foot wave length and 2- to 4-foot amplitude. These folds, their axis roughly concentric with the igneous mass, represent a miniature *décollement* of the Eagle Ford upon the more massive Buda, directly caused by the intrusion. They are not found far from the igneous rock. Where uncrumpled Eagle Ford beds are exposed near the igneous mass they dip centripetally at 5–15°. Northeast of Mustang Hill a small outlier of basalt lies above basal Eagle Ford beds and is separated from the main mass by erosion (Fig. 2). It provides clear evidence of a quasi-concordant floor of limestone dipping inward at about 3° around the intrusion.

A smaller mass of basalt nearly 3 miles S. 60° E. of Mustang Hill occurs at a similar stratigraphic horizon in the lower Eagle Ford, although exposures in the undissected upland are inadequate for detailed observation.

Within the intrusion itself, joints are the chief structural features. A roughly orthogonal joint system in the main mass leads to the typical cuboid or spheroidal boulders, but as the margin of the intrusion is approached one set of steep joints becomes dominant and closely spaced, yielding flat slabs only a few centimeters thick. These dominant joints strike tangentially to the main outline of the intrusion and range in dip from 75° outward to vertical. They are presumably tension fractures related to cooling, lying approximately normal to the long dimension of the igneous mass.

No foliation or lineation is apparent. As in other parts of this petrographic province, there is a notable absence of inclusions in the igneous

rock, no indication of assimilation of wall rock, and no dikes or apophyses.

GRAVIMETRY

Introduction

The gravity method of geophysical investigation is used to detect horizontal variations in the density of the earth. The igneous intrusive rocks of the Uvalde area are normally more dense than the surrounding sedimentary rocks, and since the Mustang Hill igneous mass is surrounded by sedimentary rocks it seemed likely that considerable information concerning the mass could by obtained by the gravity method.

A survey of this type was conducted over the Cortlandt complex in New York (Steenland and Woollard, 1952). This was a study of a rock mass composed of norite, diorite, and pyroxenite in an igneous and metamorphic terrain. The mass was much larger, and the survey less detailed than in the case of Mustang Hill. Steenland and Woollard were able to delineate two nearly vertical cylindrical masses, with shallower masses intervening.

A similar survey was conducted over Pilot Knob, a Cretaceous mafic volcanic mass in Travis County, Texas, (Romberg and Barnes, 1954). The igneous material in this case gave a strong gravity anomaly from which the authors deduced that the mass narrowed at depth.

Methods

INSTRUMENTATION: Two Worden gravity meters of identical design were employed. Transit and stadia-rod surveys established the horizontal and vertical control. A Jolly balance was used for the density determinations.

FIELD TECHNIQUES: The vertical control was established by elevation traverses throughout the survey based on sea-level datum as established by the United States Geological Survey, and the horizontal control was determined by turning plate angles and measuring distance by stadia rod. The locations and elevations of the gravity stations are shown in Figure 5. The gravity measurements were determined by first setting three base stations, Nos. 1, 16, and 33, and then adjusting the remainder of the stations on lines run between these bases.

DENSITY DETERMINATIONS: The density of the igneous rock and of the adjacent sedimentary rocks was determined by measuring the density of specimens from each lithologic unit by means of a Jolly balance. Values obtained were:

Eagle Ford shale	2.35 g/cc³
Eagle Ford limestone	2.57 g/cc³
Buda limestone	2.67 g/cc³
Grayson shale	2.21 g/cc³
Georgetown limestone	2.61 g/cc³

The average density of the sedimentary section, 2.45, was determined by taking a weighted average based on bed thicknesses. The density of the igneous rock is 2.95.

CORRECTIONS: A free-air correction, a Bouguer correction, and a latitude correction were applied to all stations, and a terrain correction was applied along the Nueces River where necessary. The free-air and Bouguer corrections were combined to form the elevation correction as described by Nettleton (1940, p. 54). The density used to correct the Bouguer effect was that of the sedimentary section, 2.45. The latitude corrections were taken from charts published for that purpose (Nettleton, 1940, p. 140). The terrain corrections were computed by the method described by Hammer (1939, p. 184–194).

Results

BOUGUER GRAVITY MAP: The gravity survey revealed a large maximum which coincides very closely with the outcrop of the igneous mass (Fig. 6). All maps are contoured in terms of gravity units. One unit equals 0.1 milligal. These data are based on an arbitrary gravity datum which is several hundred gravity units higher than absolute gravity. The large gravity maximum gives some information regarding the shape of the lower surface of the igneous mass. For instance, the surface expression of the igneous mass is two hills connected by a saddle with a broad lobe extending to the southeast, suggesting two possible sources of the intrusive material. However, the gravity anomaly contains only one peak, and it is located roughly at the same point as the westernmost hill, which is presumably above the feeder.

RESIDUAL-GRAVITY MAP: A residual-gravity map was prepared by compiling a regional map and subtracting it from the Bouguer-gravity map. This isolates the gravity effect of the igneous mass. The outline of the outcrop of the basalt appears on the residual-gravity map. The gravity anomaly overlaps the igneous mass on almost all sides and especially on the east

side. The residual-gravity map is shown by Figure 7.

Interpretation

INITIAL THICKNESS ESTIMATES: To make initial estimates of the thickness of the igneous mass, the mass was considered a semi-infinite sheet, and the formula $T = \frac{G}{2\pi\gamma\rho}$ (Nettleton, 1940, p. 114) was used. In this formula, T is the thickness in centimeters, G is the residual gravity in gals, ρ is the density in grams per cubic centimeter, and γ is the gravitational constant. This calculation resulted in an extent considerably greater that had been determined from surface geology. Profiles of these initial estimates are shown on the cross sections (Fig. 9).

INITIAL MASS CALCULATION: The formula $M = \Sigma \frac{A\Delta G}{2\pi\gamma}$ was used to calculate the anomalous mass of igneous material from the residual-gravity anomaly. This anomaly (Fig. 7) was divided into slices corresponding to the contour interval. Quantity A represents the area of each slice, ΔG the contour interval in milligals, and γ the gravitational constant. The anomalous mass thus calculated is 1.22×10^8 metric tons, and the total igneous mass 7.20×10^8 metric tons.

REFINEMENT OF SHAPE ESTIMATES: Since the initial calculation of the thicknesses gave a mass considerably larger than the mass suggested by the outcrop (Fig. 9), the interpretation was further refined by combining the gravitational and geological evidence. The hypothetical body so obtained was then evaluated by dividing it into slabs 500 feet square and 40 feet thick, and calculating the anomaly to be expected at any point as an algebraic summation of the effects of all neighboring slabs. At any given surface point, all slabs giving a vertical gravitational effect of over 0.003 milligals were taken into consideration. The formula

$$G = \frac{\gamma M}{A}\left[\tan^{-1}\frac{X_2Y_2}{Z\sqrt{X_2^2+Y_2^2+Z^2}} - \tan^{-1}\frac{X_2Y_1}{Z\sqrt{X_2^2+Y_1^2+Z^2}} - \tan^{-1}\frac{X_1Y_2}{Z\sqrt{X_1^2+Y_2^2+Z^2}} + \tan^{-1}\frac{X_1Y_1}{Z\sqrt{X_1^2+Y_1^2+Z^2}}\right],$$

derived by multiple integration, gives the effect of a single slab. In this formula, X, Y, and Z represent limits of a single slab in a co-ordinate system having the given surface point as origin. When this computed gravity effect disagreed with the observed residual-gravity anomaly, slabs were added or subtracted until a reasonable agreement was obtained. A more refined estimate of the shape of the igneous mass, as obtained by the above method, is shown on the isopach map (Fig. 8). On comparing this with the unmodified results of the first method (Fig. 9), we see that the actual mass is probably thicker near the center, in compensation for its smaller surface area.

REVISED MASS CALCULATION: A second calculation of the total mass, made by multiplying the number of slabs used above by the mass per slab, gave a figure of 5.68×10^8 metric tons. The discrepancy between the two mass calculations arises because in the first case the anomaly was contoured mathematically between gravity stations without regard for irregularities in the outcrop limits.

CONCLUSIONS: The gravity data indicate that the Mustang Hill igneous mass is a body of high density material shaped somewhat like a mushroom. The stem of the mushroom, which represents the feeder for the igneous material, is evidently located near the center of the westernmost hill, as shown on the topographic map.

The interpretations presented here are only one of several reasonable approaches to the solution of this problem. There is actually no unique solution to any gravity anomaly, and certain basic assumptions must be made for the estimation of the density distribution from which the anomaly arises. The basic assumptions made in the solution presented here were governed primarily by the existing geological evidence.

Conclusions

In the absence of well-marked internal differentiation, little can be said about the petrogenesis of Mustang Hill. Detailed comparative studies of many individual intrusions in this region will be required before the conclusions of Lonsdale (1927) are elaborated or modified. To trace the regional trends of differentiation, it is of critical importance to know the relative ages of the different intrusions; unfortunately they do not cut each other.

On questions of tectonic environment and mode of emplacement, more evidence is available. According to Barth (1956, p. 151) "vertical faulting of non-orogenic areas are (sic) the accepted prerequisites for the formation of alkalic rock suites". This prerequisite is fulfilled in the Uvalde area, where the nearly flat-lying Cretaceous beds are cut by the steep Balcones faults, and it appears to prevail in other alkalic basalt provinces. In southeast Australia, for example, "Sills and laccoliths of teschenitic dolerite . . . are found as a rule among gently dipping strata of Cretaceous to Jurassic age, and vary in thickness from a few feet to 700 feet", and "most of the rocks are olivine-bearing types with titanaugite and rare barkevikite . . . very basic and even picritic types may be present". (David, 1950, v. 1, p. 578) In the upper Paleozoic igneous rocks of the west of Scotland, where teschenites are common, the occurrences are sills, plugs, flows, and "small lenticular intrusive masses" (Tyrrell, 1912, p. 128). Kylite, corresponding to the Mustang Hill rock, is believed to be a secondary differentiate of the teschenite magma, but forms independent sills (p. 121). Among rocks "without conspicuous analcite or nepheline", the Trabboch Burn rock near Stair, Ayrshire, is described (p. 124) and is mineralogically similar to the rock of Mustang Hill.

One of the Scottish teschenites, the Lugar sill, shows strong internal differentiation (Tyrrell, 1917, p. 84–131). The differentiated layers include theralite, picrite, and peridotite in downward progression, but none corresponds to the mode of the Mustang Hill intrusion.

Gravimetric and geological evidence indicates that the Mustang Hill intrusion is a lens approximately concordant with the enclosing Eagle Ford formation. Cross sections show that it occupies a basin, flanked to the west and south by commensurate anticlines. The absence of such structures elsewhere in the area, and the presence of the crumpled limestone flags bordering the intrusion, are evidence that the folding is attributable to the intrusion.

The designation of Mustang Hill as a laccolith follows the original definition of a "laccolite" as a mass of igneous rock which "insinuated itself between two strata and opened for itself a chamber by lifting all the superior beds" (Gilbert, 1880, p. 19). Gilbert made no arbitrary division between "the sheet and the laccolite" (p. 20), but Billings (1942, p. 272) has suggested that a thickness greater than one-tenth of the diameter be taken as the criterion of a laccolith and has also stated that the floor may be concave, but is rarely seen in typical laccoliths. The thickness of the Mustang Hill intrusion has been reduced to an unknown extent by erosion, but the coarse grain of the uppermost surviving parts suggests that the 1:10 ratio was originally exceeded. Another term, lopolith, has been defined by Grout (1918, p. 518) as a "large, lenticular, centrally sunken, generally concordant intrusive mass with its thickness approximately $\frac{1}{10}$ to $\frac{1}{20}$ of its width or diameter—the type departs from a laccolith not only in form but in the probable mechanics of its intrusion" (i.e., permissive rather than forceful injection). On the basis of size, and evidence for forceful intrusion, Mustang Hill does not qualify as a lopolith.

In Vera Cruz, Mexico, there are basaltic plugs of mushroom or Christmas-tree shape around which an outer annular anticlinal fold and an inner concentric funnel depression immediately surrounding the igneous mass "is attributed to forceful injection followed by settling of the magma" (Garfias and Hawley, 1917, p. 1154).

In Ayrshire, Scotland, some of the plugs and vents show that "the beds are bent sharply down towards the wall of the rock—the result of some kind of subsidence within the vent". (Geikie, 1880, p. 469)

Emplacement of the Mustang Hill laccolith is envisioned as a forceful process bowing up the strata, followed by a subsidence on release of magmatic pressure, which led to a concave floor beneath the intrusion itself. The shape of the roof of the intrusion is unknown.

References Cited

Barth, T. F. W., 1956, Geology and petrology of the Pribilof Is., Alaska: U. S. Geol. Survey Bull. 1028-F, 160 p.

Billings, M. P., 1942, Structural geology: New York, Prentice-Hall, 473 p.

Bowen, N. L., 1940, Progressive metamorphism of siliceous limestone and dolomite: Jour. Geology, v. 48, p. 225–274

Clarke, F. W., 1900, Analyses of rocks from the laboratory of the U.S.G.S.: U. S. Geol. Survey Bull. 168, 308 p.

David, T. W. E., 1950, The geology of the Commonwealth of Australia: vol. 1, London, Edward Arnold, 747 p.

Durham, C. O., 1949, Stratigraphic relations of the Pilot Knob pyroclastics: Shreveport, La., Shreveport Geol. Soc. 17th Ann. Field Trip Guidebook, p. 102–108

Fairbairn, H. W., and Podolsky, T., 1951, Notes on precision and accuracy of optic angle determination with the universal stage: Am. Mineralogist, v. 36, p. 823–832

Friedman, I., 1951, Some aspects of the system H_2O—Na_2O—SiO_2—Al_2O_3 : Jour. Geology, v. 59, p. 19–31

Garfias, V. R., and Hawley, M. J., 1917, Funnel and anticlinal-ring structure associated with igneous intrusions in the Mexican oil fields: Am. Inst. Min. Engineers, v. 128, p. 1147–1159

Geikie, A., 1880, On the Carboniferous volcanic rocks of the basin of the Firth of Forth: Roy. Soc. Edinburgh Trans., v. 29, p. 437–518

Gilbert, G. K., 1880, Report on the geology of the Henry Mountains: U. S. Geog. Geol. Survey Rocky Mountain region, 2d. ed., 170 p.

Greenwood, R., 1956, Submarine volcanic mudflows and limestone dikes in the Grayson formation (Cretaceous) of central Texas: Houston, Texas, Gulf Coast Assoc. Geol. Soc. Trans., v. 6, p. 167–177

Grout, F. F., 1918, The lopolith, an igneous form exemplified by the Duluth gabbro: Am. Jour. Sci., ser. 4, v. 46, p. 516–522

Hammer, S., 1939, Terrain corrections for gravimeter stations: Geophysics, v. 4, p. 184–194

Hazzard, R. T., *et al.*, 1956, Part III, p. 43–72 of Four Provinces Fieldtrip Guidebook, San Angelo Geol. Soc., San Angelo, Texas, 152 p.

Hess, H. H., 1949, Chemical compositions and optical properties of common clinopyroxenes: Am. Mineralogist, v. 34, p. 621–666

Hill, R. T., 1890, Pilot Knob, a marine Cretaceous volcano: Am. Geologist, v. 6, p. 286–292

Jaeger, J. C., 1957, The temperature in the neighborhood of a cooling intrusive. sheet: Am. Jour. Sci., v. 255, p. 306–318

Johannsen, A., 1939, A descriptive petrography of the igneous rocks: 2d. ed., Chicago, Univ. Chicago Press, 1629 p.

Kennedy, G., 1947, Charts for correlation of optical properties with chemical composition of some common rock-forming minerals: Am. Mineralogist, v. 32, p. 561–573

Kennedy, W. Q., 1933, Trends of differentiation in basaltic magmas: Am. Jour. Sci., v. 25, p. 239–256

Lonsdale, J. T., 1927, Igneous rocks of the Balcones fault region of Texas: Univ. Texas Bull. 2744, 178 p.

——, 1940, Igneous rocks of the Terlingua-Solitario region, Texas: Geol. Soc. Am. Bull., v. 51, p. 1539–1626

Meixner, H., 1956, Some new occurrences of gonnardite: Mineral. Magazine, v. 31, p. 265–271

Muir, I. D., 1951, The clinopyroxenes of the Skaergaard intrusion; eastern Greenland: Mineral. Magazine, v. 29, p. 690–714

Muir, I. D., and Tilley, C. E., 1957, Contributions to the petrology of Hawaiian basalts—1. The picrite-basalts of Kilauea: Am. Jour. Sci., v. 255, p. 241–253

Murray, R. J., 1954, The clinopyroxenes of the Garbh Eilean sill, Shiant Is.: Geol. Magazine, v. 91, p. 17–31

Nettleton, L. L., 1940, Geophysical prospecting for oil: New York, McGraw-Hill, 444 p.

Osborne, F. F., and Tait, D. B., 1952, The system diopside-forsterite-anorthite: Am. Jour. Sci., Bowen Volume, pt. II, p. 413–433

Romberg, F., and Barnes, V. E., 1954, A geological and geophysical study of Pilot Knob (south), Travis Co., Texas: Geophysics, v. 19, p. 438–454

Sahama, T. G., 1952, Leucite, potash nepheline, and clinopyroxene from volcanic lavas from southwestern Uganda and adjoining Belgian Congo: Am. Jour. Sci., Bowen Volume, pt. II, p. 457–470

Sand, L. B., *et al.*, 1957, Stability relations of some minerals in the Na_2O—Al_2O_3—SiO_2—H_2O system: Econ. Geology, v. 52, p. 169–179

Sayre, A. N., 1936, Geology and groundwater resources of Uvalde and Medina counties, Texas: U. S. Geol. Survey Water-Supply Paper 678, 146 p.

Segnit, E. R., 1953, Some data on synthetic aluminous and other pyroxenes: Mineral. Mag., v. 30, p. 218–226

Sellards, E. H., and Baker, C. L. (1934), The geology of Texas, v. 2—Structural and economic geology: Univ. Texas Bull. 3401, 884 p.

Sellards, E. H., Adkins, W. S., and Plummer, F. B., 1932, The geology of Texas: v. 1—Stratigraphy: Univ. Texas Bull. 3232, 1007 p.

Shakespeare, W., 1600, King Henry IV, second part, New York, Dutton and Co., 1934, 157 p.

Smiser, J. S., and Wintermann, D., 1935, Character and possible origin of producing rock in Hilbig oilfield, Bastrop, Texas: Am. Assoc. Petroleum Geologists Bull., v. 19, p. 206–220

Steenland, N. C., and Woollard, G. P., 1952, Gravity and magnetic investigation of the structure of the Cortlandt complex, New York: Geol. Soc. Am. Bull., v. 63, p. 1075–1104

Turner, F. J., and Verhoogen, J., 1951, Igneous and metamorphic petrology: New York, McGraw-Hill, 602 p.

Tyrrell, G. W., 1912, The late Paleozoic alkaline igneous rocks of the west of Scotland: Geol. Magazine, v. 49, p. 69–80, 120–131

—— 1917, The picrite-teschenite sill of Lugar: Geol. Soc. London Quart. Jour., v. 72, p. 84–131

Vaughan, T. W., 1900, Folio no. 64 (Uvalde): U. S. Geol. Survey, Geol. Atlas of the U. S.

Vincent, E. A., 1953, Hornblende lamprophyre dykes of basaltic parentage from the Skaergaard area, E. Greenland: Geol. Soc. London Quart. Jour., v. 109, p. 21–49

Wilkinson, J. F. G., 1956a, Clinopyroxenes of olivine basalt magma: Am. Mineralogist, v. 41, p. 724–743

—— 1956b, The olivines of a differentiated teschenite sill near Gunnedah, New South Wales: Geol. Magazine, v. 93, p. 441–455

—— 1957, The clinopyroxenes of a differentiated teschenite sill near Gunnedah, New South Wales: Geol. Magazine, v. 94, p. 123–134

—— 1958, The petrology of a differentiated teschenite sill near Gunnedah, New South Wales: Am. Jour. Sci., v. 256, p. 1–39

UNIVERSITY OF HOUSTON, HOUSTON 4, TEXAS

MANUSCRIPT RECEIVED BY THE SECRETARY OF THE SOCIETY, JULY 21, 1958

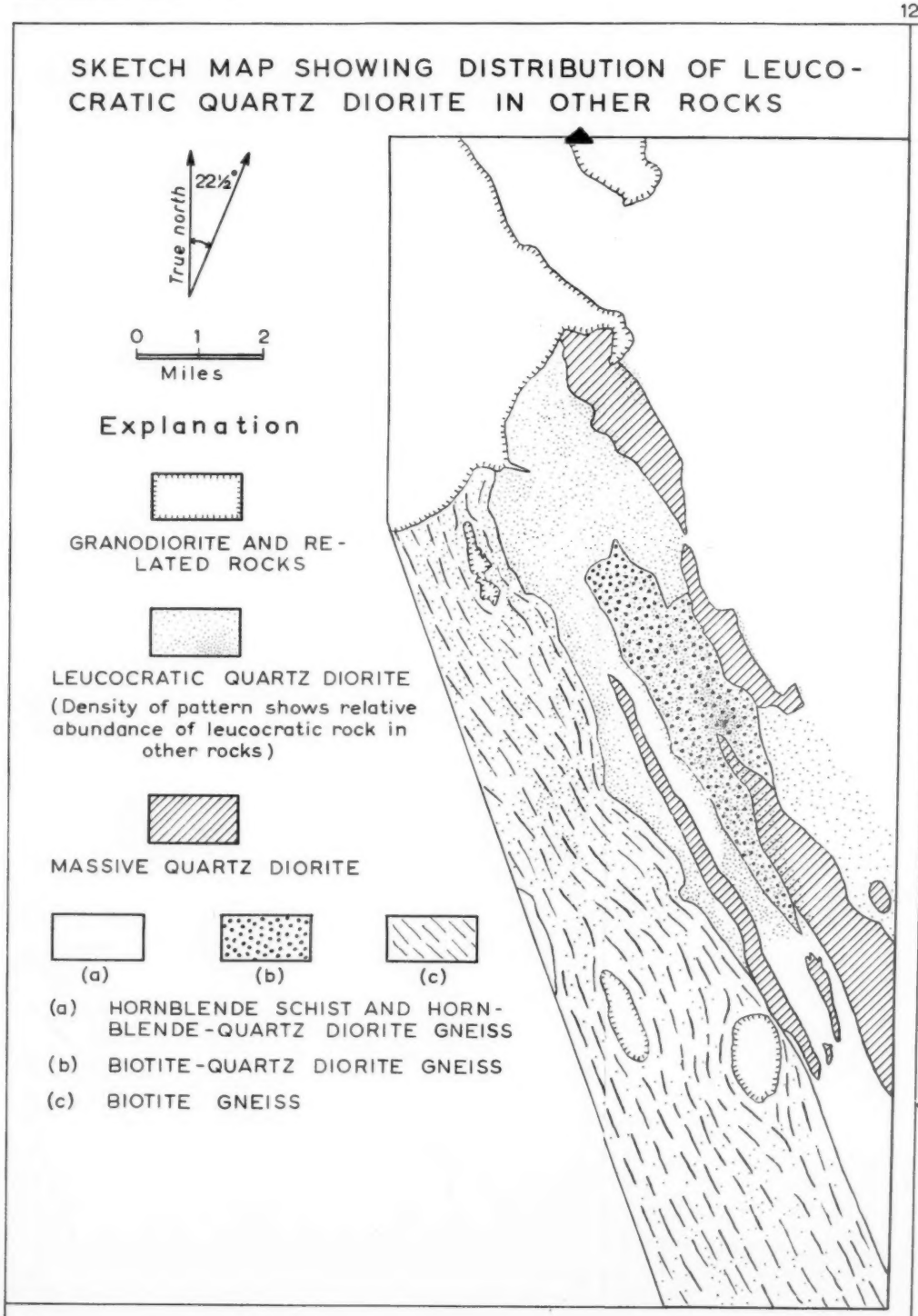
SKETCH MAP SHOWING DISTRIBUTION OF LEUCOCRATIC QUARTZ DIORITE IN OTHER ROCKS
True north
22½°
0 1 2
Miles
Explanation
GRANODIORITE AND RELATED ROCKS
LEUCOCRATIC QUARTZ DIORITE
(Density of pattern shows relative abundance of leucocratic rock in other rocks)
MASSIVE QUARTZ DIORITE
(a)
(b)
(c)
(a) HORNBLENDE SCHIST AND HORNBLENDE-QUARTZ DIORITE GNEISS
(b) BIOTITE-QUARTZ DIORITE GNEISS
(c) BIOTITE GNEISS

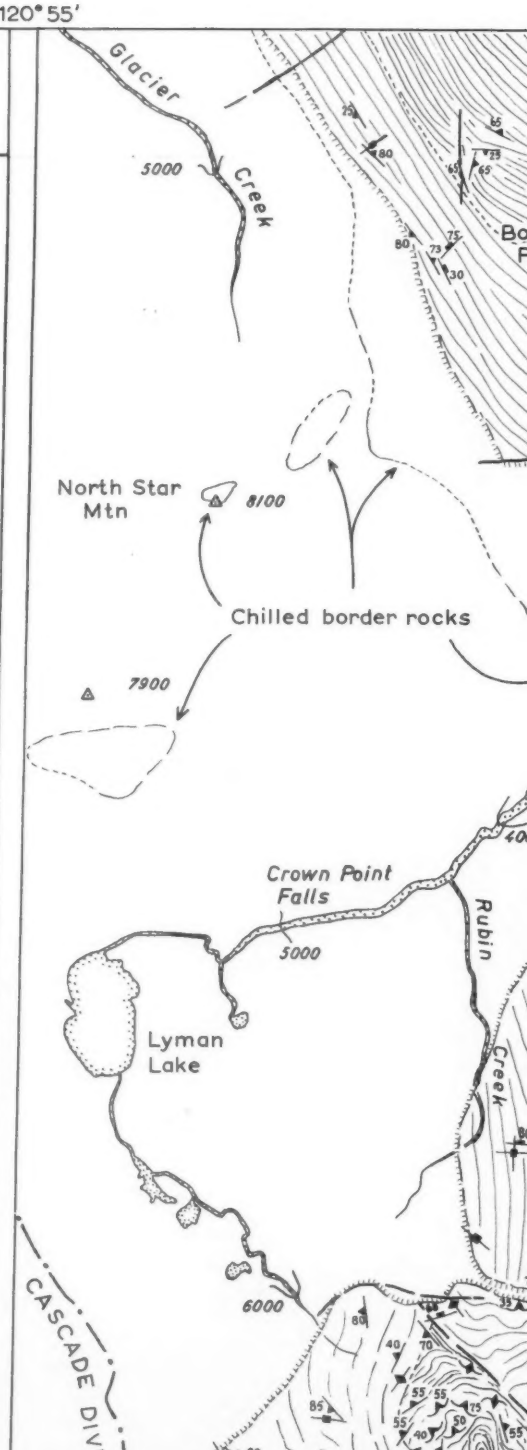
120° 55'
Glacier
5000
Creek
North Star Mtn
8100
Chilled border rocks
7900
Crown Point Falls
5000
Rubin
Lyman Lake
Creek
6000
CASCADE DIVIDE
8000

Crowder, Pl. 1

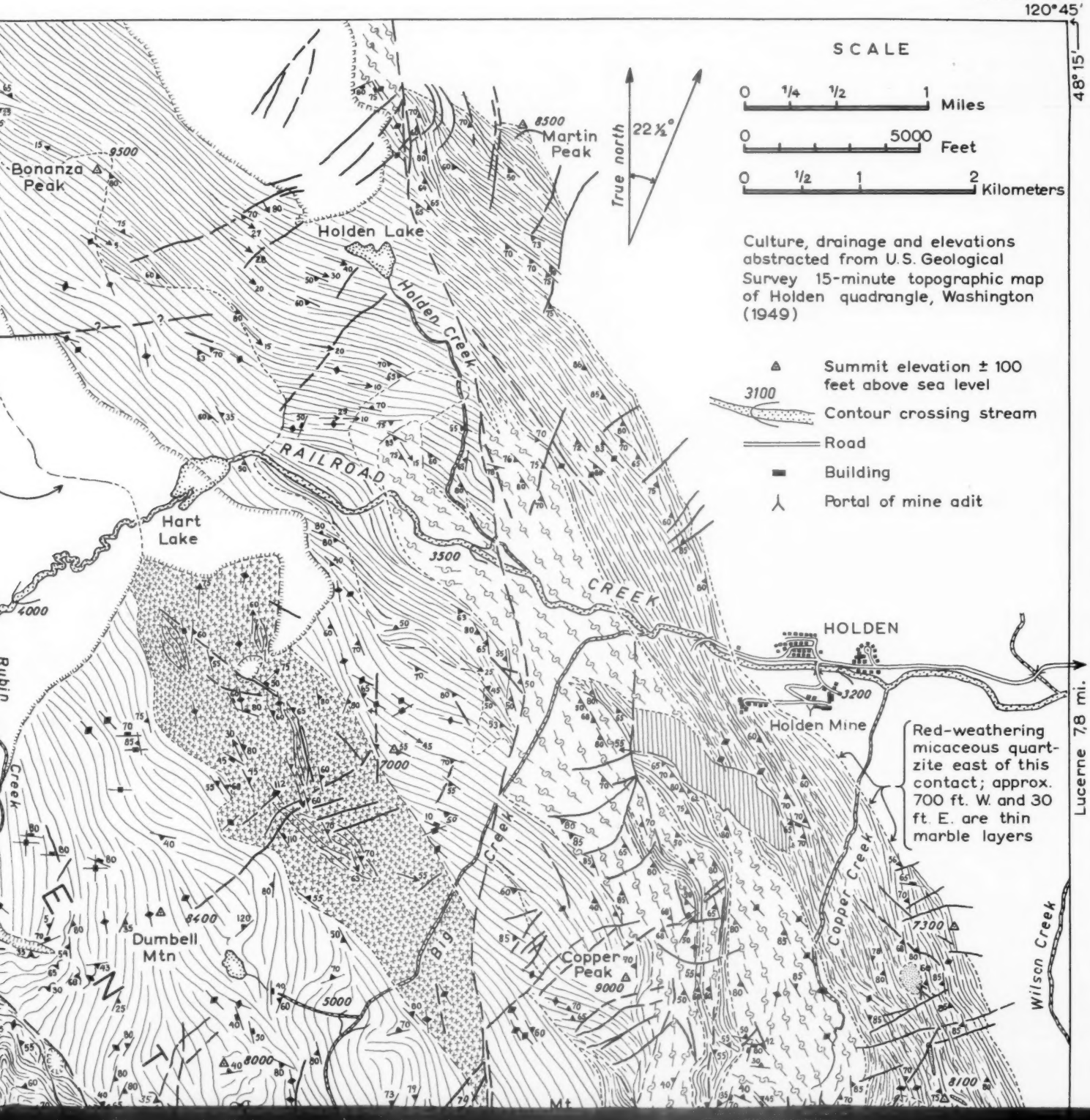
120°45'
48°15'
SCALE
0 1/4 1/2 1 Miles
0 5000 Feet
0 1/2 1 2 Kilometers
True north 22½°
Culture, drainage and elevations abstracted from U.S. Geological Survey 15-minute topographic map of Holden quadrangle, Washington (1949)
Summit elevation ± 100 feet above sea level
3100
Contour crossing stream
Road
Building
Portal of mine adit
Bonanza Peak
9500
Martin Peak
8500
Holden Lake
Holden Creek
RAILROAD
Hart Lake
4000
3500
CREEK
HOLDEN
3200
Holden Mine
Red-weathering micaceous quartzite east of this contact; approx. 700 ft. W. and 30 ft. E. are thin marble layers
Lucerne 7.8 mi.
Rubin
Creek
7000
Dumbell Mtn
8400
5000
8000
Big Creek
Copper Peak
9000
Copper Creek
7300
Wilson Creek
8100
Mt

EXPLANATION

EOCENE ROCKS POST-EOCENE ROCKS

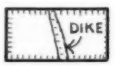

GRANODIORITE WITH CHILLED BORDER OF PORPHYRITIC – APHANITIC ROCKS; RELATED DIKES, PLUGS, AND INTRUSIVE BRECCIAS

SWAUK FORMATION

Conglomerate, grit, sandstone; a few thin coal seams.

STOCKS AND DIKES

(A) BIOTITE-QUARTZ DIORITE GNEISS
(B) FINE-GRAINED BIOTITE GRANODIORITE
(C) ULTRAMAFIC ROCKS (HORNBLENDITE AND PERIDOTITE)
(D) HORNBLENDE GABBRO AND DIORITE
(E) MAFIC DIKES

} In part older than rocks of the complex

ROCKS OF THE COMPLEX

MASSIVE QUARTZ DIORITE

(5) Biotite - hornblende - quartz diorite
Western mass badly sheared and gneissic

(6) Hornblende - biotite - quartz diorite
Some granodiorite phases

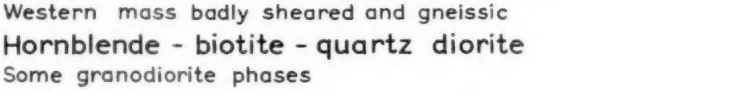

QUARTZ DIORITE GNEISS

(8) Biotite - quartz diorite gneiss
Swirled foliation very common.

ENE ROCKS

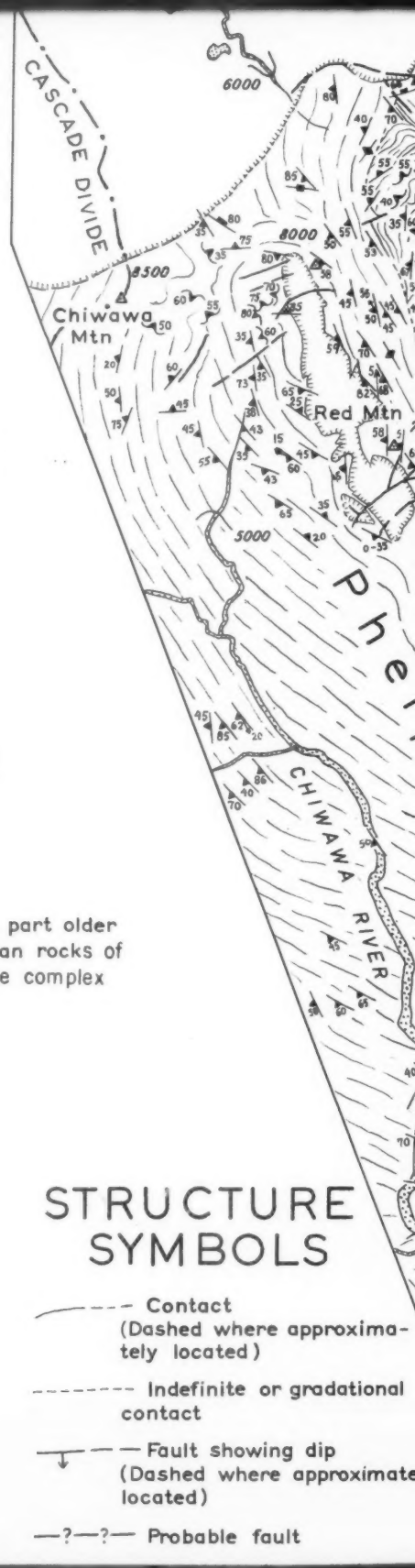

STRUCTURE SYMBOLS

Contact (Dashed where approximately located)

Indefinite or gradational contact

Fault showing dip (Dashed where approximate located)

—?—?— Probable fault

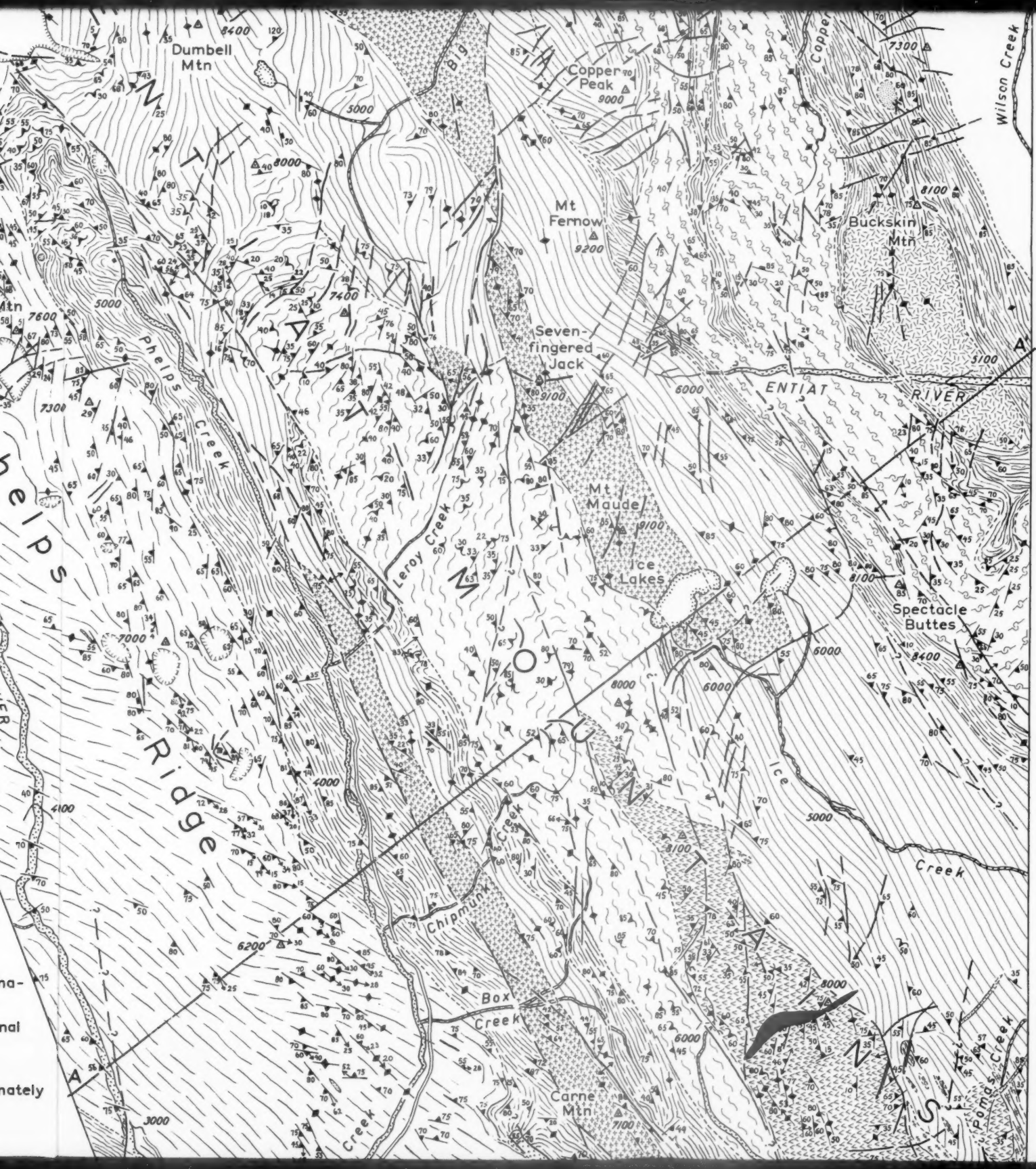
Dumbell Mtn
8400
Copper Peak
9000
Wilson Creek
7300
Mt Fernow
9200
Buckskin Mtn
8100
Seven-fingered Jack
9100
ENTIAT RIVER
Phelps Creek
Leroy Creek
Mt Maude
9100
Ice Lakes
Spectacle Buttes
8400
Ice Creek
Chipmunk Creek
Box Creek
Carne Mtn
7100
Creek
Phelps Ridge
A
A'

(E) MAFIC DIKES

PRE-EOCENE ROCKS

ROCKS OF THE COMPLEX

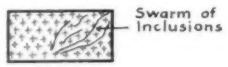

(5) (6)

MASSIVE QUARTZ DIORITE

(5) **Biotite - hornblende - quartz diorite**
Western mass badly sheared and gneissic

(6) **Hornblende - biotite - quartz diorite**
Some granodiorite phases

(8) (2) (3) (4)

QUARTZ DIORITE GNEISS

(8) **Biotite - quartz diorite gneiss**
Swirled foliation very common.

(2) **Well-foliated hornblende - quartz diorite gneiss**
Fine medium-grained. Foliation not swirled.

(3) **Granitoid hornblende - quartz diorite gneiss**
Medium-grained, swirled foliation and massive phases common.

(4) **Hornblende - quartz diorite augen gneiss**
Augen and streaks of quartz and swirld foliation common.

MIGMATITE IN HORNBLENDE SCHIST

(A) **Recrystallization type**
(a) Clots of hornblende and seams and dikes of hornblende-quartz diorite and diorite
(b) Heterogeneous mixtures of massive fine-grained to pegmatitic hornblende diorite

(B) **Replacement type**
Streaks of fine-grained light-colored hornblende-biotite-quartz diorite parallel to foliation of hornblende schist

PRE-COMPLEX ROCKS

(1) (7)

(1) HORNBLENDE SCHIST AD GNEISS

Highly variable ratio of hornblende to lit colored minerals

(7) BIOTITE GNEIS

Typically almost schistose, well segregat into light and dark layers and wisps in migmatites, garnet-aring phases common

STRUCTURE SYMBOLS

- Contact (Dashed where approximately located)
- Indefinite or gradational contact
- Fault showing dip (Dashed where approximately located)
- Probable fault
- U / D — Fault showing relative move; U upthrown block, D down block
- 30 — Strike and dip of bedding
- 10 — Strike and dip of foliation
- Strike of vertical foliation
- Horizontal foliation
- Generalized strike and dip
- Generalized strike of vertica
- 20 — Bearing and plunge of horn or mineral streaks
- 20 — Strike and dip of joints
- Strike of vertical joints

GEOLOGY B
D.F. CROWDER, F.W. CATER, C.A. HOPS
R.W. TABOR
(1950 - 1955)

Drawn by Ingrid

NUMBERS OF ROCK UNITS CORRE
NUMBERS IN TABLE 5

COSS SECTION ALONG A-A'

CHIWAUKUM GRABEI

NORTHERN ENTIAT MOUNTAINS

Ice Lakes

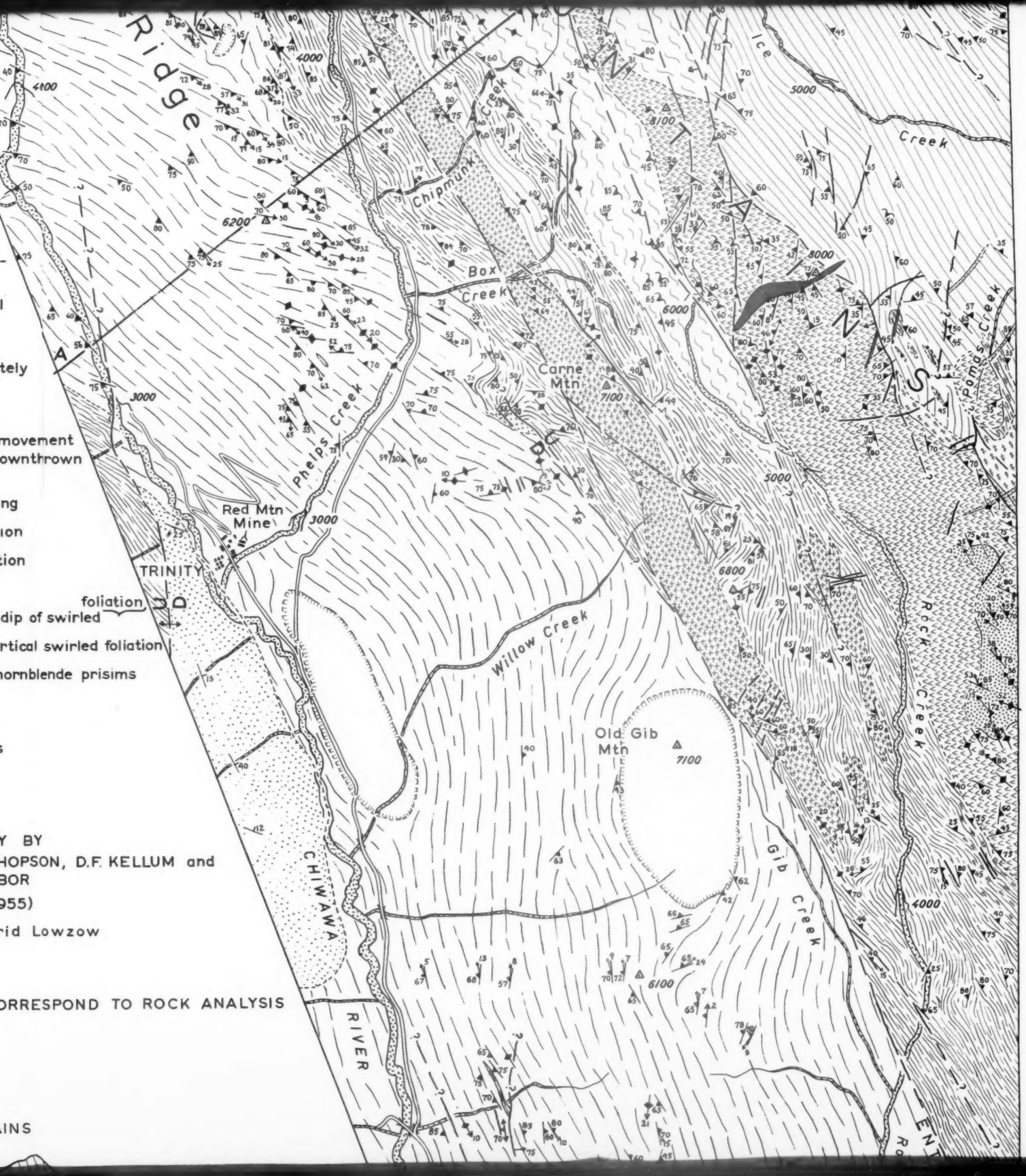
Ridge
Chipmunk Creek
Box Creek
Phelps Creek
Carne Mtn
7100
Red Mtn Mine
TRINITY
foliation
dip of swirled
rtical swirled foliation
hornblende prisims
Willow Creek
Old Gib Mtn
7100
Gib Creek
CHIWAWA
RIVER
Rock Creek
Poma Creek
Ice Creek
8100
8000
6200
6100
6800
6000
5000
4000
3000
4100
HOPSON, D.F. KELLUM and
BOR
955)
rid Lowzow
ORRESPOND TO ROCK ANALYSIS
AINS

PR

(4) Hornblende - quartz diorite augh gneiss
Augen and streaks of quartz and swirld foliation common.

MIGMATITE IN HORNBLENDE SCHIST

(A) Recrystallization type
(a) Clots of hornblende and seams and diks of hornblende-quartz diorite and diorite
(b) Heterogeneous mixtures of massive finegrained to pegmatitic hornblende diorite

(B) Replacement type
Streaks of fine-grained light-colored hornblende-biotite-quartz diorite parallel to foliation of hornblen schist

PRE-COMPLEX ROCKS

(1) HORNBLENDE SCHIST AD GNEISS
Highly variable ratio of hornblende to lit colored minerals

(7) BIOTITE GNEIS
Typically almost schistose, well segregat into light and dark layers and wisps in migmatites, garnet-aring phases common

10 Strike and dip of foliatio

Strike of vertical foliatio

Horizontal foliation

Generalized strike and di

Generalized strike of verti

20 Bearing and plunge of hor or mineral streaks

20 Strike and dip of joints

Strike of vertical joints

GEOLOGY
D.F. CROWDER, F.W. CATER, C.A. HO
R.W. TABO
(1950 - 195
Drawn by Ingri

NUMBERS OF ROCK UNITS COR
NUMBERS IN TABLE 5

COSS SECTION ALONG A-A'

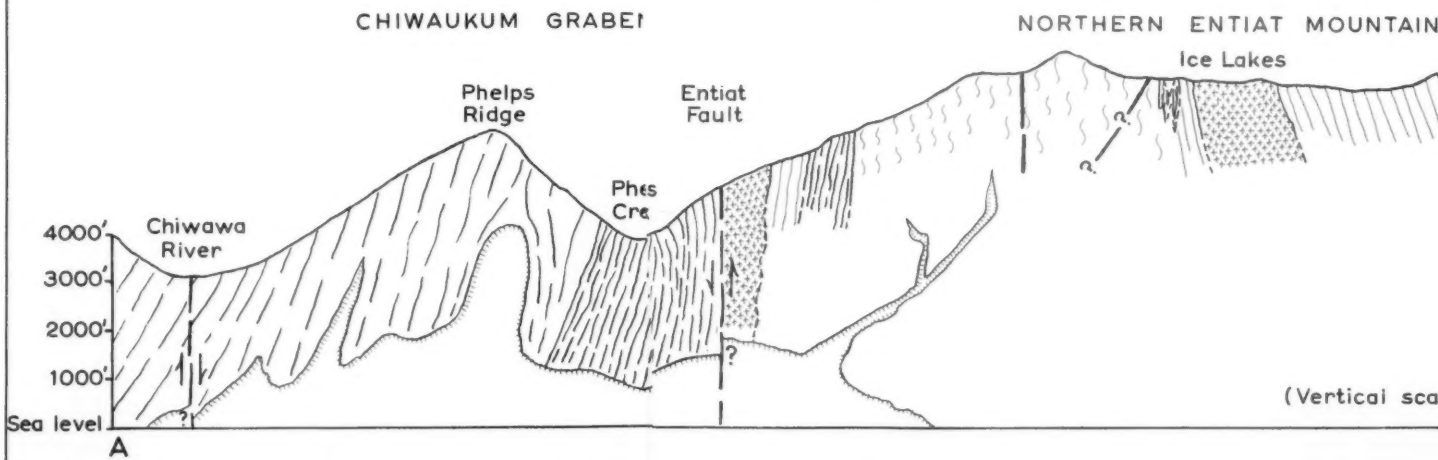

GEOLOGIC MAP OF THE NORTHER

ation

iation

foliation

d dip of swirled

vertical swirled foliation

f hornblende prisims

ts

nts

GY BY

. HOPSON, D.F. KELLUM and
ABOR

-1955)

grid Lowzow

CORRESPOND TO ROCK ANALYSIS

TAINS

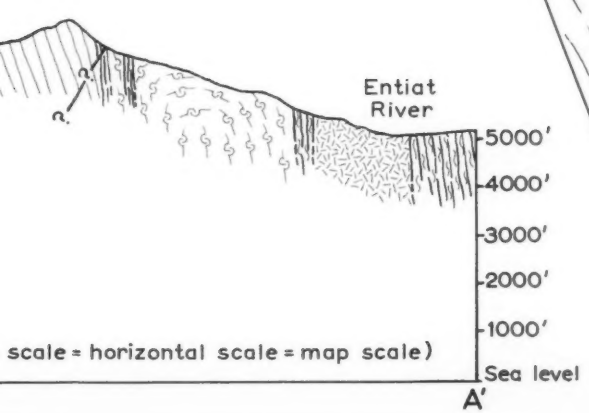

scale = horizontal scale = map scale)

ERN ENTIAT MOUNTAINS, WASHINGTON

GRANIT

sou
cor
ble
siti
me
dio
mo
sho
ho
by
in
tex
wi
the
oc
tit
tai
by
qu
m
qu
sic
ha
in
di
po
ti
en
T
sil

Introductio
General
Previous
Present
Topogra
Acknowl
Geologic
North
Holde
Terms d
Pre-compl
General

BULLETIN OF THE GEOLOGICAL SOCIETY OF AMERICA
VOL. 70, PP. 827–878, 11 FIGS., 7 PLS. JULY 1959

GRANITIZATION, MIGMATIZATION, AND FUSION IN THE NORTHERN ENTIAT MOUNTAINS, WASHINGTON

BY DWIGHT F. CROWDER

ABSTRACT

A tabular quartz diorite complex extends along the Entiat Mountains, which form a southeast-trending spur of the Northern Cascade Mountains. The country rocks of the complex are biotite gneiss, probably derived from arkosic sedimentary rocks, and hornblende schist, probably derived from basic volcanic rocks. Their present mineral composition is typical of the upper epidote amphibolite and amphibolite facies of regional metamorphism.

During regional metamorphism the biotite gneiss was granitized to biotite-quartz diorite gneiss and the hornblende schist to hornblende-quartz diorite gneiss. The metamorphic origin of these quartz diorite gneisses involving relatively little replacement is shown by their chemical and mineralogical similarity to the original biotite gneiss and hornblende schist, by their enclosing long, thin, undisturbed layers of country rocks, and by their association with migmatites formed by metamorphic processes. Here and there in the quartz diorite gneisses massive rocks with hypidiomorphic granular "igneous" textures have formed principally by recrystallization, and these features are associated with small-scale swirling of the foliation and some intrusive features, which show that the gneiss was rendered plastic and mobile during granitization.

Migmatites containing replacement bodies and secretions of leucocratic quartz diorite occur in the biotite gneiss and in most of the rocks of the complex—particularly in the biotite-quartz diorite gneiss. During the formation of the complex, the felsic material contained in the leucocratic rocks, principally sodium, potassium, and silicon, was generated by metamorphic differentiation.

During the granitization, anatectic magmas were formed by fusion of hornblende-quartz diorite gneiss, and some similar magma intruded from below. Melting without metamorphic differentiation is indicated by the chemical similarity between the anatectic quartz diorite and the parent hornblende-quartz diorite gneiss. Smearing out of inclusions and crystals and the tabular, sill-like nature of the bodies indicate that fusion may have been triggered by differential movement and shearing. The anatectic rocks contain inclusions of hornblende schist that survived both the granitization to hornblende-quartz diorite and the fusion. Crystallization differentiation of the anatectic magmas yielded potassium-rich pegmatites and local granodioritic masses. Regional metamorphism continued after the anatectic magmas in the sills had solidified; felsic metamorphic differentiates occur in leucocratic quartz diorite that partly replaces the borders of the sills. The leucocratic material was plastic and facilitated differential movement between the sill and its walls.

CONTENTS

TEXT

	Page
Introduction	828
General statement	828
Previous work	828
Present investigation	828
Topography and outcrops	829
Acknowledgments	829
Geologic setting	829
Northern Cascade Mountains	829
Holden quadrangle	830
Terms defined	832
Pre-complex rocks	833
General statement	833
Biotite gneiss	833
Hornblende schists	835
Rocks of the complex	838
General statement	838
Quartz diorite gneiss	838
Massive quartz diorite	848
Migmatites in hornblende schist	852
Leucocratic quartz diorite	855
Stocks and dikes	862
General statement	862
Quartz diorite stock	862
Granodiorite	864
Ultramafic rocks and gabbro	864
Mafic dikes	865
Relation of stocks and dikes to the complex	865

Page
Chemistry of the complex 871
Origin of the complex 874
References cited 876

ILLUSTRATIONS

Figure Page
1. Geologic reconnaissance map of the Northern Cascade Mountains 831
2. Crystalloblastic microtextures of biotite gneiss and biotite-quartz diorite gneiss ... 836
3. Porphyroblasts and crystalloblastic microtextures of hornblende schist and gneiss . 837
4. Contact of hornblende schist and quartz diorite gneiss (unit 4) 842
5. Crystallographic microtextures and porphyroblasts of hornblende-quartz diorite gneiss 844
6. Igneous-appearing features in microtextures of hornblende-quartz diorite gneiss and massive quartz diorite 845
7. Microtextures showing quartz in hornblende-quartz diorite gneiss 846
8. Visual effects of segregation 858
9. Pegmatite occurring where a layer of biotite gneiss tends to be pulled apart .. 859
10. Crystalloblastic microtexture of leucocratic quartz diorite 861
11. Changes in cation percentages of main elements during transformations 872

Plate Facing page
1. Geologic map of the northern Entiat Mountains, Washington 827
2. Polished specimens at true scale showing textures of representative rock types 830
3. Polished specimens at true scale showing textures of representative rock types 830

Following page
4. Recrystallization and metamorphic segregation in hornblende schist and ultramafic rocks 856
5. Replacement migmatite in hornblende schist and inclusions of quartz diorite gneiss 856
6. Segregation, plastic flow, and dikes of leucocratic quartz diorite in biotite gneiss and biotite-quartz diorite gneiss 856
7. Leucocratic quartz diorite in hornblende-quartz diorite gneiss 856

TABLES

Table Page
1. Composition and properties of biotite from biotite gneiss 835
2. Composition and properties of biotite from biotite-quartz diorite gneiss 843
3. Modes of massive quartz diorite 859
4. Modes of stock on Buckskin Mountain and of related dikes 862
5. Composition of rocks of complex and of host rocks 866

INTRODUCTION

General Statement

This report deals with the geology of a part of the Holden, Washington, quadrangle, most of which lies just east of the main divide of the Northern Cascade Mountains and about 70 miles northeast of Seattle (Fig. 1). The Northern Cascade Mountains are at the southwest end of the Coast Range batholith, where that enormous complex pluton disappears beneath the vast Tertiary lava flows of the northwestern United States. This report describes a part of a quartz diorite complex in the Entiat Mountains, a major southeast spur of the Northern Cascade Mountains, which joins the main divide in the Holden quadrangle. Gneiss complexes such as this can be duplicated in many parts of the world—the classic areas are in Scandinavia—but only rarely are they as excellently exposed as they are in these recently glaciated mountains of northwestern Washington. The complex is believed to have formed principally by the granitization of hornblende schists and biotite gneisses to quartz diorites. In this paper the evidence for this hypothesis is built up piecemeal in connection with the description of the various rocks.

Previous Work

Reconnaissance work by the U. S. Geological Survey (Russell, 1898; Smith and Calkins, 1904; Smith, 1904; Smith and Calkins, 1906), followed by the work of Daly (1912) along the Canadian boundary, determined some of the general features of Northern Cascades Mountains geology. Since these early days the approximate distribution of the principal rocks has been outlined by the efforts of a number of geologists, but the reconnaissance map (Fig. 1), which has been compiled from the maps of previous workers, shows by its simplicity how little is known of this large and complex area as a whole. Work within the Holden quadrangle includes Richarz' (1933) description of the rocks of the Red Mountain mine, Youngberg and Wilson's (1952) discussion of some features of the geology of the Holden mine, and Dubois' (1954, Ph.D. thesis, Univ. Washington; 1956) and Morrison's (1954, M.S. thesis, Univ. Washington) mapping of two small areas.

Present Investigation

Work on the Holden quadrangle by the U. S. Geological Survey was started in 1951,

when part of the underground workings of the Holden mine and some of the surface adjacent to the mine were mapped. The rest of the quadrangle (about 200 square miles) was mapped in the following three summers by a team of three to four geologists. In the course of this mapping a problem arose in regard to the genesis of migmatites of leucocratic quartz diorite in older rocks that required additional work; I therefore spent a fifth summer in the quadrangle (1955) studying this problem and mapping some areas at a scale of 1:24,000. This report discusses these migmatites and the adjacent quartz diorites to which they are intimately related.

Topography and Outcrops

The maximum relief in the Holden quadrangle is 7000 feet, and the highest summit altitude is 9511 feet. Heavy underbrush, large talus aprons, and glacial and fluviatile debris almost completely blanket the valley bottoms. About a third of the area is thus covered, as is evident from the distribution of structural data in Plate 1; above the brushy bottoms the outcrops are nearly continuous and exceptionally clean. The area has few roads, but all the major valleys have trails.

Acknowledgments

F. W. Cater supervised all the work in the Holden quadrangle, and he and I collaborated in the field work; C. A. Hopson, D. F. Kellum, and R. W. Tabor assisted in the mapping. Dr. R. R. Compton, Dr. C. O. Hutton, Dr. K. B. Krauskopf, and Dr. P. Misch contributed valuable discussion. A grant from the U. S. Government under the Fulbright Act (1956-1957) enabled me to make comparisons with other granitoid rocks and migmatites in Norway, to do much of the petrographic work, and to write this report while at the Mineralogisk-Geologisk Museum of the University in Oslo. Members of the staff of the Museum gave assistance, particularly Miss I. Lowzow and Miss B. Mauritz, who helped prepare the illustrations, and Mrs. B. Nilssen, who helped with the two mineral separations. B. Bruun, of the Geological Survey of Norway, made the two mineral analyses; all other chemical work was done by chemists of the U. S. Geological Survey who are named in the text. F. W. Cater and F. C. Calkins made valuable criticisms of my exposition. I am especially grateful for discussions with Prof. T. F. W. Barth, director of the Mineralogisk-Geologisk Museum in Oslo, who also put all facilities of the museum at my disposal.

Geologic Setting

Northern Cascade Mountains—The reconnaissance map of the Northern Cascade Mountains (Fig. 1) shows the general form and distribution of the principal rocks and brings out the dominant north and northwest trend of the geologic structures. The stratigraphy of the metamorphic rocks is practically unknown. Fossils are very scarce, though some late Paleozoic and Mesozoic forms have been found.[1]

Daly's interpretation of the geologic history of the region, as outlined after his traverse of the 49th parallel (1912, p. 564–577), has been accepted in the main by later workers. Waters (1955) sketched the Tertiary volcanic history of the northwestern United States and pointed out possible genetic relations between the volcanic and the plutonic rocks. In brief summary, the geologic history of the Northern Cascade Mountains as now known is as follows:

(1) In the early and middle Paleozoic the Northern Cascade Mountains were part of a highland along the Pacific coast which shed debris into the Rocky Mountain geosyncline farther east. In the late Paleozoic the Pacific coast highland sank, forming the western or Pacific geosyncline. The Rocky Mountain geosyncline rose from the sea and began shedding debris into this new basin on the west. The approximate line of junction between these two geosynclines as given by Daly is shown in Figure 1. A fragment of the ancient rocks of the floor of the Pacific geosyncline has yet to be recognized in the Northern Cascade Mountains.

(2) A major orogenesis culminated in the Mesozoic (Nevadan revolution). The Pacific geosyncline was highly deformed and metamorphosed, and extensive batholiths of granodiorite and allied rocks were emplaced. Mountains rose out of the sea, but the Rocky Mountain geosyncline to the east remained high and stable.

[1] Ordovician fossils from limestone lenses at the headwaters of the Skykomish River were recorded by W. S. Smith (1916). Smith's collection has been lost, the rocks from which it came quarried away, and the paleontologist who identified Smith's fossils is no longer living (W. S. Danner, personal communication). Recent collections from the area have yielded only Permian fossils, described by Thompson, Wheeler, and Danner (1950).

(3) Local Cretaceous geosynclines formed and were filled.

(4) In Mesozoic to early Tertiary time (Laramide revolution), widespread deformation occurred throughout both the Rocky Mountain and Pacific geosynclines. Thrusting and folding occurred on a grand scale, but no wholesale emplacement of granitoid rocks or widespread and profound metamorphism occurred, as in the Nevadan revolution.

(5) In Eocene to Pliocene time andesites were erupted along the Cascade axis, while vast amounts of tholeiitic basalt were extruded on both sides.

(6) Several batholiths were emplaced, one possibly as late as post-Miocene, but these were not nearly so extensive as those of the Nevadan revolution.

(7) In the Quaternary andesitic volcanic cones were built along the Cascade Mountains.

Rocks dating from all these major periods (except number 5) in the geologic history of the Northern Cascade Mountains can be found in the Holden quadrangle, but the rocks of the Holden quadrangle discussed in this report were formed during or before the Mesozoic Nevadan revolution.

Holden quadrangle.—The principal features of the geology of the Holden quadrangle are three northwest-trending belts of gneiss and schist (Fig. 1). The rocks in the central belt along the Entiat Mountain divide are those of the quartz diorite complex discussed in this paper; they are chiefly quartz diorite gneiss but include some massive quartz diorites (Pl. 1). On both sides of this central belt of quartz diorite are extensive conformable belts of schist and gneiss of the regional terrain, but only the rocks immediately adjacent to the central quartz diorites are discussed in this paper.

A normal fault, called by Willis (1953, p. 792) the Entiat fault, forms the west contact of the quartz diorite complex and follows the west side of the Entiat Mountains; the Entiat Mountains are in part a fault-block range. The Entiat fault also forms the east border of a large graben, a graben that ends in the southern part of the Holden quadrangle because the west-bounding fault feathers out.

The rocks discussed in this report are overlain unconformably by Eocene sedimentary rocks that crop out in small areas within the graben in the Holden quadrangle. These sedimentary rocks contain boulders of gneiss and have been correlated with the Eocene Swauk formation which, just south of the quadrangle, forms the floor of the graben.

The Entiat fault and the adjacent shattered and sheared gneissic basement rocks are cut off sharply, in the northwest part of the quadrangle, by a younger batholith of massive granodiorite. This rock apparently forms an extensive subjacent mass, for many plugs and dikes of rocks similar to a chilled border phase of the batholith have been emplaced along a broad zone parallel to the Entiat fault at least as far as the south border of the quadrangle. The granodiorite and the granitoid rocks in the southwest and northeast corners of the Holden quadrangle are not discussed in this report.

Evidence indicates that the rocks of the northern Entiat Mountains are in the core of an anticline. The northern Entiat Mountains are flanked on the west by a syncline, and reconnaissance observations by Hopson (Written communication) suggest that another syncline extends along the east flank of the Entiat Mountains outside the quadrangle. In the northern Entiat Mountains, also, the rocks on the two sides of the quartz diorite complex are much the same, even though no stratigraphic sequence is repeated.

The quartz diorites of the northern Entiat Mountains may be part of the Chelan batholith (Waters, 1932, p. 605). Hopson (1955, Ph.D. thesis, Johns Hopkins Univ.; written communications) traced rocks of this batholith almost continuously up the Entiat River valley to a point about 4 miles north of the southeast corner of the Holden quadrangle, and the rock there, a massive quartz diorite, continues northwestward into the Holden quadrangle. The distinctive biotite gneiss lying just west of the Entiat fault in the Holden quadrangle is correlated with the biotite gneiss that makes up 85 per cent of the Swakane gneiss, first described by Waters (1932, p. 615). Willis (1953) traced this gneiss northward along the Entiat Mountains from the type locality to near the southern border of the Holden quadrangle; the rock are megascopically and microscopically identical, and both contain similar minor intercalations of other gneisses and schists.

The quartz diorites in the northern Entiat Mountains were probably formed deeper in the crust than the rocks to the southeast along the trend of the Entiat Mountains or to the west of them. Erosion probably has gone deeper into the crust in the Holden quadrangle, which is

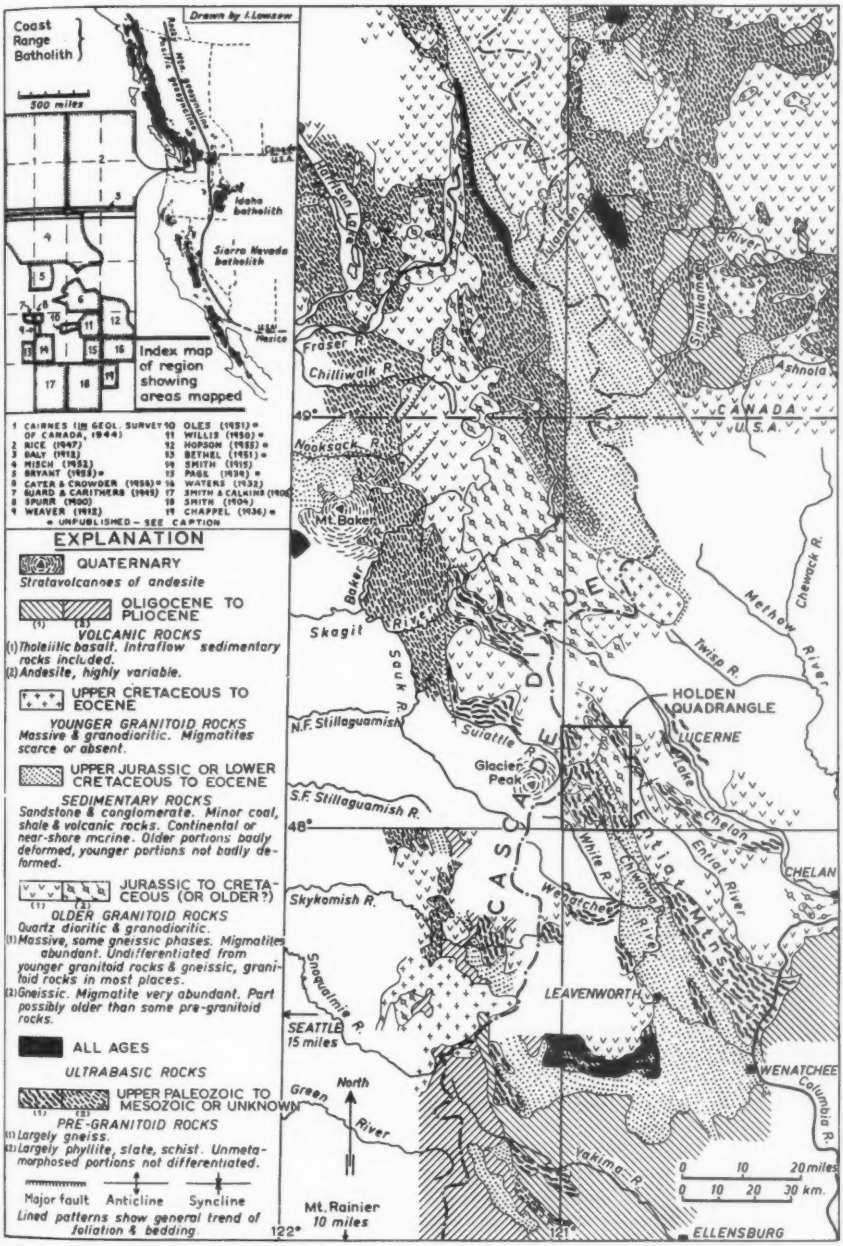

FIGURE 1.—GEOLOGIC RECONNAISSANCE MAP OF THE NORTHERN CASCADE MOUNTAINS

Unpublished sources: Bryant, Bethel, Willis, and Chappel (Ph.D. theses, Univ. Wash.), Oles (M.S. thesis, Univ. Wash.), Hopson (Ph.D. thesis, Johns Hopkins Univ.), Cater and Crowder (U. S. Geological Survey open-file report and reconnaissance), Page (Ph.D. thesis, Stanford Univ.)

near the crest of the domelike Cascade Mountains uplift, than it has on the flanks of the mountains. The Swakane biotite gneiss is not migmatitized in the foothills near Wenatchee where it was studied by Waters (1932, p. 618), although it is locally injected with pegmatites; in the more deeply eroded Holden quadrangle migmatites are a characteristic feature of this gneiss. Erosion probably has gone deeper in the upthrown Entiat Mountain fault block, east of the Entiat fault, than on the floor of the graben west of it, where the basement rocks are partly or completely blanketed with the Swauk formation; migmatites and rocks that have been granitized are more abundant east of the fault than west of it.

Terms Defined

Plutonic is used here for the deep-seated igneous rocks and the metamorphic rocks, as distinct from the volcanic and sedimentary rocks. It is used in Read's (1944, p.93) sense as one of the three main classes of rocks: plutonic, volcanic, and neptunic.

Granitoid rock is used as many geologists use the terms granite and granitic rock, in other words for a whole class of quartz-feldspar rocks of granitoid texture, of which granite, in the strict sense, is somewhat subordinate. Granitoid rock is used, because it has fewer compositional connotations than granite and granitic rock.

Granitization is used as Read (1944, p. 47) defined it: "Granitization means the process by which solid rocks are converted to rocks of granitic character without passing through a magmatic stage". Read uses granitic in the broad sense, as discussed above.

Inclusion is used for a body of rock surrounded by another rock; there is no implication concerning the origin of matrix or how the inclusions came to be in it.

Migmatite is used in this report as a descriptive term, though the original definition (Sederholm, 1907, p. 88-89, 110; 1926, p. 133-139, especially p. 135) is genetic. Sederholm believed that migmatites "look like mixed rocks" and that they were formed where host rocks were supplied with injections of magma or emanations from magma. He thought that some phases in migmatite formed by melting of the host rock. Later workers (Holmquist, 1921) believe that the supply is derived by metamorphic processes from adjacent rocks, and others believe that it is derived from distant rocks by a similar process. Wegmann (1935) and Read (1944, p. 63) agree that many migmatites look like mixtures but also say that granitoid rocks formed by replacement are migmatites even though they are essentially homogeneous. Thus such varied images are conjured up by this genetically defined word that it is impossible to use it as a descriptive term without redefining it. Until there is agreement on how migmatites were formed, a genetic definition must be avoided, and if a descriptive definition is substituted it should bring to the reader's mind a picture of a migmatite—nothing more.

A descriptive definition of migmatite is given by Turner and Verhoogen (1951, p. 294) as "those mixed rocks in which a granitic component (in the broad sense of the phrase) is clearly recognizable". This definition contains the genetic term mixed (mix and mixture commonly imply adding of one thing to another); it does not specify the nongranitic components and is incomplete without mention of scales. In composing a descriptive definition for migmatite I have tried to describe the migmatite illustrated in Sederholm's definitive paper (1907, Pls. I–VIII) and to keep close to Sederholm's statement (1926, p. 136) that migmatites "look like mixed rocks". I have used one genetic term, plutonic, in the definition because it seems agreed that migmatite forms deep in the earth:

A migmatite is made up of two or more plutonic rocks, one (or more) of which is a more granitoid rock than the other(s) and occurs in bodies big enough to provide hand specimens. Standing a few paces from a typical outcrop of migmatite one must be able to see: (1) that it is made up of two or more rocks; (2) that the more granitoid rock(s) occurs in crosscutting tabular bodies, irregular layers, pods, or less regularly shaped bodies in the other rock(s) or around pieces of the other rock(s), without destroying its (their) structural continuity; (3) that the more granitoid rock(s) makes up a significant volume (at least 10 per cent) and is rather evenly distributed. Two principal forms, one with contortion and one without, can be distinguished.

This definition excludes from migmatite many composite masses and rocks that some geologists have called migmatite; no classification can avoid some difficulty with borderline cases. The principal types of rock into which migmatite grades are rocks such as gneiss and massive granitoid rock which appear homogeneous, breccias containing unoriented inclusions, and evenly banded rocks. By

specifying that migmatites must appear composite from a distance of a few paces, and that granitoid rocks must be in bodies large enough to provide hand specimens, the definition excludes homogeneous-appearing gneiss, veined gneiss with small veins, and massive granitoid rock. The definition specifies that from a distance of a few paces the less granitoid rocks must show structural continuity. This excludes breccia containing unoriented inclusions (for example, typical intrusive breccia) and massive granitoid rock containing a few scattered inclusions or ghosts of inclusions. Banded gneisses, in which layers of more granitoid rock are straight and of uniform thickness, are excluded from migmatite by the specification that these layers must be irregular. Many of the rocks that are excluded from migmatite by this definition are formed in the same ways that migmatite forms, but this imperfection is not unusual in terminology. A granite and a diorite, for example, may form in the same way, but they are generally considered different rocks.

During the initial mapping in the northern Entiat Mountains migmatite was used as a cartographic unit, especially for migmatite in which a leucocratic quartz diorite was the granitoid rock phase. An attempt was made to map certain types of migmatite, but in most places these composite masses were considered too complex to differentiate at the scale of mapping (1:31,680). The result of this use of migmatite as a cartographic unit was that contacts that could be followed with relative ease in unmigmatized areas were lost where the rocks were intensely migmatized. During remapping the host rock of the migmatite was used as the cartographic unit, and in migmatized areas a note was made of the type, abundance, and mode of origin of the more granitoid rocks. Contacts were then detected in the migmatized areas, and the problem became comparatively simple.

Pre-Complex Rocks

General Statement

The principal host rocks of the quartz diorite complex are biotite gneiss and hornblende schists, which probably represent a series of interbedded sedimentary and volcanic rocks in the upper epidote amphibolite or the amphibolite facies of regional metamorphism. All the biotite gneiss occurs west of the complex. Where it crops out in the Holden quadrangle it is cut by dikes, sills, and irregular masses of leucocratic quartz diorite, which in many places are so numerous that the composite mass is a migmatite. The hornblende schists occur in broad belts on both sides of the complex, but they also are sparsely interlayered with the biotite gneiss and form inclusions and layers within the quartz diorite complex.

Biotite Gneiss

MEGASCOPIC APPEARANCE: The biotite gneiss is rather fine-grained and so well foliated that much of it could be called a schist (Pl. 3, fig. 1). It has a uniform appearance over large areas, but in some places, especially where it is intensely migmatized, the quartz and plagioclase are distinctly segregated from the biotite. Rocks with this good segregation of minerals were never seen in sharp contact with the more homogeneous and more schistose rocks, and many outcrops exhibit all gradations between the two. The biotite is deep red brown in hand specimens. Hornblende and epidote are locally abundant, and large crystals of kyanite were found next to a particularly large segregation of quartz (5 cm long). The accessory minerals commonly visible in hand specimens are garnet and muscovite. The marked foliation is due to the abundance of mica, principally biotite. A lineation formed by streaks of biotite in the foliation plane is common.

TREND OF FOLIATION AND LINEATION: The foliation of the biotite gneiss generally strikes northwest and is vertical or dips steeply southwest, but on the south end of Phelps Ridge it strikes generally nearly due east and is vertical or dips steeply south. The lineation is nearly horizontal or plunges south at a low to moderate angle. The only structure in the biotite gneiss that is indicated by present data is a homocline involving rocks about 12,000–17,000 feet thick dipping steeply southwest and lying west of the quartz diorite complex.

Along Phelps Ridge and at Old Gib Mountain the foliation is deflected around small plugs, which are offshoots of a batholith of granodiorite. The batholith caused little bending of the the foliation except north of Red Mountain.

Small-scale swirling of the foliation is common only in places where, as on the south side of Chiwawa Peak, the biotite gneiss is intensely migmatized; good segregation of the biotite and light minerals of the gneiss into well-defined lamellae, producing a more distinct gneissic texture, is also common in these intensely migmatized areas. The migma-

tization of biotite gneiss has made the rock more subject to plastic deformation and has caused metamorphic segregation of its minerals.

ORIGIN: The nature of the material from which the biotite gneiss was derived is obscure, for no original textures or structures were found in this rock. A sedimentary origin is suggested by: (1) the high quartz content of the gneiss (about 45 per cent), (2) thin and very long conformable layers of quartzite interbedded with similarly thin layers of garnet-hornblende schist and garnet-biotite gneiss on the south side of Chiwawa Peak and just east of Red Mountain, (3) several broad zones of garnet-rich biotite gneiss that can be traced several miles, and (4) long, thin layers of hornblende schist, commonly containing garnet, in the gneiss. These widespread intercalations of rocks of probably sedimentary origin make up only a small fraction of the biotite gneiss, but, considering the high quartz content of the gneiss itself, they tend to confirm Waters' belief (1932, p. 616) that the biotite gneiss represents "a series of metamorphosed sediments probably largely of arkosic composition".

PETROGRAPHY: Mineralogical and chemical data for the biotite gneiss are given in Table 5 (sample 7). The chief minerals of the gneiss are biotite, plagioclase (An 29 ± 3),[2] and quartz. The characteristic biotite of the biotite gneiss, though red brown in hand specimen, is reddish orange in thin section. An analysis of this characteristic biotite and its optical and physical properties are given in Table 1. The accessory constituents of the rock are garnet (almandite, a = 11.54 ± 0.02Å), muscovite, apatite, magnetite, and zircon. Hornblende is abundant in some places near intercalations of hornblende schist. Some of the rock contains a little potassium feldspar, which has no crosshatch twinning and is probably orthoclase, but most of the rocks contain none.

The microtexture of the biotite gneiss is crystalloblastic, and grain boundaries are mutually interpenetrating (Fig. 2*A*). In many thin sections, however, the texture is porphyroblastic: the quartz forms a matrix between somewhat elongate and rounded grains of plagioclase. The plagioclase porphyroblasts are unzoned, and many enclose grains of quartz and biotite. The quartz in the matrix forms small interlocking grains which, like the biotite, are comonly drawn out parallel to the foliation and bent around the porphyroblasts to produce flow structure. This fine-grained quartz probably is recrystallized from larger quartz grains in a more even-grained rock, for in some thin sections the many small interlocking grains in an aggregate of quartz will extinguish almost simultaneously under crossed nicols. Perhaps each of these aggregates was once a detrital grain in an arkosic sediment. Waters (1932) does not mention attenuated, interlocking, and clearly recrystallized interstitial grains of quartz, showing flow structure, in his description of the biotite gneisses at the south end of the Entiat Mountains; he describes a widespread cataclasis without much evidence of recrystallization. The flow structures in the Holden area near the Cascade divide may grade southward—*i.e.*, upward—into the cataclastic features that Waters observed in the foothills of the mountains, where the gneiss is less deeply eroded. These facts, taken together, suggest plastic deformation in a deep zone underlying a zone of cataclastic deformation.

Cataclastic features are common throughout the eastern part of the biotite gneiss belt, particularly on Phelps Ridge and Estes Butte, but there they are related to the Entiat fault zone and not to the general and widespread cataclasis described by Waters as occurring farther south. In thin sections the rocks from the eastern part of the biotite gneiss belt are seen to contain many microshears, and the minerals of the rock are broken, bent, and granulated. Most of these cataclastically deformed rocks are altered a little and have a bleached appearance in the field. On Phelps Ridge they are iron-stained on fractures. The alteration and staining are particularly marked near the small plugs that intrude the gneiss on Red Mountain and elsewhere and probably were caused by emanations from the plugs. Thin sections show that the biotite has altered to chlorite and magnetite, and the plagioclase to sericite. The rock contains a little disseminated pyrite, and late secondary epidote, muscovite, and orthoclase have been deposited along microscopic and megascopic shears.

[2] Plagioclase compositions given in this report were determined in thin section, without the universal stage, from maximum extinction angles. For each rock type an average composition for each of several thin sections was obtained by taking the averages of the compositions of several crystals, and the value stated for the rock is the median of these thin-section averages. The range given includes approximately 90 per cent of the individual thin section averages.

Hornblende Schists

MEGASCOPIC APPEARANCE: The hornblende schists are much more varied in composition and texture than the biotite gneiss (Pl. 2, figs. 1, 2). They are well foliated because of a planar arrangement of hornblende, and most of the hornblende needles are subparallel. In much of the fine-grained hornblende schist hornblende is about as abundant as plagioclase and quartz taken together, but in much of it the proportion of light to dark minerals varies greatly. Quartz is absent in some places and even where present is not invariably conspicuous in hand specimens. Gneissic varieties in which the light and dark minerals are more distinctly segregated, are common. Some layers of hornblende schist at the head of the Entiat River contain little or no plagioclase or quartz and are almost black. Some of the rock mapped as hornblende schists is very fine-grained and only vaguely foliated and could more appropriately be called fine-grained amphibolite. Garnet and epidote are the most common accessory minerals visible megascopically, but much of the epidote occurs in crosscutting veinlets or large pods. A little biotite is present in the hornblende schist at the Holden mine and in some of the hornblende schist interlayered with the biotite gneiss.

TABLE 1.—COMPOSITION AND PROPERTIES OF BIOTITE FROM BIOTITE GNEISS

Semiquantitative spectrographic analysis (ppm)		Chemical analysis		Physical and optical properties
B	30	SiO_2	35.49	Color of powder: deep red brown
Ba	100	Al_2O_3	20.88	
Be	.1	Fe_2O_3	1.49	Specific gravity at 20° C: 3.04 ± 0.02
Cr	3	FeO	17.72	
Cu	3	MgO	9.33	$n_\alpha = 1.587$
Sr	1	CaO	.12	$n_\beta = 1.641$
V	10	Na_2O	.30	$n_\gamma = 1.641$
Zr	10	K_2O	8.85	
		TiO_2	.59	$n_\gamma - n_\alpha = 0.054$
		P_2O_5	.06	
		MnO	.45	2V = very small
		H_2O+	2.91	X = colorless
		$H_2O\div$	1.07	Y = moderate reddish orange
		F	1.32	Z = moderate reddish orange
			100.58	
		O for F	−.55	
			100.03	

Simplified formula on the basis of O + OH + F = 12, ignoring minor substitutions:

$$K_{.9}\begin{pmatrix} Mg_{1.0} \\ Fe_{1.1} \\ Al_{.5} \end{pmatrix}\begin{pmatrix} Si_{2.7} \\ \\ Al_{1.3} \end{pmatrix}\begin{pmatrix} O \\ OH \\ F \end{pmatrix}_{12}$$

Locality: 3500 feet southeast of summit of Chiwawa Mountain, Holden quadrangle, Chelan County, Washington

Source rock: garnet-biotite gneiss cut by many dikes of leucocratic quartz diorite

Separation: electromagnetic; material apparently pure except for very small spherical and opaque inclusions in some flakes that did not effect magnetic properties sufficiently to allow these flakes to be removed.

Specific gravity: by pycnometer method, giving 3.037 and 3.044 at 20° C.

Chemical analyst: B. Brunn, Geological Survey of Norway

Spectrographic analyst: K. V. Hazel, U. S. Geological Survey (*See* Table 5 for standard sensitivities.)

ORIGIN: In the hornblende schist, as in the biotite gneiss, metamorphism has obscured the nature of the original material. The thicker and more uniform layers may once have been basic volcanic rocks. Near Red Mountain schist between them is probably also of metasedimentary origin.

PETROGRAPHY: There are so many varieties of hornblende schist that a single chemical composition and mode representing the rock

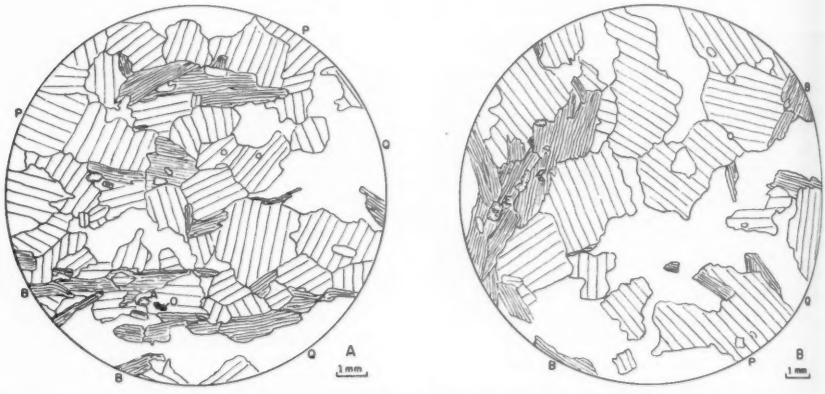

FIGURE 2.—CRYSTALLOBLASTIC MICROTEXTURES OF BIOTITE GNEISS AND BIOTITE-QUARTZ DIORITE GNEISS
A. Biotite gneiss. B. Biotite-quartz diorite gneiss. P = plagioclase, Q = quartz, B = biotite, O = ore A = apatite, E = epidote

abundant garnet and thin conformable beds of quartzite within the hornblende schist suggest that the source material was sedimentary. On the west side of Carne Mountain a thin, poddy layer of marble occurs in the hornblende schist, and near Holden the hornblende schist is in contact on the east with red-weathering finely laminated mica-quartz-diopside schist interbedded with marble. Near this contact the calcareous rocks and the hornblende schist are interbedded in layers only a few inches or a few feet thick, and in the hornblende schist about 500–750 feet west of the contact is a thin, poddy bed of marble which was traced for several miles. Therefore, the hornblende schists near Holden are either metamorphosed sedimentary rocks or are interlayered with sedimentary rocks, but the origin of the great body of hornblende schist west of the marble bed, although believed to be derived from basic volcanic rocks, is less certain.

Banded gneiss consisting of hornblende schist alternating with felsic biotite gneiss occurs in many places on the west side of the complex—for example on the divide between Rock Creek and Box Creek. Some of the felsic layers in the banded rocks were probably arkosic sedimentary beds, and the hornblende is of doubtful significance. Table 5 (sample 1), however, presents such data for a composite sample collected east of Holden Creek. Hornblende, plagioclase, and quartz are present in all thin sections examined. A few rocks consist essentially of hornblende only. The hornblende in all the schists is a common green to bluish-green variety (X = very pale yellow, Y = light green, Z = greenish blue). Common accessories are garnet, epidote, sphene, apatite, and ore; scarcer ones are augite, rutile, zircon, and allanite. Biotite occurs in some of the schist intercalated with biotite gneiss but is generally absent elsewhere.

The plagioclase varies greatly in composition. In most of the specimens it is An48 ± 5, but in rock that is migmatized or interbedded with biotite gneiss, or that contains much biotite, it is more sodic and more variable—An30 ± 10. Zoned crystals are rare, but where present the zoning is normal, and the zones are as anhedral as the grains themselves. Most of the plagioclase is dusted with secondary sericite, and the hornblende and biotite are partly altered to chlorite and magnetite. Such alteration is particularly common along Phelps Ridge.

Almost all the epidote appears to be an alteration product derived from plagioclase and

mafic minerals. Halos, patches, or veins of more sodic plagioclase occur around or near epidote inclusions in plagioclase, and near the epidote-plagioclase boundaries the epidote is associated with abundant sericite, which indicates breakdown of the plagioclase. The epidote associated with chlorite and occurring next to or within hornblende or biotite is an alteration product of the mafic mineral. Subhedral crystals of epidote enclosed in hornblende and not associated with chlorite may indicate simultaneous crystallization of the two minerals, but equilibrium between epidote and plagioclase in these rocks is nowhere clearly shown. Though plagioclase may once have been in equilibrium with epidote, retrograde metamorphism apparently has caused it to be altered to more sodic plagioclase and epidote. Possibly the later retrograde metamorphism was caused by emanations from below; this belief is supported by the widespread occurrence of epidote in small veins and pods.

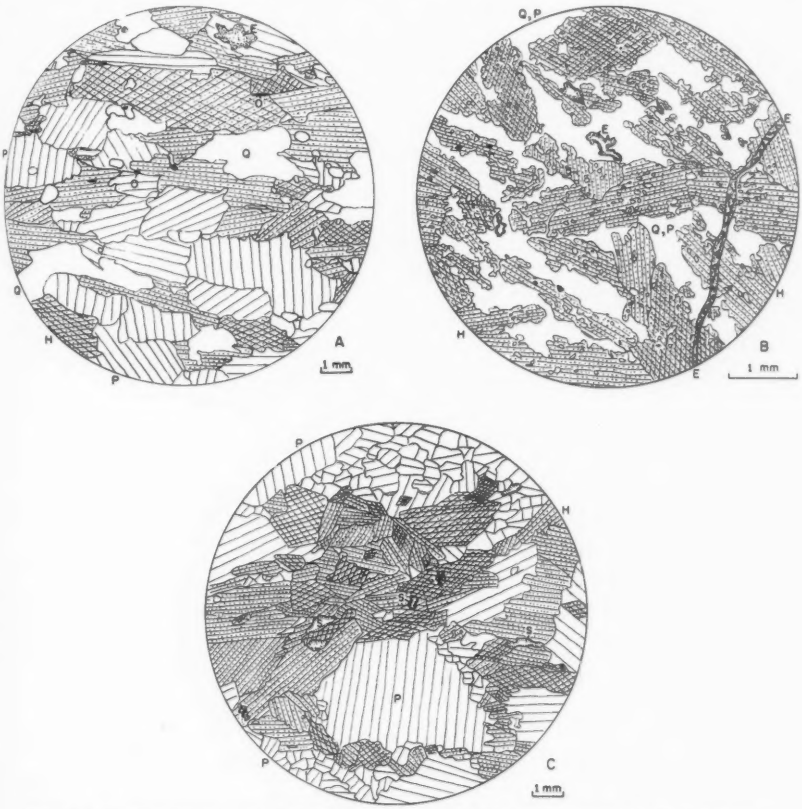

FIGURE 3.—PORPHYROBLASTS AND CRYSTALLOBLASTIC MICROTEXTURES OF HORNBLENDE SCHIST AND GNEISS

A. Hornblende gneiss. B. Hornblende porphyroblasts; plagioclase and quartz granoblastic and fine-grained. C. Plagioclase porphyroblasts and clottedhornblende. P = plagioclase, Q = quartz, H = hornblende, O = ore, E = epidote, S = sphene

The microtextures of the hornblende schists are typically metamorphic (Fig. 3). Most of the rocks consist of a mosaic of straight-sided polygons of quartz and plagioclase (granoblastic texture) enclosing a swarm of parallel, prismatic hornblende crystals, but a xenoblastic texture, in which the grains are ragged and interlocking,

is nearly as common. Many thin sections show mixtures of the two textures—of xenoblastic hornblende, for example, with granoblastic quartz and plagioclase.

Porphyroblasts of hornblende and plagioclase are common; they are anhedral and interlock with the groundmass and nearly everywhere contain many inclusions, mostly round blebs of quartz. The hornblende porphyroblasts grew by the metamorphic agglomeration of smaller grains, as shown by the hornblende-poor halos around many large, anhedral, sieve-textured hornblende porphyroblasts and similar halos around clots of small hornblende grains, only partly organized into single crystals. The plagioclase porphyroblasts are less clearly formed by metamorphic agglomeration: very few are surrounded by halos of hornblende. Many of the clots of feldspar that spot the dark schist in the area between Leroy and Willow creeks are made up of interpenetrating plagioclase crystals crowded with inclusions of hornblende, quartz, and epidote; others are single irregular crystals, also crowded with inclusions. The plagioclase in the clots and porphyroblasts is much more sodic than the plagioclase in most of the hornblende schists—oligoclase, instead of calcic andesine.

The association of hornblende and plagioclase in the hornblende schists is a characteristic of the amphibolite facies of metamorphism. If the metamorphism had been of higher grade, diopside or hypersthene, characteristic of the granulite facies, would have taken the place of hornblende (Turner and Verhoogen, 1951, p. 446). The lack of equilibrium between epidote and plagioclase makes it impossible to fix the metamorphic facies precisely, but the minerals may represent the upper part of the epidote-amphibolite facies, in which plagioclase and hornblende, even without epidote, form a stable assemblage.

Rocks of the Complex

General Statement

Rocks of the complex consist of quartz diorite gneiss, migmatite, leucocratic quartz diorite, and massive quartz diorite, all of which are believed to have evolved during one long and complex period of plutonism. The first three are believed to have formed by granitization of pre-existing rocks, and the massive quartz diorite by anatectic melting of quartz diorite gneiss.

Quartz Diorite Gneiss

GENERAL STATEMENT: The quartz diorite gneisses of the complex are granitized hornblende schists and biotite gneiss; hornblende-quartz diorite gneisses formed from the hornblende schists, and biotite-quartz diorite gneiss formed from the biotite gneiss. Locally the plastic, granitized masses have been mobilized but probably have not moved far. Granitization occurred under conditions of the amphibolite facies.

MEGASCOPIC APPEARANCE: In general the quartz diorite gneisses are distinctive and present no very difficult mapping problems. Although they all have a granitoid appearance, nearly every hand specimen differs from every other in grain size and degree of foliation and of mineral segregation. Marked variations occur within areas only a few square feet in

---

PLATE 2.—POLISHED SPECIMENS AT TRUE SCALE SHOWING TEXTURES OF REPRESENTATIVE ROCK TYPES

Figures 1–4 are of rocks cut perpendicular to foliation; Figure 5 is of a nearly massive rock. Plate illustrates granitization of hornblende schist.

FIGURE 1.—Hornblende schist typical of schists in map unit 1. Note thin seams of plagioclase porphyroblasts. (1 mile north-northwest of Buckskin Mountain)

FIGURE 2.—Hornblende gneiss typical of gneisses in map unit 1. Note coarsening of grain and beginning of segregation. (Phelps Ridge east of Red Mountain)

FIGURE 3.—Hornblende-quartz diorite gneiss typical of map unit 2. Note hornblende beginning to clot. (Half a mile west of Mt. Bonanza)

FIGURE 4.—Hornblende-quartz diorite gneiss with inclusions of hornblende schist typical of map unit 4. Note basified borders and wisps. (1½ miles southwest of Buckskin Mountain)

FIGURE 5.—Hornblende-quartz diorite gneiss typical of more massive rocks in map unit 3. Note splotchy clots and porphyroblasts of hornblende and some euhedral hornblende crystals in lower right corner. (Three quarters of a mile east of Seven-Fingered Jack)

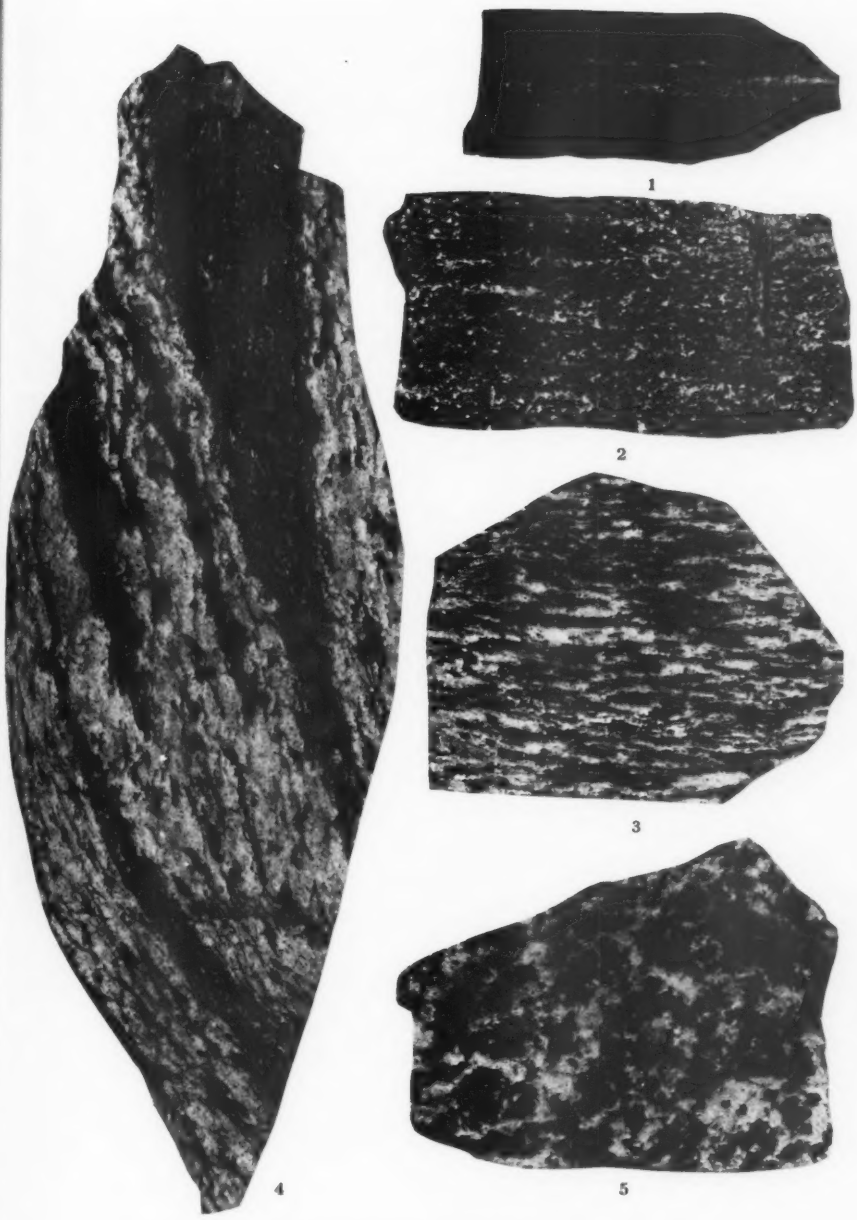

POLISHED SPECIMENS AT TRUE SCALE SHOWING TEXTURES OF REPRESENTATIVE ROCK TYPES

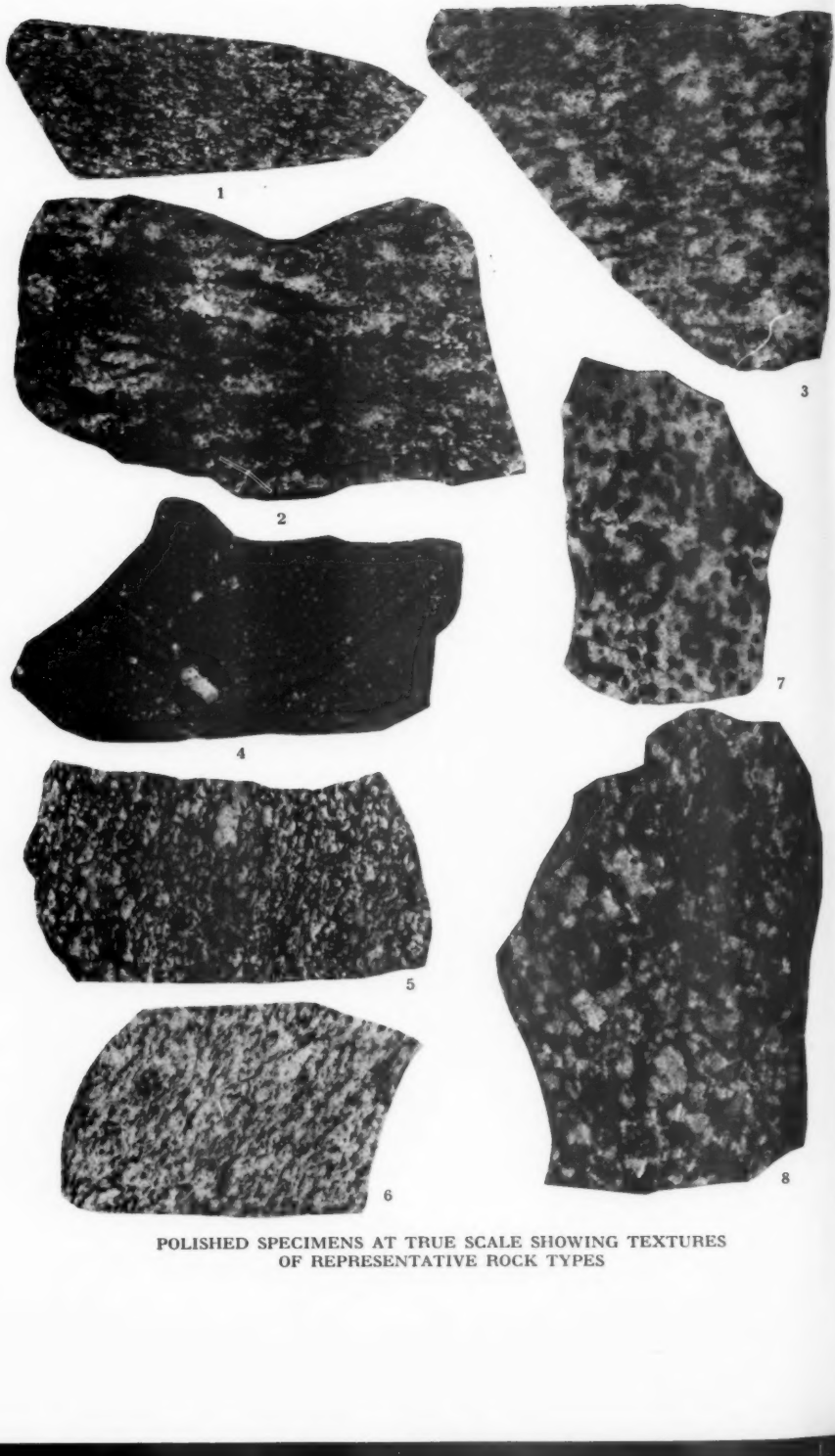

POLISHED SPECIMENS AT TRUE SCALE SHOWING TEXTURES OF REPRESENTATIVE ROCK TYPES

extent, and different rocks are so intimately mixed that they cannot be separately mapped.

The principal varieties of quartz diorite gneiss are units 2, 3, 4, and 8 on Plate 1,[3] and the distinguishing megascopic features of each are as follows:

(2) Well-foliated hornblende-quartz diorite gneiss (Pl. 2, fig. 3). Quartz is hard to detect in hand specimen. Hornblende forms long, black strings of small prisms, which give the rock a strongly gneissic appearance and a tendency to split along the foliation. This is the most nearly uniform variety of quartz diorite gneiss and is apparently a product of moderate granitization of the hornblende schist.

(3) Granitoid hornblende-quartz diorite gneiss (Pl. 2, fig. 5). In this rock hornblende forms irregular crystals and splotches, and foliation is not well developed, so that the rock looks rather igneous.

(4) Hornblende-quartz diorite augen gneiss (Pl. 2, fig. 4). This rock is characterized by augen of quartz as much as a centimeter long; quartz that is not segregated into augen forms long, narrow streaks. Hornblende occurs in short wisps. Marked segregation of the minerals makes the rocks appear rather coarse-grained; microscopic examination, however, shows them to be rather fine-grained.

(8) Biotite-quartz diorite gneiss (Pl. 3, figs. 2, 3). Biotite occurs in small scattered flakes, commonly segregated in wisps and clots. This rock is finer-grained than the hornblende-quartz diorite gneisses. Some of it is comparatively homogeneous and schistose and closely resembles the biotite gneiss west of the complex (Pl. 3, fig. 1), which is considered the parent rock. A common accessory is garnet, which occurs on the north side of Leroy Creek in crystals as much as 1 cm in diameter.

FOLIATION: A well-developed characteristic of nearly all the quartz diorite gneiss is a planar parallelism of hornblende and biotite. In a few places hornblende crystals or mineral streaks show lineation, but it is rarely distinct. The hornblende-quartz diorite gneisses commonly contain smears of hornblende-rich material parallel to the foliation whose length ranges from less than an inch to several feet. Foliation strikes, in general, north to northwest. Notable exceptions are in the upper Phelps Creek area, just south of Holden Lake, and on the south side of the Entiat River, where it strikes northeast and east.

Plate 1 shows the regular foliation trends but not the small-scale swirling of the foliation, which is evident even in small outcrops

[3] Throughout this paper, unit numbers identify rock types shown in Plate 1 and/or analyses given in Table 5.

PLATE 3.—POLISHED SPECIMENS AT TRUE SCALE SHOWING TEXTURES OF REPRESENTATIVE ROCK TYPES

Figures 1–3, 5, and 6 are of rocks cut perpendicular to foliation; Figures 4, 7, and 8 are of nearly massive rocks. Figures 1–3 illustrate granitization of biotite gneiss; Figures 7 and 8 illustrate massive and igneous rocks of the complex.

FIGURE 1.—Fine-grained schistose biotite gneiss. Typical of rocks of map unit 7 that are not intensely migmatized. (Rock Creek at 3100 feet)

FIGURE 2.—Well-segregated biotite gneiss. Texture characteristic of migmatized rocks of map unit 7. Texture also typical of the biotite-quartz diorite gneiss of map unit 8. (A quarter of a mile southeast of Chiwawa Mountain)

FIGURE 3.—Biotite-quartz diorite gneiss. Typical of rocks and dikes of map unit 8 formed from mobilized material. (Half a mile southwest of Seven Fingered Jack)

FIGURE 4.—Fine-grained hornblende-biotite quartz diorite—early dike phase of stock on Buckskin Mountain. Note euhedral plagioclase phenocrysts of this igneous rock. (Holden mine)

FIGURE 5.—Biotite-quartz diorite gneiss of stock on Buckskin Mountain. Note plagioclase porphyroclasts. (Half a mile south of Buckskin Mountain)

FIGURE 6.—Foliated biotite-quartz monzonite—late dike phase of stock on Buckskin Mountain. (Holden mine)

FIGURE 7.—Biotite-hornblende-quartz diorite from sill north of Ice Lakes which is map unit 5. Note stubby euhedral prisms of hornblende similar to those in Figure 5 of Plate 2. (Three quarters of a mile south of Hart Lake)

FIGURE 8.—Hornblende-biotite-quartz diorite from sill east of Rock Creek which is map unit 6. Note subhedral plagioclase (white) and interstitial quartz (gray). (1¼ miles northeast of Carne Mountain)

of much of the gneiss. Swirling is especially prevalent in the biotite-quartz diorite gneiss (unit 8) and is nearly lacking in the well-foliated hornblende-quartz diorite gneiss (unit 2), but except for these limitations the swirled and unswirled rocks have no systematic distribution and blend imperceptibly into each other. Over considerable areas no average strike and dip can be taken. I interpret the swirling as due to plastic flowage of solid or nearly solid masses that differ in plasticity from place to place. Had much liquid been present, the suspended crystals would show the more regular flow structure of igneous intrusions in which contortion is confined to irregularities along contacts and to protoclastic phases.

VAGUELY FOLIATED PHASES: Areas of vaguely foliated to nearly massive quartz diorite gneiss occur at random in a few places, as do the areas of swirled foliation. One of the quartz diorite gneisses, the well-foliated hornblende-quartz diorite gneiss (unit 2), lacks both vaguely foliated and swirled phases. In the other quartz diorite gneisses the more massive rocks form bodies from a few inches to many hundreds of feet across, of no particular shape, and they grade into the more gneissic rocks. Some small-scale structures indicate that the massive rock is younger than the gneiss, and that its formation is associated with mobilization of the rocks. Coarser and nearly massive streaks of quartz diorite gneiss parallel to the foliation enclose ghosts of the finer-grained gneiss (Pl. 5, fig. 5). The biotite-quartz diorite gneiss is cut by a dike of the same rock. The dike is nearly massive in some places but elsewhere shows a marked flow structure (Pl. 6, fig. 2); mobilization of the gneiss is indicated. Other indications of mobilization of the biotite-quartz diorite gneiss are abundant in migmatites containing replacement bodies of leucocratic quartz diorite. The vaguely foliated gneisses that occur in such spotty fashion cannot be relics of an original massive rock that have survived penetrative deformation or products of uniform granitization or uniform fusion. The streaks of massive rocks parallel to the foliation and the foliation of the quartz diorite gneisses, which is largely conformable to the foliation of rocks of the regional terrain, indicate the importance of the original foliation and of differential movement parallel to the foliation in controlling granitization of preexisting rocks to quartz diorite gneiss. The mixture of swirled gneiss and vaguely foliated gneiss probably resulted from differential granitization combined with differential mobilization.

FINER-GRAINED GNEISS: Gneiss that is somewhat finer-grained and less heterogeneous than the more common types and grades into them occurs in two northwest-trending zones. A zone of finer-grained gneiss in unit 3 extends from the east face of Seven Fingered Jack through the smaller Ice Lake, and another extends all along the east edge of unit 4, *i.e.*, along the east contact of the quartz diorite complex. Smaller zones of fine-grained rocks were seen in many other places throughout units 3 and 4. The fine-grained rocks look as if they had resulted from differential movements, for many enclose large crystals or clots of hornblende which have smears of small crystals (including biotite in some places) tailing out from them. Thin sections show this streaking out of mafic minerals, but they do not show any fragmental textures. I interpret the finer-grained zones as being due to concentrated differential movement, which contrasts with movement associated with the differential mobilization that caused widespread swirling of the foliation.

SHEAR FOLIATION: In the fault zone bordering the east side of the complex the rocks are so intimately sheared over such a broad area (2000 feet wide in several places) that their original foliation is obliterated. Vertical masses of mylonite from a fraction of an inch to many yards wide are common throughout the fault zone, as are smeared-out crystals of hornblende and biotite; the biotite and hornblende are largely altered to chlorite.

ANOMALOUS FOLIATION TRENDS: Foliation trends deviate markedly in some places from the prevailing northwesterly direction, and some sharp bends occur in the foliation. These anomalies are probably caused by an upwelling of plastic gneiss, particularly the biotite-quartz diorite gneiss (unit 8) and hornblende-quartz diorite augen gneiss (unit 4), which are the two most felsic quartz diorite gneisses. The best example of anomalous trend is in the biotite-quartz diorite gneiss (unit 8) about a mile northwest of Seven Fingered Jack, where its foliation closely follows a sharply curving contact of general northeasterly trend between this rock and the granitoid hornblende-quartz diorite gneiss (unit 4). The foliation here outlines a vague domal structure in rocks that strike northeast. This structure is probably due to a diapiric upwelling of more plastic and felsic biotite-quartz diorite gneiss. In the Dumbell Mountain area the foliation is hap-

hazard and suggests an irregular up-welling. Another area of possible upwelling is in the hornblende-quartz diorite augen gneiss (unit 4) on the east side of Spectacle Buttes, where the foliation delineates a domal structure. Here the foliation of this gneiss is comformable for short distances to the irregular western contact with hornblende schists, and the rock is more massive and the foliation more swirled in this area than in most other places. In the area between the summit of Copper Peak and Bonanza Peak the strike of some contacts of the quartz diorite gneiss and of some of the foliation changes from northerly to northwesterly. The best examples are near the summit of Copper Peak and on the spur of Bonanza Peak between Holden Creek and Railroad Creek. The general effect of the changes in strike is an eastward bulging both of contacts and of foliation trends. This bulging might be due to any one of the following:

(1) Preservation of a precomplex flexure in hornblende schists that have been granitized to quartz diorites.

(2) Pushing eastward by upwelling of a diapir of biotite-quartz diorite gneiss (unit 8) northwest of Seven Fingered Jack.

(3) Pushing westward by upwelling of a diapir of hornblende-quartz diorite augen gneiss (unit 4) between Copper Peak and Buckskin Mountain. (A septum of hornblende schist appears to have been wedged aside in the area a mile northeast of the summit of Copper Peak.)

(4) Pushing by later intrusions, particularly by the stock near Buckskin Mountain and by the granodiorite batholith exposed at the north end of the Entiat Mountains, which probably underlies much of the mapped area.

CONTACT RELATIONS BETWEEN QUARTZ DIORITE GNEISSES: The relations between two kinds of quartz diorite gneiss can best be observed on the south side of Bonanza Peak, where the comparatively granitoid and massive rock (unit 3) grades through a zone many hundreds of feet wide into the less granitoid, well-foliated gneiss (unit 2). This zone is only approximately located in Plate 1. The relations here indicate that the more granitoid rock is a more extensivey granitized and more plastic equivalent of the other. In the contact zone, gneiss (unit 2), which has distinct and unswirled foliation, grades into less distinctly foliated gneiss that contains some nearly massive, coarser-grained rock locally showing swirled foliation and a few vague streaks of darker gneiss. Parts of the gradational zone are only a few tens of feet wide. In one place the more massive rock, which has a swirled foliation, cuts sharply across the foliation of the more gneissic rock and is clearly the younger. A mobilized portion of the more massive gneiss (unit 3) appears to have intruded the better foliated gneiss (unit 2). The movement must have been slight, and the clear-cut intrusive relations must be local, for on Bonanza Peak and farther south the contact is irregular, and the foliation in the granitoid gneiss (unit 3) does not follow the irregularities, as would be expected if this rock were to any large extent intrusive; its foliation passes undisturbed across embayments, which indicates that it was formed in place. Other observations at the contacts between the different kinds of quartz diorite gneiss did not give evidence of relative age as clearly as that described above. At the north end of the biotite-quartz diorite gneiss (unit 8), however, the contact is abrupt, and the foliation in the gneiss curves with the contact, which indicates that this rock was intruded into the adjacent hornblende-quartz diorite gneiss; just west of Holden Creek, on the west contact of gneiss (unit 4), there is a zone of intricately swirled gneiss 200–400 feet wide, which indicates that some movement occurred at the contact but does not show the relative ages of the rocks. On the west face of Copper Peak, however, some dikelike masses of the relatively granitoid and massive gneiss (unit 3) extend into foliated gneiss (unit 2), which indicates that the granitoid gneiss is younger.

RELATIONS TO PRECOMPLEX ROCKS: The nearly ubiquitous parallelism of inclusions, the long, thin layers of older rocks in the quartz-diorite gneisses, and their many conformable contacts are most easily explained by considering that these gneisses were derived from pre-complex rocks by granitization accompanied by only minor mobilization. It is difficult to explain these features if the quartz diorite gneisses are intrusions.[4] However, the critical ends of the outcrop of the gneissic complex—where a volume increase, if it has occurred, might be clearly demonstrated by wedging aside of country rock—have not been mapped. Noble (1952) pointed out how difficult it is to prove volume

[4] Intrusion implies that host rocks have moved aside to make room for a granitoid rock mass. This process includes the growth of petroblastic granitoid masses by secretion of material in a place once occupied by the host rock, as well as the emplacement of a diapir or a magma.

increase around intrusions in areas of steeply dipping schistose rocks. For these reasons one must be particularly careful in interpreting the evidence for an origin by granitization.

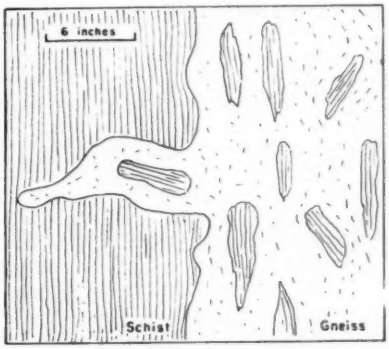

FIGURE 4.—CONTACT OF HORNBLENDE SCHIST AND QUARTZ DIORITE GNEISS (UNIT 4)

Dike interpreted as formed by intrusion of the mobilized replacement breccia on the right. From a notebook sketch, north side of Entiat River

A good picture of the general structure of the complex can be obtained by greatly enlarging Figure 4 of Plate 2. The conformable contacts are characterized by alternating layers of quartz diorite gneiss and hornblende schist. Contacts between individual layers are sharp. Sharp, conformable contacts without interlayering also occur. A gradational contact between hornblende-quartz diorite augen gneiss (unit 4) and hornblende schist was observed in the headwaters of Copper Creek; hornblende schist grades into hornblende gneiss and into quartz diorite augen gneiss in a zone several hundred feet wide; the grain size and the proportion of felsic minerals increase in the hornblende schist as the augen gneiss is approached. In the more common interlayered contacts layers of hornblende schist from a few inches to many yards thick generally alternate with similar thicknesses of quartz diorite gneiss, though in a few places the gneiss layers are much thicker. Some of the schist layers have dark, basified margins; others consist almost wholly of hornblende and contain practically no light-colored minerals, as if they had been made more basic throughout. Some hornblende schist layers can be traced until they gradually fray out into the quartz diorite gneiss. At many places on the contacts of the biotite-quartz diorite gneiss—for example on the divide between Box Creek and Rock Creek—the layers of schist and gneiss are only a few inches thick, so that the outcrop is strongly banded; it is easy in such places to confuse the biotite-quartz diorite gneiss layers with replacement sills of leucocratic quartz diorite, which are abundant in the hornblende schists and also form strongly banded rocks (Pl. 7, figs. 3, 4). Tabular dark inclusions[5] of hornblende schist and hornblende gneiss are common and widely distributed in the hornblende-quartz diorite gneisses. The inclusions range from sharply bounded streaks and lenses to streamlined, elongate bodies only a little darker and finer-grained than the surrounding gneiss. The borders of some small inclusions (*see* Pl. 2, fig. 4) have been made more mafic. Other inclusions, particularly those occurring in small clots and wisps, are nearly pure hornblende and are probably remnants of hornblende schist inclusions that have been made more mafic. Even where the enclosing gneiss is swirled, most of the tabular inclusions follow the contortions, which shows that they were incorporated before the rock was deformed. In the well-foliated hornblende-quartz diorite gneiss (unit 2) the inclusions form very long, thin layers, a few of which can be traced until they fray out into the gneiss. Many extremely long long and thin inclusions occur in the other hornblende-quartz diorite gneisses; one in the hornblende-quartz diorite augen gneiss (unit 4) on Spectacle Buttes is ½–1 inch by 40 feet. All inclusions in the hornblende-quartz diorite gneisses consist of hornblende schist or hornblende gneiss that has escaped transformation to hornblende-quartz diorite gneiss, or some ghost apparently related to these rocks; they are not foreign inclusions, as might be expected, at least in a few places, if the rocks were intrusions.

The biotite-quartz diorite gneiss (unit 8) contains inclusions of biotite gneiss as well as of hornblende schist and gneiss. The inclusions of hornblende schist and gneiss are almost everywhere in the form of long, thin layers that have sharp contacts with the enclosing gneiss; in a few places, however, the inclusions fray out into the gneiss. These layers were once interbedded with biotite gneiss—a feature common in the biotite gneiss west of the complex—which has been granitized to biotite-quartz diorite gneiss. The inclusions

[5] In this report inclusion is a descriptive term without implication of the origin of the rock that contains the inclusion.

of biotite gneiss, bodies that have escaped granitization, are ghostlike wisps and streaks grading into the biotite-quartz diorite gneiss. Larger irregular masses of biotite gneiss, also, grade into biotite-quartz diorite gneiss through gneisses intermediate in texture between those shown in Figures 1 and 2 of Plate 3.

Though the most common type of inclusion in the quartz diorite gneisses is long and thin and conformable with the foliation of the enclosing gneiss, some unoriented, angular, and sharply bounded, dark inclusions occur. These unoriented inclusions, indicative of flowage, are generally in the swirled phases of the quartz diorite gneisses. Some of them are derived from hornblende schist layers that have broken apart during mobilization of the more plastic matrix. Unoriented inclusions are fairly common in the hornblende-quartz diorite augen gneiss (unit 4) adjacent to the septum of hornblende schist on the north side of the Entiat River; here, too, a dike of the hornblende-quartz diorite augen gneiss containing unoriented inclusions cuts a septum of hornblende schist. (*See* Fig. 4.) These facts might be interpreted as indicating that the gneiss was once an igneous intrusive rock, later metamorphosed; if that is true, the igneous and perhaps massive texture in the matrix of the dike has been destroyed and a gneiss formed without affecting the sharply bounded inclusions. I believe that unoriented inclusions in swirled quartz diorite gneiss (the elongate inclusions usually follow the swirling) may be due to mobilization of breccias whose matrices formed by granitization, *e.g.*, rheomorphic

TABLE 2.—COMPOSITION AND PROPERTIES OF BIOTITE FROM BIOTITE-QUARTZ DIORITE GNEISS

Semiquantitative spectrographic analysis (ppm)		Chemical analysis		Physical and optical properties
B	3	SiO_2	35.48	Color in powder: dark brown to greenish black
Ba	100	Al_2O_3	18.15	
Cr	.1	Fe_2O_3	3.71	Specific gravity at 20°C: 3.01 ± 0.02
Cu	10	FeO	16.39	
Sr	3	MgO	9.72	$N_\alpha = 1.589$
V	10	CaO	.76	$N_\beta = 1.635$
Zr	10	Na_2O	.32	$N_\gamma = 1.635$
		K_2O	7.68	
		TiO_2	2.25	$N_\gamma - N_\alpha = 0.046$
		P_2O_5	< .01	
		MnO	.20	2V = very small
		H_2O+	4.33	X = pale greenish yellow
		$H_2O\div$	.42	Y = light olive brown
		F	.97	Z = light olive brown
			100.38	
		O for F	−.41	
			99.97	

Simplified formula on basis of O + OH + F = 12, ignoring minor substitutions:

$$K_{.7}\begin{pmatrix}Mg_{1.1}\\Fe_{1.0}\\Al_{.3}\end{pmatrix}\begin{pmatrix}Si_{2.7}\\\\Al_{1.3}\end{pmatrix}\begin{pmatrix}O\\OH\\F\end{pmatrix}_{12}$$

Locality: 2000 feet southwest of summit of Seven-Fingered Jack, Holden quadrangle, Chelan County, Washington

Source rock: biotite-quartz diorite gneiss showing signs of mobilization

Separation: electromagnetic

Specific gravity: by pycnometer method, giving 2.999 and 3.026 at 20° C.

Chemical analyst: B. Brunn, Geological Survey of Norway.

Spectrographic analyst: K. V. Hazel, U. S. Geological Survey (*See* Table 5 for standard sensitivities.)

breccias (Goodspeed, 1953), and that the dike just described may be an intrusion of such a mobilized breccia, similar to the ones shown in sharply crosscutting late veins. The quartz content of the gneisses ranges from 11 to 39 per cent.

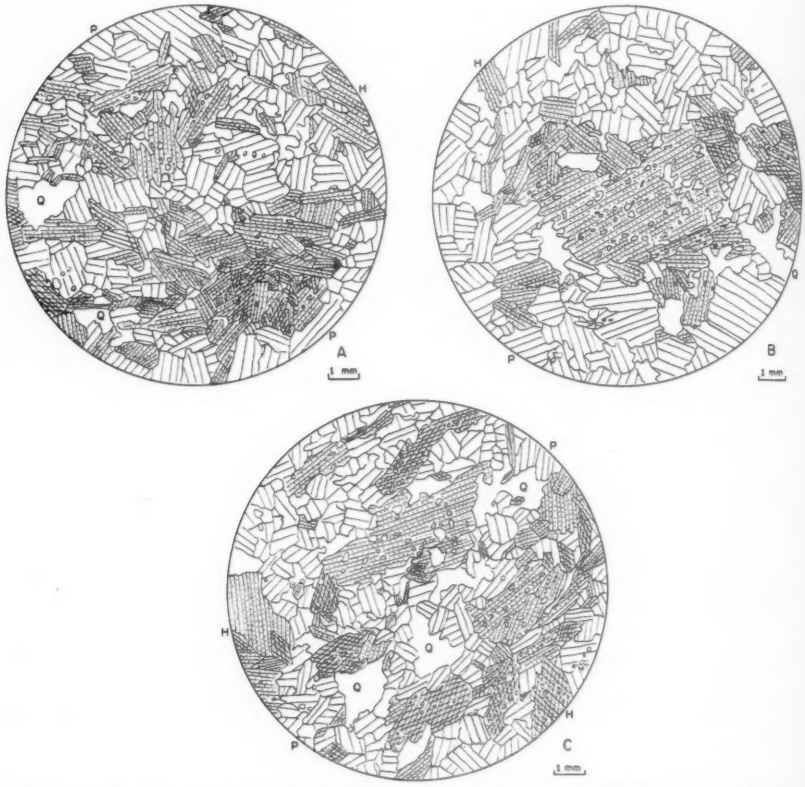

FIGURE 5.—CRYSTALLOGRAPHIC MICROTEXTURES AND PORPHYROBLASTS OF HORNBLENDE-QUARTZ DIORITE GNEISS

A. Clots of hornblende not organized into single crystals. B. Hornblende porphyroblasts, anhedral. C. Hornblende porphyroblasts, anhedral and subhedral. Texture of all three granoblastic, but some have interlocking borders. P = plagioclase, Q = quartz, H = hornblende

Figures 5 and 6 of Plate 7. The unoriented, angular inclusions, like the swirled foliation, may be another indication that the quartz diorite gneiss was locally mobilized.

PETROGRAPHY: Details of the mineralogy and composition of the quartz diorite gneisses are given in Table 5 for comparison with similar data relating to the hornblende schist and biotite gneisses. The plagioclase in the three hornblende-quartz diorite gneisses is calcic andesine, whereas that in the biotite-quartz diorite gneiss is oligoclase. Potassium feldspar is nearly absent, except in a few

The microtexture of the biotite-quartz diorite gneiss (Fig. 2B) is crystalloblastic, and the plagioclase, except for vague normal zoning in a few crystals, is characteristically anhedral and unzoned. The rocks are somewhat coarser-grained and have a better segregation of light minerals and biotite than does the Swakane biotite gneiss parent rock.

The characteristic olive-brown biotite of the biotite-quartz diorite gneiss, strikingly different in color from the orange-red biotite of the parent biotite gneiss (*see* Table 1), has been analyzed (Table 2). Color is probably not

a good indicator of the chemical composition of biotite (Hall, 1941, p. 32). It is peculiar, however, that the biotite in the biotite gneiss is reddish orange when it contains so little titanium and is not particularly rich in magnesium; in the absence of considerable magnesium, the reddish color should indicate that the biotite is rich in titanium (Hall, 1941, p. 30). Hall's data indicate that the olive-brown color of the biotite in the biotite-quartz diorite gneiss is not anomalous. Comparison of the biotite analyses of Tables 1 and 2 shows that the change to the biotite during granitization has not been profound.

The microtextures of the hornblende-quartz diorite gneisses are metamorphic (Figs. 5, 6, 7); in the more massive rocks (Fig. 5*B*) the texture is generally more interlocking (xenoblastic) than in the less massive rocks (Fig. 5*A*), which have a granoblastic texture suggesting mosaic. Some show textural features that could be igneous (Figs. 6*A*, 6*B*, 7*C*). One of the most significant features of the microtextures of the hornblende-quartz diorite gneiss is that the hornblende shows evidence of having recrystallized from small, anhedral grains in the hornblende schists to much larger, subhedral, igneous-appearing

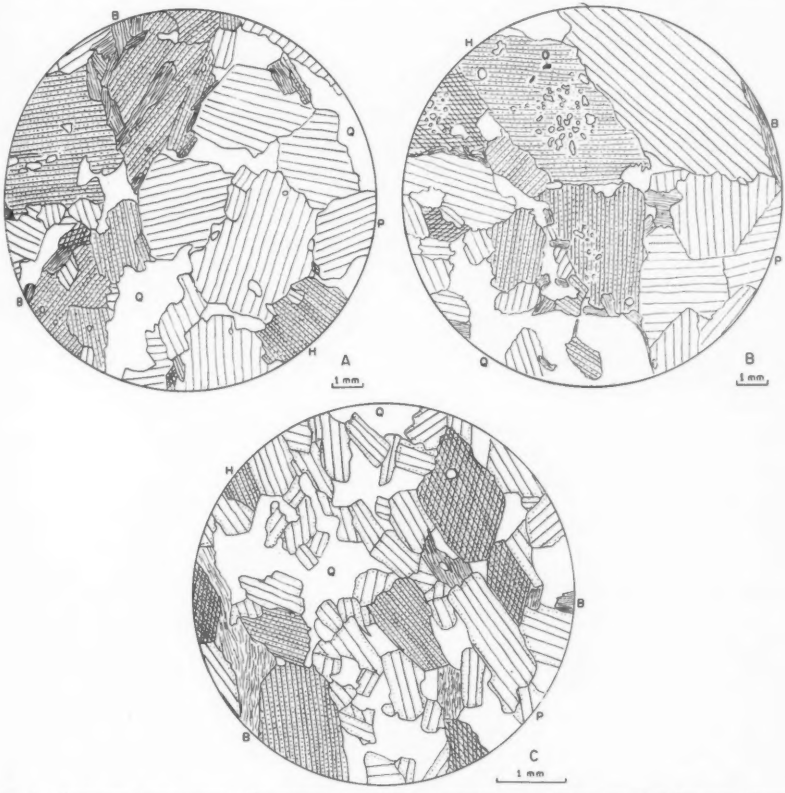

FIGURE 6.—IGNEOUS-APPEARING FEATURES IN MICROTEXTURES OF HORNBLENDE-QUARTZ DIORITE GNEISS AND MASSIVE QUARTZ DIORITE

A. Quartz, mostly interstitial, and plagioclase showing suggestions of crystal form in hornblende-quartz diorite gneiss. B. Hornblende crystal with inclusions in core and inclusion-free rim in hornblende-quartz diorite gneiss. C. Hypidiomorphic granular texture and flow structure of massive quartz diorite. P = plagioclase, Q = quartz, B = biotite, O = ore, H = hornblende. Dots around plagioclase crystals emphasize crystal form, not zoning.

crystals in some of the gneisses. Some of the hornblende schist contains sieve-textured hornblende porphyroblasts, and clots of small blende characteristic of most of the gneiss and schist. The hornblende porphyroblasts in the seams of the recrystallization migma-

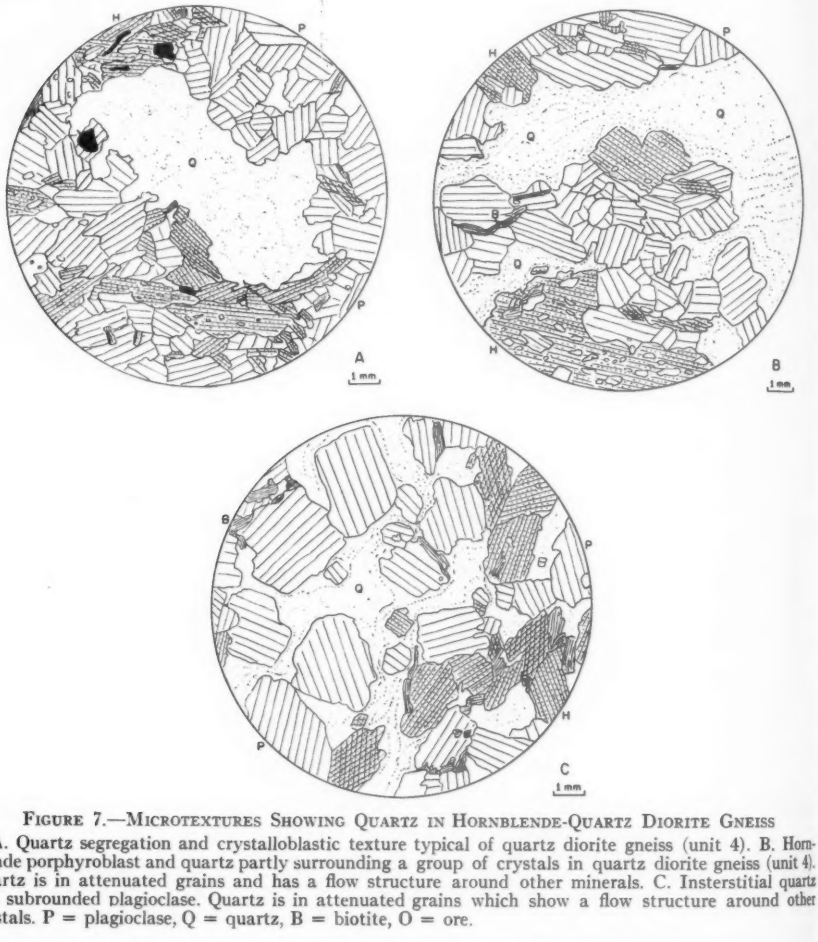

FIGURE 7.—MICROTEXTURES SHOWING QUARTZ IN HORNBLENDE-QUARTZ DIORITE GNEISS

A. Quartz segregation and crystalloblastic texture typical of quartz diorite gneiss (unit 4). B. Hornblende porphyroblast and quartz partly surrounding a group of crystals in quartz diorite gneiss (unit 4). Quartz is in attenuated grains and has a flow structure around other minerals. C. Insterstitial quartz and subrounded plagioclase. Quartz is in attenuated grains which show a flow structure around other crystals. P = plagioclase, Q = quartz, B = biotite, O = ore.

hornblende grains that have not amalgamated into single porphyroblasts; the same features are common in the hornblende-quartz diorite gneiss. (*Compare* Figs. 5*A* and 5*B* with 3*B* and 3*C*.) Figure 5*C* shows poikilitic hornblende in the hornblende-quartz diorite gneiss that has a definite suggestion of crystal form, and Figure 6*B* shows poikilitic cores surrounded by inclusion-free rims. These rims and many of the better formed hornblende crystals are green to brownish green rather than green to bluish green like the hornblende (Pl. 4, figs. 1, 2) are also subhedral to euhedral and brownish. The recrystallization of hornblende to more and more igneous-appearing crystals has occurred in the following sequence: anhedral grains (Fig. 3*A*); clots of hornblende (Figs. 3*C*, 5*A*); large sieve-textured crystals (Figs. 3*B*, 5*B*); subhedral sieve-textured crystals (Fig. 5*C*); subhedral to euhedral inclusion-free crystals (Fig. 6*B*, Pl. 4, fig. 2). Where the material that must move to effect these changes is highly mobile, as in the recrystallization migmatite, the horn-

blende in the schist has recrystallized directly into subhedral, inclusion-free crystals without passing through intermediate stages; where the material is less mobile, sieve-textured crystals develop, and where it is least mobile only clots of hornblende develop.

Recrystallization of plagioclase in hornblende-quartz diorite gneisses follows a similar course. The anhedral, unzoned grains (Fig. 5) have grown larger in schist (Figs. 3*A*, *C*), and in some of the hornblende-quartz diorite gneisses these show a suggestion of crystal form (Figs. 6*A*, 7*C*). The plagioclase porphyroblasts, unlike those of hornblende, are rarely crowded with inclusions. The better formed crystals have some irregular normal zoning, but in most grains zoning is absent.

Quartz shows no crystal form in any of the quartz diorite gneisses; it forms anhedral and interlocking crystals. In the hornblende-quartz diorite augen gneiss (unit 4), however, the quartz is segregated into large clots and wisps (Figs. 7*A*, *B*). The quartz in some of the gneisses is slightly or decidedly interstitial. (*See* Figs. 6*A*, 7*C*.)

These metamorphic changes—hornblende and plagioclase attaining better crystal form, and quartz segregating and becoming interstitial—produce metamorphic rocks whose texture looks more or less igneous. Such igneous features are most abundant near the sills of massive quartz diorite along the Entiat divide.

Thin sections reveal flow textures in the quartz of the quartz diorite gneisses, probably as a result of mobilization at a certain stage of granitization; microtextures indicate that this stage corresponds to the retreat of quartz to interstitial positions, where it formed a lubricant between the grains of other minerals. Figure 7*C* shows the typical microtexture of a rock having flow structure. The quartz occurs in a mass of small, interlocking, attenuated grains winding around the subrounded plagioclase crystals, which appear to have rolled in this matrix. In some rocks (Fig. 7*B*) whole crystal groups are surrounded or cut by flow-textured quartz. The quartz in some of these rocks appears to have behaved as a liquid, for it fills minute fractures in plagioclase crystals; it probably entered such fractures by a replacement process or by infiltration into the fracture as it opened, rather than by flowing into the fracture. The general lack of bent twin lamellae in plagioclase indicates that the deformation responsible for the flow structure of quartz was essentially plastic rather than cataclastic. Although quartz appears to have flowed in the plastically deformed quartz diorite gneisses, and many of the plagioclase crystals appear to have rolled in this plastic matrix, the hornblende and biotite crystals are ragged and dragged out, so that somewhat finer-grained and more foliated gneiss is formed by the plastic deformation. The layers of such fine-grained gneiss form zones that are probably due to plastic differential movement between thicker layers of hornblende-quartz diorite gneiss. Since one of these zones occurs along the east contact of the complex, extending all along the east part of hornblende-quartz diorite augen gneiss (unit 4), part of the complex probably moved with respect to that contact.

The association of plagioclase with common green hornblende in the hornblende-quartz diorite gneisses indicates that granitization took place under the same conditions as those of the amphibolite facies. The brownish-green hornblende that occurs sporadically in the hornblende-quartz diorite gneiss (Fig. 6*B*) and in the recrystallization migmatite (Pl. 4, figs. 1, 2) might indicate that granitization took place in the granulite facies (Eskola, 1952, p. 154). The random distribution of this brownish-green hornblende suggests, however, that emanations rather than higher temperature and pressure caused its formation.

ORIGIN: Conceivably the quartz diorite gneisses were once granitoid igneous rocks that have been recrystallized and are now metamorphic rocks. As has already been pointed out, if these gneisses were recrystallized from massive rocks with hypidiomorphic granular igneous textures, this texture in the matrix of some breccias has been destroyed without affecting the inclusions; this seems unlikely. The strongest argument against the view that any of the quartz diorite gneisses are metamorphosed igneous rocks is this: wherever these rocks have what look like igneous features—such as swirled foliation, massive phases, subhedral inclusion-free crystals, and breccias—and the age relation of these igneouslike features to metamorphic features has been determined, the metamorphic features are the older.

If the quartz diorite gneisses were formed by metamorphism of intrusive sills of magmatic quartz diorite, conformable foliation, septa, elongate inclusions, and lack of contact breccias could be expected. In the Holden quadrangle the wedging aside of older rocks, which would have occurred if the sills were intru-

sions, cannot be demonstrated. Additional mapping along the strike of the complex is needed to help settle the space problem, which will be difficult or impossible to solve in an area of steeply dipping schistose rocks (Noble, 1952). It is difficult to believe that, if the quartz diorite gneisses were originally intrusions, the space problem was alleviated by assimilation because no zones of contaminatin occur along the contacts.

Massive Quartz Diorite

GENERAL STATEMENT: The ultimate products of granitization of hornblende schists were hornblende-quartz diorite gneisses, and in places these gneisses were melted and partly mobilized, forming massive, igneous quartz diorite. Although the biotite gneiss was granitized, it did not evolve into a magma. Fusion and intrusion were localized in long, narrow zones along the Entiat Mountain divide and in a narrow zone on the west border of the complex. In a few places the magmatic rocks are gneissic as a result of flow and later shearing.

MEGASCOPIC APPEARANCE: The massive quartz diorites are homogeneous rocks that have a typically igneous appearance (Pl. 3, figs. 7, 8). The long sill extending northward from Ice Lakes (unit 5) is a medium-grained biotite-hornblende-quartz diorite, characterized by stubby, euhedral prisms of hornblende and sparse flakes of biotite. The southern extension of this sill, on the east side of Rock Creek (unit 6), contains more biotite and less well-formed hornblende crystals, and in a few places it contains some orthoclase. In small areas near Mt. Maude and Mt. Fernow the rock contains subhedral hornblende crystals up to half an inch long and clots of hornblende; in one place these clots and large crystals of hornblende are part of a quartz diorite that has a swarm of hornblende schist inclusions in it. The massive quartz diorite contains local fine-grained and gneissic phases. The sill along the west border of the complex is so badly sheared that its original texture is destroyed; it consists largely of a gneiss containing streaks of small hornblende crystals that stream from larger subhedral crystals. Despite the shearing, however, the rock of the sill has a homogeneous appearance which distinguishes it from the quartz diorite gneisses. Unlike the quartz diorite gneisses it is fairly even-grained, and its foliation, where present, is not swirled and does not vary greatly in distinctness from place to place.

FOLIATION AND LINEATION: Most outcrops of the massive quartz diorite exhibit what appears to be an igneous flow structure, marked by the planar parallelism of hornblende and biotite and accentuated by subparallel crystals of plagioclase tabular on (010). The foliation is locally emphasized by dark schlieren, and some of the rock in which the dark minerals are notably streaked out is gneissic. The foliation is vertical or nearly so and conforms to the walls of the sills. Hornblende prisms, mineral streaks, and dark, pencil-shaped inclusions commonly show a distinct lineation which, though its attitude was determined in only a few places, appears to be moderately inclined and nowhere vertical. The bending of the foliation that makes it trend north-northeast north of Dumbell Mountain was probably caused by the pressure of the adjacent intrusive batholith on the west.

INCLUSIONS: The sill north of Ice Lakes contains widely distributed inclusions, all of which consist of hornblende schist or of rocks evidently derived from it. These are clustered in definite zones parallel to the contacts and foliation but are not concentrated at the contacts. Some of the mappable zones are shown in Plate 1. No hybrid rocks occur along contacts to indicate that the sill has assimilated wall rocks. The inclusions range from sharply bounded, angular fragments to vague streaks a little finer-grained and darker than the surrounding quartz diorite. Strikingly banded rocks are formed in some places—notably east of Dumbell Mountain—where the inclusions have been drawn into long smears and rods parallel to the foliation. The inclusions were probably derived from hornblende schist of the regional terrain that has escaped both granitization to hornblende-quartz diorite gneiss (unit 3) and fusion in place to anatectic quartz diorite magma.

If the sill north of Ice Lakes is intrusive into the surrounding hornblende-quartz diorite gneiss (unit 3) and biotite-quartz diorite gneiss, inclusions of these rocks should occur in the sill; if the hornblende-quartz diorite gneiss was fused in place it would not form recognizable inclusions—especially if the zone of melting were sharply bounded, as it might be if localized along a narrow shear or stress zone. If the tabular body of massive quartz diorite is intrusive, the inclusions should be either concentrated near contacts or evenly distributed, instead of being clustered in zones. This clustering in zones would be expected, however, if the hornblende schist inclusions were relics that

have persisted through granitization and fusion. Many intrusive magmatic bodies are surrounded by zones of assimilation, and the lack of such hybrid rocks around the tabular mass north of Ice Lakes is evidence against intrusion of igneous rock. The rolling and smearing out of hornblende schist inclusions indicates differential movement, but this could be due to a stress that triggered fusion, rather than to wholesale upward movement of an intrusive sill.

The sill on the east side of Rock Creek has fewer inclusions than the sill north of Ice Lakes, its inclusions do not occur in zones, and many are concentrated at contacts. These features suggest that the sill was emplaced by intrusion rather than by fusion *in situ*. Near the roof pendants of hornblendite and pegmatite on the south side of Pomas Creek the quartz diorite is charged with inclusions of hornblendite, which are much rolled and streaked parallel to the contact (Pl. 4, fig. 4). Subhedral hornblende crystals as much as half an inch across are abundant in the quartz diorite near these inclusions, which indicates that not only they, but also the isolated clots and large crystals of hornblende which occur here and there in all the massive quartz diorite, are relics of incompletely assimilated inclusions and were not precipitated from a magma.

Just east of Peak 8000, on the east side of Rock Creek, a patch about an acre in area is occupied by a tightly packed cluster of subrounded hornblende schist inclusions, which are variously transformed, as are the hornblende schists in the recrystallization migmatite. The space between the inclusions is filled with pegmatite and aplite rich in microcline. Dikes of this rock cut the surrounding quartz diorite, which in this area contains almost 5 per cent potassium feldspar, considerably more than usual. When the inclusions broke up apparently the only material available to fill the fractures was potassium-rich magma or emanations from the local potassic phase of the surrounding quartz diorite. These potassium-rich dikes indicate that late satellitic emanations from the quartz diorite magma in the sills might be expected to be rich in potassium feldspar. Since most of the leucocratic quartz diorite that forms abundant migmatite and banded gneiss near the sills contains no potassium feldspar, the leucocratic rocks probably are not genetically related to the quartz diorite magmas.

CONTACT RELATIONS: Except for the sill bordering the Entiat fault, contacts of sills of massive quartz diorite are largely obscured by later sills, dikes, and masses of leucocratic quartz diorite. The leucocratic rocks, however, do not encroach far into the massive quartz diorite except in the north end of the sill in upper Box Creek. Within the contact zone there are indications of differential movement, between sill and wall rock, which occurred mainly in the leucocratic rocks. Along the west contact of the sill along the upper part of Rock Creek, many lenses of foliated hornblende-biotite-quartz diorite surrounded by leucocratic quartz diorite are strung out parallel to the contact; the foliation of many of the inclusions is inclined at a high angle to the streaking, and many have halos and cometlike tails of biotite-rich leucocratic quartz diorite. At this locality, despite the screen of leucocratic rocks and the differential movements, the contacts can be located within 50 feet. At Ice Lakes, along the west contact of the massive quartz diorite sill, there are alternating layers, each about a foot thick, of leucocratic quartz diorite, massive quartz diorite, and quartz diorite gneiss. The gneiss layers contain strung-out aggregates of hornblende, and the layering suggests differential movement in a zone made particularly plastic by numerous sills of leucocratic quartz diorite.

Near the Entiat fault the contacts of the sill are not obscured by leucocratic masses, but some of its critical features have been destroyed by intensive shearing. The sill there contains angular, unoriented inclusions of hornblendite and hornblende schist in several places, and similar inclusions were found in small dikes that cut the adjacent hornblende schist.

Contacts of the massive quartz diorite sills are marked by broad zones of particularly massive hornblende-quartz diorite gneiss (unit 3); these zones were not mapped. Along the east side of the sill near the Entiat fault and on the north face of Mt. Maude the more massive phases of the hornblende-quartz diorite gneiss occur in zones several hundred feet wide, and in the Dumbell Mountain area similar gneiss crops out for at least half a mile on each side of the sill. On the west side of Ice Creek the hornblende-quartz diorite gneiss near the sill has a particularly igneous appearance. These border zones of more granitic gneiss next to the sills are probably highly granitized rocks that were partly mobilized and perhaps locally melted, whereas the sills resulted from more nearly complete melting and, in places, active intrusion of this anatectic material. The ex-

posures that suggest these relations are near the lake at the headwaters of Big Creek, where irregular patches and zones of particularly massive gneiss crop out. This gneiss contains diorite gneisses. The accessory minerals are sphene, apatite, ore, and zircon; the secondary minerals are epidote, chlorite, and sericite. Potassium feldspar is scarce in most of the

TABLE 3.—MODES OF MASSIVE QUARTZ DIORITE

Volume percentages to nearest ½ per cent calculated with the Chayes point counter, using 1000–1500 points per standard thin section

	Sill on east side of Rock Creek (Table 5, sample 6)						Mean	Sill north of Ice Lakes (Table 5, sample 5)							Mean
Plagioclase	55½	50	43	49½	58½	56½	51½	53½	49½	54	55	54½	51	54½	52½
Quartz	22	25	28½	23	18½	22½	23	18	9	19	11½	11½	22½	19½	16
Hornblende	9½	9½	2	5	13½	6½	7½	16½	32	20	24	27	9	8½	20
Biotite	10½	11	13½	11½	8	4	9½	10½	3½	4½	6½	6	14	3	7
Apatite	...	+	+	+	+	+	+	+	½	+	+	+	+	+	+
Sphene	½	...	...	½	1½	+	½	...	+	+	+	+	½	+	+
Ore	½	1½	...	...	+	+	½	1	1½	2	1	½	+	½	1
Chlorite	1½	1	1	4	1	7½	2½	...	1½	+	1½	+	+	9½	2
Epidote	...	2	5½	5	...	1	2½	...	½	½	½	½	3	2½	1
Muscovite	+	+	+	1	+	½	½	½	2	+	+	+	+	2	½
K feldspar	...	...	6½	½	...	1½	2	...	...	...	...	...	...	...	...
Zircon	...	+	...	+	...	+	+	...	...	+	...	+	+	+	+
Total	100	100	100	100	100	100	100	100	100	100	100	100	100	100	100

nclusions of hornblende schist smeared out nto long streaks, and also scattered, unoriented inclusions of better foliated hornblende-quartz diorite gneiss (Pl. 5, fig. 6). These features together suggest differential movement in a very plastic mass, the more massive phases of which may have been molten. In other areas the gneiss has a more massive appearance near the sills than elsewhere but has no inclusions and lacks the intense streaking, swirling, and effects of movement that are shown in the rocks of the upper Big Creek area.

In several places on the east side of the sill near the Entiat fault the comparatively massive quartz diorite of the sill grades into quartz diorite gneiss through a transitional zone several hundred feet wide. This transitional zone contains many large, subhedral hornblende crystals that fray out into streaks of small crystals. These streaks indicate that the gneissic appearance of the rocks is partly due to late shearing.

PETROGRAPHY: The massive quartz diorites are mineralogically similar to the hornblende-quartz diorite gneisses but contain more biotite. The plagioclase is andesine (An 35–42), a little more sodic than that in the hornblende-quartz rocks, but microcline is abundant in pegmatitic phases around inclusions. Details of mineralogy and composition are given in Tables 3 and 5; typical hand specimens are illustrated in Figures 7 and 8 of Plate 3. The microtextures of the massive quartz diorites, unlike those of the hornblende-quartz diorite gneisses, are fairly uniform; all are hypidiomorphic granular (Fig. 6*C*). The plagioclase crystals are well formed and are commonly tabular parallel to (010); many are subparallel and suggest a flow structure. Although most of the plagioclase crystals are unzoned, progressively zoned and progressive oscillatory zoned crystals, which have as many as 20 rings, are not rare. Those that show oscillatory zoning are commonly better formed than those that are unzoned or normally zoned. The cores of zoned crystals contain only 1 or 2 per cent more anorthite than the rims, and the differences between oscillatory zones are even smaller. Traces of reverse zoning were noted in the sill north of Ice Lakes.

The quartz is distinctly interstitial and molds itself around the plagioclase crystals. In some sections it is attenuated and streaked out between the plagioclase, as is common in

some of the quartz diorite gneisses. In general, quartz showing a flow structure is much rarer in the massive rocks than in the gneisses.

Most of the hornblende is green to bluish green, as in most of the hornblende-quartz diorite gneisses, but in some sections it is brownish green (X = pale yellow, Y = greenish brown, Z = greenish blue) like that in the more granitoid phases of gneisses and porphyroblasts in the recrystallization migmatite. Most hornblende crystals are subhedral and have few inclusions, but there are some poikilitic grains like those in the hornblende schists and hornblende-quartz diorite gneisses. In many places elongate hornblende crystals, like tabular plagioclase crystals and flakes of biotite, are approximately parallel and give the rock a good flow structure.

Some of the biotite occurs along cleavages in hornblende or forms partial rims around hornblende, from which it appears to be derived. The amount of biotite varies considerably from place to place.

ORIGIN: It might be argued that the massive quartz diorites were formed by complete granitization of hornblende-quartz diorite gneisses and never were molten. An extensive modal-analysis survey is needed to determine accurately the degree of homogeneity of the rocks. The rocks appear homogeneous in the field, but the few modes that were measured (Table 3) indicate that their composition varies widely. Their flow structure and unoriented inclusions could be due to plastic flow in a solid rock.

Every igneous feature in the texture of the massive quartz diorites can develop in metamorphic rocks; such evidence could be used to show that the diorites never were molten. The migmatites in hornblende schist and the hornblende-quartz diorite gneisses contain subhedral to euhedral hornblende crystals, commonly brownish, that have grown in the solid state from smaller anhedra of green hornblende, and closely similar brownish hornblende crystals occur in the massive quartz diorite. Subhedral plagioclase crystals and interstitial quartz have also developed in the quartz diorite gneisses of metamorphic origin. Even some plagioclase crystals which have oscillatory zoning, probably porphyroblasts, occur in the replacement migmatite in hornblende schist. Compton (1955, p. 36) says that the normally zoned plagioclase in the granitized inclusions in the border zone of a batholith in California "is reconstituted to new oscillatory zoned grains." Apparently the igneous texture of the massive quartz diorite could have developed by metamorphism alone. However, hypidiomorphic granular textures in the metamorphic quartz diorite gneisses, which occur in contact with the massive quartz diorite, are irregularly distributed and imperfectly developed, and even if these metamorphic rocks were more highly granitized it is unlikely that this heterogeneity would be destroyed. Therefore, the strongest microscopic evidence that the massive quartz diorite is igneous rather than metamorphic is that it has a well-developed hypidiomorphic granular texture throughout each mass.

The essential minerals of the massive quartz diorite are the same as those of the adjacent hornblende-quartz diorite gneisses of similar chemical composition: they are hornblende, andesine (near An 35 to 42), quartz, and biotite. It can be argued that if the massive diorite is igneous it should contain some high-temperature minerals indicating magmatic origin. One specimen at Ice Lakes contains clinopyroxene, but if clinopyroxene was ever formed throughout the mass, virtually all of it has been converted to hornblende. This conversion would be expected, however, if the magma cooled very slowly. The granodiorite batholith at the north end of the Entiat Mountains contains some clinopyroxene in its chilled border phases; and clinopyroxene presumably was once present in the main mass, but it has been converted to hornblende and biotite, even though this batholith, as shown by its chilled border, probably cooled much more rapidly than the massive quartz diorite sills that show no signs of chilling.

The massive quartz diorite is only slightly more felsic than the hornblende-quartz diorite gneiss that melted to form the magma from which the massive rock crystallized. It is commonly argued that an anatectic magma must be much more felsic than the parent rock, because the last material to crystallize will be the first to melt. But the rate of melting and the ability of mobilized material to escape the zone of heating are equally important in determining the composition of an anatectic melt. If nothing leaves the system—if fusion is rapid there is little opportunity for constituents to leave—the melt will have the same composition as the original rock. If the melting is slow the constituents are the first to melt and that will be more felsic than the original rock, may leave the zone of heating, but the residue, if it melts, will be more mafic than the original rock. The similarity in composition of the massive quartz diorite and the parent hornblende quartz diorite gneiss in the northern Entiat Moun-

tains could indicate rapid and complete fusion of the gneiss.

The tabular form of the bodies of massive quartz diorite and the evidence of differential movement in them parallel to contacts indicate that fusion may have been triggered by shearing or intense differential movement or both. While Bennington (1956, p. 569–570) argues that mafic rocks will concentrate in the shear zone, the massive quartz diorites are slightly more felsic than their wall rocks. Bennington ignores the possibility that shearing may make the shear zone more permeable, and hence more accessible to rising felsic material, and that fusion in the shear zone would trap these felsic materials in the anatectic magma.

Migmatites in Hornblende Schist

GENERAL STATEMENT: Three types of migmatite have developed in the hornblende schists. The first type, which contains many bodies of leucocratic rock, is discussed in the later section on leucocratic quartz diorites. The other two contain no leucocratic rocks; in most places they are cut by leucocratic dikes. One of these types is characterized by transformation of the hornblende schist into spectacularly coarse-grained hornblendite or hornblende diorite pegmatite; the dominant processes in this change appear to have been metamorphic segregation and recrystallization, and these migmatites are therefore called recrystallization migmatite.[6] The second type of migmatite, which was evolved where the schists were replaced and deformed, is a strongly streaked migmatite containing elongated inclusions of altered schist in a matrix of lighter-colored, fine-grained rock. In places this replacement migmatite, as it is called, was mobilized so that dikes of it intruded adjacent rocks and even parts of the migmatite.

STRUCTURE AND PETROGRAPHY OF THE RECRYSTALLIZATION MIGMATITE: The recrystallization migmatite is best exposed on the east side of Pomas Creek and at a locality farther southeast, just outside the quadrangle, where large blocks or roof pendants of this migmatite are surrounded by the massive igneous quartz diorite of the complex. Smaller masses of the recrystallization migmatite are included in the quartz diorite gneiss throughout the area between Ice Lakes and Pomas Creek. At the Holden mine a few dioritic seams and hornblendite masses occur in the hornblende schist, and similar rocks also occur near the contact of the complex at the quadrangle boundary on the east side of Rock Creek. The structure of these composite rocks is partly illustrated in Plate 4.

Hornblende schist in areas where recrystallization migmatite is abundant contains seams and clots of hornblende diorite and hornblende-quartz diorite and clots of hornblende. The contacts of these seams and clots with the hornblende schist are gradational and irregular, and the structure of the hornblende schist is not deflected around them; the seams and clots were formed in place. Nearly all the seams occur along definite lines, which indicates that some pre-existing structure controlled their formation. In places the seams coalesce to form wider bands of diorite and quartz diorite and large clots of hornblende. In the migmatite the hornblende schist has become a vaguely foliated and fine-grained amphibolite, much of which is a heterogeneous mixture of coarser- and finer-grained phases that grade into each other (Pl. 4, fig. 2). The larger metamorphic hornblende crystals develop excellent crystal form, and few are crowded with inclusions. In some of the smaller masses of recrystallization migmatite, such as those at Ice Lakes, the schist contains round splotches of plagioclase up to 1 cm in diameter, peppered with hornblende inclusions, in a matrix of heterogeneous hornblende diorite containing needlelike hornblende crystals; these rocks grade from coarse-grained, almost pegmatitic spotted rocks to fine-grained, only slightly spotted hornblende schists.

These recrystallization migmatites grade into large masses of hornblendite and coarse hornblende diorite pegmatite containing euhedral hornblende prisms up to 6 inches long, which I believe formed by more nearly complete segregation of the minerals of hornblende schist. The spectacular hornblendites and pegmatites are mixed with medium- and coarse-grained hornblende diorites, which all contain euhedral needles of hornblende. The general structure and the gradational relationships can be pictured by imagining that the texture of the rock in Figure 2 of Plate 4 is coarsened.

In thin sections of the recrystallization migmatite as well as in the field, rims of plagioclase and quartz around hornblende porphyroblasts and rims of hornblende around plagioclase porphyroblasts are conspicuous and suggest metamorphic segregation and recrystal-

[6] I follow the scheme outlined by Ramberg (1949, p. 50–51) in classifying the more granitoid rocks in the migmatite (and the migmatite itself) as bodies formed by recrystallization, replacement, or secretion.

lization. The porphyroblasts of hornblende in the hornblende schist are anhedral, are crowded with inclusions of plagioclase and quartz, and are greenish blue to green; those in the dioritic and quartz dioritic seams contain no inclusions, are subhedral, and are commonly brownish (X = pale yellow, Y = greenish brown, Z = greenish blue). The plagioclase porphyroblasts, whether in the seams or spotting the schist, generally show a faint normal zoning and fair crystal form, whereas both zoning and subhedral form are rare in the normal plagioclase of the hornblende schist. The plagioclase in the seams is more sodic (An 30 ± 5) than that in the adjacent schist, as if some sodium had been added. Quartz is slightly more abundant in most of the seams than in the near-by hornblende schist. This may be due to segregation of quartz rather than addition of silica, though I did not note any quartz-depleted zones alongside the seams. The hornblende schist in the recrystallization migmatite is poorly foliated in most places; apparently it was recrystallized under stress-free conditions. The hornblende is seen in thin sections to form shorter, stubbier prisms than those in unmigmatized hornblende schist. Biotite, rare in the large bodies of typical hornblende schist, is a common accessory in the hornblende schist of the recrystallization migmatite, which suggests that some potassium was added during the migmatization.

Quartz, though present in most of the seams, appears to be scarce or absent in the hornblendite and hornblende diorite pegmatite, but the difference may be merely apparent, for the quartz is easy to see where concentrated in seams but becomes less conspicuous where redistributed through a mass of pegmatite derived from the schist. The plagioclase of the pegmatite ranges from labradorite to oligoclase, and it is commonly mottled and irregularly veined with more sodic plagioclase, which may have been formed by a flood of sodic solutions. The hornblende, as noted in the field, is conspicuously euhedral and forms slender prisms or even needlelike crystals.

This transformation of fine-grained hornblende schists to structureless and very coarse-grained rocks with euhedral crystals began along the foliation and along fractures, from which it spread through large masses of the rock. Despite the mineralogical differences described above and possible chemical changes, the proportions of hornblende, plagioclase, and quartz appear to have changed little during this process, as is evident in small areas (Pl. 4, fig. 2) and is also indicated by the general appearance of larger masses. For this reason, and because felsic halos commonly occur around hornblende porphyroblasts and halos of hornblende around plagioclase porphyroblasts, the migmatite is believed to have formed by metamorphic segregation and recrystallization of the minerals of the schist rather than by a replacement of the schist.

The growth of the hornblende porphyroblasts that are scattered through the schist was impeded by the surrounding grains, so that these porphyroblasts are anhedral and contain many inclusions; in the fracture-controlled seams and dikes, where material was far more mobile, the hornblende freed itself of inclusions and assumed good crystal form. The large euhedral hornblende crystals in the hornblendites and pegmatites also indicate high mobility of the material in the rock.

In short, the migmatite appears to have been derived from hornblende schists mainly through segregation and recrystallization, with little addition or subtraction of material. The process occurred under stress-free conditions, and the catalysts (fluids, ions, ichors) that promoted recrystallization and segregation did not soak through the entire mass but were channeled along fissures and foliation planes. As the largest masses of coarse-grained hornblendite and pegmatite all form inclusions or roof pendants in the magmatic phases of the complex and do not occur in the metamorphic phases, such rocks apparently could develop only when the schist was stewed in a true magma.

STRUCTURE AND PETROGRAPHY OF THE REPLACEMENT MIGMATITE: The replacement migmatite is best exposed in the Holden mine, where it is scattered through hornblende schists, and in the area between Ice Lakes and Pomas Creek, where many small masses of migmatite are surrounded by quartz diorite gneiss. The migmatite contains swarms of bannerlike inclusions of dark hornblende schist in a matrix of fine-grained, light-colored quartz diorite, as shown in Plate 5. In much of the migmatite the lighter-colored rock is like the schist—it is only slightly lighter and occurs in ill-defined streaks parallel to the foliation, which are hard to distinguish except on a perfectly clean, smooth surface.

The dark inclusions of hornblende schist have many of the same megascopic and microscopic features as the host rocks of the recrystallization migmatite. They are somewhat coarser and not so well foliated as the original hornblende schist, and in some places, particularly at the

Holden mine, they are considerably darker and finer-grained, which may indicate that they have been made more mafic. In many areas they are only vaguely foliated and resemble fine-grained quartz diorites or microdiorites. In thin section the inclusions are seen to consist of fine-grained granoblastic biotite-hornblende-quartz-plagioclase schist; the plagioclase is An 46 ± 6. Common accessory minerals are apatite, sphene, and ore; secondary minerals are chlorite, sphene (in veins), epidote, and sericite. In some sections a few of the larger plagioclase crystals are subhedral and show normal oscillatory zoning, which suggests that the rocks have an igneous history. I was unable to decide whether these zoned crystals are younger or older than the predominant metamorphic features, or whether they are porphyroclasts or porphyroblasts. Most contain three or four zones differing only 1–3 per cent in anorthite content. Some of the zones are idiomorphic, and some are irregular; some are sharply bounded, and some are gradational. Most of the margins of the plagioclase crystals are intergrown with the surrounding minerals, and one was seen that had a slight concentration of biotite and hornblende around it, like the mafic rims around porphyroblasts in the recrystallization migmatite; most crystals are free from inclusions. Some of the crystals are elongated across the undisturbed foliation of the rock.

Field evidence indicates that the light fine-grained streaks between the dark inclusions in the migmatite are of replacement origin. They consist of fine-grained biotite-hornblende-quartz diorite that has a marked foliation parallel to the streaking. The best evidences, perhaps, for a replacement origin are the fingering out of schist into the lighter rock, the complete gradation between the schist and the somewhat lighter and coarser-grained zones and seams within it (Pl. 5, fig. 1), and the persistence of foliation across all projections of the lighter rock into the schist. The general streakiness of the rocks suggests that much differential movement has occurred. The light rock might be the igneous matrix of a breccia subsequently deformed and metamorphosed, but it seems unlikely that all the features indicating replacement and the alignment of all unoriented inclusions in the original breccia could have resulted. In thin sections one sees that the lighter rock is coarser-grained than the inclusions and contains much more quartz. Most of the hornblende crystals in it, like those in many dioritic seams in the recrystallization migmatite, have no inclusions and are brownish green, which suggests that the two migmatites, though strikingly different in appearance, may be closely related in origin. Unlike the granitoid phases of the recrystallization migmatite, which lack directional features, most of the lighter streaks in the replacement migmatite have a pronounced flow texture. The quartz is interstitial, and many streaks of attenuated quartz grains bend around clusters of plagioclase and hornblende crystals and are parallel to the biotite flakes. All the quartz is in irregular interlocking grains, which shows that it was recrystallized, and there are no fragmental textures. The flow texture, like the appearance of the outcrops, suggests differential movement due to plastic deformation. The plagioclase in the light streaks has the same composition as that in the dark inclusions, and some shows oscillatory zoning. Since the field evidence indicates that the light streaks are of replacement origin, the oscillatory zoning of the plagioclase appears to have developed in a solid or nearly solid rock.

The replacement migmatite contains inclusions of some of the principal rocks in the complex—quartz diorite gneiss and leucocratic quartz diorite, and that fact raises some difficult problems (Pl. 5, fig. 4). The inclusions are angular; some foliated inclusions are unoriented with respect to the streaking and foliation of the migmatite. They occur both in the dark banners and in the lighter streaks between.

The inclusions in the light streaks appear to have been incorporated when the migmatite was mobilized. This is indicated by two dikes of replacement migmatite that contain both dark banners and lighter streaks. One of these dikes cuts sharply across the foliation of the hornblende-quartz diorite of the complex and contains disoriented, angular inclusions of foreign rocks (Pl. 5, fig. 3). The other cuts across the streaking of a large body of the replacement migmatite; in other words, a mobilized portion of the migmatite cuts a nonmobilized portion. The first-mentioned dike cuts, and contains inclusions of, leucocratic quartz diorite of the complex—a rock that elsewhere cuts the migmatite. Therefore, the mobilization of the replacement migmatite must have occurred during the formation of the leucocratic rocks.

The angular and disoriented inclusions of hornblende gneiss and hornblende-quartz diorite in the dark banners of the replacement migmatite are more difficult to explain, for they must be older than the formation and mobiliza-

tion of the migmatite. These inclusions suggest the possibility that the original rocks were once basic igneous dikes but were converted to hornblende schist without destruction of their inclusions before they were migmatized. The field evidence bearing on this possibility is conflicting. The possibility that the original rocks were once dikes is supported in the area between Ice Lakes and Pomas Creek, where masses of replacement migmatite in hornblende schist are isolated in the quartz diorites of the complex. Here the dark, fine-grained rock, which is migmatized, forms many dikelike masses that cut across the banding of the surrounding quartz diorite gneiss, which is interlayered with leucocratic quartz diorite. The migmatite is also contorted and streaked parallel to the banding and is cut by dikes of the leucocratic quartz diorite. These complex relations suggest that the rock that has been migmatized was in dikes but that these dikes were emplaced and then migmatized during deformation and during the emplacement of the leucocratic quartz diorite. Other features in the area between Ice Lakes and Pomas Creek do not suggest the possibility that the pre-migmatite rocks were dikes. From Ice Lakes southward migmatites in hornblende schist, formed both by replacement and by segregation, are concentrated in a long, narrow zone just east of the Entiat Mountain divide, and most of the larger masses of migmatite are elongated parallel to the regional trends. The migmatites thus appear to have formed in hornblende schist of the regional terrain rather than in old dikes. In the Holden mine the replacement migmatite is in hornblende schists that contain lenses and layers of marble; the dark banners in the migmatite at the mine, therefore, cannot be interpreted as old dike rock. Just how inclusions were incorporated in the dark banners in the migmatite remains unknown.

Leucocratic Quartz Diorite

GENERAL STATEMENT: Leucocratic quartz diorite occurs in complex migmatites and in banded gneisses in the western parts of the complex and in the biotite gneiss of the Holden quadrangle (Pl. 1, sketch map). During the granitization of biotite gneiss and hornblende schist into the quartz diorites of the complex, felsic material separated from the rocks by metamorphic differentiation. The felsic material collected in places where pressure was low and formed leucocratic quartz diorite by replacement and secretion. The replacement and secretion[7] migmatites and the banded gneisses thus formed are particularly abundant in the biotite gneiss and biotite-quartz diorite gneiss, but they also occur in adjacent hornblende schist and granitoid hornblende-quartz diorite gneiss (unit 3); even the massive quartz diorite magmatic rocks were partly migmatized after they had solidified. In the migmatites the masses of leucocratic rocks have an extremely wide range in form and size; they include individual porphyroblasts, splotches, and small lenses, and sills and dikes (Pls. 6, 7). There are a few small stocks of leucocratic quartz diorite. The sketch map in Plate 1 shows the distribution of the leucocratic bodies in the host rocks and those places where they are most abundant. The leucocratic quartz diorite was formed almost entirely by replacement of other rocks along definite lines. Crosscutting secretion dikes and concretions of leucocratic quartz diorite in the foliation planes occur, but in smaller volume than the replacement bodies.

MEGASCOPIC APPEARANCE: The leucocratic quartz diorite is generally massive but is obscurely gneissic in some places where mica, generally biotite, occurs as parallel flakes or as clots. It consists chiefly of plagioclase and quartz, in widely varying proportions, but most of it contains small amounts of microcline, biotite, muscovite, and epidote; garnet is a rare accessory. Potassium feldspar is extremely scarce. The rocks range in grain size from coarsely pegmatitic to fine-grained; fine- to medium-grained rocks are the most abundant. Many bodies contain rocks of differing grain size which almost everywhere grade into each other within a few inches. Small bodies of pure quartz or single crystals or clots of plagioclase occur but are much rarer than bodies of leucocratic quartz diorite.

The emplacement of the leucocratic rock has been strongly influenced by the structure of the host rock in which it occurs: the more distinctly foliated the host rock is, the greater the tendency for the leucocratic rock to develop along the foliation planes; the more massive the host rock is, the greater the tendency for the leucocratic rock to form irregular masses or dikes. The following discussion is therefore divided on the basis of the type of host rock in which the leucocratic rock occurs.

[7] I follow the scheme outlined by Ramberg (1949, p. 50–51) in classifying the metamorphic quartzofeldspathic rocks as replacement or secretion bodies.

LEUCOCRATIC ROCK IN BIOTITE GNEISS: In the biotite gneiss the leucocratic rock occurs as an integral part of the gneiss and in all gradations from pods to lines of pods to sills parallel to the foliation (Pl. 6, figs. 3, 4, 5). In biotite gneiss in which the light and dark minerals are particularly well segregated, the quartz and plagioclase occur in long lenses that grade into biotite-rich streaks. The well-segregated biotite gneisses contain lenses of leucocratic rock as much as several inches long which do not have ducts leading to them; these lie parallel to the general trend of the foliation, though the foliation is bent around them. They appear to be very much like the smaller quartz-plagioclase segregations in the gneiss except that they are somewhat coarser-grained; many of them are particularly rich in quartz, and most of them have thin rims of nearly pure biotite. They grade from separate, closely spaced lenses to lenses joined together to form irregular sills that pinch and swell. The bending of foliation around lenses indicates that the emplacement of the lenses, at least locally, was accompanied by an increase in volume of the enclosing gneiss. These small and ductless lenses cannot possibly have been intruded; the material in the lenses must have arrived by infiltration. The infiltrating material formed a body which either forced the gneiss aside as it grew or filled a space as it was opened by tectonic forces.

Dikes formed by secretion occur where felsic

PLATE 4.—RECRYSTALLIZATION AND METAMORPHIC SEGREGATION IN HORNBLENDE SCHIST AND ULTRAMAFIC ROCKS

FIGURE 1.—Seams and sills formed by segregation and recrystallization of hornblende schist. (South side of upper Pomas Creek)

FIGURE 2.—Uneven texture in schist between seams of hornblende formed by segregation and recrystallization. Note felsic rims on some seams. Pencil point for scale. (South side of upper Pomas Creek)

FIGURE 3.—Pegmatitic hornblende diorite with uneven texture. Note euhedral needles of hornblende and large hornblende crystals. (South side of upper Pomas Creek)

FIGURE 4.—Inclusions of coarse hornblende, rolled and streaked out, in massive igneous quartz diorite, near its contact with recrystallization migmatites in hornblende schist, *e.g.*, Figures 1–3. Clusters of large euhedral hornblende crystals in homogeneous igneous quartz diorite away from contacts are probably not pyrogenic but represent inclusions of hornblende schist that have been made mafic, such as those illustrated here. Pencil for scale. (South side of Pomas Creek)

FIGURE 5.—Clot of hornblende diorite formed by segregation and replacement in ultramafic rock. Compare with Figure 2. Specimen is about 7 inches high. (Holden mine)

FIGURE 6.—Hornblende diorite of coarse and uneven grain, derived by granitization of ultramafic rock. Compare with Figure 3. Specimen is about 4 inches high. (Holden mine)

PLATE 5.—REPLACEMENT MIGMATITE IN HORNBLENDE SCHIST AND INCLUSIONS OF QUARTZ DIORITE GNEISS

FIGURE 1.—Vague light-colored streaks of diorite in hornblende schist. Such rocks grade into migmatite with well-developed light-colored streaks. View about 2 feet by 2 feet. (North side of Pomas Creek)

FIGURE 2.—Biotite-quartz diorite streaks formed by replacement of hornblende schist. Note interfingering contacts. (Outlet of upper Ice Lake)

FIGURE 3.—Intrusive dike of mobilized replacement migmatite cutting quartz diorite gneiss and leucocratic quartz diorite. Note flow structure of inclusions of schist and leucocratic quartz diorite. (1 mile north of Carne Mountain)

FIGURE 4.—Inclusions of hornblende gneiss and leucocratic quartz diorite in replacement migmatite, presumably incorporated during its mobilization. View about 3 feet by 3 feet. (Outlet of upper Ice Lake)

FIGURE 5.—Seams and streaks of relatively coarse and massive hornblende-quartz diorite gneiss cutting and enclosing lenses of finer-grained gneiss near the pencil. (Three quarters of a mile south of the northern Spectacle Butte)

FIGURE 6.—Migmatite interpreted as having been formed by partial melting in a zone of intense deformation. Coarser rocks on right and unoriented inclusions near ice ax are hornblende-quartz diorite gneiss, unmelted; dark streaks are hornblende schist, also unmelted. Finer, lighter-colored massive quartz diorite may be the anatectic melt. (Three quarters of a mile southeast of Dumbell Mountain)

1

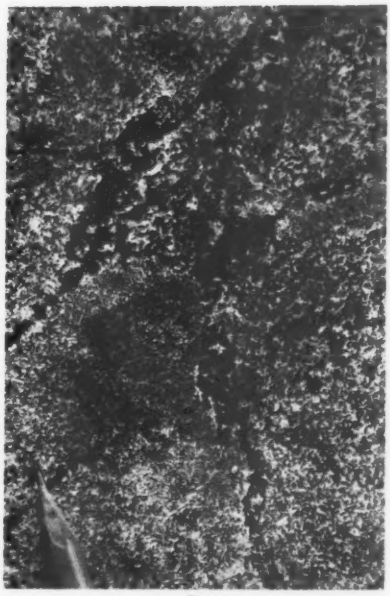

2

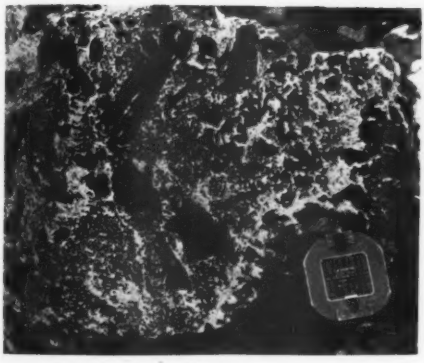

3

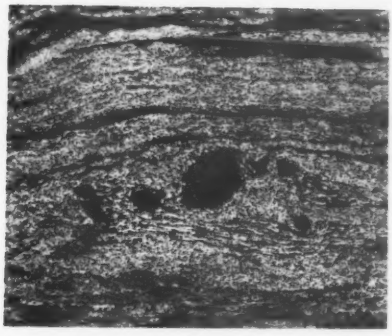

4

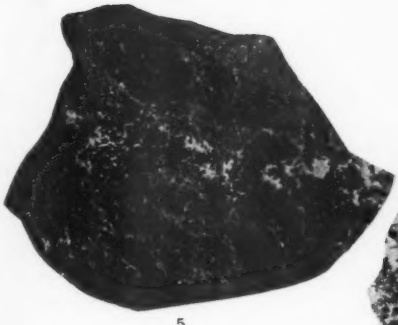

5

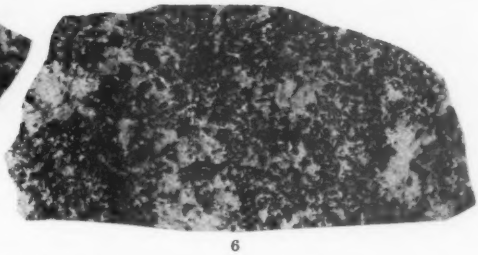

6

RECRYSTALLIZATION AND METAMORPHIC SEGREGATION IN HORNBLENDE SCHIST AND ULTRAMAFIC ROCKS

1

2

3

4

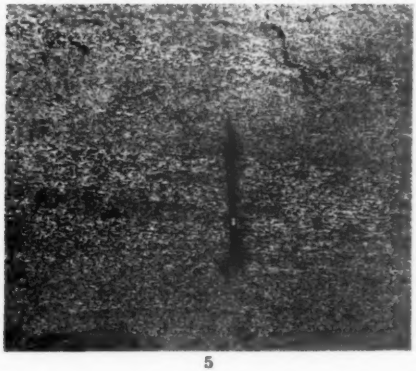

5

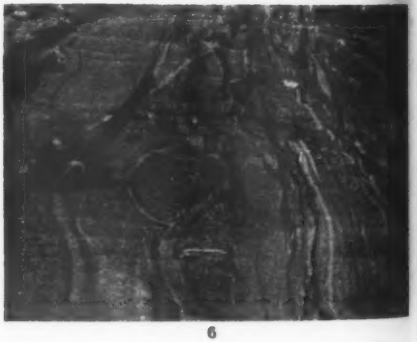

6

REPLACEMENT MIGMATITE IN HORNBLENDE SCHIST AND INCLUSIONS OF QUARTZ DIORITE GNEISS

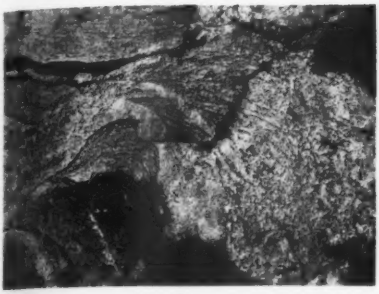

1

2

3

4

5

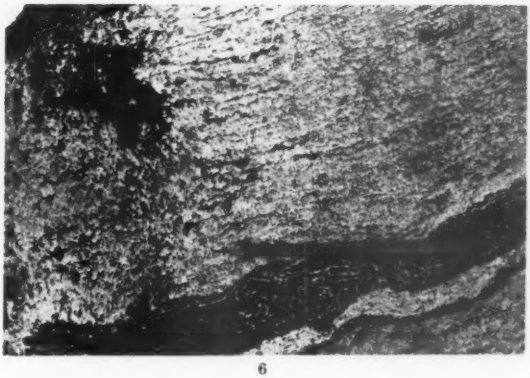

6

SEGREGATION, PLASTIC FLOW, AND DIKES OF LEUCOCRATIC QUARTZ DIORITE IN BIOTITE GNEISS AND BIOTITE-QUARTZ DIORITE GNEISS

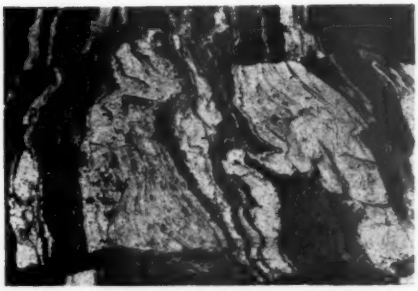

1

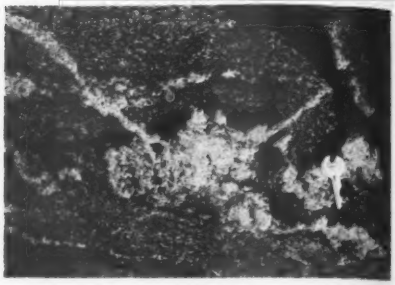

2

3

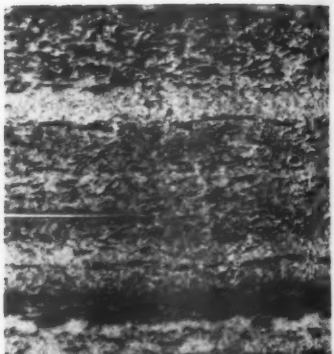

4

5

6

LEUCOCRATIC QUARTZ DIORITE IN HORNBLENDE-QUARTZ DIORITE GNEISS

materials filtered into fractures as they spread apart. These dikes are straight and of uniform widths, and some can be traced many tens of yards. Most of the contacts are sharp, and the foliation of the enclosing biotite gneiss is not distorted next to them. Displacement is obvious along some dikes that follow fault planes. The dikes formed by secretion contain practically no

---

PLATE 6.—SEGREGATION, PLASTIC FLOW, AND DIKES OF LEUCOCRATIC QUARTZ DIORITE IN BIOTITE GNEISS AND BIOTITE-QUARTZ DIORITE GNEISS

FIGURE 1.—Leucocratic quartz diorite in biotite-quartz diorite gneiss that has been formed by granitization of biotite gneiss. Compare with less intensely migmatized biotite gneiss in Figure 3. Shows the end of a thin layer of hornblende gneiss; such layers are common in the quartz diorite gneisses. (1 mile west of outlet of upper Ice Lake)

FIGURE 2.—Border of a mobilized dike with flow structure cutting well-segregated biotite-quartz diorite gneiss. The gneiss (around pencil) blends with the more leucocratic mobilized phase through a zone of slightly deformed rock 3–4 inches thick. The contact is much more gradational than most contacts of mobilized dikes in biotite gneiss as shown in Figure 4, apparently because both rocks were unusually plastic. (1 mile northwest of Mt. Maude)

FIGURE 3.—Rolled boudin of hornblende schist in plastic biotite gneiss. Note how lubrication by leucocratic quartz diorite aids the plastic deformation. Biotite gneiss is typical of migmatized areas. It has good segregation of minerals and contains leucocratic quartz diorite lenses, some with coarse biotite in and around them. Note the flow-banded, mobilized replacement dike, which is shown by the bending of the gneiss to have moved from right to left. (Three quarters of a mile west of Chiwawa Mountain)

FIGURE 4.—Mobilized replacement dike, showing flow structure, in biotite gneiss. Replacement origin is indicated by mingling of gneiss with the dike at the bottom, rims of biotite on the dike, and, near center of right margin, clots of biotite in the dike opposite biotite streaks in the gneiss. Bending of gneiss indicates that the dike moved from bottom to top. Dike is about 5 inches wide. (6 miles northwest of Chiwawa Mountain)

FIGURE 5.—Contact of secretion dike enclosing a splinter of biotite gneiss wall rock. Note lack of any contact features and complete gradation of dike material into felsic parts of the well-segregated biotite gneiss. Absence of biotite in the dike and lack of deflection of gneiss at contact distinguishes this dike from the mobilized replacement dikes in Figures 3 and 4. (A quarter of a mile southeast of Chiwawa Mountain)

FIGURE 6.—Massive biotite-quartz diorite, with biotite clot, segregated from the gneiss. Overlaps left side of Figure 1. (1 mile west of outlet of upper Ice Lake)

PLATE 7.—LEUCOCRATIC QUARTZ DIORITE IN HORNBLENDE-QUARTZ DIORITE GNEISS

FIGURE 1.—Large replacement sills and small seams and pods of leucocratic quartz diorite. Note clots of biotite, basified septa, and vague mafic streaks, all inherited from the gneiss, and contortion of all the rocks. Where such replacement sills or dikes flow plastically, flow structure develops as shown in Figures 3 and 4 of Plate 6. (1½ miles south of Dumbell Mountain)

FIGURE 2.—Replacement clots and seams of leucocratic quartz diorite. Note rims of biotite and contortions of gneiss. (1½ miles south of Dumbell Mountain)

FIGURE 3.—*Lit-par-lit* replacement sills in banded hornblende gneiss. Despite their regularity, these sills, like those in Figure 1, are thought to be largely of replacement origin. (Divide between Rock Creek and Box Creek)

FIGURE 4.—Close-up of replacement sill in banded gneiss. Note undisturbed hornblende crystals and basified septa. Needle gives scale. (Divide between Rock Creek and Box Creek)

FIGURE 5.—Replacement breccia of massive quartz diorite cut by dikes of leucocratic quartz diorite. Some inclusions still fit together; except for late faulting as in lower left, there is only a vague suggestion of movement. (North side of upper Pomas Creek)

FIGURE 6.—Mobilized replacement breccia dike of leucocratic quartz diorite showing a flow structure. The inclusions and ghosts of inclusions, though much crowded, are not rounded by flow, suggesting that they have not been carried very far. (1 mile north of Dumbell Mountain)

mafic minerals, and the one inclusion I found in a dike of this kind (Pl. 6, fig. 5) did not appear to have been forcibly ripped from the wall and rolled about. Where the dikes cut felsic segregations in the biotite gneiss, there is

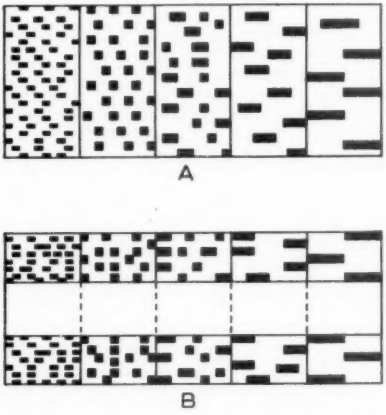

FIGURE 8.—VISUAL EFFECTS OF SEGREGATION

A. All five columns contain 15 per cent mafic material by area but variously segregated. Illustrates how segregation creates the illusion that felsic material has been added. B. All five columns contain 15 per cent mafic material as in (A) but differently segregated. Mafic material has migrated to walls of a fracture, which has been filled with felsic material secreted from the walls. There has been no volume change, and the mafic material in the walls is now 23 per cent. Shows by comparison with (A) that the increase in mafic minerals adjacent to the dike is hardly detectable in rocks whose light and dark minerals are well segregated.

no sign of a contact between the rock in the dikes and the felsic segregations; the dikes and the segregations appear to be the same rock. Some dikes have fingerlike branches projecting for short distances into the biotite gneiss, but it seems unlikely that the dikes supplied material to the myriad felsic segregations distributed through the large areas of biotite gneiss between the dikes. These straight, even, inclusion-free and particularly mafic-poor quartz diorite dikes that show no contact disturbances probably started as tectonic fractures in the gneiss, which were filled, as they opened, by felsic material filtering into them from the surrounding biotite gneiss. The dikes probably did not form by replacement. If they did it is difficult to explain their regularity, lack of contact effects, and lack of any biotite inherited from the biotite gneiss. If the dikes were intrusive, one would expect more inclusions, evidence of rolling or streaking of inclusions, flow banding, deflection of foliation in the enclosing gneiss, and possibly more differences between the dikes and the felsic parts of the biotite gneiss.

If the felsic material in the dikes was extracted from the surrounding biotite gneiss, one would expect a halo rich in basic material to occur in the gneiss. No such halo has been detected, but the heterogeneous character of the biotite gneiss would make one hard to recognize even if it were there; even a rather marked concentration of dark minerals would be difficult to detect in the field unless it occurred very near the dikes. (*See* Fig. 8.) Around small segregations and secretion lenses, however, where small distances are involved, biotite-rich halos are conspicuous, which suggests that some felsic material has been secreted from the surrounding gneiss.

The most common dikes in the biotite gneiss are leucocratic quartz diorite dikes formed by replacement of the gneiss. These are crooked and irregular compared to the dikes formed by secretion in the gneiss. Most contain some coarse-grained biotite unevenly distributed in streaks, bands, or clots in the white quartz plagioclase rock, and the contacts are marked in places by clots of coarse-grained biotite. The biotite is the same orange-red variety as that in the surrounding biotite gneiss. The foliation of the enclosing biotite gneiss passes undisturbed through many of these dikes, and most inclusions are undisturbed. Their contacts, though irregular, are sharp. These features, together, indicate a replacement origin. The more coarse-grained the dike the greater the development of clots of coarse biotite, both in the dike and at the contact; this suggests a greater mobility of basic material and more rapid diffusion in the pegmatitic bodies. The pegmatitic material generally occurs in what were probably places of lowest pressure: pods of it were formed, for example, in the crests of small folds and where layers of competent gneiss between sills of leucocratic rock tend to separate (Fig. 9). In many places the pegmatitic dikes of leucocratic quartz diorite cut all the other finer-grained bodies of leucocratic quartz diorite.

Many of the replacement and secretion dikes show signs of mobilization and intrusion (Pl. 6, figs. 3, 4). The most obvious intrusive fea-

tures are the flow structure of biotite and tabular inclusions parallel the dike walls. Some of these dikes, showing indications of flow, branch from irregular replacement dikes, sills, or pods that show little indication of movement. Even a strongly flow-banded dike (Pl. 6, fig. 4), interpreted as a mobilized replacement dike, still shows replacement features; the foliation of the enclosing gneiss is deflected in the same direction on both sides of this dike, which indicates mobilization and intrusion of plastic material in the replacement dike rather than simply differential movement within it. The quartz-feldspar rocks in the replacement and secretion dikes, sills, and smaller lenses in the biotite gneiss are very similar in megascopic appearance, although they are seen to differ in grain size and in the amount and the distribution of biotite. The source of the felsic material, therefore, is probably the same for all the various bodies.

During the emplacement of the leucocratic quartz diorite in biotite gneiss the migmatite that was formed became plastic. Most of the foliation of the well-segregated phases of the biotite gneiss, which is common in the most highly migmatized areas, is crumpled. The competent layers of hornblende schist have drifted apart, and the surrounding biotite gneiss or leucocratic quartz diorite has collapsed into the space between, producing typical boudinage structures. The biotite gneiss is more competent than the leucocratic quartz diorite. (*See* Fig. 9.) In places the biotite gneiss became so plastic that separate pieces of a hornblende schist layer were rolled (Pl. 6, fig. 3). These signs of plastic deformation are in rocks far from the complex, on the downthrown side of the Entiat fault. The numerous signs of mobilization found in the quartz diorite gneisses east of the Entiat fault, in the more deeply eroded upthrown block, are to be expected.

LEUCOCRATIC ROCK IN BIOTITE-QUARTZ DIORITE GNEISS: In the biotite-quartz diorite gneiss most of the leucocratic rock grades into the gneiss and is an integral part of it (Pl. 6, fig. 1). In areas where the gneiss is migmatized, it is well segregated into light and dark streaks, which makes the rock as a whole appear leucocratic; consequently, in the field one tends to overestimate the amount of leucocratic quartz diorite in the migmatite; only on perfectly clean outcrops that expose dikes of leucocratic rock can a comparison be made to ascertain how much of the composite mass is gneiss. Most of the leucocratic rock occurs in streaks and sills parallel to the foliation of the gneiss. The whole aspect of the migmatite suggests that the biotite-quartz diorite gneiss was thoroughly soaked with felsic material and thereby rendered plastic. The leucocratic material was not emplaced as a magma, but the exposed

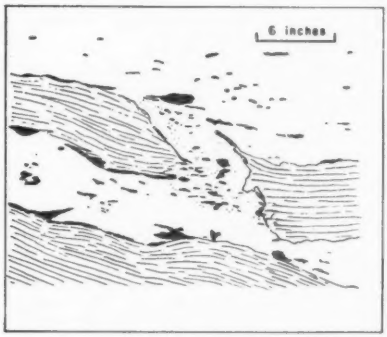

FIGURE 9.—PEGMATITE OCCURRING WHERE A LAYER OF BIOTITE GNEISS TENDS TO BE PULLED APART

Part of a migmatite consisting of alternating layers of biotite gneiss and leucocratic quartz diorite. Lined pattern = well-foliated biotite gneiss; white = leucocratic quartz diorite; black = clots of coarse-grained biotite. Where the gneiss layer appears broken, pegmatitic leucocratic quartz diorite occurs and grades into the fine- to medium-grained leucocratic quartz diorite of the main sills on either side. Shows preference of pegmatite for places of lowest pressure, where gneiss layer was probably under tension, and replacement of gneiss by pegmatitic leucocratic quartz diorite.

structures in the outcrops do not show whether the added felsic material in the replacement bodies filtered through the gneiss from an outside source or whether it is a metamorphic differentiate of the gneiss. Many of the latest dikes of leucocratic quartz diorite are straight, contain practically no dark minerals, and contain no inclusions; some of them grade along strike into the gneiss or into the heterogeneous mixtures described above. These dikes are probably formed by secretion in fractures that formed after the main period of migmatization and plastic deformation was over.

LEUCOCRATIC ROCK IN HORNBLENDE SCHIST AND GNEISS: In hornblende schist and gneiss the leucocratic rock commonly occurs in straight, parallel, and closely spaced layers from a fraction of an inch to several inches thick; the rocks formed are banded gneisses (Pl. 7, figs. 3, 4). Even though these layers are

not poddy and irregular, like most replacement layers in other rocks, they are thought to have been formed by replacement. They consist mainly of quartz and plagioclase but contain some hornblende and in places a little garnet and biotite. The hornblende is concentrated at contacts, and these contacts are somewhat gradational. The thin layers of leucocratic rock are banded, in too regular a manner to be the result of flow. Asymmetrical layers (Pl. 7, fig. 4) were probably not formed by replacement along a single foliation but by replacement along several closely spaced foliation planes, which by gradually coalescing could have partly eliminated an intervening septum and produced a single banded layer. Hornblende-rich margins and bands suggest that metamorphic differentiation has accompanied the replacement. A few mafic-free leucocratic quartz plagioclase layers that occur without contact effects or internal banding may have formed by secretion.

Some of the banding of the gneiss in the area extending north from Carne Mountain to Leroy Creek represents relict bedding. The light layers in such rocks are petrographically very similar to the biotite-quartz diorite gneiss of the complex and are easily confused with the leucocratic quartz diorite replacement layers. Unlike the layers thought to be formed by replacement they show no contact effects or banding and contain evenly distributed biotite. Some are many yards thick, yet none contain inclusions, nor do they crosscut the hornblende schists or have any features that suggest intrusive origin.

LEUCOCRATIC ROCK IN MASSIVE AND GNEISSIC HORNBLENDE-QUARTZ DIORITE: As the massive and gneissic hornblende-quartz diorite is less perfectly foliated than the biotite gneiss, the leucocratic rocks in it occur more commonly as clots, dikes, and in the matrix of breccias rather than as sills; the few sills they do form are poddy and irregular and of replacement origin (Pl. 7, figs. 1, 2). As the gneiss between the sills is generally crowded with small seams of plagioclase porphyroblasts, the layers of gneiss are in many places very ill defined and ghostlike. Large pods of leucocratic quartz diorite many hundreds of feet across grade into dikes of digested porphyroblastic quartz diorite. A large, clean surface on the east side of upper Phelps Creek reveals one of these pods, about a hundred feet across, from which dikes radiate like the spokes of a wheel. Undisturbed ghosts of the gneiss between the dikes are visible near the margins of the pod, but in the center the dike structure becomes vague; the felsic materials apparently moved outward from the network of feeder dikes into the gneiss, which they almost completely replaced. In these rocks, as in all other rocks in which occur many bodies of leucocratic quartz diorite, the foliation is contorted and swirled.

Leucocratic quartz diorite of probable replacement origin forms the matrix of breccias in both massive and gneissic hornblende-quartz diorite (Pl. 7 figs. 5, 6), especially in the gneissic rock. In some of these breccias no evidence of differential movement between inclusions appears; the inclusions are closely crowded, and many of the larger ones are joined by thin septa. These features indicate that the leucocratic quartz diorite matrix is of replacement origin, and that the breccias are replacement breccias. In places, however, breccia dikes appear to have moved (Pl. 7, fig. 6); these probably are mobilized replacement breccias. The inclusions in the dikes and breccia zones are unoriented, and mafic streaks extend from some that are lens-shaped. A wall of one dike is deformed where a large inclusion butted against it; the wall rock was evidently plastic during flow in the dike. The inclusions in the dikes are fragments of the walls, not foreign inclusions such as intrusive igneous dikes might be expected to carry upward. In some dikes the inclusions are coarser-grained than the wall rock or appear ghostlike and partly assimilated. Dikes that have flow structure occur in massive and gneissic hornblende-quartz diorite that contains abundant and widely varied replacement bodies of leucocratic quartz diorite. The leucocratic rock in all these bodies and in all the breccias has a metamorphic texture (Fig. 10).

PETROGRAPHY: Although the bodies of leucocratic quartz diorite are widely varied in form and grain size, they are found to be very similar when studied in thin section. Their chief minerals are plagioclase (oligoclase An 20 $\pm$ 2) and quartz. The principal accessory, however, is generally the same as in the host rock: in biotite gneiss it is orange-red biotite; in either massive or gneissic hornblende-quartz diorite it is commonly green to blue-green hornblende like that in the host rock but is accompanied by some biotite. The similarity of the main accessory minerals in the leucocratic quartz diorite bodies to those in their host rocks accords with the view that the leucocratic rock is largely of replacement origin and may have involved metamorphic differentiation of the host rock. Apatite, sphene, and ore gen-

erally occur as minor accessories; a pod of rutile as big as an egg was found on the border of one small pegmatitic mass on Phelps Ridge, and, in another place, coarse crystals of kyanite were found. Secondary alteration of biotite to chlorite is common and characteristic, and the plagioclase is slightly dusted with sericite. Secondary anhedral epidote is associated with sericite in altered plagioclase and with chlorite in altered biotite. Potassium feldspar is nearly absent from most of these rocks, but some microcline occurs in a few dikes near the sill on the east side of Rock Creek and on Chiwawa Mountain. Some details of mineralogical and chemical composition of the leucocratic quartz diorite are given in Table 5; sample 9 represents the typical rock.

The microtexture is metamorphic (Fig. 10): the plagioclase crystals are unzoned and anhedral, and in some bodies they are crowded with round blebs of quartz; some of the rocks have a marked flow structure where interstitial quartz is attenuated and wraps around plagioclase grains.

SOURCE OF FELSIC MATERIAL: In most places felsic material had been added to a host rock to form a leucocratic quartz diorite replacement body. A secretion body of leucocratic quartz diorite consists entirely of such felsic material. Field evidence suggests that this felsic material is probably a metamorphic differentiate of the biotite gneiss and biotite-quartz diorite gneiss; this origin is suggested by the fact that leucocratic quartz diorite is nearly everywhere a characteristic of these rocks, and that it is thoroughly mixed with them (Pl. 1, sketch map; Pl. 6; Pl. 7, fig. 1). These gneisses appear to have been thoroughly soaked with felsic material, which suggests that the material did not come into these rocks from elsewhere but was derived by metamorphic differentiation of the rocks themselves. In host rocks other than the biotite gneiss and biotite-quartz diorite gneiss, however, the felsic material does not appear to have soaked the rocks as thoroughly, because the leucocratic bodies are in comparatively well-defined dikes, sills, and pods, and over large areas these rocks contain no leucocratic quartz diorite bodies. The felsic material that filtered into these rocks apparently came from the adjacent biotite gneiss and biotite-quartz diorite gneiss from which it separated by metamorphic differentiation. Possibly the reason leucocratic quartz diorite is characteristic of, abundant in, and thoroughly mixed with the biotite gneiss and biotite-quartz diorite gneiss is not that these rocks sweated out felsic material but that, because of their comparatively excellent foliation, they were especially permeable to felsic material infiltrating from elsewhere. In the discussion of the chemistry of the complex, sodium is shown as the principal felsic material that must be added to a probable parent rock to form biotite gneiss or biotite-quartz diorite gneiss or leucocratic quartz diorite in these rocks. Thus, the source of sodium that appears to have been sweated out of the gneiss into the leucocratic quartz diorite is ultimately extraneous.

FIGURE 10.—CRYSTALLOBLASTIC MICROTEXTURE OF LEUCOCRATIC QUARTZ DIORITE

Q = quartz, P = plagioclase, M = muscovite

It is not likely that the felsic materials in the leucocratic quartz diorite were emanations derived from the magma in the massive quartz diorite sills by crystallization differentiation. There are no leucocratic phases of the massive quartz diorites, and the sodic rims on zoned plagioclase crystals in the sills are nowhere so sodic as the plagioclase in the leucocratic rocks. At the one place where magmatic differentiation is indicated—a cluster of inclusions set in a felsic matrix—the felsic matrix is rich in potassium feldspar, which is rare in most of the leucocratic quartz diorite. The sills seem very small to be the source of leucocratic bodies in biotite gneiss miles to the west, and there is no indication that the sills are offshoots of a large subjacent mass. Little leucocratic rock occurs in and near the sill along the Entiat fault, and most of the leucocratic quartz diorite in the other sills occurs only along their borders. Leucocratic quartz diorite was already developed in the rocks into which the sills were emplaced,

and it continued to form after the sills had solidified. In this way the leucocratic quartz diorite was mixed with the borders of the sills, and rotated, streaked-out inclusions of the sills in the leucocratic rock show that the mixing was accompanied by differential movement along the contact.

TABLE 4.—MODES OF STOCK ON BUCKSKIN MOUNTAIN AND OF RELATED DIKES

Figures for each rock type are the mean of 5 volume percentage modes to the nearest ½ per cent, which were calculated from thin sections with a Chayes point counter, using 1000–1500 points per standard thin section; + = less than ½ per cent.

	Early biotite-quartz diorite dikes	Main stock of biotite-quartz diorite gneiss	Late biotite-quartz monzonite dikes
Plagioclase	52	51½	36½
Quartz	27	33½	34½
Biotite	16½	13½	6
Hornblende	4	+	....
Orthoclase	½	1½	21
Chlorite	+	+	2
Total	100	100	100
Average An content of plagioclase:			
Whole crystals	43	40	27
Cores	50	45	33
Rims	32	28	21

STOCKS AND DIKES

General Statement

Along Phelps Ridge and also at Old Gib Mountain porphyritic and aphanitic rocks occur in plugs, dikes, and intrusive breccias, and many dikes of similar rocks are scattered through the northern Entiat Mountains. These rocks, which contain phenocrysts of quartz and labradorite, are related to the granodiorite batholith at the north end of the Entiat Mountains and have sharp, chilled contacts with the surrounding quartz diorite and migmatites. They are not genetically related to the complex and are not further discussed here. Other rocks, mostly intrusive bodies, occurring in and near the complex may be genetically related to it, although the nature of the relation is not clear. These include three small stocks of felsic rocks and scattered dikes and small plugs of mafic and ultramafic rocks.

Quartz Diorite Stock

Near Buckskin Mountain there is an igneous stock of gneissic quartz diorite, which was intruded, when it was in a nearly solidified state, along the northeast contact zone of the complex. The stock is surrounded by an extensive system of dikes, some older and some younger than the stock; most of these were emplaced by intrusion of magma and like the stock are much deformed and recrystallized.

Possibly the stock was intruded forcibly. The persistent layers of marble, which closely follow the east contact of the hornblende schists (Pl. 1) and the layer of hornblende schist on Copper Peak, appear to have been forced apart by the stock; they are nearly twice as far apart opposite the stock as they are near the town of Holden. The foliation of the quartz diorite gneiss adjacent to the south end of the stock is somewhat deflected, and along the west side of the stock its northeast dip changes from moderate to very steep, and its strikes follow the contact, which is sharp and steep. Not enough structural data were obtained to determine how the conspicuous biotite foliation of the stock behaves near the contacts. There is no zoning within the mass that might suggest assimilation of wall rock, and numerous inclusions occur near the contacts.

This medium-grained biotite-quartz diorite gneiss for the most part is uniform in appearance; it is characterized by elongate, rounded crystals of plagioclase surrounded by biotite (Pl. 3, fig. 5). In a few places, this dominant rock grades into a biotite-poor granodiorite. The mode of the dominant quartz dioritic rock is given in Table 4.

The microtexture of the gneissic stock is porphyroclastic. The porphyroclasts are relics of pyrogenic plagioclase, in a metamorphic matrix. They are subhedral crystals, 1–8 mm long, which have Carlsbad habit. They have either normal, oscillatory zoning or progressive zoning; cores average An 45, and rims average An 28; their over-all composition is An 40 ± 5. The normal oscillatory zoning closely follows the subhedral shape of the crystals, which is evidence that they grew in a magma. The recrystallized matrix between the porphyroclasts is fine-grained and consists of xenomorphic quartz and parallel flakes of biotite. Attenuated quartz and flakes of biotite commonly wrap

around the plagioclase crystals. The quartz and biotite that occur in strung-out clots may represent single crystals that have been crushed and recrystallized.

All stages in the abrasion, corrosion, and recrystallization of the plagioclase crystals can be observed, and some evidence indicates that the deformation and recrystallization occurred in a nearly consolidated magma. Rounded corners on euhedral grains are common. In some crystals that have oscillatory zoning, adjacent zones are not parallel; some of the outer, more sodic zones surround and truncate the zones in a subrounded or angular core. These relations probably resulted from grinding of early crystals, precipitated when the magma was nearly consolidated and before the final, most sodic plagioclase of the magma was precipitated. One plagioclase porphyroclast is cut by a fault, although the surrounding quartz was not offset or strained; the faulting may have occurred in a crystal mush before the quartz was precipitated. Narrow, unzoned twin lamellae cut through well-zoned crystals, and the best twinned crystals lack zoning; the late twinning thus appears to have been attended by obliteration of the original zoning. Twinning by itself cannot obliterate zoning; an unzoned twin lamella that cuts a zoned crystal must have been homogenized by rearrangement of ions during a recrystallization. Some of the plagioclase porphyroclasts are untwinned and unzoned; they are probably zoned crystals that have completely recrystallized.

Early dikes and masses of vaguely foliated hornblende-biotite-quartz diorite, which are gray and fine-grained, occur near the stock and in a zone extending northwest as far as the Holden mine. In these rocks a few subhedral plagioclase phenocrysts stand out distinctly from the fine-grained matrix (Pl. 3, fig. 4). The average plagioclase composition is An 43 ± 5, which is slightly more calcic than that in the stock, and the common accessory mineral is hornblende, which is rare in the stock. Details of the mineral composition of these early quartz diorite dikes are given in Table 4. The gray quartz diorites are texturally similar to the rocks of the stock, but they contain fewer oscillatory-zoned plagioclase relics, and their plagioclase crystals more commonly have wide oligoclase rims that include and interpenetrate the quartz and biotite of the matrix.

The stock and the early dikes are cut by many later dikes of fine-grained, well-foliated biotite-quartz monzonite (Pl. 3, fig. 6); these form a complex, anastomosing network throughout the area between Buckskin Mountain and the Holden mine and are best exposed in the Holden mine. These quartz monzonite dikes are rare in the northern Entiat Mountains where potassium feldspar is notably scarce. The biotite in them is characteristically red brown. The plagioclase (An 27 ± 5) is partly altered to sericite and the biotite to chlorite—both much more so than in the stock or the early dikes. Like the stock and the early dikes the microtexture of the quartz monzonite dikes is porphyroclastic. Most porphyroclasts are rounded, unzoned plagioclase crystals whose ragged borders interpenetrate with a xenomorphic matrix consisting of anhedral intergrown crystals of quartz, orthoclase, and biotite. Some of the large plagioclase crystals have normal oscillatory zoning parallel to their subhedral outlines, and most are oriented to form a flow structure in the crystalloblastic matrix. These crystals appear to be older pyrogenic inclusions in a metamorphic matrix in which they have been rolled.

The assumption that the quartz monzonite dikes are offshoots of the biotite-quartz diorite stock is based on the fact that (1) the dikes are concentrated in a zone near the stock, and (2) they are petrographically similar to leucocratic phases of the stock, especially in containing red biotite and abundant potassium feldspar.

Certain compositional features of the stock and its satellites indicate that the varieties may have evolved through normal crystallization differentiation of a magma. In the progression from early dikes to stock to late dikes, the plagioclase shows a marked decrease in anorthite content. The proportion of mafic minerals also decreases (*see* Table 4): hornblende is common in the early dikes, rare in the stock, and absent in the late dikes, whereas potassium feldspar is abundant in the late dikes, where plagioclase and biotite are commonly altered. Other magmatic features are the oscillatory zoning in subhedral to euhedral porphyroclasts of plagioclase and a definite order of crystallization. Hornblende and plagioclase crystallized first, in subhedral, inclusion-free crystals; the quartz and orthoclase in the matrix are molded around these early crystals. Apart from these magmatic features visible in thin sections, intrusive origin is indicated by the homogeneous character of the stock, its sharp contacts, and the evidence that it pushed its walls aside.

The stock and its satellites probably were emplaced along the border of the complex when this border was a hot zone undergoing granitiza-

tion and plastic deformation. Deformation near the east contact of the complex, where the stock and its satellites occur, is shown by: (1) the streakiness of the replacement migmatite in hornblende schist parallel to the contact of the complex where this migmatite is abundant, combined with a porphyroclastic texture in its light streaks; (2) a fine-grained eastern border phase of the hornblende-quartz diorite augen gneiss (unit 4), which also has a porphyroclastic texture. That the stock has shared in this deformation is indicated by the foliation, porphyroclastic texture, and elongation of the stock parallel to the contact with the complex; the satellitic dikes of the stock are also schistose and have a porphyroclastic texture. The protoclastic texture of the stock and many of its satellites shows that the deformation was contemporaneous with the late stages in the freezing of the magmas. Most of the late quartz monzonite dikes cut in all directions across the streaking of the replacement migmatite in the hornblende schist; this shows that the main differential movement parallel to the contact of the complex had ceased before emplacement of these dikes.

Granodiorite

East of Rock Creek there is a stock of fine-grained, igneous biotite granodiorite This rock has a foliation marked by flakes of biotite and a lineation marked by streaks of biotite; both these structures maintain a uniform trend in that part of the stock that is within the quadrangle. The rock is massive and is uniform in appearance except near its contacts, where it contains numerous unoriented, angular inclusions of quartz diorite. Its microtexture is hypidiomorphic granular.

Ultramafic Rocks and Gabbro

In the Holden mine and on Buckskin Mountain are a few small dikes and plugs of ultramafic rocks—hornblendite and peridotite—some of which have gabbroic and dioritic phases. Half a mile west of the mine is a mass of gabbro that may be related to these rocks.

Most of the ultramafic rocks are hornblendites. Their mineralogy and texture is highly varied, and their original character has been largely masked by alteration and granitization. The hornblende is greenish brown but is rimmed and in places replaced by tremolite; its iron formed magnetite dust in the tremolite. In some of the rocks the amphibole is nearly all tremolite; in some it is all greenish-brown hornblende. Red-orange biotite is a common accessory in both the hornblendic and tremolitic facies, and long needles of apatite are abundant in both. Less common than the hornblendites are altered olivine hornblendites or hornblende peridotites. Most of the hornblende in these rocks also is greenish brown. Most of the pyroxene is clinopyroxene, which forms inclusions in hornblende. Olivine generally is present only in small amount, but in a few places it makes up as much as a third of the rock. In one specimen it forms inclusions in hypersthene crystals. The olivine is much altered to antigorite and magnetite, and the hornblende to tremolite and magnetite. Angular inclusions of wall rocks occur in the ultramafic rocks at some places near the contacts with the surrounding hornblende schist and the replacement migmatite in hornblende schist; these contacts are generally sharp.

Granitization of the ultramafic rocks formed gabbro and diorite of granular texture in the Holden mine and in ultrabasic parts of the gabbro stock southwest of the mine. The ultramafic rocks contain clots and seams of labradorite, and as the labradorite becomes abundant the rocks grade into hornblende diorite and gabbro (Pl. 4, figs. 5, 6).

The stock just southwest of Holden may be an igneous intrusion to which the ultramafic rocks in the Holden area appear related. At one place in the Holden mine ultramafic rocks and their granitized equivalents extend continuously from the mine workings to a place well under the outcrop of the stock. Both in the outcrop and in the mine the stock contains hornblendite masses that are variously granitized, but their relation to the main gabbro of the stock was not observed. The main part of the stock is a medium-grained hornblende gabbro with a striking panidiomorphic-granular texture that shows the crystallization sequence clinopyroxene-hornblende-plagioclase. The hornblende, which is brown and forms euhedral crystals with cores of clinopyroxene, is slightly altered to tremolite. The labradorite is subhedral and has well-defined progressive zoning from labradorite to oligoclase. Apatite in long needles is a common accessory, and a little brown biotite is present. Quartz, orthoclase, and muscovite, all probably secondary, occur in very small amounts. The contact of the stock is sharp where observed, and at one place the margin contains numerous unoriented, angular inclusions of hornblende schist. The stock occurs in the border zone of the complex

where particularly intense differential movement occurred during its formation. The stock is massive, which probably means it was intruded after this period of deformation.

The origin of the ultramafic rocks is not clear. Gobs of hornblendite grading into diorite are found in limited amounts in the Holden mine in recrystallization migmatites in hornblende schist; perhaps the large masses of hornblendite also formed by recrystallization and segregation of hornblende schist. The ultrabasic rocks, which contain clinopyroxene, hypersthene, and olivine, are probably magmatic differentiates related to the gabbro stock on Copper Peak, which appears to be igneous.

Mafic Dikes

Late black aphanitic dikes that cut all the rocks of the complex are widespread in the northern Entiat Mountains. Most of them are typical hornblende-plagioclase lamprophyres—spessartites. They are concentrated along the mountain divide and occur in swarms along the crest for a mile south of Dumbell Mountain and near the divide west of Ice Lakes. In both these areas they trend west, are vertical and straight, and have knife-sharp contacts. In the area between Ice Lakes and Pomas Creek many similar dikes, some of which have good columnar jointing, lie parallel to and within the west-dipping shear zone near the divide. The largest of the basic dikes (Pl. 1) have aphanitic chilled margins, which grade into medium-grained or fine-grained hornblende diorite cores characterized by abundant euhedral needles of hornblende. Specimens from one of the large dikes, and from a columnar-jointed, aphanitic to fine-grained dike in a dike swarm on the Entiat Mountain divide between the two forks of Box Creek, show a similarity in thin section to specimens from the gabbro stock southwest of Holden. They consist of hornblende diorite, which has a panidiomorphic-granular texture. The hornblende is greenish brown, euhedral, and rimmed with tremolite. Subhedral plagioclase crystals that have normal zoning are molded around the hornblende crystals. Some of the plagioclase crystals are larger than average and include grains of hornblende. No pyroxene was noted. Apatite is an abundant accessory and forms needles up to 3 mm long. Quartz is scarce and appears to be late, for it is interstitial and intimately intergrown with plagioclase.

Relation of Stocks and Dikes to the Complex

The mafic and ultramafic stocks and dikes which appear igneous do not all have the same relation to the complex. Some of the ultramafic rocks (olivine hornblendites and hornblende peridotites) are older than the complex and were granitized like hornblende schist and biotite gneiss during its formation. Although gabbro stock near Holden is petrographically very similar to some of these early ultramafic rocks and even contains similar ultramafic phases, it was intruded after the main period of deformation and granitization. The late mafic dikes are petrographically very like the gabbro stock near Holden, but, as is shown by their chilled margins, they were intruded after the complex had cooled. It is difficult to show that any of these probable igneous rocks are genetically related to the complex.

Many masses of hornblendite and hornblende diorite were formed in recrystallization migmatite by intense local metamorphic segregation and recrystallization of hornblende schist and are genetically related to the complex. These rocks are petrographically similar to the ultramafic and mafic rocks which appear to be igneous. It might be suggested that these mafic and ultramafic rocks that appear igneous are also genetically related to the complex and were formed by metamorphic processes at depth in the complex and were mobilized, intruded, and then granitized during this plutonism. Experimental evidence shows that an ultramafic magma cannot exist below 1000° C. (Bowen and Tuttle, 1949, p. 455). But there is no evidence for the metamorphic origin of the hypersthene,[8] olivine, and clinopyroxene in the ultramafic rocks of the northern Entiat Mountains. The late basic dikes which have chilled margins and columnar joints are certainly igneous and probably not genetically related to the plutonism that formed the complex.

The quartz diorite stock on Buckskin Mountain and the granodiorite stock on the east side of Rock Creek may be genetically related to the complex. The stocks have a gneissic foliation parallel to the regional structural trends, and the Buckskin Mountain stock is much metamorphosed. The stock east of Rock Creek, which is not metamorphosed where

[8] Hypersthene derived from hornblende does occur as rims around small inclusions of hornblende schist in the igneous granodiorite batholith at the north end of the Entiat Mountains.

TABLE 5.—COMPOSITION OF ROCKS OF COMPLEX AND OF HOST ROCKS

WEIGHT PERCENTAGES OF OXIDES

	1	2	3	4	5	6	7	8	9	10	11
SiO_2	53.8	56.9	53.2	68.9	57.5	61.8	73.9	72.9	75.3	75.9	74.2
Al_2O_3	15.8	17.9	18.7	14.3	18.0	17.0	13.4	13.7	15.1	14.1	15.5
Fe_2O_3	2.6	2.7	3.0	2.1	2.7	2.1	.6	1.6	.1	.6	.48
FeO	8.1	4.2	5.2	2.6	3.9	3.5	2.5	2.4	.2	.90	.33
MgO	4.8	3.7	4.5	1.7	3.6	2.4	1.3	.8	.2	.64	.32
CaO	7.6	7.3	8.5	4.7	6.9	5.2	2.7	2.3	2.7	2.0	1.8
Na_2O	3.9	3.4	3.3	3.5	3.8	3.8	3.5	5.0	5.3	3.2	3.8
K_2O	.87	.66	.51	.42	1.0	1.7	1.6	.9	.8	2.1	3.4
TiO_2	.95	.59	.76	.41	.98	.71	.....	.....	.....	.16	.08
P_2O_5	.16	.24	.29	.21	.32	.33	.....	.....	.....	.06	.04
MnO	.25	.14	.15	.11	.12	.11	.....	.....	.....	.03	.01
H_2O	1.4	1.5	1.3	.76	1.0	1.2	.5	.4	.3	.96	.64
CO_2	.10	<.05	.07	<.05	.07	.05	.....	.....	.....	<.05	<.05
Total	100.3	99.2	99.5	99.7	99.9	99.9	100.0	100.0	100.0	100.7	100.6

CATION PERCENTAGES[a]

Si	50.4	53.8	50.3	65.6	53.9	58.3	70.2	69.4	70.2	71.8	69.1
Al	17.5	20.3	20.8	16.0	19.9	18.9	15.0	15.2	16.4	15.6	17.0
Fe +3	1.9	1.9	2.2	1.5	1.9	1.5	.4	1.2	.1	.5	.3
Fe +2	6.4	3.3	4.1	2.1	3.0	2.8	2.0	1.9	.2	.7	.3
Mg	6.8	5.3	6.4	2.4	5.1	3.4	1.8	1.2	.3	.9	.4
Ca	7.7	7.6	8.6	4.8	6.9	5.2	2.7	2.3	2.7	2.0	1.8
Na	7.1	6.3	6.0	6.5	6.9	6.9	6.1	8.3	9.5	5.8	6.9
K	1.1	.8	.6	.5	1.2	2.0	1.6	.5	.6	2.5	4.0
Ti	.7	.4	.6	.3	.7	.5	.....	.....	.....	.1	.1
P	.1	.2	.2	.2	.3	.3	.1	.....	.....	.1	.1
Mn	.2	.1	.1	.1	.1	.1	.1	.....	.....	.....	.....
H_2O	(9.9)	(9.4)	(8.2)	(4.8)	(6.2)	(7.5)	(3.0)	(2.7)	(1.7)	(6.1)	(4.0)
C	.1	.....	.1	.....	.1	.1	.....	.....	.....	.....	.....
Total	100.0	100.0	100.0	100.0	100.0	100.0	100.0	100.0	100.0	100.0	100.0
Associated anions											
O	151.5	157.1	154.8	168.8	157.5	162.7	164.8	165.8	165.4	172.9	170.7
OH	9.9	9.4	8.2	4.8	6.2	7.5	3.0	2.7	1.7	6.1	4.0

MEASURED MODES[b]

Plagioclase	25	43½	48	43	52½	51½	44½	53½	59½	40	40

Associated anions											
O	151.5	157.1	154.8	168.8	157.5	162.7	164.8	165.8	165.4	172.9	170.7
OH	9.9	9.4	8.2	4.8	6.2	7.5	3.0	2.7	1.7	6.1	4.0

MEASURED MODES[b]

Plagioclase	25	43½	48	43	52½	51½	44½	53½	59½	40	40
% An	(30–50)	(44±5)	(44±5)	(39±5)	(42±5)	(35±5)	(29±3)	(20±2)	(20±2)	(29±5)	(25±6)
Quartz	9½	18	11	39	16	23	42	38	35	50	30
Hornblende	60½	31	37	14	20	7½	.....	.....	.....	.....	.....
Biotite	+	2	1	2	7	9½	12	5	1	3	3
Apatite	+	+	+	+	+	+	+	+	+	.....	.....
Sphene	½	+	+	+	+	½	.....	.....	+	.....	.....
Ore	1	+	½	1½	1	½	+	1	+	+	.....
Chlorite	1	2	1½	½	2	2½	.....	1	½	.....	2
Epidote	½	3	1	+	1	2½	.....	½	1	.....	.....
Muscovite	1	½	+	+	½	½	½	1	2½	2	5
K feldspar	.....	.....	.....	+	.....	2	1	+	½	5	20
Calcite	½	.....	.....	.....	.....	.....	.....	.....	.....	.....	.....
Garnet	½	.....	.....	.....	.....	.....	+	+	.....	.....	.....
Zircon	.....	.....	.....	+	+	+	+	.....	.....	.....	+
Kyanite	.....	.....	.....	.....	.....	.....	.....	.....	.....	.....	+
Total	100	100	100	100	100	100	100	100	100	100	100

CALCULATED MODES[c]

Plagioclase	30.0	46.5	44.5	46.0	52.8	53.0	44.5	53.5	59.5	42.0	41.5
% An	17	44	42	37	43	35	29	20	20	33	22
Quartz	6.8	17.2	10.1	34.5	12.7	21.0	42.0	38.0	35.0	42.3	33.6
Hornblende	54.1	26.8	37.0	13.1	17.8	6.2	.....	.....	.....	.....	.....
Biotite	.....	2.8	2.1	2.1	9.8	7.8	12.0	5.0	1.0	6.5	1.6
Apatite	.3	.5	.5	.5	.8	.7	.....	.....	.....	.6	.....
Sphene	.6	.3	.3	.3	.3	.6	.....	.....	.....	.....	.....
Ore	3.2	2.0	2.2	2.3	.5	1.1	.....	1.0	.....	.5	.4
Chlorite	1.0	1.0	1.0	.7	3.0	3.0	.....	1.0	.5	.....	.6
Epidote	.8	2.4	1.6	.....	1.6	.4	.....	.5	1.0	.....	.....
Muscovite	2.5	.5	.5	.5	.5	1.0	.5	1.0	2.5	2.0	5.0
K feldspar	.....	.....	.....	.....	.....	4.0	1.0	.....	.5	6.0	14.0
Calcite	.2	.....	.2	.....	.2	.2	.....	.....	.....	.....	.....
Garnet	.5	.....	.....	.....	.....	.....	.....	.....	.....	.....	.....
Kyanite	.....	.....	.....	.....	.....	.....	.....	.....	.....	.4	3.3
Total	100.0	100.0	100.0	100.0	100.0	100.0	100.0	100.0	100.0	100.0	100.0

TABLE 5.—*Continued*

MOLECULAR NORMS[d]

	1	2	3	4	5	6	7	8	9	10	11
Q	2.1	11.3	6.3	32.1	10.9	17.4	37.8	35.9	34.1	41.6	32.2
C	.....	.....	.....	.....	.....	.8	1.9	1.8	.9	3.2	2.5
Or	5.5	4.0	3.0	2.5	6.0	10.0	8.0	2.5	3.0	12.5	20.0
Ab	35.5	31.5	30.0	32.5	34.5	34.5	30.5	41.5	47.5	29.0	34.5
An	23.3	33.0	35.5	22.5	29.5	23.0	13.5	11.5	13.5	10.0	9.0
Σ salic	66.4	79.8	74.8	89.6	80.9	85.7	91.7	93.2	99.0	96.3	98.2
Wo	5.4	1.4	2.2	.....	.8	.....	.....	.....	.....	.....	.....
En	13.6	10.6	12.8	4.8	10.2	6.8	3.6	2.4	.6	1.8	.8
Fs	9.8	4.0	5.0	2.2	2.8	3.2	3.8	2.6	.2	.6	.....
Mt	2.9	2.9	3.3	2.3	2.9	2.3	.6	1.8	.2	.8	.5
Il	1.4	.8	1.2	.6	1.4	1.0	.....	.....	.....	.2	.2
Ap	.3	.5	.5	.5	.8	.8	.3	.....	.....	.3	.3
Cc	.2	.....	.2	.....	.2	.2	.....	.....	.....	.....	.....
Σ femic	33.6	20.2	25.2	10.4	19.1	14.3	8.3	6.8	1.0	3.7	1.8
Calculated % An	40	51	54	41	47	40	31	22	22	26	21

MESONORMS[e]

Q	2.7	13.6	8.1	33.5	14.4	22.4	42.1	37.4	34.5	43.3	33.2
C	.....	.....	.....	.....	.....	.8	3.3	1.8	.9	3.7	2.9
Or	4.2	.....	.....	.....	.....	1.5	1.8	.....	2.2	10.3	19.2
Ab	35.5	31.5	30.0	32.5	34.5	34.5	30.5	41.5	47.5	29.0	34.5
An	9.5	29.5	30.0	22.5	27.5	23.0	12.5	11.5	13.5	9.0	8.0
Σ salic	51.9	74.6	68.1	88.5	76.4	82.2	90.2	92.2	98.6	95.3	97.8
Ho	41.3	10.5	16.5	.....	6.0	.....	.....	.....	.....	.....	.....
Bi	2.1	6.4	4.8	4.0	9.6	13.6	9.9	4.0	1.3	3.5	1.3
Hy	.....	4.4	5.4	4.2	2.8	.....	.....	2.0	.....	.....	.....
Mt	2.8	2.8	3.3	2.2	2.8	2.2	.6	1.8	.1	.7	.4
Il	1.4	.8	1.2	.6	1.4	1.0	.....	.....	.....	.2	.2
Ap	.3	.5	.5	.5	.8	.8	.3	.....	.....	.3	.3
Cc	.2	.....	.2	.....	.2	.2	.....	.....	.....	.....	.....
Σ femic	48.1	25.4	31.9	11.5	23.6	17.8	10.8	7.8	1.4	4.7	2.2
Calculated % An	21	48	50	41	44	40	27	22	22	24	19

TRACE-ELEMENT CONTENT[f]

5 B	0	3	0	0	0	0	0	0	0	1	1

Σ femic	48.1	25.4	31.9	11.5	23.6	17.8	10.8	7.8	1.4	4.7	2.2
Calculated % An	21	48	50	41	44	40	27	22	22	24	19

TRACE-ELEMENT CONTENT[1]

5 B	0	3	0	0	0	0	0	0	0	1	1
.5 Ba	100	10	10	3	10	10	100	70	90	300	300
.05 Be	0	0	0	0	0	0	.2	0	0	.1	.1
1 Co	3	3	3	1	1	.1	1	.8	.8	.5	0
.6 Cr	3	1	10	.3	3	3	8	4	4	2	0
.05 Cu	10	3	3	1	1	1	2	1	40	2	1
1 Ga	3	3	3	1	3	3	2	2	2	1	1
1 Ni	3	0	0	0	0	0	2	.5	.5	.6	.5
1 Pb	10	0	0	0	0	0	2	3	1	2	3
.5 Sc	3	1	1	1	1	1	.8	.8	.3	0	0
1 Sr	30	100	30	30	30	30	20	30	60	70	40
1 V	30	1	1	1	1	1	3	2	1	4	2
1 Y	3	1	1	1	1	1	3	3	1	0	0
.1 Yb	—	.1	.1	.1	.1	.1	.2	.2	.1	0	0
.8 Zr	—	1	10	1	3	10	30	30	10	3	3
Total	198.0	127.1	72.1	40.4	54.1	60.2	144.2	147.3	210.7	386.2	351.6

1. Hornblende schist and gneiss, east side of Holden Creek. Composite sample of 4 selected chips. P. L. D. Elmore and S. D. Botts, analysts

2. Well-foliated hornblende-quartz diorite gneiss, north and east sides of Mt. Bonanza to Copper Peak. Composite sample of 7 selected specimens. P. L. D. Elmore, K. E. White, and S. D. Botts, analysts

3. Granitoid hornblende-quartz diorite gneiss, south and west sides of Mt. Bonanza to Ice Creek and Mt. Fernow. Composite sample of 9 selected specimens. P. L. D. Elmore, K. E. White, and S. D. Botts, analysts

4. Hornblende-quartz diorite augen gneiss, Spectacle Buttes to Copper Creek. Composite sample of 10 selected specimens. P. L. D. Elmore, K. E. White, and S. D. Botts, analysts

5. Biotite-hornblende-quartz diorite, south side of Hart Lake to Mt. Maude. Composite sample of 7 selected specimens. P. L. D. Elmore, K. E. White, and S. D. Botts, analysts

6. Hornblende-biotite-quartz diorite, east side of Rock Creek. Composite sample of 8 selected specimens. P. L. D. Elmore, K. E. White, and S. D. Botts, analysts

7. Biotite-quartz-plagioclase gneiss, Estes Butte and Phelps Ridge. Calculated from mode; K_2O and Na_2O determined with flame photometer by B. Bruun, Geological Survey of Norway

TABLE 5.—*Concluded*

8. Biotite-quartz diorite gneiss, west side of Entiat Mountains. Calculated from mode; K_2O and Na_2O determined with flame photometer by B. Bruun, Geological Survey of Norway

9. Leucocratic quartz diorite replacement dikes and masses, west side of Entiat Mountains. Calculated from mode; K_2O and Na_2O determined with flame photometer by B. Bruun, Geological Survey of Norway

10. Leucocratic granodiorite pods in biotite gneiss, south side of Chiwawa Mountain. Composite sample of several hundred randomly selected chips. P. L. D. Elmore, K. E. White, and S. D. Botts, analysts

11. Leucocratic granodiorite pegmatitic dikes in biotite gneiss, south side of Chiwawa Mountain. Composite sample of several hundred randomly-selected chips. P. L. D. Elmore, K. E. White, and S. D. Botts, analysts

Analyses numbers also refer to map-unit numbers on Plate 1 and in the text
Samples 1–6, 10, 11 analyzed by methods similar to those described by Shapiro and Brannock (1956)

[a] As proposed by Barth (1955). *See* Figure 11 for comparison of the cation percentages of the rocks recalculated to a standard cell of 160 oxygen anions

[b] Volume percentages to nearest ½ per cent; + means less than ½ per cent. Samples 1–9 calculated from thin sections with a Chayes point counter; 1000–1500 points per standard thin section. Samples 10 and 11 are estimated

[c] Volume percentages calculated from the chemical analyses. Biotite formulas used: $K_{(.8\text{ to }1.0)}$ $Fe_{(1.0\text{ to }1.2)}$ $Mg_{(.7\text{ to }1.0)}$ $Al_{(1.6\text{ to }2.0)}$ $Si_{(2.7\text{ to }3.1)}$ $(O, OH)_{12}$. Hornblende formulas used: $Na_{(.3\text{ to }.8)}$ $K_{(.1\text{ to }.02)}$ $Fe_{(1.2\text{ to }1.8)}$ $Ca_{(1.3\text{ to }1.8)}$ $Al_{(2.3\text{ to }3.4)}$ $Si_{(6.4\text{ to }7.1)}$ $(O, OH)_{24}$

[d] As proposed by Barth (1952, p. 76–82)

[e] As proposed by Barth (1955, p. 350–352)

[f] Semiquantitative spectrographic analyses expressed in parts per million (ppm); standard sensitivities are noted to left of element symbol; 0 = element was not detected; — = element was not looked for. Analysts: H. J. Roe, sample 1; K. E. Valentine, samples 2–6; S. Berman, samples 7–9; H. Bastron, samples 10 and 11. Sensitivities of elements that were looked for but were not detected are listed below. If a specimen number is noted after the element symbol, it means that in that sample the element was not looked for. Ag .01, As 10, Au 1, Bi 5, Cd 5, Ce 30, Cs 800 (1, 7–11), Dy 6 (1, 7–11), Er 3 (1, 7–11), Eu 3 (1, 7–11), Gd 6 (1, 7–11), Ge 1, Hf 7 (10, 11), Hg 80, Ho 1 (1, 7–11), In 0.4, Ir 30, La 3, Li 10 (1, 7–11), Lu 5 (1, 7–11), Mo 0.5, Nb 1, Nd 6 (7 to 11), Os 100 (10–11), Pd 3, Pr 10 (1, 7–11), Pt 3, Rb 7000 (1, 7–11), Re 40, Rh 4, Ru 8, Sb 10, Sn 1, Sm 8 (1, 7–11), Ta 100, Tb 10 (1, 7–11), Te 80 (1, 10, 11), Th 50, Tl 40, Tm 1 (1, 7–11), U 80 (1), W 50, Zn 8

studied, was probably intruded somewhat later than the stock on Buckskin Mountain. Perhaps some anatectic magma, generated at depth during formation of the complex, was intruded upward into the complex both during and a short time after the main period of granitization and deformation. Hornblende-quartz diorite gneiss appears to have melted to form the anatectic magma for which the massive quartz diorite of the complex solidified and the biotite gneiss and the biotite-quartz diorite gneiss may also have melted at depth to form a more felsic anatectic magma.

Chemistry of the Complex

The following discussion is based on the 11 chemical analyses given in Table 5. I assume that the changes that occurred during the formation of the complex were approximately volume for volume. The main basis for this assumption is the lack of any evidence of major pushing aside by the quartz diorite gneiss and massive quartz diorite, the abundant replacement features in the quartz diorite gneisses and associated migmatites, and the evidence for anatectic origin of the massive quartz diorites. Volume-for-volume changes must be evaluated by comparing the compositions of equal volumes of rock before one was changed into the other. Barth (1948) describes a method for doing this without elaborate calculations. He shows that equal volumes of rocks—especially of those belonging to the same metamorphic facies—contain approximately the same number of oxygen ions, and he proposes that units of 160 oxygen ions be used as a standard for comparing equal volumes. I have recalculated the analyses expressed in oxides to the percentage of the various cations associated with 160 oxygen ions and have plotted these percentages in Figure 11, where the vertical scale is such that a given change in the cation percentage of any element is represented by about the same vertical distance. This diagram is simply a graphic method of comparison. Field relations are relied upon to indicate the origin of the rocks and to establish the genetic grouping used in the diagram.

The problem of the original source rock of much of the hornblende schist has not been solved in the field, but it may be considered from a chemical basis. The lack of relict structures in most of the hornblende schists, however, suggests that they may have formed from massive igneous rocks, and an igneous parent rock, probably basalt, is also indicated by the fact that the hornblende schist (*see* Table 5) contains more Na_2O than K_2O and more CaO than MgO, as do many igneous rocks. A volume-for-volume change of average basalt to the hornblende schist of the northern Entiat Mountains requires subtraction of potassium, calcium, and magnesium, and perhaps of a very little iron, and an addition of sodium and a little silicon. Similar changes (except the addition of sodium) are indicated by further metamorphism and transformation of the hornblende schist to hornblende-quartz diorite gneiss. Andesite and graywacke, which are also plotted as possible source rocks, would require addition, not subtraction, of iron, magnesium, and calcium to become hornblende schist.

Field evidence indicates that the biotite gneiss is a metamorphosed arkosic sediment. Except for an increase in sodium and a decrease in potassium, the chemical changes necessary to convert an average arkose to biotite gneiss are relatively minor.

The hornblende schists are varied in composition, and this fact would presumably be reflected in the chemical composition of hornblende-quartz diorite gneisses derived from them by granitization. The hornblende-quartz diorite augen gneiss (unit 4) differs more chemically from the analyzed hornblende schist than do the other two hornblende-quartz diorite gneisses (units 2, 3); the greatest difference is in silicon: the augen gneiss contains almost 40 per cent quartz in the mode. Perhaps the parent rock of the hornblende-quartz diorite augen gneiss was a hornblende schist rather different in composition from the hornblende schist analyzed. For example, this gneiss could have been derived from average graywacke, without any significant change of composition except a decrease of potassium.

As shown by the trends of the curves in Figure 11 between hornblende schist and all three hornblende-quartz diorite gneisses, hornblende schist can be transformed to hornblende-quartz diorite gneiss by rather small changes—largely subtraction of elements. Some of the chemical changes required are remarkably small: for example, a unit cell of the hornblende schist need lose only 7.4 cations and gain 4.4 cations to become a unit cell of the granitoid hornblende-quartz diorite gneiss (unit 3). If the very large oxygen anions, which make up most of the volume of a rock, are imagined as remaining fixed in position while the small cations migrate, this movement of the 7.4 and 4.4 cations involve only about 6

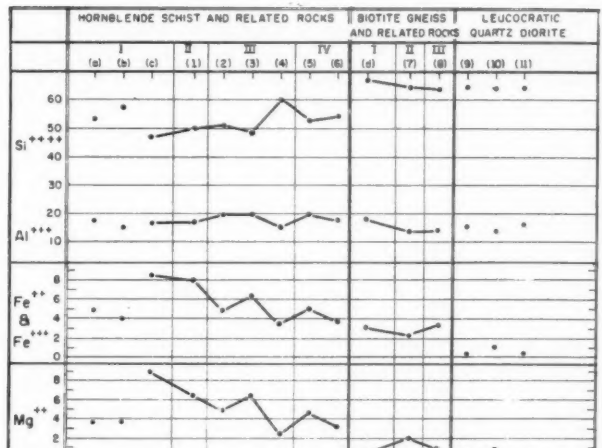

FIGURE 11.—CHANGES IN CATION PERCENTAGES OF MAIN ELEMENTS DURING TRANSFORMATIONS

Cation percentages per unit cell of 160 oxygen anions, as suggested by Barth (1948), plotted on the vertical axis on a scale adjusted for all elements but Si, so that unit change vertically equals approximately the same percentage change in the cation percentage. Significant changes are thus made visible without obscuring changes in the major constituents. The rocks are arranged on the horizontal axis into groups that field evidence indicates are genetically related. Lines connect most probable source rock for hornblende schist or biotite gneiss on the left with progressively more transformed phases of them on the right.

Hornblende schist and related rocks:

I. Possible source rocks of hornblende schist: (a) average andesite (Daly, 1933, p. 16); (b) average graywacke (Pettijohn, 1949, p. 250); (c) average basalt (Daly, 1933, p. 17)

II. Hornblende schist: (1) (Table 5, analysis 1)

III. Hornblende-quartz diorite gneisses formed by granitization of hornblende schist; granitoid appearance and indications of flowage increase from left to right: (2) well-foliated hornblende-quartz diorite gneiss (Table 5, analysis 2); (3) granitoid hornblende-quartz diorite gneiss (Table 5, analysis 3); (4) hornblende-quartz diorite augen gneiss (Table 5, analysis 4)

IV. Anatectic igneous rocks derived by melting of hornblende-quartz diorite gneiss: (5) hornblende-quartz diorite, melted *in situ* (Table 5, analysis 5); (6)hornblende-biotite-quartz diorite, intrusive, possibly derived by fusion at depth (Table 5, analysis 6)

(*Continued foot of next page*)

per cent of the movable material (200 cations) in the two rocks being compared. If the volumes of both the 200 cations and the associated anions in the two unit cells are considered, the movement of the cations is only a fraction of 1 per cent of the volume of the rocks.

The transformation of biotite gneiss to biotite-quartz diorite gneiss is nearly isochemical except for an increase of sodium and a decrease of potassium, which indicates that the transformation is chiefly a process of metamorphic segregation of the minerals of the biotite gneiss rather than a profound replacement.

To sum up, the transformation of basalt to hornblende schist and then to hornblende-quartz diorite gneiss, and of arkose to biotite gneiss and then to biotite-quartz diorite gneiss, requires rather small changes in chemical composition, mainly subtraction of potassium, iron, magnesium (?), and calcium (?). Some sodium had to be added to transform average basalt to hornblende schist and average arkose to biotite gneiss and then to biotite-quartz diorite gneiss. The sodium may have been derived from subjacent rocks by metamorphic differentiation. There is a vague suggestion from the trend of the curves in Figure 11 that the required sodium could have been given off in the transformation of hornblende schist to hornblende-quartz diorite gneiss, a process which appears to yield sodium.

As mentioned above, iron, magnesium, and calcium were expelled during many of the transformations, and the destination of these mafic elements is not entirely known. Some of the iron, magnesium, and calcium ions have migrated to inclusions that have been made more mafic, to septa, and to borders of replacement bodies, but since no quantitative data on the composition and size of these bodies are available, no accurate estimate can be made of their importance as a reservoir of the expelled mafic ions. A rough estimate can be made by calculating how many iron, magnesium, and calcium ions would be needed to convert a given volume of the analyzed hornblende schist to an equal volume of pure hornblendite—a process that occurred locally, as field evidence indicates. Approximately 40 ions of calcium, magnesium, and iron would be needed, provided a large amount of silicon and aluminum is expelled. When hornblende schist is transformed to either massive or gneissic hornblende-quartz diorite, approximately 8 calcium, magnesium, and iron ions, on the average, are given off. Approximately 5 volumes (40/8) of hornblende schist can thus be converted to quartz diorite while the rejected ions are used to convert 1 volume of hornblende schist to hornblendite. Figure 4 of Plate 2 shows that on this small scale the process of making inclusions more mafic probably uses all the rejected mafic ions, but on a larger scale it is difficult to be sure. Unfortunately for this hypothesis, only a few of the inclusions consist of essentially pure hornblendite. Mapped septa make up only about 10 per cent of the zone of massive and gneissic hornblende-quartz diorite; but this figure might be doubled by layers and inclusions too small to be mapped, and in that event the ratio of inclusions to gneiss would approach the 1 in 5 ratio required. The process of making inclusions more mafic may have utilized a sizable amount of the mafic material rejected during granitization.

The concept of metasomatic fronts can be applied to the migration of sodium during regional metamorphism in the northern Entiat Mountains. On the east side of the complex hornblende-quartz diorite gneisses appear to have formed from hornblende schist by subtracting sodium; on the west side biotite-quartz diorite gneiss was formed from biotite gneiss by an addition of sodium. If a zone of addition of sodium (a sodium "front") overlay a zone of subtraction of sodium in the complex while it was being metamorphosed, then the rocks on the east side of the complex must have been deeper seated than those farther west. Rocks east of the Entiat fault, in the upthrown,

---

Biotite gneiss and related rocks:

I. Possible source rock of biotite gneiss: (d) average arkose (Pettijohn, 1949, p. 259)
II. Biotite gneiss: (7) (Table 5, analysis 7)
III. Biotite-quartz diorite gneiss formed by granitization of biotite gneiss: (8) (Table 5, analysis 8)

Leucocratic quartz diorite:

Forms replacement bodies in rocks 1, 3, 5, 6, 7, and 8, particularly in 7 and 8
(9) Main dikes and masses (Table 5, analysis 9); (10) pegmatitic concretions (Chiwawa Mountain area) (Table 5, analysis 10); (11) pegmatitic dikes (Chiwawa Mountain area) (Table 5, analysis 11).

deeply eroded block, are more highly metamorphosed and migmatized and therefore were formed at greater depth than those west of the fault. Evidence for the existence of a potassium front is not clear.

The massive quartz diorites appear to contain more sodium and potassium than the hornblende-quartz diorite gneiss formed by granitization of hornblende schist. The concentration of sodium and potassium in the anatectic rocks may be due in part to crystallization differentiation after the anatectic magma had formed. It could have been concentrated in the zone of melting before fusion occurred and be derived by metamorphic differentiation during the transformation of hornblende schist to hornblende-quartz diorite gneiss—a process that appears to yield potassium and perhaps sodium—and the transformation of arkose to biotite gneiss and then to biotite-quartz diorite gneiss—a process that appears to yield potassium. The mobile metamorphic differentiates rich in sodium and potassium may have been channeled into a shear zone, in which they were trapped as a result of fusion triggered by intense differential movement.

Pegmatite bodies of leucocratic quartz diorite (units 10, 11) contain more potassium than do any of the rocks in which they occur. The added potassium was probably derived from arkose and basalt by metamorphic differentiation during their transformation to biotite gneiss and hornblende schist and then to quartz diorite gneiss, because these transformations apparently require a subtraction of potassium.

Leucocratic quartz diorite, represented except for the relatively minor pegmatitic phases by analysis 9, has been formed principally by replacement of rocks (units 1, 3, 5, 6, 7, 8) and is far more abundant in the biotite gneiss (unit 7) and biotite-quartz diorite gneiss (unit 8) than in the other rocks.

The replacement of biotite-quartz diorite gneiss by leucocratic quartz diorite is isochemical, except for a decrease in iron ions. The leucocratic quartz diorite in biotite-quartz diorite gneiss (Pl. 6, fig. 1) appears to be the felsic material left behind by segregation of felsic and mafic material rather than floods of foreign felsic material soaked into the rock. Replacement of biotite gneiss by leucocratic quartz diorite (unit 9) requires decrease of potassium and increase of sodium but very little other change. To form either biotite gneiss from arkose or biotite-quartz diorite gneiss from biotite gneiss a significant addition of sodium is apparently required. The sodium, which appears to be the principal material added to form leucocratic quartz diorite from these rocks, is therefore not derived from them, as it appears to be at first glance, but from some other source.

From the amounts of trace elements in the principal rocks of the complex (Table 5), some possible changes in the abundance of those elements during the formation of the complex can be stated. Transformation of hornblende schist to hornblende-quartz diorite gneiss and of biotite gneiss to biotite-quartz diorite gneiss was attended by a decrease of a few trace elements (Ba, Cr, Cu, Ni), although only the change in Ba may be significant, but by no appreciable change of other trace elements (B, Be, Co, Ga, Sr, Yb).

The biotite gneiss and the biotite-quartz diorite gneiss are exceptionally rich in zirconium, a fact that might be explained by supposing that both rocks were derived from an arkosic sediment rich in detrital zircon.

The leucocratic quartz diorites, which probably contain metamorphic differentiates of other rocks of the complex, are slightly enriched in barium, copper, and strontium but are not so notably enriched in the trace elements that are commonly found in felsic rocks which contain magmatic differentiates.

Origin of the Complex

Principal events in the development of the complex are believed to have been as follows:

(1) Biotite gneiss and hornblende schist, derived principally from arkosic and basaltic rocks, were subjected to particularly intense metamorphism in a zone trending northwestward along the present site of the Entiat Mountains, and were consequently transformed to hornblende and biotite-quartz diorite gneisses.

(2) In the center of this zone the hornblende-quartz diorite gneisses were in turn transformed to particularly massive quartz diorite gneiss and locally melted to form anatectic magma, much of which moved and differentiated only slightly.

(3) Elements driven off by metamorphic differentiation—potassium, sodium, and silicon—collected largely in localities of low pressure and formed bodies of leucocratic quartz diorite.

The evidence that the quartz diorite gneisses of the complex originated by granitization and never became molten is:

(1) The several bodies of quartz diorite gneiss have a tabular form, which is parallel to structures in the older rocks.

(2) The foliation and the widely distributed elongate inclusions and layers of older rocks within them are conformable, which suggests *lit-par-lit* granitization.

(3) The texture of the rocks is metamorphic.

(4) Replacement and recrystallization migmatites are present, rather than a dike complex with intrusive features, in and around the quartz diorite gneisses.

(5) There is no evidence that older rocks have been pushed aside.

(6) Gneissic quartz diorite grades into biotite gneiss and hornblende schist.

(7) The gneisses and the parent rocks are chemically similar—particularly the biotite-quartz diorite gneiss and the biotite gneiss.

(8) There is a heterogeneous and gradational mixture of gneiss and more massive rock and of regularly foliated gneisses and gneisses that have swirled foliation.

The evidence for the magmatic origin of the massive quartz diorites is:

(1) They are massive and homogeneous.

(2) Nearly everywhere their texture is igneous—*i.e.*, a definite order of crystallization is shown by interstitial quartz between subhedral crystals of plagioclase and hornblende and by the presence of oscillatory zoning in the plagioclase crystals.

(3) They have flow structure, indicated by a regular foliation rather than a contorted foliation, such as would be produced by flow of a plastic mass of mobilized metamorphic rock.

(4) Evidence of crystallization differentiation is indicated by the potassium-rich pegmatite between pieces of disrupted inclusions.

That the massive quartz diorites formed nearly in place is indicated by the following similarities to the hornblende-quartz diorite gneisses formed by granitization of hornblende schist:

(1) There is no assimilation along contacts and no evidence of pushing aside of older rocks.

(2) Inclusions are concentrated in zones in the middle of one of the sills, not at contacts.

(3) Most of the tabular inclusions are parallel to the walls, which may indicate little movement.

(4) They contain inclusions of the same hornblende schist that forms widespread and numerous inclusions in the hornblende-quartz diorite gneisses, but none of the hornblende-quartz diorite gneisses themselves, presumably because they were melted to form the anatectic magma. These inclusions of hornblende schist probably escaped fusion because they have been made more mafic during granitization and are thus schists rich in hornblende, even hornblendites, of relatively high melting point.

(5) The massive quartz diorite rocks are chemically similar to their probable parent rocks.

The features that indicate formation in place are best shown by the sill north of Ice Lakes and the one along the Entiat fault but less by the sill on the east side of Rock Creek; this sill has fewer inclusions and may be an intrusive magmatic rock formed by melting of hornblende-quartz diorite gneiss at a greater depth.

The complex appears to be confined to a remarkably narrow and sharply defined belt, but migmatites occur throughout the biotite gneisses west of the Entiat fault, and if this depressed area could be re-elevated and eroded, exhuming more intensely migmatized rocks, the contacts of the complex would probably appear broadly gradational and irregular on the west. If an anticline was formed in the original biotite gneiss and hornblende schist, mobile, infiltrating material would have tended to gather in the low-pressure area in the crest and thus to localize the quartz diorites. Though our present knowledge (Fig. 1) suggests the anticlinal position of the northern Entiat Mountains, the evidence is far from conclusive. Alternatively, the present zone of quartz diorites may once have been a zone of differential stress, which became a channel for rising mobile material when stress was relieved by shearing. Most of the differential movement for which evidence can be seen is parallel to the regional trends of the host rocks. In nearly every locality, and on all scales, the quartz diorites of the complex occur in sill-like bodies that are nearly, if not exactly, parallel to the foliation of older rocks. Structural control of replacement bodies, either by shearing or by foliation, implies that the materials that effected the transformations did so by moving along grain boundaries and incipient fractures, rather than by diffusion through crystal grains.

In the southern Entiat Mountains Waters

(1932, p. 616) observed that the Swakane biotite gneiss, which correlates with the biotite gneiss in the northern Entiat Mountains, is in contact with granodiorite gneiss, and that the contact is not "interwoven". The biotite gneiss contains increasing amounts of quartz toward the contact. From these facts Waters infers "deposition of arkose derived from the granodiorite directly on the surface of the plutonic mass, followed by dynamic metamorphism of both rocks"; in essence this is the mantled-dome hypothesis later proposed by Eskola (1948). One might attempt to apply the mantled-dome hypothesis to explain certain features in the northern Entiat Mountains. The rocks between the biotite gneiss on the west side of the quartz diorite complex in the Holden quadrangle and the gneiss along Lake Chelan near Lucerne, which is also biotite gneiss, consist mainly of granitoid rocks (Fig. 1). The hornblende schists and metasedimentary rocks in the northeast corner of the Holden quadrangle, on the east side of the quartz diorite complex, form a relatively thin septum within a broad belt of granitoid rocks. It is possible, therefore, that the quartz diorite complex is on the west side of a northwest-trending anticline of granitoid rocks mantled with biotite gneiss. The contact between such a mantle and the old basement would be a zone of differential stress and active granitization (Eskola, 1948, p. 467). The stress might have triggered fusion of hornblende-quartz diorite gneiss along the mantled anticline, and some of the anatectic magma (such as the massive quartz diorite sill east of Rock Creek) formed minor late intrusions in the same zone. These possibilities seem unlikely because reconnaissance suggests that the structure between Lake Chelan and the Entiat Mountains is a syncline rather than an anticline, and there is no clear evidence of more than one period of metamorphism.

The controversy over the origin of the granitoid rocks is no longer so much over how they form as over the relative abundance of the granitized masses and the magmatic masses and the source of the magmas and the granitizing emanations. This study of a small area indicates that, at the level of erosion represented, about 25 per cent of the granitoid rocks are magmatic and 75 per cent granitized. Three possible sources of the magma that forms granitoid rocks are: (1) differentiates of a basaltic magma, (2a) melting of the original granitic crust of the earth, and (2b) melting of the sedimentary and volcanic rocks in a tectogene. Evidence from the northern Entiat Mountains points to the last alternative. Three principal alternatives for the origin of the emanations are: (1) magmatic differentiation, (2a) metamorphic differentiation of a tectogene, and (2b) metamorphic differentiation of the crustal or subcrustal material around a tectogene; evidence from this study indicates that the emanations are sweated from the tectogene. Very little chemical change is needed to effect many of the transformations in the northern Entiat Mountains. The dominant process does not appear to be replacement but recrystallization and metamorphic segregation—*i.e.*, the emanations appear to have acted more as catalysts to granitization than as suppliers of new material.

All the rocks in the northern Entiat Mountains may be treated as parts of two stratigraphic units—a unit on the west of biotite gneiss and all rocks derived from it, and a unit on the east of hornblende schist and its derivatives. Igneous intrusion played a minor role. Although the original biotite gneiss and hornblende schist have been granitized and migmatized and in places even melted, it is still possible to find traces of their structure and chemical composition in the quartz diorites formed from them.

References Cited

Barth, T. F. W., 1948, Oxygen in rocks: Jour. Geology, v. 56, p. 50–60.

—— 1952, Theoretical petrology: N. Y., John Wiley & Sons, 387 p.

—— 1955, Presentation of rock analyses: Jour. Geology, v. 63, p. 348–363

Bennington, K. O., 1956, Role of shearing, stress and pressure in differentiation as illustrated by some mineral reactions in the system MgO-SiO_2-H_2O: Jour. Geology, v. 64, p. 558–577

Bowen, N. L., and Tuttle, O. F., 1949, The system MgO-SiO_2-H_2O: Geol. Soc. America Bull., v. 60, p. 439–460

Compton, R. R., 1955, Trondhjemite batholith near Bidwell Bar, California: Geol. Soc. America Bull., v. 66, p. 9–44

Daly, R. A., 1912, Geology of the North American Cordillera at the forty-ninth parallel: Canada Geol. Survey Mem. 38, 857 p.

—— 1933, Igneous rocks and the depths of the earth: N. Y. and London, McGraw-Hill Book Co., Inc., 598 p.

Dubois, R. L., 1956, Petrology of the Holden mine area, Washington (Abstract): Geol. Soc. America Bull., v. 69, p. 1766

Eskola, P. E., 1948, The problem of mantled gneiss domes: Geol. Soc. London Quart. Jour., v. 104, p. 461–476
— 1952, On the granulites of Lapland: Am. Jour. Sci., Bowen Volume, p. 133–171
Geological Survey of Canada, 1944, Hope, Yale and New Westminster districts, British Columbia: Canada Dept. Mines and Res., Mines and Geology Br., Bur. Geology and Topography map no. 737A
Goodspeed, G. E., 1953, Rheomorphic breccias: Am. Jour. Sci., v. 251, p. 453–469
Guard, A. K., and Carithers, W., 1945, Geology and ore deposits of the Sultan Basin, Snohomish County, Washington: State of Wash. Div. Mines and Geology Bull. 36, 90 p.
Hall, A. J., 1941, Relation between colour and chemical composition in the biotites: Am. Mineralogist, v. 26, p. 29–33
Holmquist, P. J., 1921, Typen und nomenklatur der adergestine: Geol. Fören. Stockholm Förh., Band 43, p. 612, 631
Misch, Peter, 1952, Geology of the Northern Cascades, Washington: The Mountaineers, v. 55, no. 13, p. 4–22
Noble, J. A., 1952, Evaluation of criteria for the forcible intrusion of magma: Jour. Geology, v. 60, p. 34–57
Pettijohn, F. J., 1949, Sedimentary rocks: N. Y., Harper and Brothers, 526 p.
Ramberg, Hans, 1949, The facies classification of rocks: a clue to the origin of quartzo-feldspathic massifs and veins: Jour. Geology, v. 57, p. 18–54
Read, H. H., 1944, Meditations on granite; Part II: Geologists Assoc. London Proc., v. 55, pt. 2, p. 45–93
Rice, H. M. A., 1947, Geology and mineral deposits of the Princeton Map Area, British Columbia: Canada Geol. Survey Mem. 243, 136 p.
Richarz, Stephen, 1933, Peculiar gneisses and ore formations in the eastern Cascades, Washington: Jour. Geology, v. 41, p. 757–768
Russell, I. C., 1898, A preliminary paper on the geology of the Cascade Mountains of northern Washington: U. S. Geol. Survey 20th Ann. Rept., pt. 2, p. 83–210
Sederholm, J. J., 1907, Om granit och gneis, deras uppkomst, upp trädande och utbredning inom urberget i Fennoscandia: Comm. Geol. Finlande Bull. 23, 110 p.
— 1926, On migmatites and associated Pre-Cambrian rocks of southwestern Finland, Part II, The region around the Barosundsfjord w. of Helsingfors and neighboring areas: Comm. Geol. Finlande Bull. 77, 143 p.
Shapiro, Leonard, and Brannock, W. W., 1956, Rapid analysis of silicate rocks: U. S. Geol. Survey Bull. 1036C, p. 19–56
Smith, G. O., 1904, Mt. Stuart folio: U. S. Geol. Survey Geol. Atlas, folio 106, 10 p.
Smith, G. O., and Calkins, F. C., 1904, A geological reconnaissance across the Cascade Range near the forty-ninth parallel: U. S. Geol. Survey Bull. 235, 103 p.
—— 1906, Snoqualmie folio: U. S. Geol. Survey Geol. Atlas, folio 139, 14 p.
Smith, W. S., 1915, Petrology and economic geology of the Skykomish Basin: Columbia School Mines Quart., v. 36, p. 154–185
—— 1916, Stratigraphy of the Skykomish Basin, Washington: Jour. Geology, v. 24, p. 559–583
Spurr, J. E., 1900–1901, The ore deposits of Monte Cristo, Washington: U. S. Geol. Survey 22d Ann. Rept., pt. 2, p. 777–865
Thompson, M. L., Wheeler, H. E., and Danner, W. R., 1950, Middle and upper Permian fusulinids of Washington and British Columbia: Cushman Found. for Foram. Research Contr., v. 1, pts. 3 and 4, p. 46–63
Turner, F. J., and Verhoogen, Jean, 1951, Igneous and metamorphic petrology: N. Y., McGraw-Hill Book Co., Inc., 620 p.
Waters, A. C., 1932, Petrologic and structural studies of the Swakane gneiss, Entiat Mountains, Washington: Jour. Geology, v. 40, p. 604–633
—— 1955, Volcanic rocks and the tectonic cycle, p. 703–712 *in* Poldervaart, A., *Editor*, Crust of the earth: Geol. Soc. America Special Paper 62, 762 p.
Weaver, C. E., 1912, Geology and ore deposits of the Index mining district: Wash. Geol. Survey Bull. 7, 104 p.
Wegmann, C. E., 1935, Zur deutung der migmatite: Geol. Rundschau, Band 26, p. 305–350
Willis, C. L., 1953, The Chiwaukum graben, a major structure of central Washington: Am. Jour. Sci., v. 251, p. 789–797
Youngberg, E. A., and Wilson, T. L., 1952, The geology of the Holden mine: Econ. Geology, v. 47, p. 1–12

U. S. Geological Survey, Denver, Colo.
Manuscript Received by the Secretary of the Society, May 16, 1958
Publication Authorized by the Director, U. S. Geological Survey

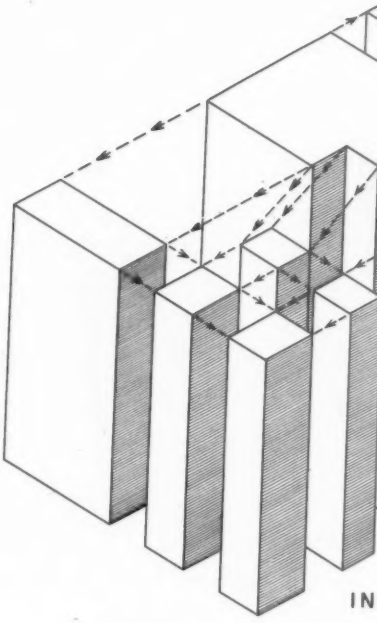

IN

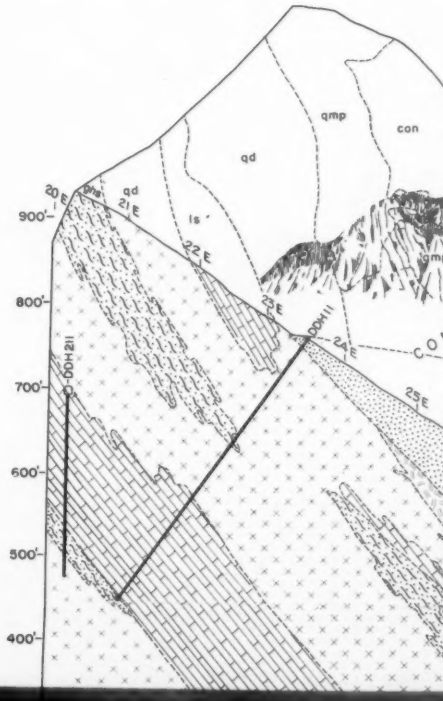
qmp
con
qd
ls
20 E
21 E
22 E
23 E
24 E
25 E
900'
800'
700'
600'
500'
400'
DDH 11
DDH 21

INDEX DIAGRAM

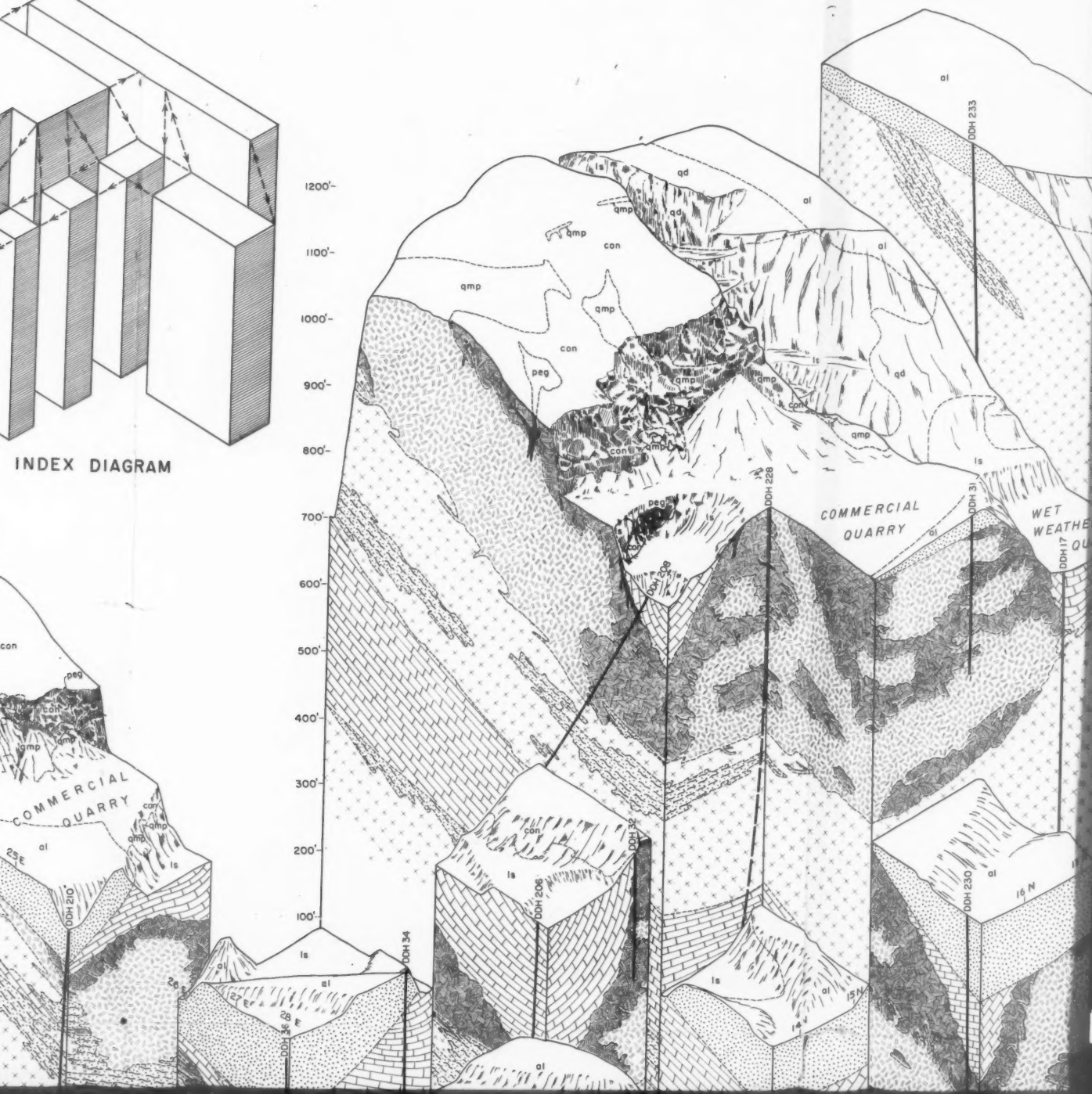

DIAGRAM

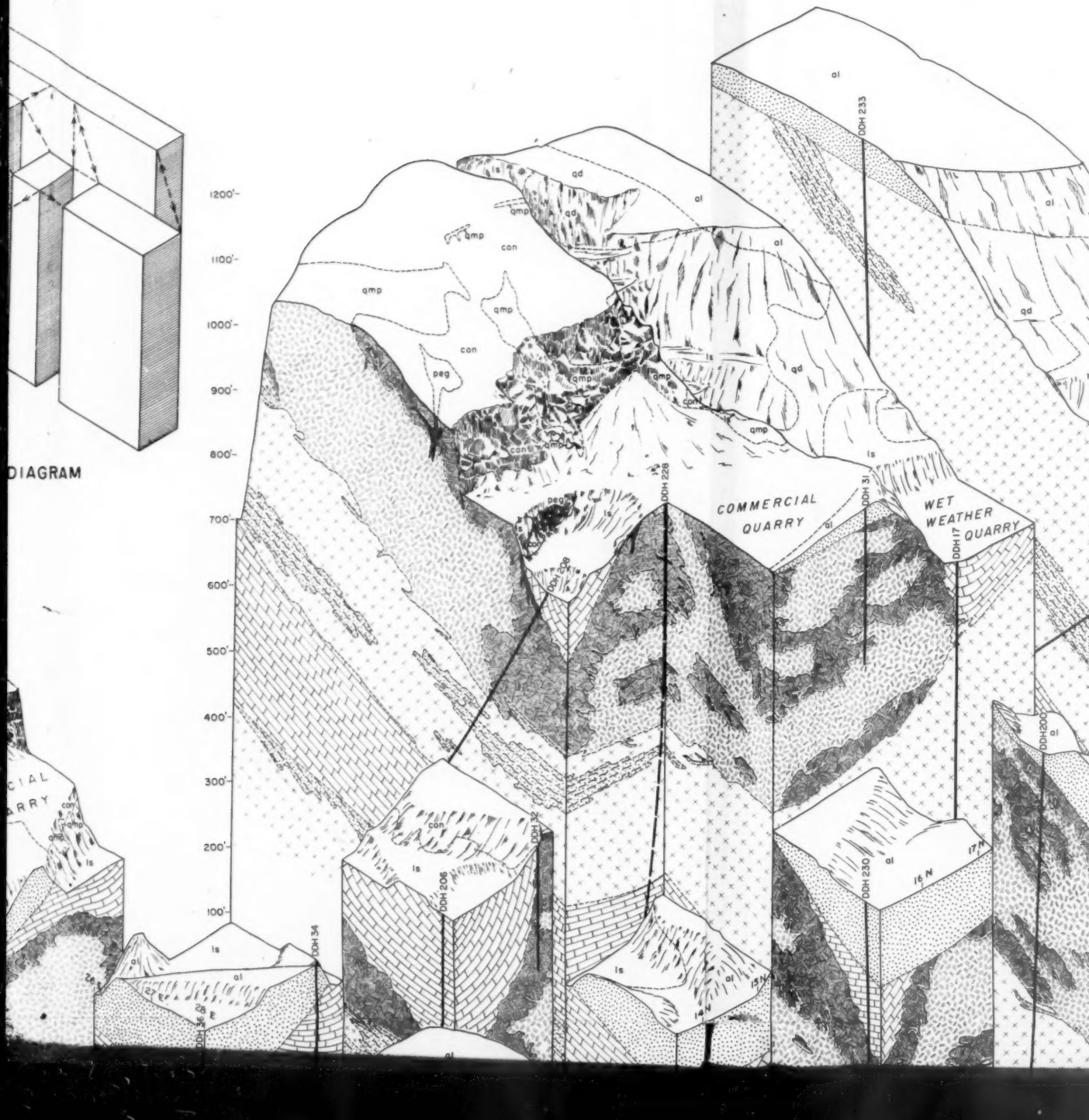
1200'
1100'
1000'
900'
800'
700'
600'
500'
400'
300'
200'
100'
al
qd
qmp
con
peg
ls
DDH 233
DDH 228
DDH 31
DDH 17
DDH 206
DDH 34
DDH 230
DDH 200
COMMERCIAL QUARRY
WET WEATHER QUARRY
16 N
17 N
14 N
15 N

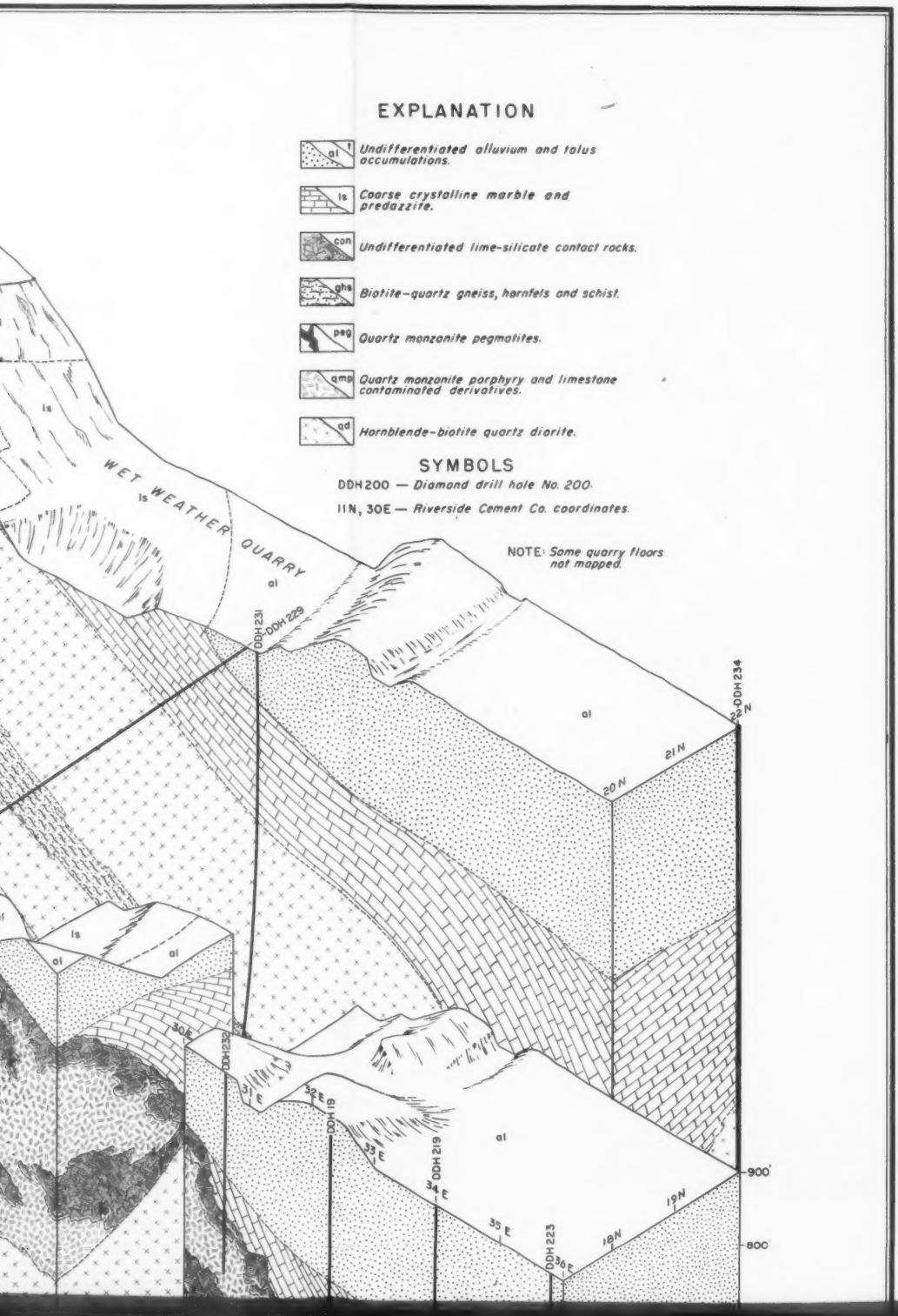
EXPLANATION
al
Undifferentiated alluvium and talus accumulations.
ls
Coarse crystalline marble and predazzite.
con
Undifferentiated lime-silicate contact rocks.
ghs
Biotite-quartz gneiss, hornfels and schist.
peg
Quartz monzonite pegmatites.
qmp
Quartz monzonite porphyry and limestone contaminated derivatives.
qd
Hornblende-biotite quartz diorite.
SYMBOLS
DDH 200 — Diamond drill hole No. 200.
11N, 30E — Riverside Cement Co. coordinates.
NOTE: Some quarry floors not mapped.
WET WEATHER QUARRY
DDH 231
DDH 229
DDH 234
22 N
21 N
20 N
19 N
18 N
30 E
31 E
32 E
33 E
34 E
35 E
36 E
DDH 232
DDH 219
DDH 223
900'
800'

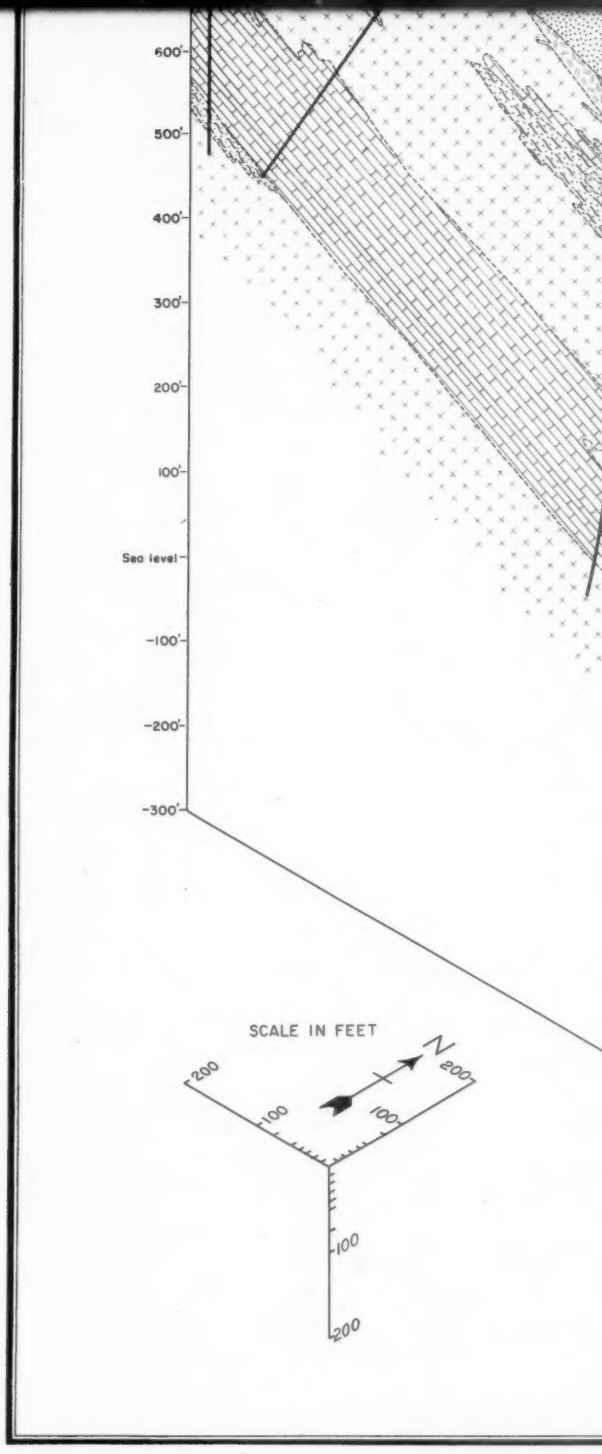
600'
500'
400'
300'
200'
100'
Sea level
-100'
-200'
-300'
SCALE IN FEET
200
100
N
200
100
100
200

E

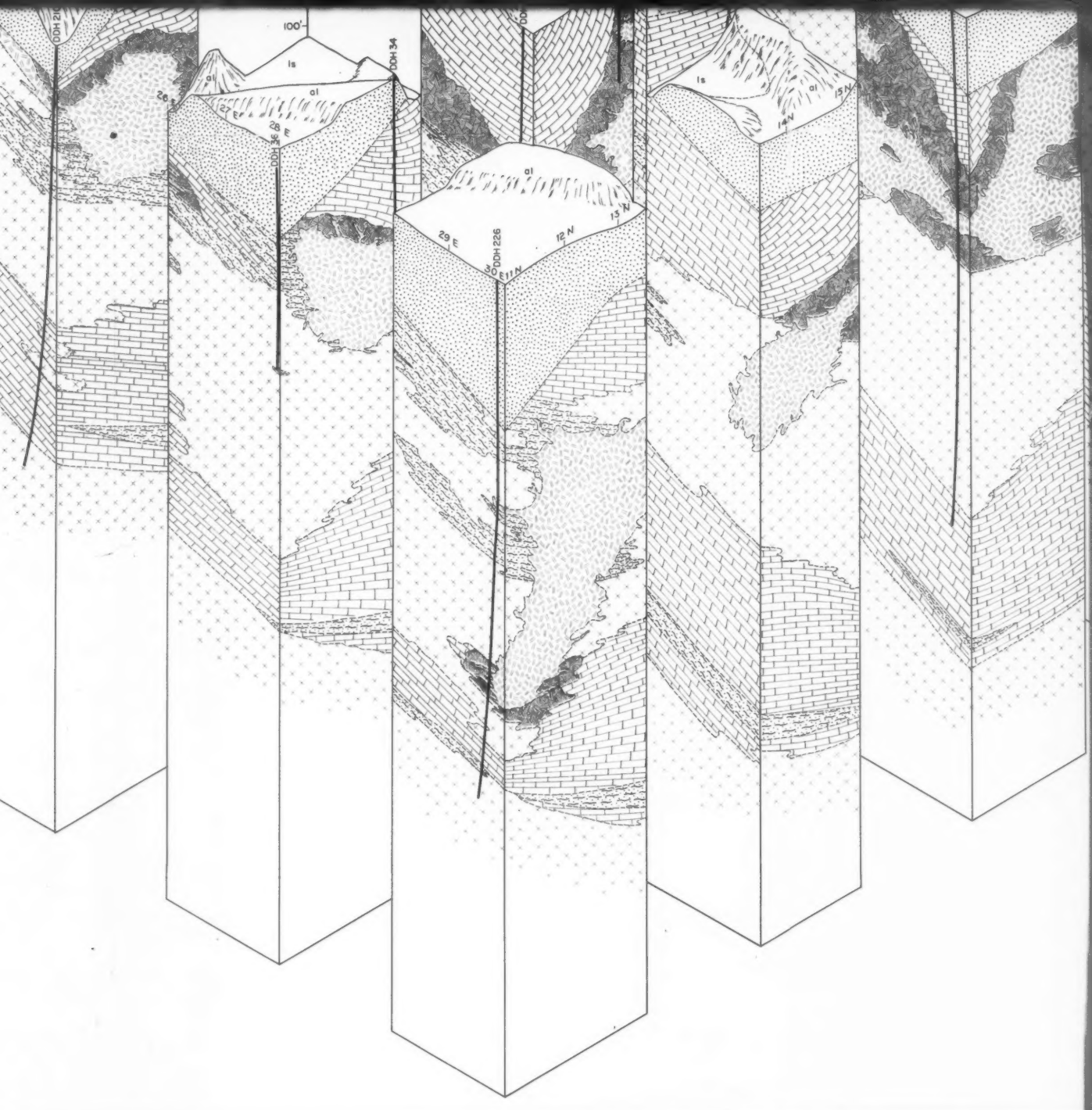

EXPLODED ISOMETRIC BLOCK DIAGRAM OF THE COMMERCIAL QUARRY.

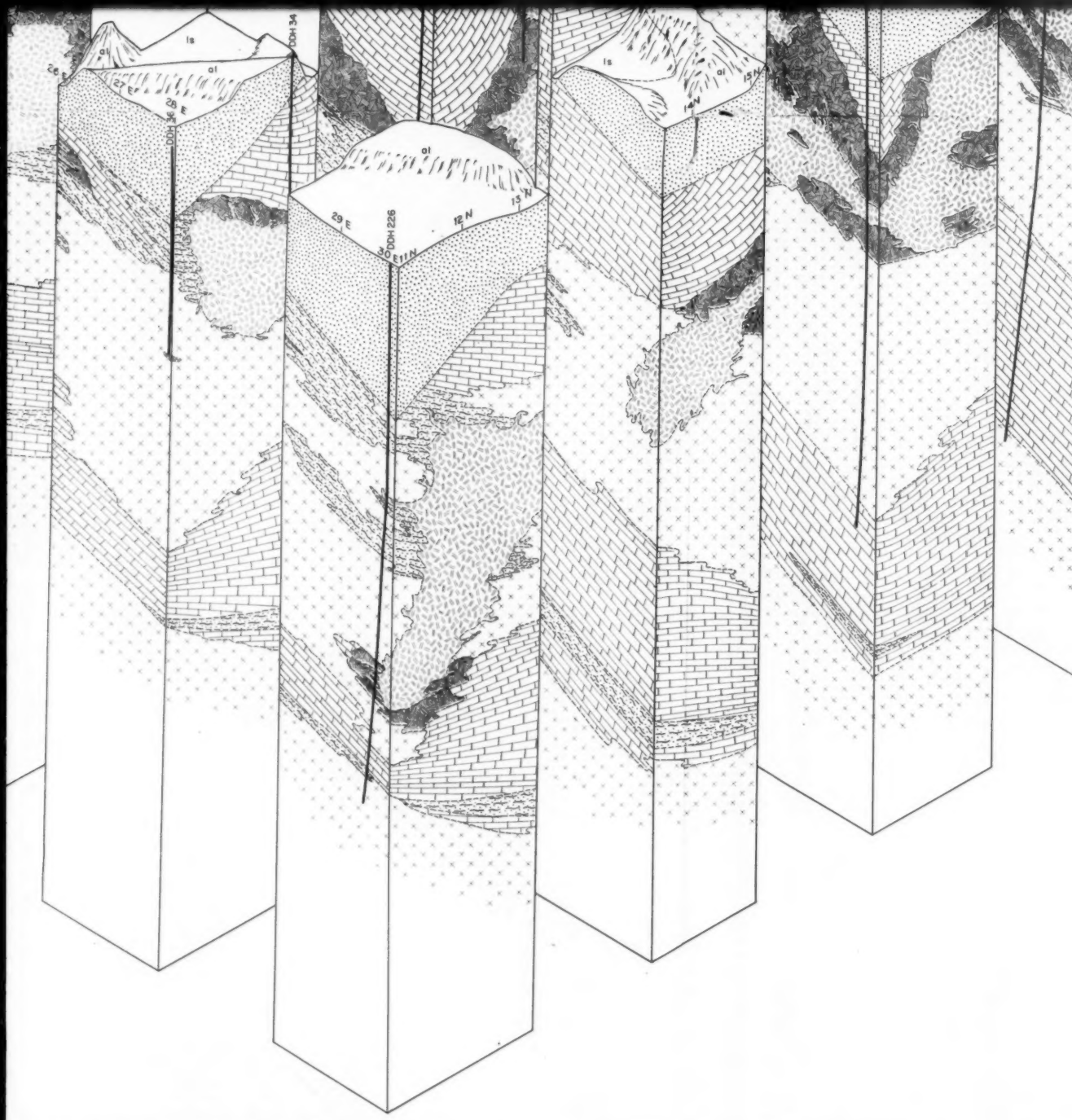

ED ISOMETRIC BLOCK DIAGRAM OF THE COMMERCIAL QUARRY, CRES

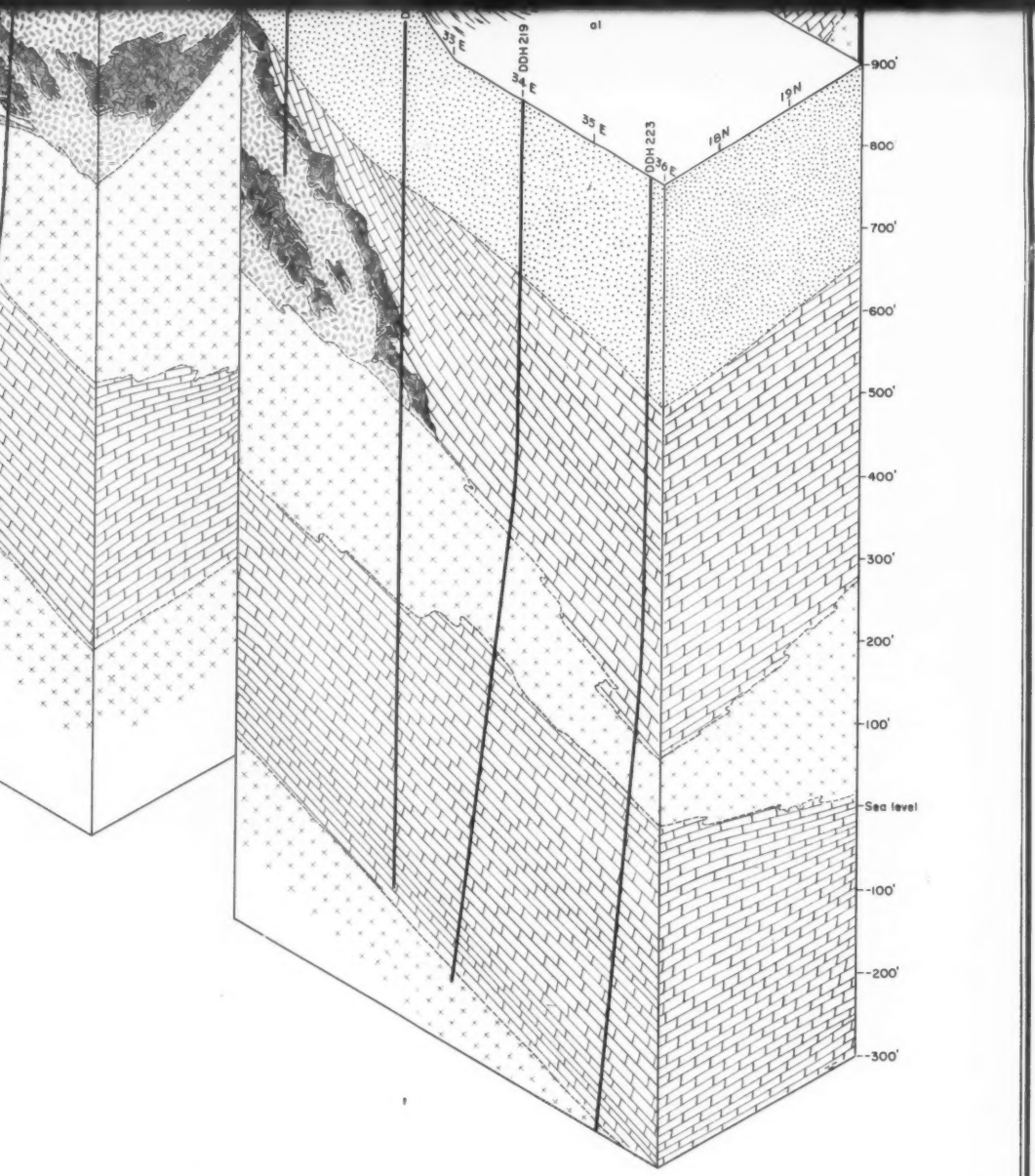

ESTMORE, CALIFORNIA

BULLETIN OF THE GEOLOGICAL SOCIETY OF AMERICA
VOL. 70, PP. 879–920, 6 FIGS., 10 PLS. JULY 1959

CONTACT METAMORPHISM OF MAGNESIAN LIMESTONES AT CRESTMORE, CALIFORNIA

By C. Wayne Burnham

Abstract

The contact-metamorphic rocks at Crestmore, California, occur between magnesian marbles and a plutonic mass of quartz diorite (Bonsall tonalite) and between the same marbles and a relatively small pipelike hypabyssal mass of quartz monzonite porphyry.

The marbles are preserved as two crudely lenticular bodies about 400 and 500 feet thick, respectively, that occur as screens in the quartz dioritic intrusive rocks of the southern California batholith. Both bodies, which are very similar petrographically, are composed of alternating layers of predazzite and coarsely crystalline calcite marbles and are nearly free of silica, alumina, iron, and the alkalies.

The quartz diorite that engulfed the marbles is contaminated locally very near the contacts where minor monzonitic and gabbroic variants are present. Its exomorphic effects on the carbonate rocks consist mainly of: (1) the formation of metasomatic silicate contact rocks that generally are less than 1 foot thick and are composed of diopside, wollastonite, and grossularite; and (2) the conversion of nearly all the magnesium-bearing carbonate beds to periclase marbles, which subsequently were altered to predazzites.

In contrast, the younger quartz monzonite porphyry, which was injected into the upper or Sky Blue marble unit, is nearly all contaminated as a result of reactive assimilation of marble. Moreover, its exomorphic silicate aureole is as much as 50 feet thick and contains the numerous complex mineral assemblages for which Crestmore is famous. Several lines of evidence indicate that much of this aureole was formed prior to the final consolidation of the porphyry intrusive mass.

The thicker parts of the silicate contact aureole that surrounds the quartz monzonite porphyry exhibit the following well-defined zonal distribution of mineral assemblages, as traced outward from the intrusive body: (1) a garnet zone that is composed of grossularite and lesser amounts of wollastonite and diopside; (2) a zone characterized by only one mineral, idocrase; and (3) a zone in which monticellite is the most abundant mineral, but in which there are various amounts of clinohumite, cuspidine, ellestadite, forsterite, melilite, merwinite, perovskite, spinel, spurrite, tilleyite, and xanthophyllite. This zonation of mineral assemblages reflects a corresponding zonation in the bulk chemical composition of the rocks, as shown by changes in the ratio of metasomatic to indigenous constituents (Si + Al + Fe/Ca + Mg) from 0.66 in the monticellite zone, through 1.15 in the idocrase zone, to 1.62 in the garnet zone.

There also is a strong tendency toward a mineralogical zonation within the monticellite zone, such that clinohumite, forsterite, spurrite, and spinel are concentrated in the silica-poor and calcite-rich outer part, and merwinite, cuspidine, and melilite in the more silica-rich inner part. Hence, a sequential occurrence of mineral assemblages and a change in bulk chemical composition can be traced inward toward the intrusive mass from unmetasomatized marbles. Moreover, textural features reveal a corresponding paragenetic sequence in which the more highly metasomatized assemblages appear to have formed at the expense of those that were less metasomatized.

Available evidence indicates that: (1) the contact-metamorphic mineral assemblages at Crestmore and their zonation are largely the compositionally controlled products of silica, alumina, and iron metasomatism of relatively pure magnesian limestones; (2) temperatures of 625°C. or higher were reached prior to the introduction of silica into the present monticellite-zone rocks; and (3) the so-called "high-temperature" assemblages, such as monticellite, spurrite, and melilite, formed directly from the magnesian marbles without the intervention of "lower-temperature" steps that involve diopside, wollastonite, and grossularite. Therefore, it is proposed that contact metamorphism at Crestmore should be viewed as progressive metasomatism with consequent decarbonation at elevated temperatures rather than as progressive decarbonation attendant simply upon rising temperature.

CONTENTS

TEXT

	Page
Introduction	880
General statement	880
Location and historical sketch	881
Present study	881
Acknowledgments	881
Geologic setting	883
Petrology	884
Pre-batholith metasedimentary rocks	884
Igneous rocks	886
Quartz diorite	886
Quartz monzonite porphyry	890
Contaminated rocks	893
Quartz monzonite pegmatites	897
Contact rocks	899
General statement	899
Monticellite zone	901
Idocrase zone	908
Garnet zone	911
Summary and comparison	912
Origin of the contact rocks	915
References cited	918

ILLUSTRATIONS

Figure	Page
1. Generalized geologic map of the Crestmore Hills	882
2. Generalized geologic map of faces of the Commercial Quarry	885
3. Idealized north-south cross section through quartz monzonite porphyry intrusion at Crestmore	900
4. Tetrahedral composition diagram for part of the system Ca-Mg, Fe^{+2}-Si-Al, Fe^{+3}	913
5. Variations in composition of the rocks in the contact aureole at Crestmore as compared with the parental Sky Blue marble	914
6. P_{CO_2}-T curves for the reactions: $CaCO_3 + SiO_2 = CaSiO_3 + CO_2$ and $2CaSiO_3 + 3CaCO_3 = 2Ca_2SiO_4.CaCO_3 + 2CO_2$	916

Plate	Facing page
1. Exploded isometric block diagram of the Commercial Quarry, Crestmore, California	879

	Following page
2. Air photograph of the Crestmore hills and plant, mine, and quarries of the Riverside Cement Company	882
3. Oblique aerial view of the Commercial Quarry, Crestmore, California	
4. Exposures in the Commercial Quarry	
5. Photomicrographs	
6. Photomicrographs	
7. Photomicrographs	
8. Photomicrographs	908
9. Photomicrographs	
10. Geologic map of faces of the Commercial Quarry, Crestmore, California	920

TABLES

Table	Page
1. Chemical composition of the Sky Blue marble	886
2. Mineral composition of the quartz diorite and allied rocks	887
3. Chemical composition of the quartz diorite	888
4. Mineral composition of the quartz monzonite porphyry	891
5. Chemical composition of the quartz monzonite porphyry	892
6. Mineral composition of the contaminated rocks	894
7. Chemical composition of the contaminated rocks	895
8. Chemical composition of prehnite and "orthoclase" from pegmatite	898
9. Chemical composition of monticellite-zone rocks and minerals	902
10. Chemical composition of idocrase-zone rocks and minerals	903
11. Chemical composition of garnet-zone rocks and minerals	904

INTRODUCTION

General Statement

The contact-metamorphic deposits at Crestmore, California, have received much attention from mineralogists and petrologists during the past four decades principally because they contain a large number of minerals, many of which are presumed to indicate extraordinary conditions of metamorphism. Attention was focused early on the identification of the many new and rare minerals that were found in the deposits (Eakle and Rogers, 1914; Eakle, 1914, 1916, 1917, 1920, 1921, 1925, 1927; Rogers, 1918, 1929; Foshag, 1920a, 1920b, 1924; Larsen and Foshag, 1921; Tilley, 1928; Larsen and Dunham, 1933; Moehlman and Gonyer, 1934), and later preliminary studies were made of rock textures (Dunham, 1933) and mineral paragenesis (J. W. Daly, 1935). Few investigators (Daly, 1935; Woodford *et al.*, 1941) have dealt with the geologic mode of occurrence of the minerals and mineral assemblages, and no one has studied in detail the rocks or the spatial and genetic relationships of the metamorphic-mineral assemblages to the parental carbonate and intrusive rocks. The present studies were undertaken largely to obtain detailed information on these features and relationships because a knowledge of them is essential to an understanding of contact-metamorphic processes—the ultimate objective of this work. Consequently, this paper, which is a first step toward the ultimate objective, consists mainly of a detailed description of the rocks at Crestmore and a discussion of their modes of formation.

Location and Historical Sketch

The Crestmore quarries and mine of the Riverside Cement Company lie at the eastern end of the Jurupa Mountains, 50 miles east of Los Angeles and 3 miles north of Riverside. The original quarry site on Chino Hill (Fig. 1; Pl. 2), known as the Chino Quarry, was opened in 1908 for "limestone" (marble) to be used in the manufacture of portland cement. In the years immediately following, other quarries were opened on the north and east sides of Sky Blue Hill. The quarry on the east side of this hill, known as the Commercial Quarry (Fig. 1; Pls. 1, 2, 3, and 10), was worked primarily for riprap and is the site of the original discovery of the complex mineral assemblages for which Crestmore is famous (Eakle and Rogers, 1914.) However, in 1947 a small amount of "limestone" was quarried from the lower levels of this opening for the manufacture of cement. During World War II the old North Star and Lone Star quarries on the north side of Sky Blue Hill were nearly obliterated by the westward extension of the Wet Weather quarry. Moreover, underground mining operations, in which a modified system of block-caving is employed, have nearly obliterated the original Chino Quarry. They also have yielded the major part of the "limestone" obtained from the Crestmore deposits.

Present Study

This study of contact metamorphism at Crestmore was undertaken in 1950 and has been carried on intermittently to the present. It has been greatly facilitated by information obtained from extensive diamond drilling by the Riverside Cement Company during 1951 and 1952. Part of this information pertains to the spatial distribution of the rocks and is summarized in the exploded block diagram (Pl. 1); another part, obtained from a detailed petrographic study of many thousands of feet of drill core, constitutes the basis for much of the text discussion. An opportunity seldom is afforded for a detailed three-dimensional study of such petrologically important deposits as those at Crestmore, and it is largely due to knowledge of the third dimension that many of the genetic, as well as the spatial, relationships of the rocks are now more clearly defined.

The results of the field work, which was done mainly in 1951 and 1952, are presented in part in the generalized geologic map of Figure 1, the detailed geologic map of Plate 10, and the exploded block diagram (Pl. 1). Plate 10 was made as an overlay on the oblique aerial photograph (Pl. 3) and has essentially the same direction of view as Plate 1. A preliminary report summarizing part of this work already has been published (Burnham, 1954), but much of the information that is embodied in the present paper, especially on the chemical composition of the Crestmore rocks, has been obtained since then. Moreover, many experimental data on contact-metamorphic processes have been obtained recently and, although these data do not appear directly in this paper, many of the interpretations and conclusions are influenced by them.

There are many still unsolved problems connected with the Crestmore deposits, especially those involving the retrograde alteration products of prograde minerals. Even though these retrograde minerals present a separate petrologic problem that doubtless is worthy of further detailed study, they have been ignored for the most part in this study because they are not directly involved in the prograde contact metamorphism, the primary concern of this work.

Acknowledgments

The writer is grateful for the wholehearted co-operation of the officials of the Riverside Cement Company, and especially for their generosity in allowing him complete access to diamond-drill records and cores. He also has derived much benefit from discussion of the problem with Messrs. R. H. Wightman and C. D. Chandler of the mining department. The problem was first suggested by Dr. A. O. Woodford, and both he and Dr. R. H. Jahns have offered many valuable suggestions and criticisms in the course of the work. The manuscript has been read critically by Dr. Jahns, and his detailed comments and suggestions are greatly appreciated.

Sixteen complete chemical analyses of Crestmore rocks were financed by a grant from The Penrose Bequest of The Geological Society of America, and the funds for the aerial photograph in Plate 3 were provided by the Claremont Graduate School. The cost of approximately 200 thin sections and of drafting Plates 1 and 10 was borne by the California Institute of Technology. Laboratory facilities for this work have been generously provided by the California Institute of Technology and the Pennsylvania State University.

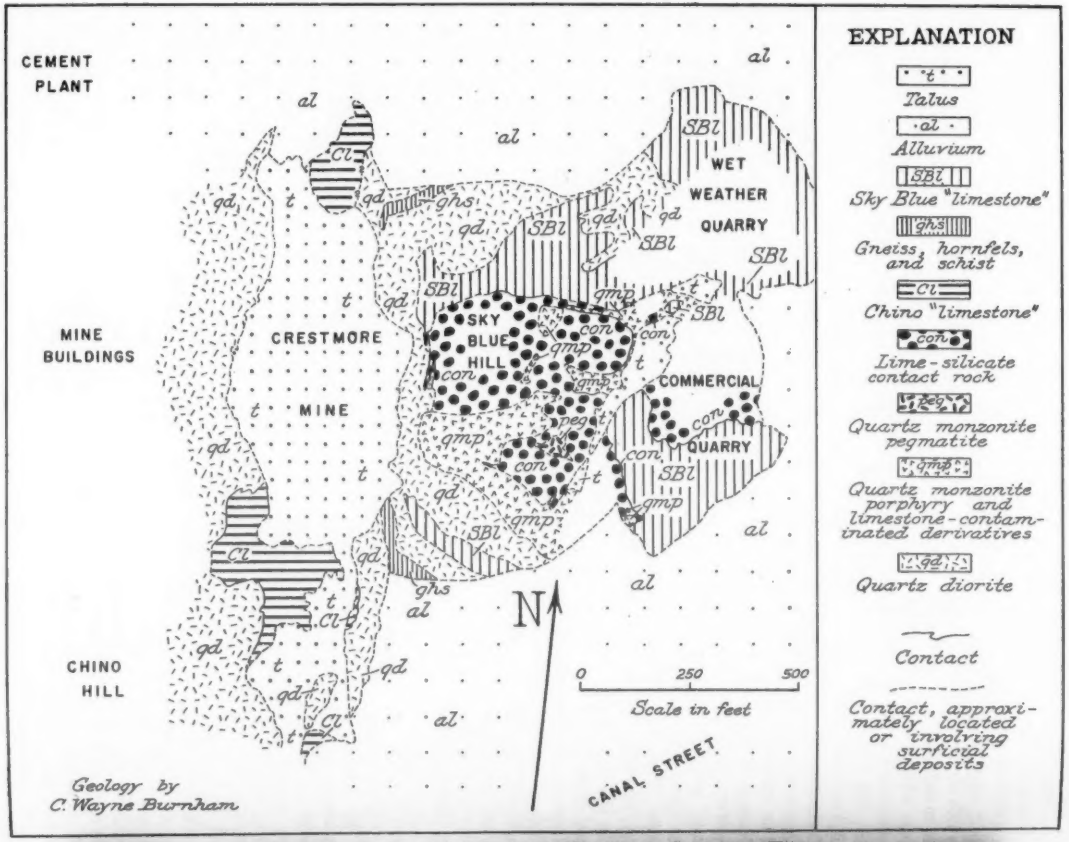

FIGURE 1.—GENERALIZED GEOLOGIC MAP OF THE CRESTMORE HILLS
Continued with Plate 2

FIGURE 1.—GENERALIZED GEOLOGIC MAP OF THE CRESTMORE HILLS
Continued with Plate 2

AIR PHOTOGRAPH OF THE CRESTMORE HILLS AND PLANT, MINE, AND QUARRIES OF THE RIVERSIDE CEMENT COMPANY

Contacts between major rock units are shown by dashed and dotted lines (see Fig. 1). MacPherson Aerial Surveys photograph.

OBLIQUE AERIAL VIEW OF THE COMMERCIAL QUARRY, CRESTMORE, CALIFORNIA
R. C. Frampton photograph.

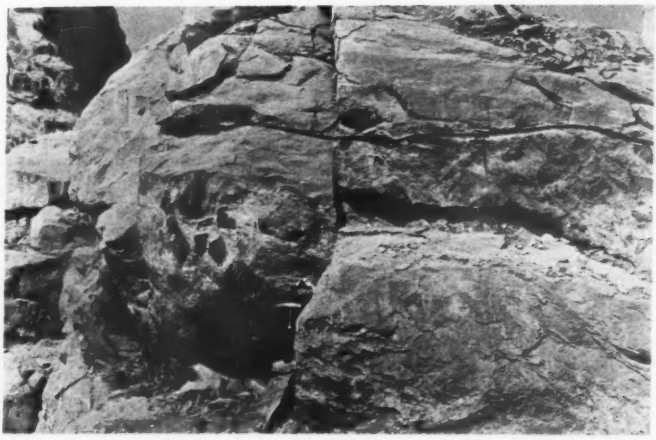

FIGURE 1

FIGURE 2

FIGURE 3

EXPOSURES IN THE COMMERCIAL QUARRY

OBLIQUE AERIAL VIEW OF THE COMMERCIAL QUARRY, CRESTMORE, CALIFORNIA
R. C. Frampton photograph.

FIGURE 1

FIGURE 2

PHOTOMICROGRAPHS

Geologic Setting

The carbonate rocks in which the contact deposits at Crestmore occur form part of a thick sequence of predominantly siliceous metasedimentary rocks that are widespread in the Peninsular Ranges of southern California. They appear to be either late Paleozoic (Woodford *et al.*, 1941) or Triassic (MacKevett, 1951) and commonly occur as screens in the plutonic rocks of the southern California batholith (Larsen, 1948).

The country rock in which the metasedimentary screens at Crestmore occur is a quartz diorite of early late Cretaceous age (Larsen *et al.*, 1954). This quartz diorite is equivalent to the Bonsall tonalite of Larsen (1948) and constitutes the northernmost exposures of the intrusive rocks of the southern California batholith. Locally, and apparently only at Crestmore, both the metasedimentary rocks and the quartz diorite are intruded by a relatively small body of aplitic quartz monsonite porphyry, the age of which is unknown. It is with this body of porphyry that the complex contact-metamorphic mineral assemblages are associated.

The major structural features of the Crestmore area are relatively simple, although locally and on a small scale the metasedimentary rocks are highly deformed. The greatest deformation occurs in the marbles and clearly is related to the intrusion of the quartz diorite and quartz monzonite porphyry magmas. In general, the bedding in the metasedimentary rocks strikes slightly west of north and dips moderately eastward. The steepest dips (up to 80°) occur in the vicinity of Crestmore Mine (Pl. 2), but in the eastern part of the area the dip is uniformly about 20°. Generally concordant attitudes are exhibited by the foliation in the quartz diorite and by the contacts between the quartz diorite and the metasedimentary screens throughout the northern part of the batholith.

The relatively minor structural features in the Crestmore area are somewhat complex. The lower body of marble (called the Chino limestone by Woodford *et al.*, 1941, the Chino Quarry limestone by J. W. Daly, 1935, and the Chino Hill limestone by Eakle, 1917) has been deformed into a shallow eastward-plunging syncline, whereas directly above this syncline the upper marble body (called the Sky Blue limestone by Woodford *et al.*, 1941) has been arched into an eastward-plunging anticline. The Chino marble body has been thinned considerably in the trough of the syncline and thickened correspondingly on the limbs. Numerous small rolls and crenulations in the thickened limbs, with their axes plunging roughly parallel to the axis of the larger syncline, indicate that these deformational features were produced in large part by the intrusion of the sill-like mass of quartz diorite that lies between the two marble units, as shown in Plate 1. Similarly, it appears that the anticline in the Sky Blue marble was produced by the forcible intrusion of the quartz monzonite porphyry magma.

Another noteworthy structural feature at Crestmore is a small steeply dipping fault that strikes about N. 65° E. across the south slope of Sky Blue Hill and into the Commercial Quarry (Fig. 2; Pl. 10). Slickensides in the Commercial Quarry, which plunge about 25° southwest, and the offset of the metasedimentary rocks above

---

PLATE 4.—EXPOSURES IN THE COMMERCIAL QUARRY

FIGURE 1.—Contact between garnet-contaminated rock breccia and Sky Blue marble above station *G* (Fig. 2; Pl. 10).

FIGURE 2.—Garnet-contaminated rock breccia above station *F* (Fig. 2; Pl. 10). Calcite has been partially leached from the pegmatitic matrix, leaving angular cavities.

FIGURE 3.—Well-zoned prehnite-, calcite-, and wollastonite-bearing pegmatite below station *C* (Figure 2; Pl. 10).

PLATE 5.—PHOTOMICROGRAPHS

FIGURE 1.—Graphic intergrowth of wollastonite and potassium feldspar in pegmatitic contaminated rock. The feldspar of the intergrowth is interstitial to plagioclase and quartz, as in Plate 7, figure 2. Crossed nicols, ×65.

FIGURE 2.—Contact between predazzite (lower right) and monticellite-zone rock. Represents the limit of contact metasomatism associated with the intrusion of quartz monzonite porphyry. Crossed nicols, ×6.

Crestmore Mine indicate that the displacement along this fault has been about 4 feet in a left-lateral oblique sense. This fault does not appear to extend westward to the footwall of the Chino marble and therefore is presumed to die out within this carbonate body.

Petrology

Pre-Batholith Metasedimentary Rocks

Although the pre-batholith rocks throughout the northern part of the Peninsular Ranges are predominantly siliceous, those at Crestmore are mainly calcareous. Several thousand feet of the siliceous metasediments occur in the Jurupa Mountains west of Crestmore, and inasmuch as they have a persistent eastward dip, it appears that the marbles overlie the siliceous rocks. A similar sequence occurs about 30 miles south of Crestmore, where about 15,000 feet of siliceous metamorphic rocks are capped by magnesian marbles.

The noncalcareous metasediments at Crestmore consist largely of feldspathic biotite-quartz gneisses, schists, and hornfelses. They occur mainly between the Chino and Sky Blue marbles and locally interfinger with both these units. They also locally underlie the Chino marble (Pl. 1). The gneisses commonly are ptygmatically folded and injected *lit-par-lit* by quartzo-feldspathic material, especially near contacts with igneous rocks.

The contacts between the siliceous metasediments and the marbles generally are sharp, as the transition from noncalcareous siliceous rocks to nonsiliceous marbles commonly is spanned in a single thin section. Locally, however, the contacts are somewhat more gradational, and the resulting transition rocks are pyroxene- and/or wollastonite-rich gneisses and schists. Whether diopsidic pyroxene or wollastonite predominates in these rocks depends largely upon the magnesium content of the original sediments.

The marble units appear to be crudely lenticular, although locally their shapes are somewhat irregular owing to deformation and interfingering with the siliceous metasediments. The two bodies thicken toward the east and tend to converge, although they do not join in the area of the quarries. About 2000 feet east of the quarries the Chino marble is nearly 400 feet thick, and the Sky Blue marble is more than 500 feet thick.

The chemical and petrographic features of both marble units are similar in every respect. They are composed in part of alternating layers of predazzite and light-gray coarsely crystalline calcite marble; the remainder consists of relatively magnesium-poor calcite marbles. Most of the predazzites occur in the lower part of the Chino marble and in the upper part of the Sky Blue marble. The layers of predazzite clearly reflect the bedding in the original limestones, as they are parallel to relict bedding in the marbles and to the intercalated siliceous metasediments. They also are roughly parallel to a zone of metamorphosed chert nodules that occurs about 100 feet above the footwall of the Chino marble.

The predazzites at Crestmore closely resemble predazzites from other localities (Pl. 6, fig. 5), and the occurrence of periclase in the cores of brucite grains (Pl. 6, fig. 3) clearly indicates that the brucite is of secondary origin. This conclusion is confirmed by the deformed lamellae in the calcite around the brucite grains, which evidently resulted from the increase in volume upon hydration of the periclase to form brucite, as suggested by Eakle (1917). The magnesium content of the predazzites, calculated as the carbonate, rarely exceeds 25 per cent by weight of the rock. Consequently, none of the original carbonate beds was dolomite, although many of them were dolomitic or magnesian limestones. Not all the magnesium occurs in brucite, however, for some beds in the central parts of the Chino marble, which locally are called "fish-scale lime", contain as much as 20 per cent $MgCO_3$. This rock is readily distinguished from the surrounding calcite marbles by its smaller grain size and "scaly" texture. Whether the magnesium in this rock occurs as separate discrete grains of dolomite admixed with calcite, as partly unmixed dolomite in calcite hosts, or as a metastable solid solution in the calcite has not been determined.

Two chemical analyses of the Sky Blue marble are presented in Table 1. These analyses are of composite samples of diamond-drill core and represent the entire body of rock as it was encountered in the drill holes. These composite samples of drill core, as well as all others described in this paper, are identified by the hole number and footage of AX-size core included, as measured from the collar of the hole. Also, individual specimens of drill core are identified by hole number, distance in feet from the collar, plus distance in inches beyond the last footage marker. The differences in the analyses arise largely because the sample from drill hole No. 230 (analysis 2) represents a smaller thickness of the lower, less predazzite-rich part of the Sky Blue marble. Although this sample is not truly

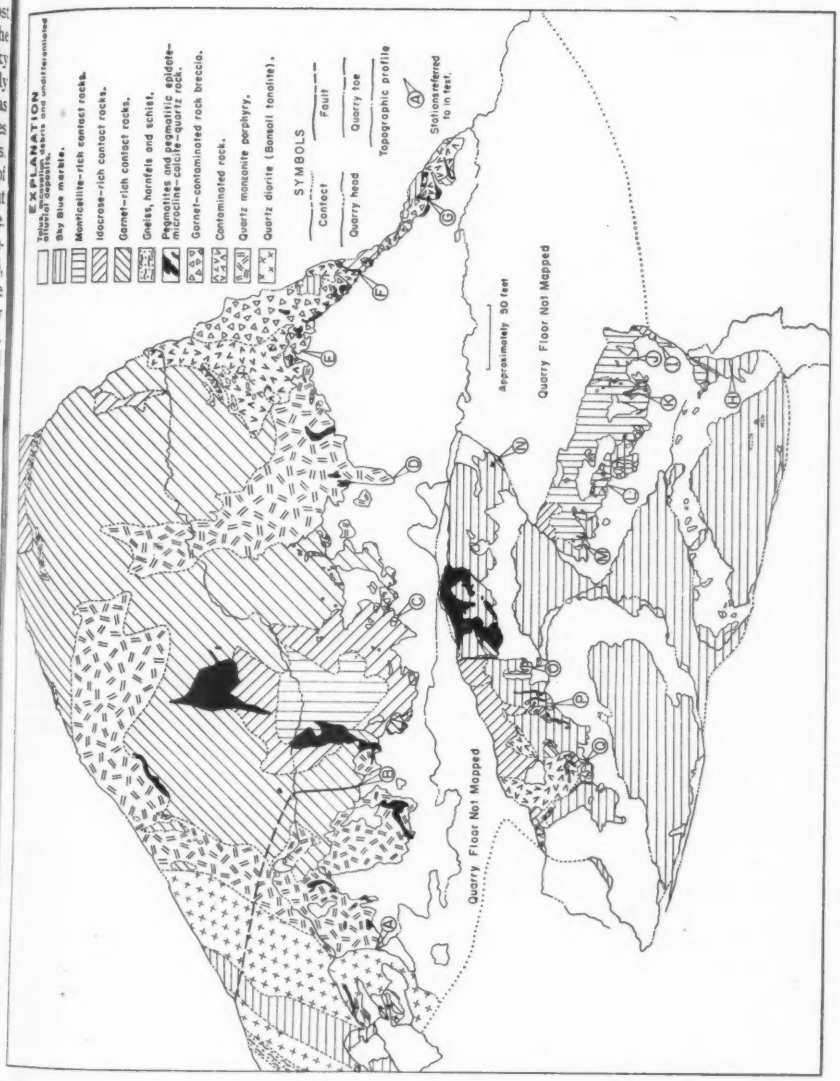

FIGURE 2.—GENERALIZED GEOLOGIC MAP OF FACES OF THE COMMERCIAL QUARRY, CRESTMORE
(See Pl. 10 for detailed map.) Compare with Plate 3.

representative of the part of the Sky Blue marble that was involved in the contact metamorphism, it was selected for analysis because all the major rock types were encountered in this one hole. An opportunity was thus afforded for direct comparisons of rock types that are sequentially associated in space.

TABLE 1.—CHEMICAL COMPOSITION OF THE SKY BLUE MARBLE

H. B. Wiik, analyst (Weight per cent)

Constituent	1	2
SiO_2	0.10	0.17
TiO_2	0.02	0.02
Al_2O_3	0.24	0.37
Fe_2O_3	0.00	0.00
FeO	0.22	0.14
MnO	0.01	0.01
MgO	5.42	8.15
CaO	51.20	49.21
Na_2O	0.00	0.08
K_2O	0.00	0.00
P_2O_5	0.17	0.17
H_2O+	1.94	3.55
H_2O-	0.08	0.00
CO_2	40.62	38.40
S	0.01	0.02
SO_3	0.00	0.00
F	0.02	0.02
Cl	0.01	0.00
BaO	0.02	0.02
Total	100.08	100.33
Less O for S and F		0.01
		100.32

1. Petrographically representative composite-core sample of the Sky Blue marble (DDH 206, 4–213 feet).

2. Composite core sample of the upper part of the Sky Blue marble (DDH 230, 108–225 feet).

In order that a more accurate over-all comparison of rock types could be made, another composite core sample was selected from drill hole No. 206. This sample is petrographically representative of the part of the Sky Blue marble that was involved in the contact metamorphism, and the analysis of it, presented in column 1 of Table 1, is used as the basis for comparison with the contact rocks that were derived from the marble.

One of the more important compositional features of the Sky Blue marble is its very low content of SiO_2 and Al_2O_3. This is somewhat surprising in view of the intimate association of the marble units with siliceous metasedimentary rocks. Also, there is sufficient H_2O in the Sky Blue marble to account for essentially all the MgO as brucite, and there is just enough CO_2 to satisfy the CaO in calcite. Consequently very little magnesium occurs in minerals other than brucite.

A discussion of the contact-metamorphic features in the pre-batholith rocks is deferred to later sections. It will suffice here to mention that the mode of occurrence of the predazzites is inconsistent with a gross introduction or redistribution of magnesium during metamorphism of the original carbonate rocks. Moreover, the amount of magnesium in the predazzites is compatible with a syngenetic origin, perhaps as algal limestones (Chave, 1954), although a diagenetic origin also appears possible.

Igneous Rocks

Quartz diorite.—The country rock of the Crestmore region is principally a hornblende-biotite quartz diorite, the Bonsall tonalite of Larsen (1948), and constitutes the northernmost known exposures of the intrusive rocks of the southern California batholith. The quartz diorite is the only rock type of this great composite batholith that is exposed in the immediate vicinity of the quarries, although both the San Marcos gabbro and the Woodson Mountain granodiorite crop out near by in the Jurupa Mountains, and the Rubidoux Mountain granite underlies Rubidoux Mountain only about 2.5 miles south of Crestmore.

The more homogeneous facies of quartz diorite generally are of medium to coarse grain and possess an hypautomorphic texture. The plagioclase is a calcic andesine that contains approximately 44 per cent of the anorthite end member. Although this rock appears to be of uniform composition, some distinct local variations result in types that range from quartz monzonite to hornblende gabbro, as can be seen in Table 2.

Modal analyses 1, 2, and 3 of Table 2 are of samples from different parts of the area and appear megascopically to be typical of the quartz diorite. Column 4, which is an average of the first three analyses, is therefore considered to represent the average mineral composition of the quartz diorite. Although this aver-

age is only an approximation, it corresponds closely to the mineral composition of the Bonsall tonalite about 13 miles south of Crestmore, as determined by Larsen (1948, p. 66) and presented in column 5 of Table 2. Moreover, the hypothetical chemical composition of the "average quartz diorite" (Table 3, column 2) corresponds closely to the chemical composition of the same sample of Bonsall tonalite (Table 3, analysis 1). The main discrepancy is in the $Al_2O_3+Fe_2O_3/MgO+FeO$ ratio and probably arises from assumptions, based on optical properties, regarding the chemical composition of the ferromagnesian minerals.

TABLE 2.—MINERAL COMPOSITION OF THE QUARTZ DIORITE AND ALLIED ROCKS
(Weight per cent)

Mineral	1	2	3	4	5	6	7	8	9	10	11	12	13	14
Plagioclase	55.8	55.1	53.9	54.9	52	69.7	49.4	39.2	34.3	74.1	34.9	46.5	53.2	51.1
Potassium feldspar	0.5	0.5	tr	0.3	..	0.2	0.5	22.6	19.5	tr	30.5	0.4	..	..
Quartz	17.6	19.4	24.4	20.5	22	18.1	8.8	23.5	17.9	3.5	..	..	..	..
Pyroxene	0.7	tr	4.3	1.7	..	..	tr	..	0.7	2.0	29.6	42.6	26.7	1.6
Hornblende	17.4	12.6	2.7	10.9	9	3.7	20.8	6.3	16.3	14.4	..	..	8.8	38.6
Biotite	7.7	12.5	14.8	11.7	15	8.1	20.5	7.8	10.4	6.0	..	..	10.3	8.3
Opaque minerals	0.4	tr	tr	0.1	..	tr	tr	0.5	0.4	..	3.5	2.5	1.0	0.4
Sphene	..	..	..	..	1	..	..	tr	0.5	..	1.3	7.3	..	..
Apatite	tr	tr	..	tr	..	0.2	tr	tr	tr	..	0.2	0.7	..	..
Total	100.1	100.1	100.1	100.1	99	100.0	100.0	99.9	100.0	100.0	100.0	100.0	100.0	100.0
Anorthite content of plagioclase	42	42	47	44	45	42	43	44	38	53	42	60	44	44–53

1. Quartz diorite (No. 210-503 + 90)
2. Quartz diorite (No. 210-626 + 24)
3. Quartz diorite (No. 230-742 + 1)
4. Quartz diorite (Average of 1, 2, and 3)
5. Bonsall tonalite from 2 miles west of Valverde (Larsen, 1948, p. 66, SLRE 138-28).
6. Leucocratic quartz diorite (No. 208-620 + 84).
7. Melanocratic quartz diorite (No. 208-253 + 0).
8. Granodiorite (No. 206-385 + 108).
9. Granodiorite (No. 201-237 + 14).
10. Hornblende gabbro (No. 214-546 + 108).
11. Pyroxene monzonite (No. 225-786 + 115).
12. Pyroxene gabbro (No. 215-213 + 20).
13. Dioritic inclusion in quartz diorite (No. 208-253 + 68b).
14. Dioritic inclusion in quartz diorite (No. 210-513 + 12b).

Although the total ferromagnesian mineral content of each of the three "typical" samples of quartz diorite is about the same, their relative proportions in each sample are very different. Moreover, there appears to be a direct relationship between the quartz and biotite contents of the rock and an inverse relationship between the quartz and hornblende contents.

Minor leucocratic variants of the quartz diorite are represented by analysis 6, Table 2, and minor melanocratic variants are represented by analysis 7. Analyses 8 and 9 represent more extreme granodioritic variants of the "quartz diorite", and analysis 10 is of a more extreme gabbroic variant. It is probable that many of these variations in mineral composition reflect differences in the nature and degree of assimilative reaction and consequent contamination of the quartz diorite magma by various kinds of wall rocks. For example, a carbonate wall-rock environment affects the marginal phases of the quartz diorite in two different ways: within 1 or 2 feet of the calcareous rocks the normal quartz diorite in some places grades into a quartz-poor, potassium feldspar-rich pyroxene monzonite like that represented by analysis 11, Table 2, and in other places grades into a quartz and potassium feldspar-poor pyroxene gabbro (analysis 12). These two types of contaminated rock differ mainly in the high potassium feldspar content of the monzonite and the higher anorthite content of the plagioclase in the gabbro. They are similar, however, in that both are desilicated, as compared with the parental quartz diorite, and both contain pyroxene instead of hornblende and biotite.

The process by which an initially oversaturated magma, by assimilative reaction with carbonate rocks, becomes more syenitic on the one hand and more gabbroic on the other is discussed more fully in the section on contaminated rocks. That it is of widespread occurrence is attested by the numerous discussions of it in connection with the origin of alkaline rocks (*cf.* Shand, 1923; R. A. Daly, 1933; Smyth, 1927; Bowen, 1928).

A characteristic feature of the quartz diorite throughout large parts of the southern California batholith is the occurrence of dark inclusions (Hurlbut, 1935; Larsen, 1948). Near the

margins of some plutons many of the inclusions are subangular blocks several feet across; in other places they are vaguely bounded schlieren or dark wisps. Hurlbut has demonstrated that

TABLE 3.—CHEMICAL COMPOSITION OF THE QUARTZ DIORITE

(Weight per cent)

Constituent	1	2
SiO_2	62.28	62.2
TiO_2	0.72	0.1
Al_2O_3	16.68	19.0
Fe_2O_3	0.78	1.8
FeO	5.30	4.8
MnO	0.07	..
MgO	2.23	1.2
CaO	5.72	5.5
Na_2O	3.50	3.7
K_2O	1.49	1.3
H_2O-	0.04	..
H_2O+	0.55	0.3
CO_2	0.00	..
P_2O_5	0.11	..
S	0.11	..
BaO	0.06	..
ZrO_2	....	..
Total.....	99.64	99.9

1. Bonsall tonalite 2 miles west of Valverde as reported by Larsen (1948, p. 66). A modal analysis of the same sample is presented in column 5, Table 2.

2. Hypothetical chemical composition of the quartz diorite computed from the average mineral composition as given in column 4, Table 2.

in some places the inclusions originally were San Marcos gabbro, although in others many of them are composed of metasedimentary rocks. The inclusions in the quartz diorite of the Crestmore area consist of both igneous and metasedimentary rocks, but the igneous material does not appear to have been San Marcos gabbro originally. Instead, most of the igneous inclusions appear to represent early marginal phases of the quartz diorite, some of which might have been contaminated through assimilation of calcareous metasedimentary rocks. One such product of contamination is represented by analysis 12, Table 2, and inclusions that might well have been derived from this type of contaminated rock are represented by analyses 13 and 14.

The inclusion that is represented by analysis 14 has a porphyritic (or pseudoporphyritic) texture (Pl. 6, fig. 1). The large grains of plagioclase, which have an anorthite content of about 53 per cent, could be phenocrysts or porphyroblasts, although many of them occur in clusters of three, four, or more anhedral individuals that might be relicts of an originally coarser-grained rock. Even the phenocrystlike grains are highly corroded and contain abundant biotite and hornblende inclusions near their margins. Moreover, the "groundmass" plagioclase contains about 44 per cent anorthite, the same as the plagioclase of the nonporphyritic inclusions and the average quartz diorite. It is therefore suggested that most of these inclusions have been largely altered toward quartz diorite composition from an originally slightly more mafic and coarser-grained igneous rock.

The structural elements of the quartz diorite consist of: (1) abundant ellipsoidal inclusions of gabbroid rock which show preferred orientation of their axial elements, producing a planar structure; (2) strong gneissic layering commonly developed near contacts with limestone; and (3) a planar structure that rarely is detected in hand specimen or thin section, but which clearly is a cause of a consistent westerly deflection of vertically directed diamond-drill holes. All these elements strike approximately north and dip moderately eastward, although minor local deformation produces considerable departures from this general attitude.

Foliation is well developed in some of the ellipsoidal dark inclusions in the quartz diorite, but in the majority of them, especially in the "porphyritic" type, it is not conspicuous. Where it is developed, it lies in the *ab* plane of the ellipsoids and is parallel to the plane of foliation in the quartz diorite. Although many of the inclusions are not conspicuously foliated, the quartz diorite in contact with them commonly exhibits a strong preferred orientation of mineral grains (Pl. 6, fig. 6). This phenomenon is interpreted as a result of differential flow in a very viscous quartz diorite magma.

The gneissic layering in the quartz diorite commonly is produced by the planar orientation of shreds and plates of biotite along relatively closely spaced shear zones (Pl. 6, fig. 4). In Plate 6, figure 2, which is an enlargement of the top part of Plate 6, figure 4, a considerable amount of sphene is arranged sawtooth fashion parallel to the cleavage of surviving shreds of biotite. The sphene occurs in a matrix of chlorite, quartz, and residual biotite and is interpreted as a product of the deuteric altera-

tion of titaniferous biotite. This occurrence of sphene is a common feature in the quartz diorite in many parts of the batholith, but it is of especial importance here, for it indicates that the foliation had developed prior to the deuteric alteration of the biotite and hence probably before the final consolidation of the quartz diorite magma.

The intrusion of the quartz diorite magma produced considerable deformation in the marbles, as has been described in the previous section. In general, the deformation consists of relatively small domical arches in the footwall portion of the Chino marble and antithetic anticlines and synclines in the hanging-wall portions of the Chino marble and footwall portions of the Sky Blue marble (Pl. 1). The quartz diorite rarely intrudes the marbles discordantly to an appreciable extent; hence it is suggested that these deformational features perhaps are the result of flowage in the marbles under the intrusive pressures of a highly viscous quartz diorite magma. The attitudes of these deformational features also indicate that the quartz diorite magma was injected upward from the east, approximately up the dip of the metamorphic units. Thus, the mass of quartz diorite that lies between the two bodies of marble is essentially a sill (Pl. 1), although it is contiguous with the main mass of quartz diorite on the north, east, and south, and perhaps also on the west originally.

The largest example of a mass of quartz diorite, or derivative thereof, that has "punctured" the footwall of the Chino marble is a nearly vertical pipelike body, as much as 50 feet in diameter, that was encountered in Crestmore Mine. This pipe was fringed with masses, several feet thick, of pyrrhotite, sphalerite, and other sulfides in a calcite matrix. Similar though much smaller axinite-bearing pipes and dikes have been encountered more recently in the southern end of the mine. The junction of the large pipe with the underlying quartz diorite has not been exposed in the mine workings, but the smaller pipes and/or dikes in the south end of the mine appear to extend into the marbles from near the crest of one of the small domical arches in the footwall of the Chino marble.

The silicate contact zones between quartz diorite and the marbles are less than 1 foot thick in most places and rarely are more than 2 feet thick. The minerals most characteristic of these zones are brownish grossularite, grass-green diopside, and colorless wollastonite. Minor amounts of quartz and clinozoisite are present locally on the igneous side of the contact zone, whereas spinel-group minerals, rarely in association with a few small crystals of clinohumite, occur on the marble side. Also, scattered grains of sulfides commonly occur both in the contact rock and in the marbles very near the contacts.

Contact effects, other than for formation of the narrow silicate zone which represents the extent of silica, alumina, and iron metasomatism associated with the quartz diorite magma, consist of the recrystallization of all the relatively pure limestone beds to coarse-grained calcite marbles, and the formation of periclase marbles from the magnesium-bearing beds. The formation of the predazzites at the expense of the periclase marbles through the hydration of the periclase to form brucite appears to have occurred during the waning stages of the quartz diorite intrusive activity, as the occurrence of periclase in surface outcrops and in diamond-drill holes indicates that neither weathering nor ground-water action was the cause of the alteration.

Other contact effects, which are largely thermal in nature, are represented by reaction rims of wollastonite around recrystallized chert nodules that occur in a bed of calcite marble about 100 feet above the footwall of the Chino marble. Similarly, sugary white wollastonite, commonly with minor amounts of pale grossularite and/or green diopside, occurs locally in both marble bodies as lenticular masses a few inches thick. These masses apparently represent small lenses of initially silty or argillaceous limestone.

Small flakes of brown phlogopite occur locally disseminated through the predazzites. Near the quartz diorite contacts these flakes commonly are green instead of brown and resemble somewhat the green xanthophyllite that occurs in the contact aureole which surrounds the quartz monzonite porphyry. Small graphite flakes also are commonly disseminated through the marbles, and locally near the footwall of the Chino marble graphite is sufficiently abundant to form calcitic graphite schist.

The masses of predominantly siliceous metamorphic rocks that were engulfed by the sill-like body of quartz diorite between the two marble units locally contain lenses of magnesian marble, some of which are several feet thick. Most of the thicker lenses are surrounded by zones as much as a foot thick of diopside-wollastonite-grossularite rock, and some of the thinner lenses have been completely converted to this rock. The more magnesian (diopsidic) of

these small lenses appear to have been favorable sites for the deposition of sulfides, chiefly pyrrhotite, chalcopyrite, and loellingite.

In the extreme northeastern corner of the area shown in Plate 1, the siliceous metamorphic rocks between the two marble units grade into a wollastonite-rich schist that also contains considerable amounts of pale-green diopside, brown grossularite, and calcite. This rock appears to have formed largely by thermal metamorphism of silty and argillaceous limestone during the intrusion of the quartz diorite.

Quartz monzonite porphyry.—Blocky masses of light-gray quartz monzonite porphyry are exposed in both the southern and northern parts of the upper face of the Commercial Quarry (Fig. 2; Pl. 3). The southern and structurally lower mass is the exposed part of an irregular pipe that was intruded upward from the east along the contact between the Sky Blue marble and the underlying quartz diorite (Pl. 1). The northern and structurally higher mass also is the exposed part of an irregular pipe that was intruded upward from the east, but it lies entirely within the Sky Blue marble. However, the mass from which this latter pipe branches lies mainly along or very near the contact between the Sky Blue marble and quartz diorite and extends westward up the dip beneath Sky Blue Hill. Another relatively large mass of quartz monzonite porphyry underlies the floor of the northern part of the Commerical Quarry, and it is with this body that the contact rocks exposed on the lower levels of the Commercial Quarry between stations *I* and *N*, Plate 10, are associated. As indicated in Plate 1, the source of the quartz monzonite porphyry apparently lies southeast of the Crestmore area.

The texture of the porphyry is mainly xenomorphic porphyritic, as shown in Plate 7, figure 5, but in detail it is highly variable, especially with respect to grain size and relative abundance of plagioclase phenocrysts. The phenocrysts, which constitute as much as 26 per cent of the rock, generally are anhedral and range from 1 to 7 mm in diameter. Their anorthite content ranges from 30 to 50 per cent, depending upon the amount of contamination by limestone, but the average is about 37 per cent. In contrast, the anorthite content of the plagioclase in the fine-grained groundmass ranges from 25 to 33 per cent, and the average is about 30 per cent. Locally, where phenocrysts are nearly lacking, as at station *D*, the rock is aplitic and consists of fine-grained anhedral plagioclase, potassium feldspar, quartz, and minor subhedral pyroxene.

The mineral composition of the less contaminated phases of the quartz monzonite porphyry is represented by analyses 1–3 of Table 4. The sample represented by analysis 1 is practically the same as that represented by chemical analysis 1 of Table 5. Moreover, the average chemical composition of the less contaminated porphyry, as given in column 3 of Table 5, corresponds fairly closely to the average mineral composition given in column 3 of Table 4. However, a comparison of the norm with the mode reveals a considerable discrepancy in the potassium feldspar/plagioclase ratio. This feature persists throughout the quartz monzonite porphyry and its contaminated derivatives and is attributed to the occurrence of relatively large amounts of sodium in the potassium feldspar of the porphyry and in the pyroxene (aegerinaugite) of the highly contaminated rocks.

The pyroxene of the less contaminated quartz monzonite porphyry, which generally is a light-green diopsidic augite, occurs largely as small subhedral crystals or clusters of crystals disseminated through the rock. In places the clusters resemble relatively large (up to 3 mm) poikilitic or poikiloblastic crystals, as shown in Plate 7, figure 3, and suggest that much of the pyroxene might have crystallized after some of the feldspar and quartz.

The interiors of some of the larger bodies of quartz monzonite porphyry, especially the pipe that underlies the northern part of the Commercial Quarry, are considerably more porphyritic than the outer parts. Both the mineral composition (analysis 12, Table 4) and the chemical composition (analysis 4, Table 5) indicate that these more porphyritic rocks are somewhat more contaminated than the average quartz monzonite porphyry (column 14, Table 4, and column 6, Table 5). Also, their texture and mode of occurrence suggest a cooling history somewhat different from that of the finer-grained, more aplitic rocks.

Within a few feet of the contacts with quartz diorite, the quartz monzonite porphyry generally contains 2 to 5 per cent of dark minerals, mainly hornblende and biotite instead of pyroxene (analyses 4–8, Table 4). Moreover, the sphene in this rock commonly contains cores of ilmenite or titaniferous magnetite, whereas the sphene of the "normal" porphyry is free of oxides. The major differences in the bulk chemical composition of this hornblende- and

biotite-bearing porphyry (analysis 5, Table 5), as compared with the "normal" porphyry (column 3, Table 5), are: greater TiO_2, total iron oxide, P_2O_5, H_2O, and S contents, and a lower SiO_2 content. Whether these differences are due mainly to differences in contaminating materials or the lack of appreciable contamination by limestone is uncertain. Had the quartz monzonite porphyry magma not intruded the Sky Blue marble, perhaps the entire body would have crystallized as a biotite- and/or hornblende-bearing quartz monzonite such as the apophysis that occurs in quartz diorite very near the footwall contact of the porphyry beneath Sky Blue Hill (*cf.* analysis 7, Table 4).

The less contaminated quartz monzonite porphyry represented by analysis 3, Table 4, and analysis 1, Table 5, is for the most part confined to the interiors of the larger masses. The bulk of the porphyry has been slightly more contaminated through the assimilation of limestone. The chemical composition of these slightly more contaminated variants of the porphyry is represented by analysis 2, Table 5, and the mineralogical variation in these rocks by modal analyses 9–13, Table 4. The 15½ feet of drill core that makes up the chemically analyzed composite sample includes the specimens that are represented by modal analyses 9 and 11, Table 4. These analyses correspond to the norm, except for the usual and previously mentioned discrepancy in the potassium feldspar/plagioclase ratio.

TABLE 4.—MINERAL COMPOSITION OF THE QUARTZ MONZONITE PORPHYRY
(Weight per cent)

Mineral	1	2	3	4	5	6	7	8	9	10	11	12	13	14
Plagioclase	30.2	29.4	29.8	35.7	33.4	22.7	25.2	29.3	25.2	28.3	29.1	38.5	29.0	29.9
Potassium feldspar	30.8	37.9	34.4	30.6	37.0	38.4	26.2	34.2	31.9	37.5	31.8	23.7	34.4	32.6
Quartz	34.1	27.2	30.7	24.3	24.8	36.8	45.2	33.8	34.7	26.9	28.7	24.2	23.2	29.0
Pyroxene	4.2	4.8	4.5	1.5	0.6	..	..	0.5	6.8	6.8	9.4	11.8	11.4	7.0
Hornblende	..	..	..	4.2	3.4	0.5	..	..	..	..	..	..	..	0.2
Biotite	..	..	..	..	..	1.7	3.3	1.3	..	..	..	..	..	0.1
Opaque minerals	..	..	..	tr	tr	tr	..	tr	..	..	..	..	..	tr
Sphene	0.7	0.8	0.8	3.8	0.8	tr	..	1.1	0.9	0.5	0.9	1.7	2.0	1.1
Apatite	..	..	..	..	..	..	..	..	0.5	..	..	..	..	0.1
Total	100.0	100.1	100.2	100.1	100.0	100.1	99.9	100.2	100.0	100.0	99.9	99.9	100.0	100.0
Plagioclase phenocrysts	12.3	5.3	8.8	12.3	13.0	?	..	?	7.3	14.9	16.2	26.0	9.0	..
Anorthite content of plagioclase	26–30	29–?	28	27–28	33–42	30	32	31	31–27	27–37	28–36	33–50	25–35	32

1. Least contaminated quartz monzonite porphyry (No. 228-181 + 72).
2. Very slightly contaminated quartz monzonite porphyry (No. 220-37a).
3. Average of 1 and 2.
4. Quartz monzonite porphyry near contact with quartz diorite (No. 217-16b).
5. Quartz monzonite porphyry near contact with quartz diorite (No. 216-12).
6. Quartz monzonite porphyry near contact with quartz diorite (No. 228-327 + 96).
7. Quartz monzonite dike in quartz diorite (No. CWB-8).
8. Average of 4, 5, 6, and 7.
9. Slightly contaminated quartz monzonite porphyry (No. 230-310 + 60).
10. Slightly contaminated quartz monzonite porphyry (No. 230-338½ + 42).
11. Slightly contaminated quartz monzonite porphyry (No. 230-317 + 82).
12. Slightly contaminated quartz monzonite porphyry (No. 230-327 + 66).
13. Slightly contaminated quartz monzonite porphyry (No. 232-256 + 42).
14. Weighted-average bulk mineral composition of the quartz monzonite porphyry.

In order that the bulk mineral composition of the quartz monzonite porphyry body as a whole might be estimated, an average that is weighted according to the estimated relative volumes of the different types was computed (column 14, Table 4). A weighted-average bulk chemical composition was computed in similar manner and is presented in column 6, Table 5. Although the chemical analyses are of large composite samples, whereas the modal analyses are of individual thin sections, the two averages are nearly equivalent, again except for the feldspar ratio.

The quartz monzonite porphyry is marked by joints, flow layering, and a weak lineation. Near station *A* (Fig. 2; Pl. 10) in the southern part of the Commercial Quarry, two sets of joints are conspicuous. One set, which is parallel to the plane of foliation and flow layering,

TABLE 5.—CHEMICAL COMPOSITION OF THE QUARTZ MONZONITE PORPHYRY

(Weight per cent) H. B. Wiik, analyst.

Constituent	1	2	3	4	5	6
SiO_2	74.15	71.52	72.84	70.46	69.36	71.78
TiO_2	0.22	0.32	0.27	0.30	0.50	0.31
Al_2O_3	12.15	13.14	12.65	13.25	13.21	12.91
Fe_2O_3	0.32	0.39	0.36	0.25	0.64	0.39
FeO	1.93	1.43	1.68	1.78	3.28	1.83
MnO	0.03	0.02	0.03	0.02	0.03	0.02
MgO	0.29	0.82	0.56	1.28	0.93	0.76
CaO	2.69	4.00	3.35	4.63	3.86	3.73
Na_2O	4.10	3.42	3.76	3.02	3.34	3.53
K_2O	3.30	4.12	3.71	4.28	3.48	3.86
P_2O_5	0.04	0.04	0.04	0.09	0.12	0.06
H_2O+	0.30	0.44	0.37	0.40	0.52	0.21
H_2O-	0.03	0.00	0.02	0.08	0.00	0.02
CO_2	0.00	0.00	0.00	0.00	0.00	0.00
S	0.00	0.00	0.00	0.04	0.30	0.04
SO_3	0.00	0.00	0.00	0.00	0.00	0.00
F	0.00	0.00	0.00	0.02	0.03	0.01
Cl	0.00	0.00	0.00	0.00	0.00	0.00
BaO	0.03	0.02	0.03	0.02	0.02	0.02
Total	99.58	99.68	99.67	99.92	99.62	99.48
Less O for S and F	..	..	..	0.01	0.08	..
				99.91	99.54	
			Norm			
Quartz	33.25	31.15	..	29.30	32.20	..
Orthoclase	19.52	22.91	..	25.30	20.01	..
Albite	34.63	28.92	..	25.52	29.25	..
Anorthite	4.95	6.28	..	12.73	11.97	..
Diopside	6.72	7.86	..	7.80	..	..
Wollastonite	1.04	1.69	..	1.32	..	..
Hypersthene	..	..	..	..	5.42	..
Magnetite	0.46	0.46	..	..	0.97	..
Pyrite	..	..	..	..	0.10	..
Total	100.57	99.27	..	101.97	99.92	..

1. Least contaminated quartz monzonite porphyry obtainable (DDH 228, 183–214 feet).
2. Very slightly contaminated quartz monzonite porphyry (DDH 230, 313–328½ feet).
3. Average of columns 1 and 2. Representative of the main mass of less contaminated quartz monzonite porphyry.
4. Highly porphyritic quartz monzonite porphyry (DDH 230, 328½–340 feet).
5. Quartz monzonite porphyry in contact with quartz diorite (DDH 228, 318½–337 feet).
6. Weighted-average bulk chemical composition of the quartz monzonite porphyry intrusive mass at Crestmore.

strikes N. 48° W. and dips 28° northeast near the footwall contact with quartz diorite but strikes N. 30° W. and dips 30° northeast near the hanging-wall contact with contact rock. The other set strikes nearly east and dips 86° S. to 87° N. The intersection of these two sets of joints defines a lineation near the footwall that nearly coincides with another lineation formed by the preferred orientation of mineral grains. Moreover, these lineations are approximately parallel to the direction of flow of the magma, as determined by the shape and suspected source area of the porphyry intrusive mass.

The quartz monzonite porphyry appears to have been intruded as a pipelike body, 200–300 feet in diameter, upward and northward from points beneath the southeast corner of the area, as shown in Plate 1. The wall rocks of the pipe in this part of the area are quartz diorite and a small remnant of the Chino marble. At the intersection of the pipe with a large fragment of siliceous metasedimentary rocks that underlies and interfingers with the lower members of the Sky Blue marble, the pipe branches into two smaller pipes, one of which extends westward along the contact between quartz diorite and the metasedimentary rocks. The other pipe extends northward and upward through the remnant of metasedimentary rocks and more quartz diorite into the Sky Blue marble. Within the Sky Blue marble the porphyry forms a complex network of anastomosing pipes and stringers, the larger bodies being directed either westward along and near the footwall contact or steeply upward into the marble. As closely as can be determined, the porphyry extends only a short distance northward beyond the south wall of the Wet Weather Quarry.

The intrusion of the porphyry magma produced profound deformational effects in the Sky Blue marble. In general the marble was arched into an eastward-plunging anticline, the axis of which lies in the northernmost part of the Commercial Quarry. The northern limb of this anticline forms the south walls of the Wet Weather and Wet Weather Extension quarries and is relatively uniform and steeply dipping. In contrast, the southern limb is very irregular in attitude owing to bosslike protrusions from the main mass of porphyry in the core of the anticline and to deformational effects around the porphyry pipe that underlies the southern part of the Commercial Quarry and the south slope of Sky Blue Hill.

These deformational features, which clearly are associated with the quartz monzonite porphyry intrusive mass, as shown in Plate 1, indicate that the porphyry made room for itself largely by displacing the Sky Blue marble. This conclusion is supported by the fact that the relative amounts of calcium in the contaminated and uncontaminated facies of the porphyry indicate that certainly less than 15 per cent, and probably less than 10 per cent, of the space now occupied by the porphyry and related igneous rocks can be accounted for by the assimilation of Sky Blue marble.

Contaminated rocks.—The contaminated rocks described here are genetically related to the quartz monzonite porphyry and have been derived from it through contamination of the porphyry magma by magnesian marble (the Sky Blue marble). Nearly all gradations exist between essentially uncontaminated quartz monzonite porphyry and a gabbroic rock of the composition indicated by analysis 1, Table 6, or a kalisyenitic rock of the composition indicated by analysis 18; consequently the grouping of the contaminated and uncontaminated rocks is somewhat arbitrary. That is, the rocks represented by analyses 9–13, Table 4, actually are contaminated rocks, but the degree of contamination is relatively slight as compared with the rocks represented in Table 6, except analysis 11, Table 4, which is transitional.

The contaminated rocks may be subdivided into two principal types that generally can be distinguished by differences in color, texture, composition, and occurrence. The less extensive type commonly is very dark and occurs as small pipelike masses or stringers in garnet-rich contact rocks and as small lenticular bodies in the more extensive lighter-colored contaminated rock. Most of the small masses of contaminated rock near station *C* (Pl. 10) are of this type. Syenodiorites are the most abundant of the dark contaminated rocks, but quartz diorites, diorites, and gabbros also are common (analyses 1–9, Table 6). The average, as shown in column 10, Table 6, is a syenodiorite and is approximately equivalent chemically to the composite sample represented by analysis 2, Table 7. The discrepancies between the mode and the norm of these rocks arise not only from the occurrence of sodium in the potassium feldspar but also from potassium in the plagioclase and sodium in the pyroxene.

A comparison of the average dioritic contaminated rock (column 10, Table 6) with the parent quartz monzonite porphyry (column 3, Table 4) emphasizes the effects of the assimilation of limestone on the mineral composition of the resultant rocks. The more obvious of these

TABLE 6.—MINERAL COMPOSITION OF THE CONTAMINATED ROCKS
(Weight per cent)

Mineral	1	2	3	4	5	6	7	8	9	10	11	12	13	14	15	16	17	18	19	20	21
Plagioclase	45.8	52.3	52.5	46.1	44.5	62.8	56.3	55.2	44.5	51.1	35.7	19.9	47.6	35.2	20.2	18.1	29.5	..	51.3	50.6	28.2
Potassium feldspar	..	0.5	0.8	2.4	6.7	9.4	11.4	21.0	21.1	8.1	26.1	38.1	38.3	40.3	56.9	58.3	43.0	80.6	4.3	18.1	44.5
Quartz	..	..	..	12.1	..	..	..	..	..	1.3	23.3	1.2	4.7	..	1.7	2.9	5.6	..	4.3	14.6	..
Pyroxene	51.6	45.6	42.5	38.2	43.2	26.3	30.2	22.4	32.2	36.9	13.2	39.3	8.6	23.0	15.9	19.0	19.8	12.2	7.5	6.1	19.8
Hornblende	..	..	..	..	..	..	0.4	..	..	tr	..	..	..	..	..	..	..	..	22.8	4.5	4.5
Biotite	..	..	..	..	..	..	..	..	..	..	..	..	..	..	..	..	..	..	8.7	3.3	0.7
Opaque minerals	tr	tr	tr	tr	tr	tr	tr	tr	tr	tr	tr	tr	tr	tr	tr	0.7	0.1	tr	1.1	2.9	tr
Sphene	2.6	1.5	4.2	1.0	5.6	1.5	1.7	1.4	2.0	2.4	1.7	1.5	0.8	1.5	5.3	0.9	1.9	0.4	..	..	2.3
Apatite	tr	tr	tr	0.3	tr	tr	tr	tr	0.1	tr	tr	tr	tr	tr	tr	tr	tr	tr	tr	tr	tr
Wollastonite	..	..	..	..	..	..	..	..	..	..	..	..	..	..	..	..	..	7.0	..	..	..
Total	100.0	99.9	100.0	100.1	100.0	100.0	100.0	100.0	99.9	99.8	100.0	100.0	100.0	100.0	100.0	99.9	99.9	100.2	100.0	100.1	100.0
Plagioclase phenocrysts	..	..	..	..	..	..	..	..	..	..	17.3	..	..	9.8	..	..	..	..	..	22.5	..
Anorthite content of plagioclase	70	40	34	31	39	40	26–44	47	32	40	32–37	38	43	36–42	33	33	37	..	40–44	37–46	30

1. Gabbro (No. 208-233 + 66).
2. Diorite (No. 221-39a).
3. Titaniferous diorite (No. 208-223 + 60).
4. Quartz diorite (No. 221-38a1).
5. Titaniferous syenodiorite (No. 208-223 + 78).
6. Syenodiorite (No. 232-256 + 8).
7. Syenodiorite (No. 219-34f).
8. Syenodiorite (No. 200-63 + 115).
9. Syenodiorite (No. 208-233 + 106).
10. Average of 1–9 that represents the dark contaminated rocks.
11. Quartz monzonite (No. 222-40f).
12. Monzo-syenite (No. 208-223 + 75).
13. Monzonite (No. 200-63 + 48).
14. Monzonite (No. 232-53c).
15. Syenite (No. 230-310 + 24).
16. Syenite (No. 232-226 + 60).
17. Average of 11–16 that represents the light-colored contaminated rocks.
18. Kalisyenite (No. 226-46g).
19. Hornblende diorite (No. 200-235½ + 36).
20. Syenodiorite (No. 200-220 + 24).
21. Monzonite (No. 222-40e).

effects are the virtual disappearance of quartz and an enormous increase in the pyroxene content. There also is a marked decrease in the potassium feldspar content and a concomitant increase in the plagioclase content. Moreover, the pyroxene is aegerinaugite instead of diopsidic augite, as in the less contaminated quartz monzonite porphyry, or diopside as in the contact rocks. These mineralogical differences are reflected in the chemical composition by a pronounced decrease in the SiO_2 content (desilication) and concomitant large increases in CaO, MgO, FeO, Fe_2O_3, and TiO_2 contents of the contaminated rock (*cf.* analysis 2, Table 7, with column 3, Table 5). Together with a notable increase in the Al_2O_3 content and decrease in the K_2O content, these differences in composition indicate that the process of formation of the dioritic contaminated rocks is essentially one of basicification.

Relatively small masses of dark schistose rocks are common, especially in the northern part of the Commercial Quarry and above station *K* (Pl. 10). In some of these masses the schistosity is well developed, but in others it is detectable only microscopically as numerous shear fractures along which there has been some displacement and granulation. These schistose rocks clearly are closely related to the dioritic contaminated rocks, for there is a continuous gradation between them, and it is suggested that they are metamorphosed early apophyses of contaminated quartz monzonite porphyry. Mineralogically the schistose rocks differ from the parent contaminated rocks in the occurrence of hornblende and biotite, as shown in analyses 19–21, Table 6. These minerals appear to have formed at the expense of pyroxene, and their preferred orientation indicates that they are of metamorphic origin. It is noteworthy in this connection that there is a direct relationship between the ratio of hornblende plus biotite to pyroxene and the degree of development of schistosity.

The more common type of contaminated rock, which is represented compositionally by analyses 11–16, Table 6, and analysis 3, Table 7, generally is lighter in color, less porphyritic, and coarser-grained. It occurs as relatively large masses that locally have engulfed blocks of garnet-rich contact rocks and smaller masses of dioritic contaminated rock, especially the schistose type. In fact, there is strong evidence that the metamorphism of the schistose rock is closely related to the intrusion of the lighter-colored contaminated rock. Generally the masses of light-colored contaminated rock are marginal to the main bodies of quartz monzonite porphyry and doubtless grade into them.

The mineral composition of the more com-

TABLE 7.—CHEMICAL COMPOSITION OF THE CONTAMINATED ROCKS

(Weight per cent) H. B. Wiik, analyst.

Constituent	1	2	3
SiO_2	61.07	57.91	60.22
TiO_2	0.66	0.60	0.80
Al_2O_3	14.57	14.82	14.56
Fe_2O_3	0.79	1.90	0.60
FeO	3.07	3.57	2.93
MnO	0.07	0.08	0.06
MgO	1.97	2.59	1.64
CaO	8.36	10.46	7.31
Na_2O	3.42	4.67	3.36
K_2O	5.40	2.77	6.97
P_2O_5	0.11	0.11	0.17
H_2O+	0.24	0.50	0.60
H_2O-	0.00	0.00	0.00
CO_2	0.00	0.00	0.00
S	0.00	0.00	0.00
SO_3	0.00	0.00	0.00
F	0.02	0.02	0.03
Cl	0.00	0.00	0.00
BaO	0.17	0.15	0.23
Total	99.92	100.15	99.48
Less O for S and F			0.01
			99.47
Norm			
Quartz	9.78	7.78	5.16
Orthoclase	31.86	16.34	41.14
Albite	28.92	39.46	28.40
Anorthite	8.48	11.20	4.11
Diopside	17.74	21.38	8.13
Wollastonite	4.68	3.68	9.27
Magnetite	1.16	2.76	0.88
Total	102.62	102.60	97.09

1. Intermediate contaminated rock that megascopically appears to be representative of the contaminated rocks as a whole (DDH 232, 238–242 feet).

2. Typical dark contaminated rock (DDH 200, 80–88 feet).

3. Typical light-colored contaminated rock (DDH 230, 309–313 feet).

mon type of contaminated rock varies considerably, as shown by analyses 11–16, Table 6. Although generally these rocks are more leucocratic than the dioritic group described heretofore, the feature that serves to distinguish them as a group is their higher content of potassium feldspar. Facies of these syenitic contaminated rocks that are transitional with the quartz monzonite porphyry are represented by analyses 11 and 13 (*cf.* analysis 13, Table 4). Column 17 is an average of analyses 11–16 and is nearly representative of the entire group of syenitic contaminated rocks.

A comparison of this average with the less contaminated quartz monzonite porphyry (column 3, Table 4) indicates again that the main effects of contamination are a marked decrease in the quartz content and a concomitant increase in the pyroxene content. However, unlike the dioritic contaminated rocks, the average syenitic contaminated rock contains more potassium feldspar than the parental quartz monzonite porphyry and about the same amount of plagioclase, although the plagioclase generally is slightly more calcic. The pyroxene content of the syenitic rock, although much greater than that of the quartz monzonite porphyry, is only about half that of the dioritic contaminated rock; hence the differences in color.

The chemical composition of typical syenitic contaminated rock (analysis 3, Table 7) corresponds closely to the average mineral composition given in column 17, Table 6. The discrepancy between the mode and the norm is considerably smaller for this rock than for the dioritic contaminated rock or the quartz monzonite porphyry, indicating that there is less sodium in the potassium feldspar and pyroxene. This syenitic rock also contains considerably less SiO_2 and more CaO and K_2O than does the less contaminated quartz monzonite porphyry. It is neither as desilicated nor as enriched in CaO, MgO, and total iron as the dioritic contaminated rock, but it contains a great deal more K_2O.

An extreme effect of potassium enrichment associated with the contamination of the quartz monzonite porphyry magma by carbonate rocks is a kalisyenitic rock such as that shown in Plate 7, figure 1 and represented by analysis 18, Table 6. This rock is uncommon at Crestmore, having been found on the surface only between stations *I* and *M* in the Commercial Quarry. It occurs as small stringers in monticellite-rich rocks that are surrounded by light-colored sheaths of dense fine-grained diopside-grossularite-wollastonite rock, some of which are thicker than the stringers themselves. Most of the feldspar in this rock is microcline, but some of the grains are untwinned and have the very small optic angles suggestive of sanidine.

Although most of the schistose rocks that already have been described appear to be metamorphosed dioritic contaminated rock, the mass above station *K*, Plate 10, is believed to have been kalisyenite originally. All the plagioclase in this rock that is reported in analysis 21, Table 6, occurs in perthitic intergrowths with untwinned potassium feldspar and indicates that the original feldspar was intermediate in composition. However, the relatively calcic nature of the plagioclase (sodic andesine) suggests that perhaps some calcium was introduced during metamorphism and accompanying exsolution.

A common feature of the syenitic rocks that might be connected with the phenomenon of potassium enrichment is the occurrence of two types of potassium feldspar. One type, which is relatively coarse-grained and commonly occurs as phenocrysts (Pl. 7, figs. 4 and 6), has the optical properties of sanidine, whereas the other type, which commonly is fine-grained and interstitial to the other minerals, appears to be orthoclase. The latter type also forms small veinlets along intergranular boundaries, as in Plate 7, figure 2, and graphic intergrowths with wollastonite as in Plate 5, figure 1. These features suggest that the two types of potassium feldspar also represent two stages of formation, an earlier coarse-grained sanidine stage and a later interstitial orthoclase stage.

Wollastonite also occurs in the stringers of kalisyenitic contaminated rock, such as that represented by analysis 18, Table 6, and shown in Plate 7, figure 1, but it does not form graphic intergrowths with the potassium feldspar in them. This feature is compatible with the interpretation that the potassium feldspar in these rocks is equivalent to the earlier sanidine stage in the rocks that contain two potassium-rich feldspars, whereas the potassium feldspar in the graphic intergrowths is equivalent to the later orthoclase stage.

Although the contaminated rocks at Crestmore have more than one mode of occurrence, they provide much information about the relationships of metasomatism to intrusion, of metasomatism to assimilative reaction, and of assimilative reaction to the development of rocks with alkaline affinities. The dioritic contaminated rocks occur generally as small stringers and pipelike bodies in garnet-rich

contact rock, as above station *C*, Plate 10. These stringers are so abundant near the summit of Sky Blue Hill, above the face of the Commercial Quarry, that the entire mass has been mapped as undifferentiated "garnet rock—contaminated rock mixture." The dioritic contaminated rocks have produced slight, if any, contact-metamorphic effects on the garnet-rich wall rocks, but the stringers that penetrate idocrase- or monticellite-rich rock commonly are surrounded by several centimeters of light-colored diopside-wollastonite-grossularite rock. These features strongly suggest that the stringers were injected into an already formed contact aureole. Moreover, the occurrence of many relatively small, somewhat metamorphosed inclusions of this rock within larger bodies of syenitic contaminated rock indicates that the dioritic rocks represent relatively early phases of the quartz monzonite porphyry intrusive mass.

In fact, the dioritic contaminated rocks appear to be the initial crystallized product that resulted from the assimilation of marble by the quartz monzonite porphyry magma, and the syenitic contaminated rocks may be the product of crystallization of the residual magma, minus some silica, alumina, and iron that were lost through metasomatism. That is, the heat required for the reactive assimilation of the carbonate rocks was obtained largely from the heat of crystallization of the minerals with which the magma was saturated, minerals that produced rocks of syenodioritic to gabbroic composition. The addition of calcium and magnesium increased the proportions of the cafemic constituents in the crystallized product and at the same time desilicated the magma to an extent somewhat greater than their molecular equivalence. The residual magma, somewhat desilicated and impoverished in the cafemic constituents but enriched in potassium, became further desilicated through the evolution of silica-bearing, carbon dioxide-rich, aqueous metasomatizing solutions, and the residuum crystallized as rocks of syenitic to kalisyenitic composition.

The syenitic contaminated rocks commonly contain angular blocks of garnet-rich contact rock or constitute the matrix of a garnet-contaminated rock breccia, as in Plate 4, figures 1 and 2. The contact between this garnet-contaminated rock breccia and the predazzites generally is sharp, as shown in Plate 4, figure 1, and rarely is there as much as 2 cm of intervening diopside-wollastonite-grossularite contact rock. Inasmuch as the contaminated magma produced little, if any, contact zone against predazzite, it could not have produced the highly metasomatized large blocks of garnet rock that occur in contaminated rock adjacent to the contact with predazzite. Hence it appears that much of the syenitic contaminated rock was intruded into already formed contact rock. Moreover, several features of the contact rocks associated with the quartz monzonite pegmatites clearly indicate that the pegmatites also were intruded into an already formed contact aureole. Consequently it is concluded that large-scale contact metasomatism preceded final emplacement of the porphyry intrusive mass and related pegmatites.

Quartz monzonite pegmatites.—Pegmatite dikes cut the contact rocks, contaminated rocks, and marginal parts of the quartz monzonite porphyry. They clearly are related to the porphyry, for all gradations between the two rocks types have been found in a single dike or lens. Generally these pegmatitic rocks occur as veinlike or dikelike bodies and stringers in the contact rocks or along the contact between the contact rocks and marble, but many smaller masses, either thinly lenticular or ovoid, occur within the main bodies of quartz monzonite porphyry. The ovoid masses generally are somewhat less than 1 foot in diameter, but the thinly lenticular bodies range in thickness from about one-fourth of an inch to 3 feet or more.

The pegmatite dikes and lenses that occur in the marginal parts of the porphyry have two preferred attitudes, the most common of which is parallel to a poorly developed set of joints that strikes N. 15° W. and dips 50°–80° E. The less common preferred attitude of the pegmatites is parallel to a well-developed set of joints that strikes N. 30°–45° W. and dips 28°–30° northeast. These pegmatite bodies commonly grade imperceptibly into the porphyry, although some of the lenses have sharp contacts. Mineralogically they are very similar to the parent porphyry, as they contain mainly oligoclase-andesine, potassium-rich feldspar (perthite), and quartz. In addition, highly altered pyroxene crystals up to 2 cm long, or brown andradite garnet crystals as much as 1 cm in diameter, occur in or near the cores of some of the ovoid masses. Unlike most of the pegmatites associated with the quartz diorite country rock, the quartz monzonite pegmatites rarely contain schorl or axinite.

The pegmatites form well-defined dikes that commonly cut the rocks of the contact aureole, but they rarely penetrate the marbles more than a few feet. Those larger dikes that reach

the marble contact generally spread out along it to form sheetlike bodies, such as below station *C* and near station *N*, Plate 10. This feature, together with the relationship between the dikes and the joints in the marginal parts of the porphyry, indicates that fractures and zones of weakness along the contacts exercised considerable control in the emplacement of the pegmatite bodies.

TABLE 8.—CHEMICAL COMPOSITION OF PREHNITE AND "ORTHOCLASE" FROM PEGMATITE

(Weight per cent)

Constituent	1	2	3
SiO_2	44.04	44.10	64.54
TiO_2	0.03	..	..
Al_2O_3	24.77	24.20	20.86
Fe_2O_3	0.20	..	tr
FeO	0.00	..	..
MgO	0.01	..	tr
CaO	26.99	25.20	1.86
Na_2O	0.00	..	1.18
K_2O	0.00	..	11.85
H_2O (total)	4.20	5.86	0.52
P_2O_5	0.01	..	..
MnO	0.00	..	..
Total	100.25	99.36	100.81

1. Brown to flesh-colored prehnite from zoned pegmatite below station *C*, Plate 10; W. F. Blake, analyst.

2. "Brown prehnite" from pegmatite; reported by Eakle (1917).

3. "White orthoclase" from pegmatite; reported by Eakle (1917).

The major minerals of the pegmatite dikes are essentially the same as in the pegmatite bodies within the porphyry, except that locally, as north of station *B*, below station *C*, and at station *N*, euhedral andradite garnets as much as 2 cm across are important constituents of the dikes. Allanite also occurs sparingly as black euhedral crystals as much as 2 cm long in the more feldspar-rich parts of some zoned pegmatite bodies.

A subhorizonal lenticular apophysis from a large andradite-bearing pegmatite extends into garnet-rich contact rock below station *C*. This lens is nearly 20 feet across, as much as 3 feet thick, and has a well-defined zonal structure as shown in Plate 4, figure 3. The wall zone consists of coarse-grained oligoclase and microcline-quartz graphic intergrowths. The next zone inward consists mainly of chalky white oligoclase and microcline with subordinate quartz. The core consists largely of massive quartz with minor amounts of wollastonite, in blades up to 25 cm long, and crude rhombohedral crystals of calcite.

The intermediate zone of chalky white feldspar overlying the core commonly contains vuggy masses of brown to flesh-colored prehnite, analyses of which are presented in Table 8. The small vugs are lined with euhedral crystals of prehnite, on which are perched abundant crystals of quartz and rare datolite and laumontite. Larger vugs, some more than a foot across, also are common in the white, feldspar-rich intermediate zone above the core. They generally are lined with oligoclase and microcline crystals that are as much as 10 cm across, and the microcline contains graphic intergrowths of quartz. A few greenish epidote crystals up to 2 cm long are perched on the feldspars, and the entire contents of the vugs are coated with a thin layer of hyalite opal.

Perhaps it would appear that the coexistence of quartz, calcite, and wollastonite in the core of this zoned pegmatite, which presumably crystallized under essentially closed-system conditions, should provide an indication of the conditions of crystallization. However, inasmuch as neither the partial pressure of CO_2 nor of H_2O at the time of crystallization is known, only an approximate lower-temperature limit can be established. A lower limit of about 400°C. for the crystallization of the core assemblage is based on P-T relations of the reaction: xonotlite = wollastonite + water, as determined by D. A. Buckner (1955, unpub. MS thesis, The Pennsylvania State University) and by the writer.

Scattered patches and veinlike masses of pegmatitic epidote-microcline-oligoclase-calcite-quartz rock in garnet-rich contact rock are common on the upper face of the Commercial Quarry between stations *E* and *F*, Plate 10. Near station *E* they consist mainly of quartz, oligoclase, microcline, and epidote, but northward away from the contact with contaminated porphyry the ratio of calcite to quartz increases. Thus near station *F* the veinlets consist largely of coarsely crystalline greenish-gray calcite that encloses large euhedral crystals of epidote and smaller euhedral crystals of oligoclase along the walls. The calcite-rich veinlets commonly pene-

trate well into idocrase-zone rocks, and locally 2 cm or more of the idocrase wall rocks adjacent to the veinlets has been converted into epidote-rich rocks. Except for their coarse and variable grain size, these rocks bear little resemblance to the average quartz monzonite pegmatites, but they very closely resemble the quartz-rich cores of the larger, zoned pegmatites. However, they generally contain more epidote and less wollastonite than the cores, especially at greater distances from the porphyry contact. The absence of wollastonite from quartz-calcite contacts in many of these veinlets indicates either lower temperatures or higher partial pressures of CO_2 than in the cores of the zoned pegmatites. The field evidence indicates that perhaps both lower temperatures and higher CO_2 pressures prevailed in the veinlets at greater distances from the porphyry contact.

An andradite-bearing pegmatite very similar to, and perhaps contiguous with the one below station *C*, occurs below station *N* along the contact between idocrase-rich rock and marble. Southeastward along the quarry face this pegmatite thins to a discontinuous sheet or mesh of microcline and bladed wollastonite. The contact zone between this wollastonite-microcline pegmatite and marble generally is 1 cm or less in thickness and consists of diopside, wollastonite, and grossularite. Locally, however, the rocks are in knife-sharp contact, and microcline crystals are embedded in calcite.

Contact Rocks

General statement.—An aureole of contact-metamorphic rocks that ranges from 1 inch to 50 feet in thickness surrounds the quartz monzonite porphyry and related igneous rocks where they have invaded the Sky Blue marble beneath the Commercial Quarry and Sky Blue Hill. The thinner parts of the aureole generally separate the marbles from contaminated rock or pegmatite and consist largely of diopside, wollastonite, and grossularite. The thicker parts of the aureole, however, generally separate the marbles from the main masses of quartz monzonite porphyry and commonly exhibit a well-defined zonal arrangement of mineral assemblages, as shown in Figure 3.

A mineral zoning in the contact aureole at Crestmore was first suggested by Larsen and Foshag (1921) in their description of the new mineral merwinite, which occurs associated with monticellite, spurrite, melilite, spinel, and idocrase a considerable distance from the intrusive contact, beyond the "garnet zone." Also, Woodford *et al.* (1941) described a "local zoning" on the south wall of the Wet Weather Quarry where blue marble is backed by brown monticellite rock, which in turn is backed by an idocrase-diopside zone. However, there was some uncertainty connected with these observations, and little importance was attached to them. Thus, although a faint suggestion of local zoning has been recognized previously, it was not until a vast amount of subsurface data from diamond-drill cores (Pl. 1) was combined with detailed surface mapping (Pl. 10) that a general zonal distribution of mineral assemblages within the contact aureole was detected. The recognition of this general zonation and the understanding in part of its nature and origin are regarded as the major contributions of this work.

The mineral zones of the contact aureole, as shown in Figure 3, are arranged in the following manner outward from the contact with the quartz monzonite porphyry intrusive mass: (1) a garnet zone that is composed chiefly of brown grossularite and lesser amounts of wollastonite and diopside; (2) an idocrase zone that is characterized by only one mineral, idocrase; and (3) a monticellite zone in which monticellite is the most abundant mineral, but in which there are variable amounts of clinohumite, cuspidine, ellestadite, forsterite, melilite, merwinite, perovskite, spinel, spurrite, tilleyite, and xanthophyllite. Outside the monticellite zone lie the nearly silica-free unmetasomatized marbles. However, locally within a few feet of the monticellite-zone contact the marbles have been secondarily recrystallized and colored blue as a consequence of the contact metasomatism. Perhaps these blue marbles should be considered as constituting a fourth zone in the contact aureole, although no new mineral assemblages have formed in them.

In addition to the aureole that surrounds the quartz monzonite porphyry in the Sky Blue marble there are large masses of contact rock that have been partially enveloped by the porphyry and its contaminated derivatives. Most of these masses form a complex interconnected network and consist entirely of the garnet-zone assemblage (diopside, wollastonite, and grossularite), but the central parts of some of the larger masses contain abundant idocrase.

An accurate estimate of the total amount of contact rock that was produced by replacement of the Sky Blue marble as a result of intrusion of the quartz monzonite porphyry magma is difficult to make, owing to the irregular shapes

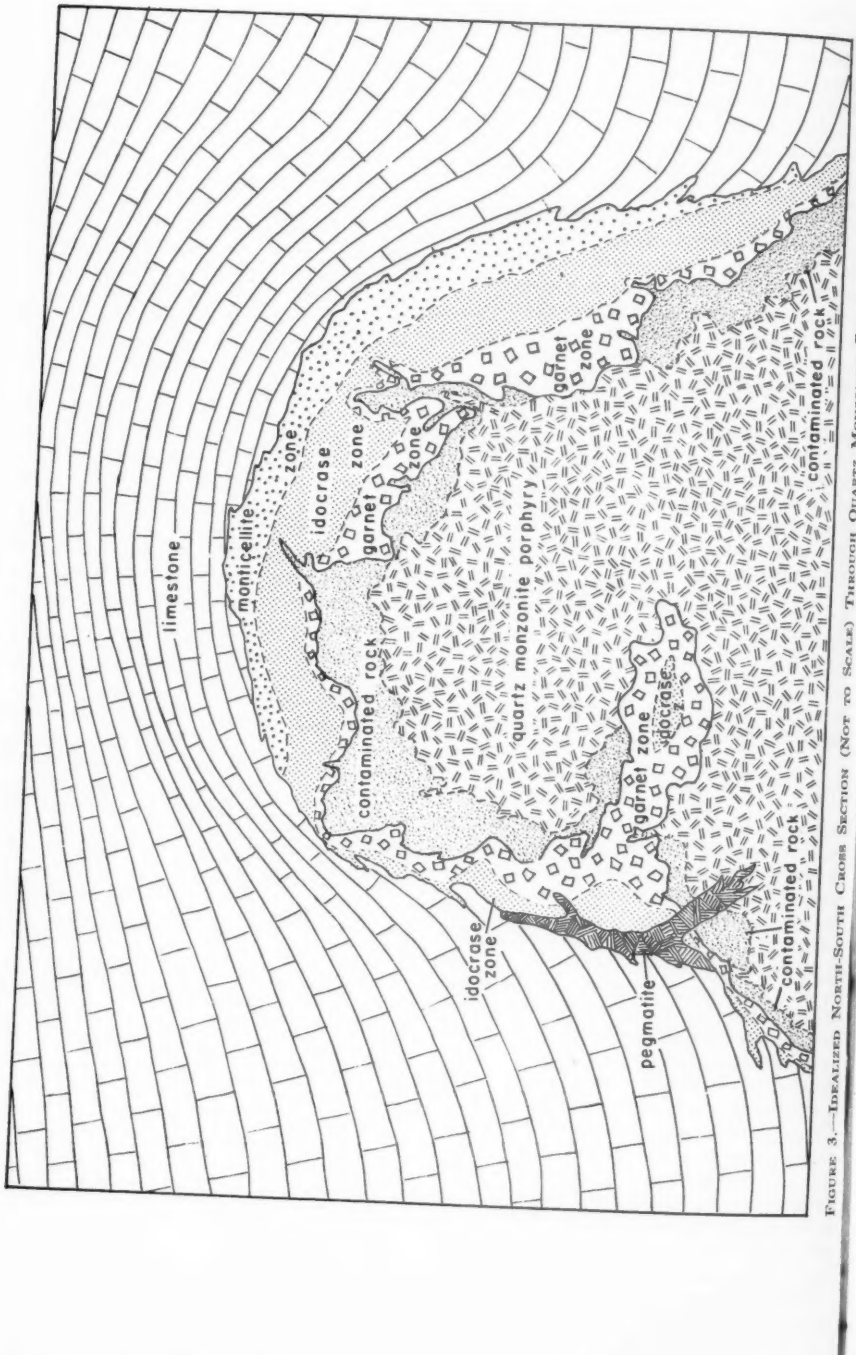

FIGURE 3.—IDEALIZED NORTH-SOUTH CROSS SECTION (NOT TO SCALE) THROUGH QUARTZ MONZONITE PORPHYRY INTRUSION AT CRESTMORE

FIGURE 3.—IDEALIZED NORTH-SOUTH CROSS SECTION (NOT TO SCALE) THROUGH QUARTZ MONZONITE PORPHYRY INTRUSION AT CRESTMORE

and distribution of the remnants within the intrusive mass; also the extent of erosion is unknown. However, a comparison of the relative amounts of these rocks indicates that the total volume of quartz monzonite porphyry and related igneous rocks is about ten times that of the contact rocks. This estimate, together with another that there is somewhat more contaminated rock than uncontaminated quartz monzonite porphyry, indicates that essentially all the silica in the contact aureole could have been obtained by desilication of the original quartz monzonite porphyry magma as a consequence of the assimilation of marble.

In succeeding parts of this section each of the three zones of the contact aureole will be described in detail, beginning with the outermost (monticellite) zone and proceeding inward through the idocrase and garnet zones to the contact with igneous rocks. This sequence of discussion is adopted because the available evidence indicates that it is essentially the time sequence of formation of the mineral assemblages which are characteristic of each zone. This is not intended to imply, however, that the present monticellite-zone rocks formed before the idocrase- and garnet-zone rocks, or that there is no overlap of the zones. On the contrary, it is probable that some of the rocks of all three zones formed contemporaneously, but it appears that idocrase-zone rocks formed largely from pre-existing monticellite-zone assemblages, and garnet-zone rocks formed from idocrase-zone assemblages. Moreover, there is considerable overlap of the zones within the aureole, although it is largely a unidirectional overlap. That is, idocrase and even some of the minerals that are characteristic of the garnet zone commonly occur in the outer part of the monticellite zone, but idocrase rarely, and monticellite-zone minerals never, have been found in the inner part of the garnet zone.

The overlap of mineral assemblages that are characteristic of each zone produces a gradation between zones and makes the definition of inter-zone boundaries somewhat arbitrary. Hence, the boundaries between one zone and another are here defined and mapped (Pl. 10) as those surfaces within which the characteristic minerals of each of the two zones occur in approximately equal proportions. This applies only to the zones within the aureole, however, as the boundary between the marbles and the contact aureole occurs where silicate-bearing assemblages, generally with excess calcite, replace the brucite-calcite assemblage.

The mineralogical differences from zone to zone are accompanied by corresponding differences in chemical composition, as shown by a comparison of the first analyses in Tables 9, 10, and 11.[1] The general relationships among the major components in each of the zones, as shown in these tables, are essentially as deduced previously (Burnham, 1954) on the basis of the chemical composition of the characteristic minerals in each zone. That is, the atomic ratio of the major metasomatic constituent (Si) to the indigenous constituents (Ca + Mg) in monticellite and several other monticellite-zone minerals is nearly 1:2, whereas in idocrase it is 1:1.5, and in the three garnet-zone minerals it is 1:1. However, the chemical analyses provide a much firmer basis on which to establish these relationships and also permit a quantitative comparison of other important constituents, such as aluminum and iron. These comparative relationships will be discussed more fully following the detailed descriptions of the zones.

Monticellite zone.—The rocks of the monticellite zone may be grouped according to the relative abundance in them of each of the major characteristic minerals. These groups may then be arranged into a sequence that corresponds approximately to the sequence in which they are encountered upon proceeding inward through the zone toward the intrusive rocks. This also appears to correspond approximately to the sequence of their formation, as interpreted from textural relationships. No evidence has been found that would indicate reversals in the sequence, although locally some of the intermediate steps appear to have been bypassed in the formation of a given assemblage.

The sequence begins with calcite-rich assemblages in contact with marbles and proceeds through clinohumite-forsterite[2], monticellite, melilite, spurrite, tilleyite, and cuspidine to merwinite-rich assemblages. Merwinite-rich

[1] The composite samples represented by these analyses are petrographically representative of the respective zones and were prepared by splitting and "quartering" all the diamond-drill core (AX size) from contact to contact in each zone as it was encountered in the drill hole. Core recovery was greater than 95 per cent for all samples.

[2] Both clinohumite and forsterite have been identified in these rocks by optical and X-ray methods, but it has not been practicable to distinguish between them in every thin section.

TABLE 9.—CHEMICAL COMPOSITION OF MONTICELLITE-ZONE ROCKS AND MINERALS
(Weight per cent)

Constituent	1	2	3	4			5				6	7	8		9
				a	b	c	a	b	c	d			a	b	
SiO_2	36.92	33.59	37.69	36.02	37.46	37.46	33.34	34.92	37.4	36.5	17.31	16.74	35.50	35.58	24.09
TiO_2	0.19	0.13	0.20	.. *	..	..	0.00	tr	0.0	tr	..	..	..	0.03	..
Al_2O_3	2.01	7.40	2.57	..	..	..	0.36	1.17	0.5	1.3	0.13	42.70	0.66	0.35	0.61
Fe_2O_3	1.59	0.80	1.75	..	..	..	0.80	0.27	1.0	0.3	0.22	2.85	0.00	0.07	0.12
FeO	2.57	2.28	1.14	2.82	2.94	3.98	1.26	1.80	1.6	2.0	..	0.41	1.22	0.36	..
MnO	0.19	0.11	0.07	..	..	0.52	0.19	0.07	0.2	0.1	0.01	..	..	0.02	..
MgO	20.24	20.37	10.54	24.74	25.32	22.78	19.26	21.54	24.5	23.7	0.47	20.03	11.62	12.34	0.43
CaO	32.70	32.66	37.73	34.36	35.14	35.20	39.37	37.75	34.4	35.7	55.18	13.09	49.96	50.69	57.75
Na_2O	0.04	0.06	0.07		..	..	0.23	0.16	0.3	0.2	..		..	..	..
K_2O	0.00	0.00	0.02		..	..	..	..	..	..	..		..	..	..
P_2O_5	0.03	0.02	0.15		..	..	tr	tr	tr	tr	3.06		..	..	..
H_2O+	1.05	0.62	1.00	1.25	..	0.15	0.30	0.17	0.4	0.2	0.53	4.49	0.94	0.44	1.09
H_2O-	0.15	0.27	0.42	loss	..	..	0.03	0.02	tr	tr	0.10	loss	0.12	0.00	..
CO_2	1.75	2.00	6.10	on	..	..	..	..	..	..	0.61	on	..	..	15.82
S	0.00	0.00	0.00	ign.	..	..	..	..	..	..	..	ign.	..	..	..
SO_3	0.13	0.13	0.15		..	..	4.57	1.91	0.0	0.0	20.69		..	..	..
F	0.00	0.00	0.02		..	..	..	..	..	..	0.57		..	..	..
Cl	0.00	0.00	0.01		..	..	..	..	..	..	1.64		..	..	..
BaO	0.04	0.00	0.00	..	..	..	..	..	..	..	..	..	..	..	..
Total	99.60	100.44	99.63	99.19	100.86	100.09	99.71	99.78	100.3	100.0	100.52	100.31	100.02	99.88	99.91
Less O for F and Cl											0.61				
											99.91				

* Constituent not reported in published analysis.

1. Composite core sample that is petrographically representative of the monticellite-zone rock—H. B. Wiik, analyst (DDH 208, 46–65 feet).
2. Nearly ideal monticellite-zone rock—H. B. Wiik, analyst (DDH 208, 116–126 feet).
3. Atypical monticellite-zone rock that is in contact upward with rock represented by analysis 2, Table 1, and downward with rock represented by analysis 2, Table 10—H. B. Wiik, analyst (DDH 230, 228½–240 feet).
4. (a) Brown monticellite as reported by Eakle (1916 and 1917)—Gordon Surr, analyst; (b) Monticellite as reported by Eakle (1917)—Gordon Surr, analyst; (c) Monticellite as reported by Moehlman and Gonyer (1934).
5. (a) "Sulfate-bearing monticellite" as reported by Kouvo (1952)—O. Kouvo, analyst; (b) "Sulfate-bearing monticellite" as reported by Kouvo (1952)—O. Kouvo, analyst; (c) Analysis 5 (a) recalculated after subtraction of the SiO_2 and CaO equivalent of SO_3 in ellestadite (analysis 6) that was present in the analysed sample; (d) Analysis 5 (b) recalculated in the same manner as analysis 5 (c).
6. Ellestadite as reported by McConnell (1937).
7. Xanthophyllite (valuevite) as reported by Eakle (1916 and 1917).
8. (a) Merwinite as reported by Larsen and Foshag (1921); (b) Merwinite as reported by Neuvonen (1952)—H. B. Wiik, analyst.
9. Tilleyite as reported by Larsen and Dunham (1933).

rocks, in turn, grade inward into idocrase-rich rocks of the idocrase zone. Although monticellite is the most abundant and widespread mineral in this zone, locally it is less abundant than calcite or other minerals of the sequence, and rarely it is absent. Calcite also is widespread, both in residual masses and secondary veinlets, throughout all the zones of the contact aureole.

TABLE 10.—CHEMICAL COMPOSITION OF IDOCRASE-ZONE ROCKS AND MINERALS

(Weight per cent)

Constituent	1	2	3	4
SiO_2	39.68	41.70	37.41	9.62
TiO_2	0.48	0.54	..*	..
Al_2O_3	9.49	9.67	17.89	..
Fe_2O_3	3.19	4.14	3.16	..
FeO	1.14	0.78	0.47	..
MnO	0.07	0.10	1.52	0.77
MgO	6.77	3.01	4.80	..
CaO	34.49	38.00	33.78	54.44
Na_2O	0.09	0.00	0.35	..
K_2O	0.00	0.00	..	..
P_2O_5	0.15	0.17	..	20.85
H_2O+	1.05	0.90	0.62	tr
H_2O-	0.01	0.03	..	tr
CO_2	2.85	0.84	..	2.10
S	0.05	0.03	..	..
SO_3	0.00	0.00	..	12.28
F	0.02	0.03	..	..
Cl	0.00	0.00	..	..
BaO	0.00	0.00	..	..
Total	99.53	99.94	100.00	100.06
Less O for S and F	0.02	0.02		
	99.51	99.92		

*Constituent not reported.

1. Composite sample of drill core that is petrographically representative of the idocrase zone—H. B. Wiik, analyst (DDH 208, 65–116 feet).

2. Composite sample of drill core which represents the idocrase-rich rocks that are contiguous upward with monticellite-zone rocks represented by analysis 3, Table 9, and downward with garnet-zone rocks represented by analysis 2, Table 11—H. B. Wiik, analyst (DDH 230, 240–263½ feet).

3. Green idocrase reported by Eakle (1917). Recalculated disregarding 1.06 per cent CuO in original analysis—J. B. Wright, analyst.

4. Pink wilkeite reported by Eakle (1914).

The contacts between monticellite-zone rocks and the coarsely recrystallized marbles generally are very sharp (Pl. 5, fig. 2). On one side of this contact is the assemblage calcite-brucite, with minor spinel and rare ellestadite; on the other side is the assemblage calcite-clinohumite (plus some forsterite) -monticellite-spinel, with minor ellestadite and rare perovskite very near the contact. The clinohumite and forsterite in this example are confined to a zone about 1 cm or less in thickness adjacent to the contact. In other places these two minerals comprise zones that are several centimeters thick, but in all known occurrences they separate the brucite marbles from monticellite-rich rocks.

The abrupt disappearance of brucite at the contact with monticellite-zone rocks is accompanied by an equally abrupt change in the nature of the calcite. The calcite associated with brucite generally is "dusty" with microscopic inclusions and is highly deformed adjacent to the brucite grains, whereas the calcite associated with silicates on the other side of the contact generally is clear and undeformed. The contact between these two types of calcite in Plate 5, figure 2, is readily traced microscopically and coincides with the contact between brucite- and clinohumite-bearing rocks. The coincidence of these contacts suggests a causal relationship between the secondary recrystallization of the calcite and the conversion of brucite to clinohumite (also forsterite and monticellite), but which is cause and which is effect is uncertain. Perhaps the water released in the conversion of brucite to a silicate plays an important role in this connection.

Inasmuch as the Sky Blue marble is essentially free of silica (Table 1), the contact between the monticellite-zone rocks and the marble represents the limit of silica metasomatism associated with the intrusion of the quartz monzonite porphyry magma. This also generally is the limit of alumina and iron metasomatism, although locally spinel and magnetite extend several centimeters beyond the silicate contact into the predazzites. Scattered crystals of ellestadite, which contain about 17 per cent SiO_2 (analysis 6, Table 9), also locally extend a few centimeters into brucite-bearing marbles, but most occurrences of this mineral are in the more calcite-rich parts of the monticellite zone.

The lack of silica in the Sky Blue marble and the spatial distribution of clinohumite-forsterite clearly indicate that one of the first reactions to occur upon the metasomatic introduction of SiO_2 into the predazzites was as follows:

7. Xanthophyllite (valuevite) as reported by Eakle (1916 and 1917).
8. (a) Merwinite as reported by Larsen and Foshag (1921); (b) Merwinite as reported by Neuvonen (1952)—H. B. Wiik, analyst.
9. Tilleyite as reported by Larsen and Dunham (1933).

$$9Mg(OH)_2 + 4SiO_2 \rightarrow 4Mg_2SiO_4 \cdot Mg(OH)_2 + 8\,H_2O. \quad (1)^3$$

9 brucite + 4 silica → 1 clinohumite + 8 water.

brucite now in the predazzites formed from periclase subsequent to the metamorphism associated with the quartz monzonite porphyry. However, there is no petrographic evidence to

TABLE 11.—CHEMICAL COMPOSITION OF GARNET-ZONE ROCKS AND MINERALS

(Weight per cent)

Constituent	1	2	3	4		5
				a	b	
SiO_2	42.89	41.91	35.77	51.77	50.42	56.50
TiO_2	0.52	0.50	..*	..	..	..
Al_2O_3	10.07	10.02	21.30	..	..	0.12
Fe_2O_3	8.14	5.28	3.98	2.12	0.51	0.23
FeO	1.82	0.75	0.60	..	..	0.00
MnO	0.22	0.11	..	..	..	..
MgO	2.43	3.67	0.78	..	0.60	17.80
CaO	32.39	36.28	36.30	44.85	48.29	25.56
Na_2O	0.24	0.00	0.20			..
K_2O	0.13	0.00	..			..
P_2O_5	0.11	0.13	..			..
H_2O+	0.57	0.80	1.23			0.58
H_2O-	0.04	0.00	..	1.02	0.07	0.22
CO_2	0.80	0.36	..	loss on ign.	loss on ign.	..
S	0.04	0.04	..			..
SO_3	0.00	0.00	..			..
F	0.02	0.02	..			..
Cl	0.00	0.00	..			0.00
BaO	0.00	0.00	..	..	..	..
Total	100.43	99.87	100.16	99.76	99.89	101.01
Less O for S and F.	0.02	0.02				
	100.41	99.85				

* Constituent not reported in published analysis.

1. Composite sample of diamond-drill core that is petrographically representative of the garnet-zone rocks—H. B. Wiik, analyst (DDH 228, 230–251 feet).

2. Composite sample of diamond-drill core that is contiguous upward with rock represented by analysis 2. Table 10—H. B. Wiik, analyst (DDH 230, 263½–276 feet). Sample is atypical of garnet-zone rock, owing to abnormally high wollastonite content.

3. Massive cinnamon-colored garnet as reported by Eakle (1917)—J. B. Wright, analyst.

4. (a) Granular white wollastonite as reported by Eakle (1917); (b) Clear crystals of wollastonite as reported by Eakle (1917).

5. Pale-green diopside from idocrase-rich rock as reported by Merriam and Laudermilk (1936). The diopside in garnet-rich rocks is darker green and presumably contains more iron.

Possibly this reaction was preceded by the dehydration of the brucite to periclase or the indicate that the reacting mineral was periclase instead of brucite. Moreover, the nature of the clinohumite and other humite-group minerals, which consist structurally of brucite interlayered with forsterite, indicates that they are more closely related stability-wise to brucite than to periclase. It also is possible that other

[3] Virtually all the SiO_2 that is involved in this and later reactions is of metasomatic origin, as the Sky Blue marble contains less than 0.2 per cent SiO_2 (Table 1). Also, the irreversible nature of this and later reactions is discussed in the section on the origin of the contact rocks.

more silica-poor members of the humite group, such as chondrodite, formed as intermediate steps in reaction (1), although only clinohumite[4] has been positively identified.

The very limited extent of the clinohumite occurrences indicates that its compositional stability field under the prevailing P-T conditions was very small and its formation was followed closely by the reaction:

$$2[4Mg_2SiO_4 \cdot Mg(OH)_2] + SiO_2 \rightarrow 9Mg_2SiO_4 + 2H_2O. \quad (2)$$

2 clinohumite + 1 silica → 9 forsterite + 2 water.

Actually, the clinohumite reaction probably was bypassed in many places, and forsterite formed directly from brucite or periclase, whichever was stable under the prevailing P-T conditions. However, forsterite itself is narrowly restricted in its occurrence at Crestmore, as shown in Plate 5, figure 2, and generally gives way within a few centimeters of the contact to monticellite-rich assemblages. This feature and the occurrence of monticellite crystals with forsteritic cores strongly suggest that much of the monticellite formed according to the following reaction:

$$Mg_2SiO_4 + 2CaCO_3 + SiO_2 \rightarrow 2CaMgSiO_4 + 2CO_2 \quad (3)$$

1 forsterite + 2 calcite + 1 silica → 2 monticellite + 2 carbon dioxide.

This reaction is the first to involve calcite and hence is the first to represent a decarbonation, although all three reactions involve silica in progressively increasing amounts.

Neither serpentine, talc, tremolite, diopside, nor wollastonite were formed near the contact with the marbles. The absence of these minerals indicates that temperatures somewhat greater than 400°C. were reached at this distance from the intrusive contacts prior to the introduction of the silica. It also indicates a deficiency in silica throughout, for all these minerals except serpentine should have formed even at much higher temperatures if enough silica has been present.

It might be expected from the foregoing that the continued metasomatic introduction of silica in excess of the amount required to fix all the magnesium in monticellite would result in the formation of one of these more silica-rich minerals such as diopside or wollastonite. However, diopside and wollastonite are uncommon in the outer part of the monticellite zone, whereas spurrite is abundant. Moreover, spurrite commonly forms rims around and intergrowths in monticellite, as shown in Plate 8, figure 5, indicating that the next step in the sequence involves the following reaction:

$$5CaCO_3 + 2SiO_2 \rightarrow 2Ca_2SiO_4 \cdot CaCO_3 + 4CO_2. \quad (4)$$

5 calcite + 2 silica → 1 spurrite + 4 carbon dioxide.

Although this reaction appears to follow that for the formation of monticellite in the silica-metasomatized magnesian marbles, the occurrence of spurrite-rich rock directly in contact with calcite marbles indicates that it is one of the first reactions involving silica to occur in the magnesium-free marbles. Occurrences of this type are not as common as would be expected from the amount of magnesium-free Sky Blue marble, owing to the extensive metasomatic introduction of magnesia into the monticellite-zone rocks (*cf.* analysis 1, Table 9, with analysis 1, Table 1).

Locally the more calcite-poor, spurrite-rich rocks of the monticellite zone contain abundant tilleyite. Its mode of occurrence is very similar to that of spurrite, with which it is generally associated, although it ordinarily does not extend as far outward toward the contact with marble as does spurrite. It also forms vermicular intergrowths with monticellite that resemble the spurrite-monticellite intergrowths in Plate 8, figure 5, but rims of tilleyite around monticellite have not been found. The available evidence indicates that tilleyite could have formed in two ways, either directly from calcite and silica as in the spurrite reaction (4) or from spurrite as follows:

$$2Ca_2SiO_4 \cdot CaCO_3 + CO_2 \rightleftarrows Ca_3Si_2O_7 \cdot 2CaCO_3. \quad (5)$$

1 spurrite + 1 carbon dioxide ⇄ 1 tilleyite.

Which of the two reactions was more important in a given place depends largely upon the CO_2 pressure and the availability of spurrite. The almost ubiquitous association of tilleyite with spurrite suggests that reaction (5) generally was important.

The textural evidence leaves some doubt as to whether the next step in the sequence involves the formation of cuspidine or merwinite, but this may be in part a reflection of the fact that although cuspidine is widespread at Crestmore, it is not a major constituent in any of the assemblages studied. The occurrence of cuspidine poikiloblastically enclosing both

[4] The "Mineral O" of Woodford, *et al.* (1941) and the "chondrodite" of Burnham (1954) have been identified as clinohumite by X-rays.

spurrite and tilleyite suggests that much of it might have formed at the expense of these minerals as follows:

$$4(2Ca_2SiO_4 \cdot CaCO_3) + 2SiO_2 + 5H_2O \rightarrow 5Ca_4Si_2O_7(OH)_2 + 4CO_2, \quad (6a)$$

4 spurrite + 2 silica + 5 water → 5 cuspidine + 4 carbon dioxide,

or

$$4(Ca_3Si_2O_7 \cdot 2CaCO_3) + 2SiO_2 + 5H_2O \rightarrow 5Ca_4Si_2O_7(OH)_2 + 8CO_2. \quad (6b)$$

4 tilleyite + 2 silica + 5 water → 5 cuspidine + 8 carbon dioxide.

The inner parts of the monticellite zone commonly consist of assemblages in which merwinite is the chief mineral. Generally the merwinite forms vermicular or subgraphic intergrowths in monticellite as in Plate 8, figure 1, granular aggregates as in Plate 8, figure 3, or irregular grains that appear to have partly replaced monticellite-spurrite intergrowths as in Plate 8, figure 5. It also forms vermicular intergrowths with cuspidine as in Plate 8, figure 3, but this occurrence appears to be relatively uncommon. Ovoid crystals of melilite such as those in Plate 8, figure 5 are abundant in the merwinite-rich rocks as are poikiloblastic crystals of idocrase.

The textural features shown in Plate 8, figure 5 are of especial interest for the information they provide on the paragenetic relationships among certain minerals in the monticellite zone. For example, in the lower left part of this photomicrograph, there is a large crystal of monticellite that encloses a subgraphic intergrowth of spurrite and a polysynthetically twinned crystal of merwinite. The merwinite is everywhere separated from calcite by monticellite or the monticellite-spurrite intergrowth, and the monticellite is in turn separated from calcite by a thin rim of spurrite. Similar relationships are exhibited by the tropical fishlike feature in the upper right part of the photomicrograph. The "eye" of this fish possesses a "pupil" of calcite, a "cornea" of spurrite, and a "white" of monticellite-spurrite intergrowth. The "body" of the fish consists of merwinite surrounded by monticellite; and along the underside a thin rim of spurrite separates the monticellite from calcite. These features, which are common in the merwinite-rich rocks, suggest that the merwinite is in reaction relationship to the monticellite-spurrite intergrowths as follows:

$$5CaMgSiO_4 + 2(2Ca_2SiO_4 \cdot CaCO_3) + SiO_2 \rightarrow 5Ca_3Mg(SiO_4)_2 + 2CO_2. \quad (7a)$$

5 monticellite + 2 spurrite + 1 silica → 5 merwinite + 2 carbon dioxide.

However, merwinite can also form from the monticellite-spurrite mixtures without additional silica, although excess silica probably would promote its formation at low CO_2 pressures; thus:

$$2CaMgSiO_4 + 2Ca_2SiO_4 \cdot CaCO_3 \rightleftarrows 2Ca_3Mg(SiO_4)_2 + CaCO_3. \quad (7b)$$

2 monticellite + 1 spurrite ⇄ 2 merwinite + 1 calcite.

The formation of merwinite-bearing assemblages completes the sequence in which silica is the only metasomatic constituent involved. However, as a comparison of the first analyses in Tables 1 and 9 reveals, alumina, iron, and magnesia also are important metasomatic constituents and must be considered in any comprehensive discussion of the monticellite-zone rocks.[5] They complicate the somewhat oversimplified picture that has just been presented, although the complications are not numerous for the following reasons: (1) magnesium that was introduced metasomatically tends merely to enhance the effects of the indigenous magnesium, (2) ferrous iron closely resembles magnesium in its effects, and (3) ferric iron closely resembles aluminum. Consequently, as a metasome, alumina is second only to silica in the importance of its effects on the mineral assemblages in the contact aureole at Crestmore.

Monticellite-zone minerals that contain aluminum (also ferric iron) as an essential component are not readily arranged into a sequence as are the aluminum-free silicates, although they exhibit a very well-defined zonal distribution in the contact aureole as a whole. The only suggestion of zoning within the monticellite zone, however, is provided by the distribution of spinel (and magnetite) with respect to the aluminosilicates melilite and xanthophyllite.

Spinel is most common in the outer part of the monticellite zone, where it is associated with forsterite or monticellite in calcite-rich rock, as in Plate 8, figure 6. It also occurs in the predazzites several centimeters beyond the monticellite-zone contact and indicates that

[5] Perhaps H_2O and CO_2 also should be considered as metasomes, but inasmuch as their effects are discussed in a later section they are excluded from the immediate discussion.

locally some alumina was transported beyond the limits of silica metasomatism. Spinel-bearing assemblages extend well into the monticellite zone, but spinel is rare in the merwinite-rich inner part. The mode of occurrence of the spinel and the absence of features which would indicate that it had formed from a pre-existing aluminum-rich mineral suggest that much of the spinel formed as follows:

$$Mg(OH)_2 + Al_2O_3 \rightleftarrows MgAl_2O_4 + H_2O, \quad (8a)^6$$

1 brucite + 1 alumina $\rightleftarrows$ 1 spinel + 1 water,

or

$$MgO + Al_2O_3 \rightleftarrows MgAl_2O_4. \quad (8b)$$

1 periclase + 1 alumina $\rightleftarrows$ 1 spinel.

The rare brittle mica xanthophyllite commonly occurs as bright-green tabular crystals very near the contact between the predazzite and monticellite zone, in rock very similar to that shown in Plate 8, figure 6, but in place of the spinel. It also occurs throughout the monticellite zone and in the outer part of the idocrase zone, but in these occurrences it is colorless and interstitial to the other silicates as in Plate 8, figures 2 and 4. Generally spinel is absent from rocks that contain xanthophyllite, and the occurrence of residual spinel cores in some of the tabular xanthophyllite crystals suggests that the latter mineral has formed in part at the expense of spinel, perhaps according to the reaction:

$$2MgAl_2O_4 + CaCO_3 + SiO_2 + H_2O \rightarrow Ca(Mg_2Al)(Al_2Si)O_{10}(OH)_2 + CO_2 \quad (9)$$

2 spinel + 1 calcite + 1 silica + 1 water $\rightarrow$ 1 xanthophyllite + 1 carbon dioxide.

Melilite, which according to its optical properties consists of about 60 per cent gehlenite and 40 per cent akermanite, is an abundant mineral in the monticellite zone and commonly is associated with xanthophyllite, as in Plate 8, figure 4. It also occurs in the monticellite-bearing, calcite-rich outer part of the monticellite zone, as in Plate 8, figure 6, where it is easily mistaken for monticellite owing to similarities in crystal habit and birefringence. The paragenetic relationships between melilite and the other two aluminous minerals are not clear; nor are they clear between melilite and monticellite, although the occurrence of poikiloblastic crystals of melilite enclosing monticellite crystals, as in Plate 8, figure 4, suggests that it is in part later than monticellite. However, the common occurrence of thin "rims" of spurrite that are molded to melilite grains, as in Plate 9, figure 5, strongly suggests that melilite preceded the spurrite. Moreover, the occurrence of oriented rods of merwinite in melilite in Plate 9, figure 3, leaves little doubt that melilite was the host. Thus it appears that much of the melilite formed after monticellite and before spurrite or merwinite, but apparently not at the expense of the monticellite. Consequently it is suggested that it formed mainly from calcite and metasomatically introduced silica, alumina, and perhaps magnesia as follows:

$$10CaCO_3 + 2MgO + 3Al_2O_3 + 7SiO_2 \rightarrow 3Ca_2Al_2SiO_7 \cdot 2Ca_2MgSi_2O_7 + 10CO_2 \quad (10)$$

10 calcite + 2 magnesia + 3 alumina + 7 silica $\rightarrow$ 3 melilite ($Ge_{60}Ak_{40}$) + 10 carbon dioxide.

Actually, whether melilite or spurrite (or tilleyite) formed at this stage probably would depend largely upon the availability of alumina in the metasomatizing fluids.

A comparison of the first analyses in Tables 1 and 9 clearly reveals that at least half the magnesium in the monticellite-zone rocks has been introduced metasomatically. This introduction, as mentioned previously, has enhanced the effects of the magnesium already in the rocks by increasing the proportions of magnesium-bearing minerals. It also has resulted in the formation of magnesium-bearing minerals such as melilite and merwinite in rocks that originally were magnesium-free calcite marbles and has therby tended to obscure the original interbedded nature of the predazzites and calcite marbles. Locally magnesia metasomatism has been so intense that the original predazzites have been converted to a calcite-poor spinel-forsterite rock. The formation of this rock clearly represents a gross removal of calcium as well as an introduction of magnesium.

Very few textural relationships provide conclusive evidence for a paragenetic sequence of minerals, but the repeated occurrence of features that indicate a certain paragenetic relationship and the absence of contradictory indications are at least highly suggestive. Thus, although the sequence that has been presented is based largely on inconclusive evidence, it is wholly consistent with all the known facts,

[6] A comparison of Tables 1 and 9 indicates that 90 per cent or more of the aluminum in the monticellite-zone minerals is of metasomatic origin.

especially the sequential changes in chemical composition of the rocks.

However, certain discrepancies exist between the paragenetic relationships described here and those described by Dunham (1933) that were based on samples obtained from the Wet Weather Quarry. Dunham (p. 474) lists the following four pairs of minerals as occurring in intergrowths: wollastonite-tilleyite, wollastonite-gehlenite, wollastonite-vesuvianite, and merwinite-grossularite. The second mineral in each pair was presumed to have formed subsequent to the first. Although no satisfactory explanation for this discrepancy is forthcoming, intergrowths between these mineral pairs of the type Dunham describes have not been observed in the detailed examination of more than 100 thin sections of Crestmore contact rocks. On the other hand, poikiloblastic crystals of grossularite and idocrase commonly enclose irregular remnants of merwinite, but graphic or vermicular intergrowths of these minerals have not been observed. A factor that should be considered in attempts to resolve these discrepancies is the close resemblance of wollastonite to cuspidine in thin section; subgraphic intergrowths of tilleyite and cuspidine are widespread at Crestmore. Wollastonite also closely resembles melilite in thin section, and in this connection Dunham (Fig. 2*A*, p. 476) presents a *camera lucida* drawing that shows oriented inclusions of "merwinite in wollastonite" which strikingly resemble the oriented rods of merwinite in melilite[7] shown in Plate 9, figure 3.

Idocrase zone.—The distribution of rocks in which idocrase is the major mineral constituent is shown in Figure 2 and Plate 10. One of the more important features of this distribution is that idocrase-rich rocks lie on the intrusive side of the monticellite-zone rocks in all places where the two are associated. Idocrase is the only characteristic mineral of this zone, although the rare mineral wilkeite appears to be confined to

[7] This melilite ($Ge_{60}Ak_{40}$) has been positively identified by X rays.

Plate 6.—Photomicrographs

Figure 1.—Phenocrystlike relict of plagioclase (An_{33}) in partially assimilated mafic xenolith engulfed by quartz diorite. Crossed nicols, ×16.

Figure 2.—Enlargement of top of Figure 4 of this plate, showing sawtooth arrangement of sphene parallel to cleavage in surviving shreds of chloritized biotite. Plain light, ×40.

Figure 3.—Predazzite. Partial pseudomorph of fibrous brucite after octahedral periclase in calcite matrix. Plain light, ×16.

Figure 4.—Foliation in quartz diorite near contact with Chino marble. Plain light, ×16.

Figure 5.—Predazzite. Brucite pseudomorphous after periclase in calcite. Note deformation of lamellae in calcite adjacent to brucite. Compare with Figure 3 of this plate. Crossed nicols, ×16.

Figure 6.—Contact between quartz diorite and the xenolith shown in Figure 1 of this plate. Note preferred orientation of the large plagioclase (An_{44}) crystals in the quartz diorite (right-hand side). Crossed nicols, ×16.

Plate 7.—Photomicrographs

Figure 1.—Kalisyenitic contaminated rock. Small grains with excellent cleavage are wollastonite. Crossed nicols, ×16.

Figure 2.—Pegmatitic contaminated rock. Potassium feldspar constitutes veinlet along contact between quartz and plagioclase. The same interstitial potassium feldspar forms "host" for wollastonite intergrowth in Plate 5, figure 1. Crossed nicols, ×40.

Figure 3.—Poikilitic or poikiloblastic crystal of diopsidic augite in slightly contaminated quartz monzonite porphyry. Plain light, ×16.

Figure 4.—Monzonitic contaminated rock. The perthitic plagioclase is oligoclase and the pyroxene (lower left) is aegerinaugite (see analysis 4, Table 6). Crossed nicols, ×40.

Figure 5.—Petrographically representative quartz monzonite porphyry (see analysis 11, Table 4, and analysis 2, Table 5). Note the general anhedral character of the grains. Crossed nicols, ×16.

Figure 6.—Syenitic contaminated rock within 1 cm of contact with garnet-rich contact rock. Sanidine phenocryst is partially rimmed with myrmekite and contains a bladelike crystal of wollastonite. Dark area (at top left) consists of andraditic garnet. Crossed nicols, ×16.

FIGURE 1

FIGURE 2

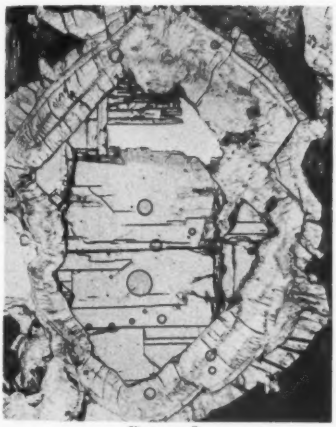

FIGURE 3

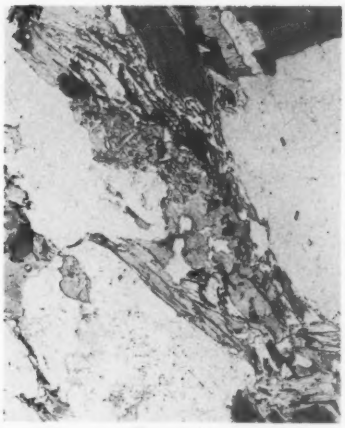

FIGURE 4

FIGURE 5

FIGURE 6

PHOTOMICROGRAPHS

FIGURE 1

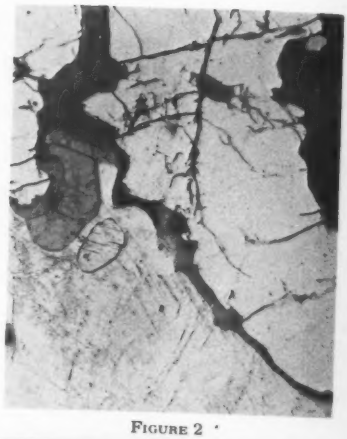

FIGURE 2

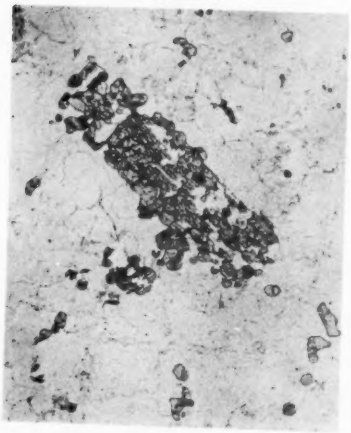

FIGURE 3

FIGURE 4

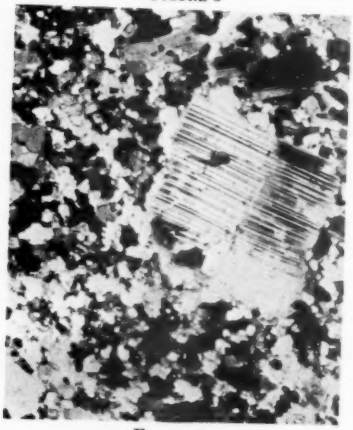

FIGURE 5

FIGURE 6

PHOTOMICROGRAPHS

FIGURE 1

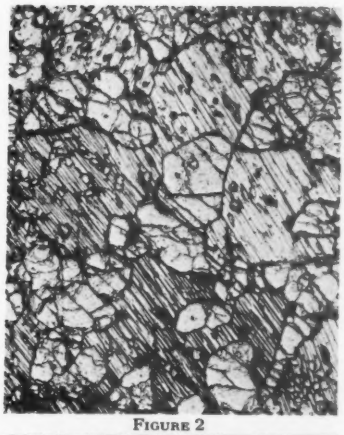

FIGURE 2

FIGURE 3

FIGURE 4

FIGURE 5

FIGURE 6

PHOTOMICROGRAPHS

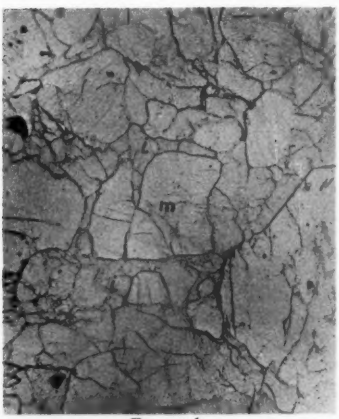

FIGURE 1

FIGURE 2

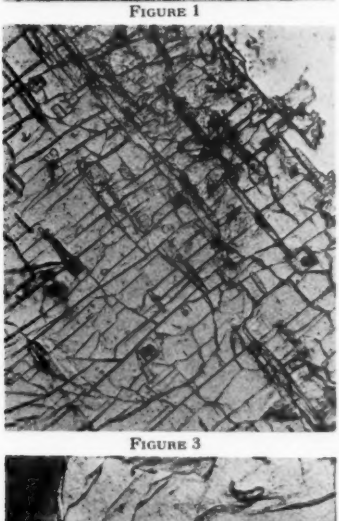

FIGURE 3

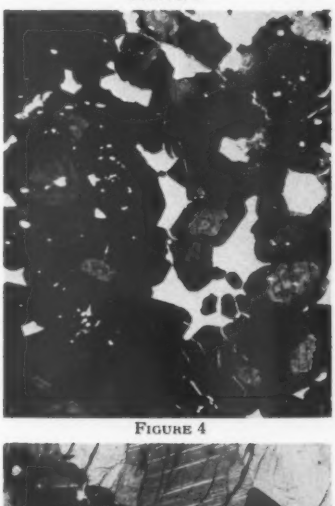

FIGURE 4

FIGURE 5

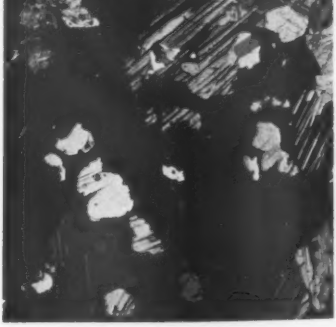

FIGURE 6

PHOTOMICROGRAPHS

idocrase-rich rocks. However, wilkeite is so rare at Crestmore, having been found only along the ridge between the Commercial and Wet Weather quarries and in diamond-drill hole No. 230 (Pl. 1), that its true affinities are somewhat uncertain.

Although idocrase is the only characteristic mineral of the idocrase zone, it is by no means the only common one. The occurrence of this zone, sandwiched between the monticellite and garnet zones, and the gradational nature of the transition from one zone to another result in the association of a relatively large number of minerals with the predominant idocrase. However, the kinds of associated minerals in the outer part of the zone differ from those in the inner part, as would be expected from the mineral composition of the adjacent zones. Thus, monticellite, merwinite, melilite, spurrite, and xanthophyllite are common in the outer part of the zone (Pl. 8, fig. 2; Pl. 9, figs. 1 and 6), whereas diopside, wollastonite, and grossularite are abundant in the inner part. Calcite (Pl. 9, fig. 4) is common throughout the idocrase zone and the contact aureole in general.

The occurrence of either diopside, wollastonite, or grossularite as a minor constituent of the monticellite-zone rocks, especially in the inner part of the zone, already has been described and is attributed to a local "flooding" by metasomatic silica. These minerals, singly or in pairs, are somewhat more common in the outer part of the idocrase zone (Pl. 9, fig. 2), bringing the total number of different minerals in a single thin section to as many as seven. Hence, a larger number of minerals is likely to be found in a given specimen from the outer part of the idocrase zone than in one from either of the other two zones.

Certain common textural features, such as those shown in Plate 9, figures 1 and 6, clearly indicate that idocrase has replaced monticellite-

---

PLATE 8.—PHOTOMICROGRAPHS

FIGURE 1.—Monticellite-zone rock. Vermicular or subgraphic intergrowths of merwinite and monticellite in matrix of granular monticellite, tilleyite, and spurrite. Crossed nicols, ×40.

FIGURE 2.—Monticellite-zone–idocrase-zone transition rock. Colorless xanthophyllite interstitial to subhedral and euhedral idocrase. Plain light, ×16.

FIGURE 3.—Monticellite-zone rock. Top left: intimate intergrowths of merwinite in monticellite and cuspidine. Center: fine vermicular intergrowths of the same minerals. Lower right: granular merwinite. Crossed nicols, ×16.

FIGURE 4.—Monticellite-zone rock. Wheat-shaped crystals of monticellite enclosed in idocrase (left), xanthophyllite (center), and melilite (right). Plain light, ×16.

FIGURE 5.—Monticellite-zone rock. Lower left: polysynthetically twinned merwinite and vermicular spurrite in monticellite host which is rimmed with spurrite. Upper right: merwinite (in extinction) rimmed with monticellite (light) and spurrite. Top left and lower right: crystals of melilite ($Ge_{60}Ak_{40}$) in calcite. Crossed nicols, ×40.

FIGURE 6.—Monticellite-zone rock. Wheat-shaped crystals of monticellite (and less abundant melilite) with spinel in calcite. Plain light, ×16.

PLATE 9.—PHOTOMICROGRAPHS

FIGURE 1.—Monticellite-zone–idocrase-zone transition rock. Monticellite (*m*) partially replaced by idocrase (*i*). Plain light, ×40.

FIGURE 2.—Idocrase-zone rock. Intimate intergrowth of wollastonite (at extinction) and monticellite. Diopside at top left and idocrase at bottom right. Crossed nicols, ×16.

FIGURE 3.—Monticellite-zone rock. Rods of merwinite in melilite ($Ge_{60}Ak_{40}$) have two orientations perpendicular to each other and apparently in the (110) plane of the melilite. Opaque inclusions in some merwinite rods are magnetite. Plain light, ×40.

FIGURE 4.—Idocrase-zone rock. Zoned crystals of idocrase with intersitial calcite. Zonation is of abnormal interference colors, olive green in the cores and ultra blue in the rims. Crossed nicols, ×16.

FIGURE 5.—Monticellite-zone rock. "Spines" of spurrite along boundaries between melilite grains. Crossed nicols, ×40.

FIGURE 6.—Monticellite-zone–idocrase-zone transition rock. Merwinite (polysynthetically twinned) partially replaced by large poikiloblastic crystals of idocrase (dark). Crossed nicols, ×40.

zone minerals. Similarly, textural relationships suggest that monticellite-zone minerals in the outer part of the idocrase zone locally have been replaced by garnet-zone minerals, presumably as a result of "flooding" by silica and alumina. However, other textural relationships involving these minerals, as in Plate 9, figure 2, are somewhat ambiguous. For example, the monticellite-wollastonite intergrowths shown in this photomicrograph are thought by the writer to have formed from the monticellite-spurrite, monticellite-merwinite, or monticellite-cuspidine intergrowths as a result of "flooding" by silica, whereas they are tentatively interpreted by Harker and Tuttle (1956b) as the result of decomposition of akermanite. Arguments in support of the replacement origin are: (1) the rock consists mainly of diopside and idocrase, indicating an excess of silica; (2) similar types of intergrowths between monticellite and spurrite, merwinite, or cuspidine are very common in the monticellite zone; (3) most of the intergrowths in this specimen involve diopside instead of wollastonite; and (4) the intergrowths grade into relatively large clean crystals of wollastonite or diopside that are in parallel optical orientation. Arguments against the decomposition hypothesis are: (1) the melilite that is abundant throughout the monticellite zone is gehlenitic instead of akermanitic; (2) to the writer's knowledge, akermanite never has been found as a contact-metamorphic mineral; and (3) the hypothesis should but does not explain the much more prevalent identical-type intergrowths of monticellite and diopside in the same thin section. It is probable that akermanite-rich solid solutions do not ordinarily occur in contact-metamorphic rocks because of their instability in the presence of water vapor and the greater stability of idocrase in these systems.

The chemical composition of the idocrase-zone rocks is represented by analysis 1 in Table 10. The composite sample of drill core, on which this analysis was made, was obtained by splitting and quartering the entire section of core from contact to contact and is regarded as petrographically representative of the idocrase-zone rocks. The section of drill core represented by analysis 2, Table 10, is petrographically atypical owing to the presence of abnormally large amounts of wollastonite, but was selected for analysis because it is contiguous upward with the monticellite-zone rock represented by analysis 3, Table 9, and downward with the garnet-zone rock represented by analysis 2, Table 11.

The differences in composition between the idocrase- and monticellite-zone rocks, as shown by a comparison of the first analyses in Tables 9 and 10, are in the direction that would be anticipated from their mineralogical differences and the closer proximity of the idocrase zone to the quartz monzonite porphyry intrusive mass, the source of silica, alumina, and iron. The magnitude of these differences perhaps is not as great as might be expected, but the important factor in the formation of a given mineral assemblage is not the absolute amounts of the metasomatic constituents, but their amounts relative to calcium and magnesium. Thus, the fact that the ratio Si + Al + Fe/Ca + Mg in the idocrase zone is about 1.7 times greater than in the monticellite zone supports the interpretation, based on petrographic evidence, that the idocrase-rich rocks formed largely at the expense of the monticellite-zone assemblages.

The number of reactions by which the idocrase at Crestmore could have formed is relatively large, owing to the several different monticellite-zone minerals and assemblages that can be converted into idocrase through the addition of appropriate amounts of silica, with or without alumina (and iron). However, inasmuch as monticellite, spurrite, merwinite, and melilite are the most abundant monticellite-zone minerals near the idocrase-zone contacts, the following general reaction which involves these minerals will serve to represent the conversion of all monticellite-zone assemblages to idocrase:

$$\begin{aligned} &CaMgSiO_4 + 2(2Ca_2SiO_4 \cdot CaCO_3) \\ &\quad + 3Ca_3MgSi_2O_8 + 4Ca_{10}Mg_2Al_6Si_7O_{35} \\ &\quad + 15SiO_2 + 12H_2O \rightarrow \\ &\quad 6Ca_{10}Mg_2Al_4Si_9O_{34}(OH)_4 + 2CO_2 \qquad (11) \end{aligned}$$

1 monticellite + 2 spurrite
+ 3 merwinite + 4 melilite ($Ge_{60}Ak_{40}$)
+ 15 silica + 12 water →
6 idocrase + 2 carbon dioxide.

Reaction (11) is not given as the only, or even the most prevalent, reaction by which idocrase was formed, but merely as one that is representative. In fact, a comparison of the aluminum contents of the idocrase and monticellite zones indicates that much metasomatic alumina as well as silica generally was involved in the formation of idocrase-zone assemblages. Consequently much less melilite than is indicated in reaction (11) ordinarily would have been involved, and this is in agreement with its general abundance relative to monticellite, spurrite, and merwinite.

Garnet zone.—Large masses of rock that consist mainly of brown grossularite garnet with subordinate amounts of wollastonite and diopside are perhaps the most prominent feature of the contact aureole at Crestmore. It is estimated from surface exposures and diamond-drill data that about 60 per cent by volume of the contact aureole consists of garnet-zone rock; and inasmuch as grossularite composes about 60 per cent of this rock, it is the most abundant contact-metamorphic mineral at Crestmore. Rocks that consist essentially of the wollastonite-diopside-grossularite assemblage have the following modes of occurrence: (1) as essentially the only rock of the contact zones between the quartz diorite and marbles, (2) as the innermost zone of the contact aureole that surrounds the quartz monzonite porphyry intrusive mass, (3) as large masses that are partly or wholly enveloped by quartz monzonite porphyry, (4) as contact zones as much as 1 foot thick that separate bodies of pegmatite from marbles or other zones of the aureole, and (5) as sheaths as much as 1 foot thick that surround small pipes and stringers of contaminated rock in monticellite- or idocrase-zone rocks.

The first of these modes of occurrence has been described in connection with the quartz diorite. The innermost zone of the aureole and the inclusions of garnet-rich rock in quartz monzonite porphyry are very similar mineralogically and texturally, although the inclusions appear generally to contain more wollastonite. Locally the aureole garnet-zone rocks that overlie the larger bodies of quartz monzonite porphyry are brecciated (*e.g.* above stations *B*, *E*, *F*, and *G*, Pl. 10). The matrix of the more intensely brecciated rock generally consists of contaminated rock, some of which is slightly pegmatitic. The interstices of the fragments in the less intensely brecciated rock, as near station *B*, commonly are filled with calcite and wollastonite or calcite, diopside, and scapolite. However, between stations *E* and *F* some of these interstices are filled with pegmatitic epidote - microcline - oligoclase - calcite - quartz rock. The brecciation very probably was caused by intrusive activity in the main pipelike bodies of quartz monzonite porphyry magma after the formation of the brittle garnet-rich contact rock.

The contact zones that border the quartz monzonite pegmatites generally are less than 25 cm thick. The thicker zones separate the pegmatites from idocrase- and monticellite-zone rocks, whereas the thinner zones, which commonly are less than 1 cm thick, separate the pegmatites from marbles. In fact, near station *N* (Pl. 10) microcline crystals are embedded in coarsely crystalline calcite with no megascopically visible contact zone between them. Generally, however, both this body and the one below station *C* are separated from the Sky Blue marble by a centimeter or more of fibrous wollastonite with or without minor amounts of green diopside and pale-pink grossularite.[8]

The contact zones of the relatively large pegmatite body north of station *B* afford an excellent illustration of the differential contact effects of the same igneous body on different zones of the contact aureole. In the lower part of the quarry face this pegmatite is in contact on the south with aureole garnet-zone rocks, and except perhaps for a slight enrichment in wollastonite near the dike, there is no megascopically visible contact effect. On the north, however, the pegmatite cuts idocrase-zone rocks and is separated from them by approximately 15 cm of diopside-rich rock that contains only minor amounts of wollastonite and grossularite. The wollastonite occurs mainly in contact with the quartz and feldspars of the pegmatite, and the grossularite occupies an intermediate position. This diopside-rich zone continues upward along the contact between the pegmatite and monticellite-zone rocks, although it diminishes considerably in thickness.

The fifth mode of occurrence of the wollastonite-diopside-grossularite assemblage is as sheaths 5–25 cm thick that surround small pipes or stringers of contaminated rock where they penetrate idocrase- and monticellite-zone rocks. Regardless of the composition of the contaminated rock, whether syenitic or dioritic, the sheaths are all similar in that they consist mainly of light-colored, fine-grained grossularite, wollastonite, and diopside. The wollastonite generally is concentrated near the contacts, and the diopside is more abundant in the outer parts of the sheaths. Thus, they exhibit the same kind of zoning as occurs in the contact rocks adjacent to pegmatites, although the sheaths generally contain a much larger proportion of grossularite.

Although the wollastonite-diopside-grossularite borders of the pegmatites and sheaths around the contaminated-rock pipes and stringers are quantitatively only minor features of the contact aureole, they are nonetheless

[8] The wollastonite-rich rock along much of the contact below station *C* has been altered to opal (cristobalite).

important because they illustrate the fact that monticellite-zone rocks never, and idocrase-zone rocks rarely, occur in contact with igneous rocks at Crestmore. Moreover, the ubiquitous occurrence of the wollastonite-diopside-grossularite assemblage bordering igneous bodies that have been intruded into idocrase- and monticellite-zone rocks clearly indicates that the garnet-zone rocks have formed largely at the expense of these other contact rocks.

This interpretation is supported by the chemical data in Table 11, for the atomic ratio of metasomatic to indigenous constituents (Si + Al + Fe/Ca + Mg) in analysis 1 is 1.64, approximately 1.4 times as large as in the idocrase-zone rocks and 2.5 times as large as in the monticellite-zone rocks. Thus it appears that the idocrase-zone rocks could have been converted into garnet-zone rocks if the ratio of metasomatic to indigenous constituents was increased as follows:

$$Ca_{10}Mg_2Al_4Si_9O_{34}(OH)_4 + 3SiO_2 \rightarrow 2Ca_3Al_2Si_3O_{12} + 2CaMgSi_2O_6 + 2CaSiO_3 + 2H_2O. \quad (12)$$

1 idocrase + 3 silica → 2 grossularite + 2 diopside + 2 wollastonite + 2 water.

In this reaction, all three characteristic minerals of the garnet zone can be produced from the single characteristic mineral of the idocrase zone simply by the addition of silica. This is an oversimplification of the actual process of conversion, of course, for alumina as well as silica was a constituent of the metasomatizing solutions, and some magnesia clearly was removed in the process. However, both these added factors have only a modifying effect on reaction (12) in that they would tend to increase the yield of grossularite relative to diopside and wollastonite and thereby produce a rock that compositionally more closely resembles the garnet-zone rocks at Crestmore.

Summary and comparison.—The general geological features of the contact rocks and their spatial relationships to the quartz monzonite porphyry and related igneous rocks are schematized in Figure 3. Although this cross-sectional diagram is somewhat idealized, it nevertheless illustrates the general spatial relationships of the various types of rock. Thus, the monticellite zone occurs as an incomplete outer carapace mainly over the thicker parts of the contact aureole. The idocrase zone, and locally even the garnet zone, also occurs in contact with the parental marbles but generally only where the aureole is relatively thin. Garnet-zone rocks nearly everywhere separate igneous rocks from other zones of the contact aureole, and consequently idocrase-zone rocks rarely, and monticellite-zone rocks never, have been found in contact with igneous rocks.

The thicker parts of the contact aureole generally are in contact with relatively uncontaminated quartz monzonite porphyry, whereas the thinner parts of the aureole are in contact with the thicker masses of contaminated rock. Contaminated rocks also occur as stringers and small pipelike bodies in all three zones of the aureole but are everywhere separated from aureole contact rocks by minerals of the garnet-zone assemblage regardless of the zone in which they occur. The same contact relationships are associated with the pegmatite bodies that cut all the zones of the contact aureole and locally penetrate marbles for short distances.

The petrological relationships within and between zones of the contact aureole are readily summarized with the aid of Figure 4, in which the compositions of each of the zones and its minerals are represented. Only the prograde metamorphic minerals that occur at Crestmore are represented in the diagram. Moreover, inasmuch as there are eight major components involved in the natural system and only four corners to the tetrahedron, the ferric iron is combined with aluminum, and ferrous iron is combined with magnesium, and it is assumed that water and carbon dioxide are present in excess.[9] Thus simplified, the chemical composition of each zone of the aureole and of the parental predazzite marbles can be represented on the diagram as points *P*, *M*, *I*, and *G*.

The course by which the composition of representative monticellite-zone rock (*M*) is attained from the parental predazzite marbles (*P*) passes through the following equilibrium assemblages: (1) calcite-brucite (or periclase)-clinohumite-spinel, (2) calcite-clinohumite-forsterite-spinel, (3) calcite-forsterite-spinel-xanthophyllite, (4) calcite-forsterite-monticellite-xanthophyllite, (5) calcite-monticellite-xanthophyllite-melilite, (6) calcite-monticellite-spurrite (or tilleyite)-melilite, and (7) monticellite-spurrite-merwinite-melilite. Monticellite-rich assemblages that contain small amounts of idocrase- and/or garnet-zone minerals also are encountered very near *M*. Whether the course actually is as indicated by the line *P*-*M* is determined by local conditions during metamorphism, especially the degree

[9] The roles of water and carbon dioxide are discussed in the next section.

and timing of magnesia metasomatism with respect to silica and alumina metasomatism.

It is remarkable that this sequence of assemblages is essentially the same sequence in which they are encountered upon proceeding inward toward the quartz monzonite porphyry intrusive mass from the contact with Sky Blue marble. Moreover, it is essentially the same as the paragenetic sequence and therefore provides strong support for the sequence of reactions 1-10. The fact that the principal assemblages in the monticellite zone are equilibrium assemblages indicates that chemical equilibrium, although perhaps not fully attained, was closely approached within relatively small volumes of rock.

The conversion of monticellite-zone assemblages to idocrase-rich rocks is represented in Figure 4 by passage from *M* to *I* and, as indicated, involves the introduction of silica and alumina and the removal of magnesia. Similar gains and losses are involved in the conversion of idocrase-rich assemblages to the garnet-zone assemblage (from *I* to *G*). It is noteworthy that *I* and *G* lie near the high-silica boundaries of their respective equilibrium assemblages and that *M* oversteps this boundary slightly. This phenomenon is expressed by the "unidirectional overlap" of mineral assemblages and the metasomatic "flooding" of silica (and alumina) outward from the intrusive mass.

Figure 5 facilitates a more precise comparison of each zone in the contact aureole with the others and with the parental Sky Blue marble in terms of gains and losses in major constituents. The data in this diagram have been obtained from the first analyses in Tables 1, 5, 7, 9, 10, and 11 through a recomputation based on the assumption that a unit volume of Sky Blue marble remained constant during conversion to calc-silicate contact rock. Although this assumption is not strictly valid, it doubtless holds as a first approximation.

The largest loss in the conversion of Sky Blue marble to monticellite-zone rock is in the carbon (CO_2) content, as expected, but a considerable and somewhat unsuspected loss also occurs in the calcium content. The direction of migration of the replaced calcium is uncertain; perhaps it makes up part of the secondary calcite veins that occur both within the contact aureole and in the Sky Blue marble near the contact. The relatively minor loss in the hydrogen (H_2O) content is probably not as large as it was originally, owing to the occurrence of

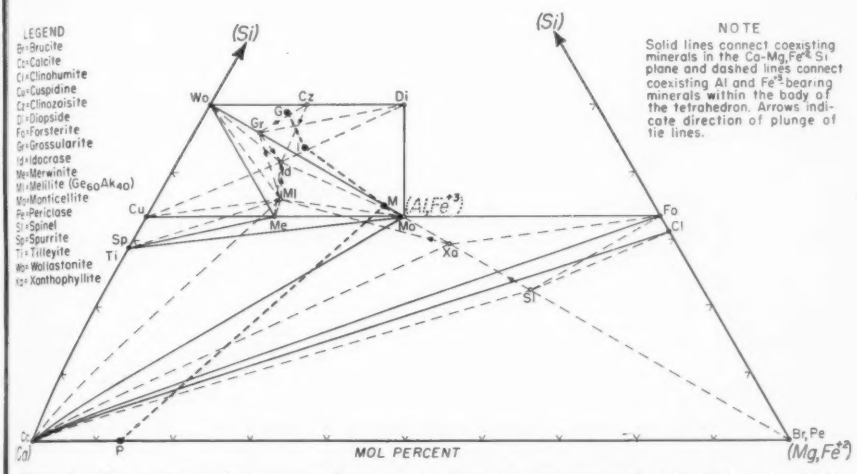

FIGURE 4.—TETRAHEDRAL COMPOSITION DIAGRAM FOR PART OF THE SYSTEM CA-MG, Fe^{+2}-SI-AL, Fe^{+3}

The Al, Fe^{+3} apex is at the eye of the observer. Only those minerals that occur in the contact aureole at Crestmore are represented. *P*, predazzite (analysis 1, Table 1); *M*, monticellite-zone rock (analysis 1, Table 9); *I*, idocrase-zone rock (analysis 1, Table 10); *G*, garnet-zone rock (analysis 1, Table 11). *P* lies essentially on the Ca-Mg, Fe^{+2}-Si base of the tetrahedron, whereas *M*, *I*, and *G* lie 4.6, 13.1, and 17.6 per cent above the base, respectively.

hydrous alteration products of anhydrous prograde minerals in the monticellite zone.

The principal gain in the conversion of the marble became "stuffed" with metasomatic constituents during the conversion to monticellite-zone rocks.

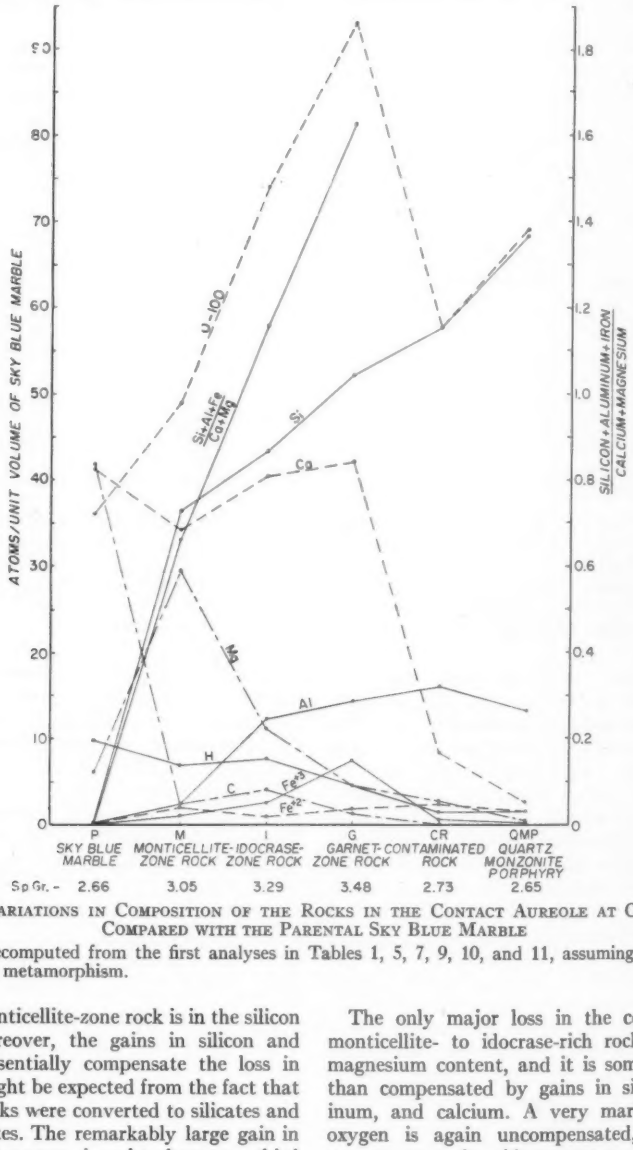

FIGURE 5.—VARIATIONS IN COMPOSITION OF THE ROCKS IN THE CONTACT AUREOLE AT CRESTMORE AS COMPARED WITH THE PARENTAL SKY BLUE MARBLE

Data are recomputed from the first analyses in Tables 1, 5, 7, 9, 10, and 11, assuming constancy of volume during metamorphism.

marble to monticellite-zone rock is in the silicon content. Moreover, the gains in silicon and aluminum essentially compensate the loss in carbon, as might be expected from the fact that carbonate rocks were converted to silicates and aluminosilicates. The remarkably large gain in magnesium, however, is only about one-third compensated by the loss in calcium, and the appreciable gain in oxygen is uncompensated. Consequently, each unit volume of original

The only major loss in the conversion of monticellite- to idocrase-rich rocks is in the magnesium content, and it is somewhat more than compensated by gains in silicon, aluminum, and calcium. A very marked gain in oxygen is again uncompensated, and as a consequence the idocrase-zone rocks have become further "stuffed" with metasomatic constitutents during their formation.

This "stuffiing" appears to have continued

in the formation of the garnet-zone rocks, as the relatively minor losses in magnesium, carbon, and hydrogen are more than compensated by gains in silicon, aluminum, and iron, and the large gain in oxygen is once again uncompensated. Consequently the garnet-zone rocks (sp. gr. = 3.48), which are the most intensely metasomatized of all the contact rocks, contain about 40 per cent more atoms per unit volume than the original marbles (sp. gr. = 2.66), and oxygen makes up nearly half this increase.

A comparison of the ratios of metasomatic constituents to indigenous constituents (Si + Al + Fe/Ca + Mg) reveals a very sharp and nearly uniform increase from essentially zero in the Sky Blue marble through 0.66 in monticellite-zone rocks and 1.15 in idocrase-zone rocks to 1.62 in garnet-zone rocks. The large and systematic increase in this ratio is regarded as petrologically more important than gains and losses in individual elements, as it appears to be the underlying cause for the zonal arrangement of mineral assemblages in the contact aureole at Crestmore.

Origin of the Contact Rocks

The concept advanced by Bowen (1940), that the metamorphism of siliceous limestones and dolomites involves essentially a progressive thermal decarbonation, is taken as the starting point in this discussion on the origin of the contact rocks at Crestmore. Accordingly, the progressive metamorphism of carbonate rocks is capable of exhibiting 13 steps[10], each of which is represented by a univariant reaction (except those that involve tremolite). Also, for each of these reactions there is a univariant P-T curve, and the phase assemblage that is stable on the low-temperature side of it is not stable on the high-temperature side. Consequently, the occurrence of one of these assemblages indicates that the temperature at which it becomes unstable has not been attained. Moreover, if metamorphism is purely thermal and the CO_2 pressure remains constant, the appearance of each new mineral assemblage on the high-temperature (right) side of the following reactions generally indicates the attainment of a certain temperature of metamorphism.

(*a*) $3CaMg(CO_3)_2 + 4SiO_2 \rightleftarrows CaMg_3(SiO_3)_4 + 2CaCO_3 + 4CO_2$.
3 dolomite + 4 quartz ⇄ 1 tremolite + 2 calcite + 4 carbon dioxide.

(*b*) $CaMg_3(SiO_3)_4 + 5CaMg(CO_3)_2 \rightleftarrows 6CaCO_3 + 4Mg_2SiO_4 + 4CO_2$.
1 tremolite + 5 dolomite ⇄ 6 calcite + 4 forsterite + 4 carbon dioxide.

(*c*) $CaMg_3(SiO_3)_4 + 2CaCO_3 + 2SiO_2 \rightleftarrows 3CaMgSi_2O_6 + 2CO_2$.
1 tremolite + 2 calcite + 2 quartz ⇄ 3 diopside + 2 carbon dioxide.

(*d*) $2CaCO_3 + 3CaMg_3(SiO_3)_4 \rightleftarrows 5CaMgSi_2O_6 + 2Mg_2SiO_4 + 2\ CO_2$.
2 calcite + 3 tremolite ⇄ 5 diopside + 2 forsterite + 2 carbon dioxide.

(*e*) $CaMg(CO_3)_2 \rightleftarrows CaCO_3 + MgO + CO_2$.
1 dolomite ⇄ 1 calcite + 1 periclase + 1 carbon dioxide.

(*f*) $CaCO_3 + SiO_2 \rightleftarrows CaSiO_3 + CO_2$.
1 calcite + 1 quartz ⇄ 1 wollastonite + 1 carbon dioxide.

(*g*) $CaMgSi_2O_6 + Mg_2SiO_4 + 2CaCO_3 \rightleftarrows 3CaMgSiO_4 + 2CO_2$.
1 diopside + 1 forsterite + 2 calcite ⇄ 3 monticellite + 2 carbon dioxide.

(*h*) $CaMgSi_2O_6 + CaCO_3 \rightleftarrows Ca_2MgSi_2O_7 + CO_2$.
1 diopside + 1 calcite ⇄ 1 akermanite + 1 carbon dioxide.

(*i*) $Mg_2SiO_4 + CaCO_3 \rightleftarrows CaMgSiO_4 + MgO + CO_2$.
1 forsterite + 1 calcite ⇄ 1 monticellite + 1 periclase + 1 carbon dioxide.

(*j*) $CaCO_3 + 2\ CaSiO_3 \rightleftarrows 2\ Ca_2SiO_4 \cdot CaCO_3 + CO_2$.
1 calcite + 2 wollastonite ⇄ 1 spurrite + 1 carbon dioxide.

(*k*) $Ca_2MgSi_2O_7 + CaCO_3 \rightleftarrows Ca_3Mg(SiO_4)_2 + CO_2$.
1 akermanite + 1 calcite ⇄ 1 merwinite + 1 carbon dioxide.

(*l*) $CaSiO_3 + 2Ca_2SiO_4 \cdot CaCO_3 \rightleftarrows 3Ca_2SiO_4 + CO_2$.
1 wollastonite + 1 spurrite ⇄ 3 larnite + 1 carbon dioxide.

A comparison with reactions 1–12 reveals that the reactions given here generally are not those by which the contact-metamorphic assemblages at Crestmore are thought to have formed, nor is the sequence of their occurrence the same. Consequently, one might conclude, as did Turner and Verhoogen (1951, p. 377), that the mineral assemblages at Crestmore possibly represent nonequilibrium associations. This is not supported, however, by the evidence presented in the preceding section or by laboratory experience.[11] Moreover, the conclusion does not necessarily follow, for Bowen (1940) considered in detail only the series of equilib-

[10] Tilley (1951) has increased this number to 17 with the addition of two reactions that involve talc and one each for tilleyite and rankinite.

[11] Although most of these reactions are relatively sluggish in "dry" systems, the presence of even a trace of water vapor is sufficient for the establishment of equilibrium, generally within a few hours.

rium assemblages that would arise in response to increased temperatures under conditions of constant pressure and appropriate fixed chemical composition and tended to minimize the quartz-wollastonite, as spurrite is unstable in the presence of excess silica. In either case wollastonite could have formed under equilibrium conditions as low as 400°C. On the other

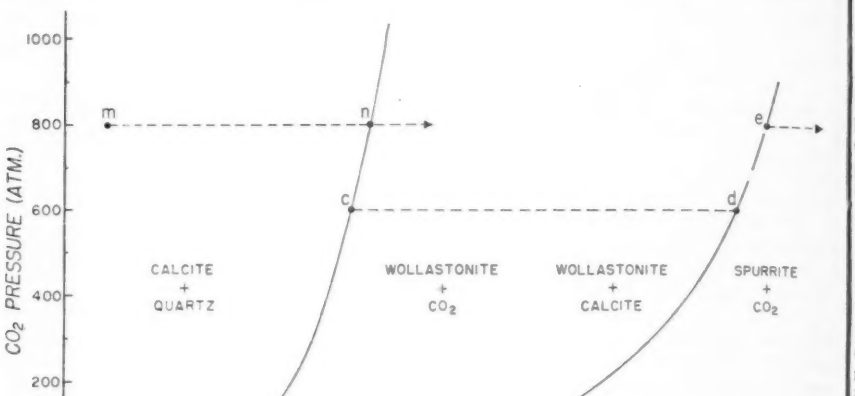

FIGURE 6.—P_{CO_2}-T CURVES FOR THE REACTIONS: $CaCO_3 + SiO_2 = CaSiO_3 + CO_2$ AND $2CaSiO_3 + 3CaCO_3 = 2Ca_2SiO_4 \cdot CaCO_3 + 2CO_2$

Data from Harker and Tuttle (1956a), Tuttle and Harker (1957), and unpublished work by the writer.

effects of the partial pressure of CO_2 and metasomatic changes in composition. Consequently, he visualized the path of metamorphism of a siliceous limestone more or less as represented by the line *m-n* in Figure 6 (*cf.* Bowen, 1940, Fig. A). However, this is merely one of several possible paths of metamorphism if the effects of changes in composition and CO_2 pressure, which really is a compositional factor[12], are taken into account.

The particular path taken in any natural example of metamorphism is determined primarily by the initial composition of the carbonate rocks and the physical nature of the system. Thus, if the original rock consisted essentially of quartz and calcite in a mol ratio $SiO_2/CaCO_3$ less than unity, and the system was closed to the escape of CO_2, the path of metamorphism can be represented approximately by the line *a-b-c-d-e* in the P-T diagram (Fig. 6). However, if the mol ratio $SiO_2/CaCO_3$ was greater than unity, metamorphism would have ended with the mineral assemblage

[12] The effect of CO_2 is not due to the pressure it exerts but to its concentration; hence it is more appropriately considered as a compositional factor.

hand, if the original siliceous carbonate rocks had been magnesian and/or argillaceous, reactions at lower temperatures to form mineral such as talc, tremolite, diopside, and grossular ite could have produced CO_2 pressures comparable to those indicated by the path *m-n* in Figure 6, as visualized by Bowen (1940, Fig. A). Consequently, wollastonite would not have formed unless temperatures of perhaps 650°C were reached, and then only if there was excess silica. Thus, although wollastonite could occur in equilibrium assemblages as a product of regional metamorphism, it should be very rare.

A somewhat different path would be followed if an initially siliceous carbonate rock were thermally metamorphosed under conditions that would permit the escape of CO_2, as indicated by the line *a-b-f* in Figure 6. This path would be unaffected by the formation of magnesium- and aluminum-bearing minerals at lower temperatures. Hence it is possible for many siliceous carbonate rocks to be metamorphosed to wollastonite-bearing rocks at temperatures as low as 400°C., provided the initial SiO_2 content exceeded the amount necessary to satisfy the magnesium, aluminum

and iron. Moreover, spurrite also could form at temperatures as low as 625°C. if the ratio SiO_2/CaO in the earlier formed wollastonite-bearing rock is less than unity. Consequently, spurrite might form in the thermal metamorphism of near-surface rocks at temperatures that barely would be sufficient for the formation of wollastonite in deep-seated siliceous carbonates. In reality, however, natural systems probably are neither entirely open nor entirely closed to the escape of CO_2, and therefore the paths of thermal metamorphism of siliceous carbonate rocks generally lie somewhere between the extremes outlined.

On the other hand, if the carbonate rocks initially were essentially free of silica, as they were at Crestmore, the path of metamorphism can be greatly different from those already considered. This is due mainly to two implications of the initial absence of silica. First, the formation of silicates depends upon the metasomatic introduction of silica, and second, the initial products of reaction with it are determined largely by the time relationships between its introduction and the introduction of heat. Thus, if silica is introduced early in the thermal history, the path of metamorphism would be essentially the same as if the carbonate rock had been initially siliceous. However, if the silica is introduced later in the thermal history, as it is thought to have been at Crestmore, the path of metamorphism very well might be as indicated by the line *g-h* in Figure 6. Consequently, it is possible, and indeed highly probable, that under certain conditions of contact metamorphism, spurrite would form directly from calcite and metasomatic silica (*cf.* reaction 4), and wollastonite could form later at the expense of spurrite.

Wollastonite can form from spurrite either by an increase in the CO_2 pressure as a consequence of the conversion of calcite to spurrite or by silica metasomatism in excess of the amount required for spurrite. However, inasmuch as the amount and rate of evolution of CO_2 are directly dependent upon the amount and rate of introduction of silica, the CO_2 pressure at the existing temperature might or might not in a given case reach the stability field of wollastonite. It might if the contact aureole constitutes an appreciable part of the entire carbonate body, as the volume throughout which the CO_2 can diffuse and dissipate is relatively small. It might not, on the other hand, if the volume of the carbonate body is very large as compared with the contact aureole, or if metamorphism occurs very near the earth's surface.

The wollastonite-forming reaction which occurs in response to increased CO_2 pressure is reversible, whereas the reaction which occurs in response to silica metasomatism is irreversible. However, the fact that metasomatic reactions commonly are irreversible (*cf.* reactions 1–12 with reactions *a–e*) does not prevent them from yielding equilibrium products, for the major controlling factor is the relationship between the rate of introduction of the metasomatic reactant and the rate of reaction. Consequently, contact metasomatism, which is essentially an open-system process, can readily produce equilibrium mineral assemblages.

The application of these principles to the contact metamorphism at Crestmore is more readily accomplished by comparison of the effects produced in the same carbonate rock units by two different intrusions, the quartz diorite and the quartz monzonite porphyry. Metasomatism associated with the quartz diorite magma produced a relatively thin silicate contact aureole that consists almost entirely of the garnet-zone assemblage (wollastonite, diopside, and grossularite), whereas metasomatism associated with the quartz monzonite porphyry magma produced a much thicker contact aureole that exhibits a well-defined zonation of mineral assemblages, with the garnet-zone assemblage innermost with respect to the intrusive mass and the monticellite-zone assemblage (spurrite, monticellite, melilite, and other minerals) outermost.

The differences in mineral composition of the two aureoles probably are due mainly to differences in the pressure-temperature relationships during intrusion and metamorphism. Inasmuch as the quartz diorite, which is part of a deep-seated batholith, completely engulfed the limestone units, the CO_2 that was rapidly evolved in the thermal decomposition of the magnesium carbonate component of the marbles (reaction *e*) probably could not escape. Consequently, the partial pressure of CO_2 was too high for the formation of the monticellite-zone assemblages at the prevailing temperatures.[13]

[13] Evidence obtained from petrographic and field relationships, as described earlier in this paper, clearly suggests that the quartz diorite magma was largely crystalline at the time of intrusion into the marbles and therefore probably in the lower-temperature part of its crystallization range. Conversely, the same kind of evidence suggests that the quartz monzonite porphyry magma was in the upper part of its crystallization range. However, in

The quartz monzonite porphyry, on the other hand, was intruded later as a relatively small pipelike hypabyssal body into already formed brucite (or periclase)-bearing marbles, and hence the partial pressures of CO_2 probably were very low, at least during the earlier stages of silica metasomatism. Consequently, monticellite-zone assemblages formed upon initial metasomatic introduction of silica into the marbles even though the temperatures probably were not much, if any, higher than during the formation of the garnet-zone assemblage in the quartz diorite contact aureole.

In conclusion, field, petrographic, chemical, and experimental studies all clearly indicate that: (1) the quartz monzonite porphyry contact aureole at Crestmore is largely the product of silica, alumina, and iron metasomatism of an initially silica-poor magnesian marble; (2) the silica did not reach the outer part of the aureole (the monticellite zone) until the marbles there had been heated perhaps to 625°C. or higher; (3) owing to these initially high temperatures and low CO_2 pressures, minerals such as spurrite, monticellite, and melilite formed directly from the metasomatized marbles without the intervention of the "lower-temperature" steps which involve wollastonite, diopside, and grossularite; and (4) the zonal distribution of mineral assemblages is not the result of differences in temperature and/or pressure, but merely differences in the intensity of metasomatism, as reflected by the markedly different silica, alumina, iron, and magnesia contents of the three zones. Consequently, it is proposed that the contact metamorphism at Crestmore, and perhaps numerous other places, should be viewed as progressive metasomatism with consequent decarbonation at elevated temperatures rather than progressive decarbonation attendant simply upon rising temperatures.

Such a view of contact metamorphism naturally places greater emphasis on compositional factors than on temperature and is therefore not entirely compatible with the thermal decarbonation concept. Temperature is merely one of the factors that govern the occurrence of a specific metamorphic-mineral assemblage; in the contact metasomatism of carbonate rocks, compositional factors, including the relative amounts (partial pressures) of carbon dioxide, commonly exert a greater influence than temperature on the mineral assemblages produced. Development of these mineral assemblages at equilibrium under given conditions of temperature, pressure, and final bulk composition is fundamentally dependent upon the course of compositional changes, especially in volatile content, during metasomatism (*cf.* Turner and Verhoogen, 1951, p. 428). It is suggested, therefore, that contact metamorphic deposits might well be considered in terms of the nature and extent of metasomatism, for it is only on this basis that valid interpretations can be made in connection with temperatures of metamorphism.

view of the compositional relationships between the two rocks, it is probable that the quartz monzonite porphyry magma was not appreciably hotter than the quartz diorite magma.

References Cited

Bowen, N. L., 1928, The evolution of the igneous rocks: Princeton, N. J., Princeton Univ. Press, 334 p.

—— 1940, Progressive metamorphism of siliceous limestone and dolomite: Jour. Geology, v. 48, p. 225–274

Burnham, C. W., 1954, Contact metamorphism at Crestmore, California: Calif. Div. Mines Bull. 170; Ch. VII, p. 61–70

Chave, K. E., 1954, Aspects of the biogeochemistry of magnesium (Part) 1, Calcareous marine organisms: Jour. Geology, v. 62, p. 266–283

Daly, J. W., 1935, Paragenesis of the mineral assemblage at Crestmore, Riverside County, California: Am. Mineralogist, v. 20, p. 638–65

Daly, R. A., 1933, Igneous rocks and the depths of the earth: N. Y., McGraw-Hill Book Co., 508 p.

Dunham, K. C., 1933, A note on the texture of the Crestmore contact rocks: Am. Mineralogist, v. 18, p. 474–477

Eakle, A. S., 1914, Some contact metamorphic minerals in crystalline limestone at Crestmore (Abstract): Geol. Soc. America Bull., v. 25, p. 125

—— 1916, Xanthophyllite in crystalline limestone: Jour. Wash. Acad. Sci., v. 6, p. 332–335

—— 1917, Minerals associated with crystalline limestone at Crestmore, Riverside County, California: Univ. Calif., Bull. Dept. Geol., v. 10, p. 327–360

—— 1920, New and rare minerals formed in limestone by contact metamorphism (Abstract): Geol. Soc. America Bull., v. 31, p. 162–163

—— 1921, Jurupaite, a new mineral: Am. Mineralogist, v. 6, p. 107–109

—— 1925, Foshagite, a new silicate from Crestmore, California: Am. Mineralogist, v. 10, p. 97–9

—— 1927, Famous mineral localities: Crestmore, Riverside County, California: Am. Mineralogist, v. 12, p. 319–321

Eakle, A. S., and Rogers, A. F., 1914, Wilkeite, a new mineral of the apatite group and okenite its alteration product: Am. Jour. Sci., v. 3 p. 262–267

Foshag, W. F., 1920a, Thaumasite (and spurrite from Crestmore, California: Am. Mineralogist, v. 5, p. 80–81

Foshag, W. F., 1920b, Plazolite, a new mineral from Riverside, California: Am. Mineralogist, v. 5, p. 183–185
— 1924, Centrallasite from Crestmore, California: Am. Mineralogist, v. 9, p. 88–90
Harker, R. I., and Tuttle, O. F., 1956a, Experimental data on the P_{CO_2}-T curve for the reaction: calcite + quartz = wollastonite + carbon dioxide: Am. Jour. Sci., v. 254, p. 239–256
— 1956b, The lower limit of the stability of akermanite ($Ca_2MgSi_2O_7$): Am. Jour. Sci., v. 254, p. 468–478
Hilbut, C. S., 1935, Dark inclusions in a tonalite of southern California: Am. Mineralogist, v. 20, p. 609–630
Hauvo, O., 1952, A variety of monticellite from Crestmore, California: Bull. Comm. Géol. Finlande, No. 157, (Compte Rendu Soc. Géol. Finlande, No. 25), p. 7–11
Larsen, E. S., 1948, Batholith and associated rocks of Corona, Elsinore, and San Luis Rey quadrangles, southern California; Geol. Soc. America Mem. 29, 182 p.
Larsen, E. S., and Dunham, K. C., 1933, Tilleyite, a new mineral from the contact zone at Crestmore, California: Am. Mineralogist, v. 18, p. 469–473
Larsen, E. S., and Foshag, W. F., 1921, Merwinite, a new calcium-magnesium orthosilicate from Crestmore, California: Am. Mineralogist, v. 6, p. 143–148
Larsen, E. S., Gottfried, D., Haffe, H., and Waring, C. L., 1954, Age of the southern California, Sierra Nevada, and Idaho batholiths (Abstract): Geol. Soc. America Bull., v. 65, p. 1277
MacKevett, E. M., 1951, Geology of the Jurupa Mountains, San Bernardino and Riverside Counties, California: Calif. Div. Mines, Special Rept. 5, 14 p.
McConnell, D., 1937, The substitution of SiO_4- and SO_4- groups for PO_4- groups in the apatite structure; ellestadite, the end member: Am. Mineralogist, v. 22, p. 977–986
Merriam, R., and Laudermilk, J. D., 1936, Two diopsides from southern California: Am. Mineralogist, v. 21, p. 715–718
Moehlman, R. S. and Gonyer, F. A., 1934, Monticellite from Crestmore, California: Am. Mineralogist, v. 19, p. 474–476
Neuvonen, K. J., 1952, Heat of formation of merwinite and monticellite: Am. J. Sci., Bowen Volume, p. 373–380
Rogers, A. F., 1918, An American occurrence of periclase and its bearing on the origin and history of calcite-brucite rocks: Am. Jour. Sci., v. 46, p. 581–586
—— 1929, Periclase from Crestmore near Riverside, California, with a list of minerals from this locality: Am. Mineralogist, v. 14, p. 462–469
Shand, S. J., 1923, The problem of the alkaline rocks: Geol. Soc. S. Africa Trans., v. 25, p. 19–32
Smyth, C. H., 1927, The genesis of alkaline rocks: Am. Philos. Soc. Proc., v. 66, p. 535–580
Tilley, C. E., 1928, On a custerite-bearing contact rock from California: Geol. Mag., v. 65, p. 361–372
—— 1951, A note on the progressive metamorphism of siliceous limestones and dolomites: Geol. Mag., v. 88, p. 175–178
Turner, F. J., and Verhoogen, J., 1951, Igneous and metamorphic petrology: N. Y., McGraw-Hill Book Co., 602 p.
Tuttle, O. F., and Harker, R. I., 1957, Synthesis of spurrite and the reaction wollastonite + calcite = spurrite + carbon dioxide: Am. Jour. Sci., v. 255, p. 226–234
Woodford, A. O., Crippen, R. A., and Garner, K. B., 1941, Section across Commercial Quarry, Crestmore, California: Am. Mineralogist, v. 26, p. 351–381

College of Mineral Industries, Division of Earth Sciences, The Pennsylvania State University, University Park, Pennsylvania
Manuscript Received by the Secretary of the Society, July 2, 1958
Contribution No. 870, Division of the Geological Sciences, California Institute of Technology

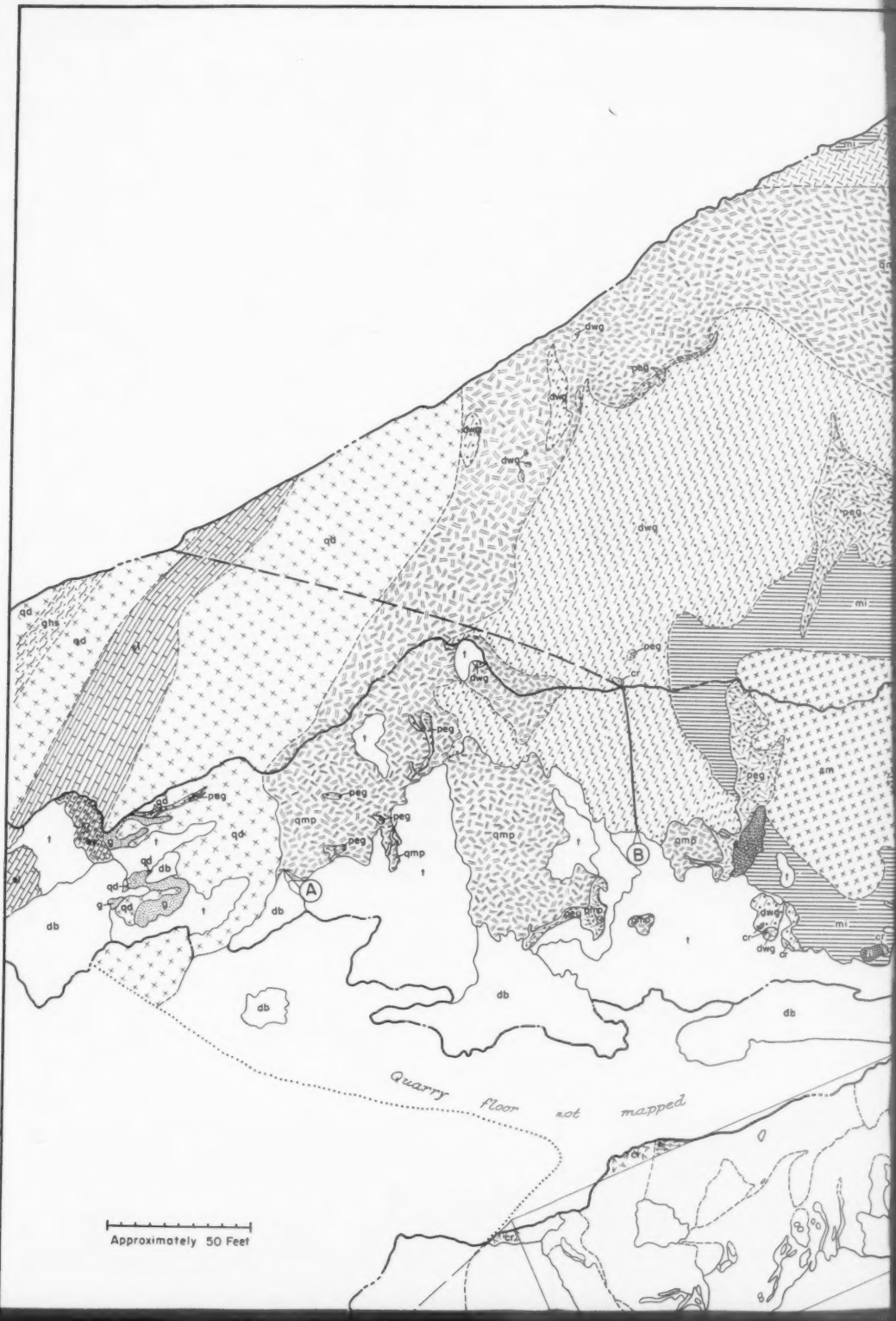
dwg
peg
qd
ghs
mi
qmp
db
A
B
Quarry floor not mapped
Approximately 50 Feet

mi
qmp
gc
sch
gbx
peg
cr
sm
dg
db
sl
dwg
bc
imr
E
C
D
N
M

EXPLANATION

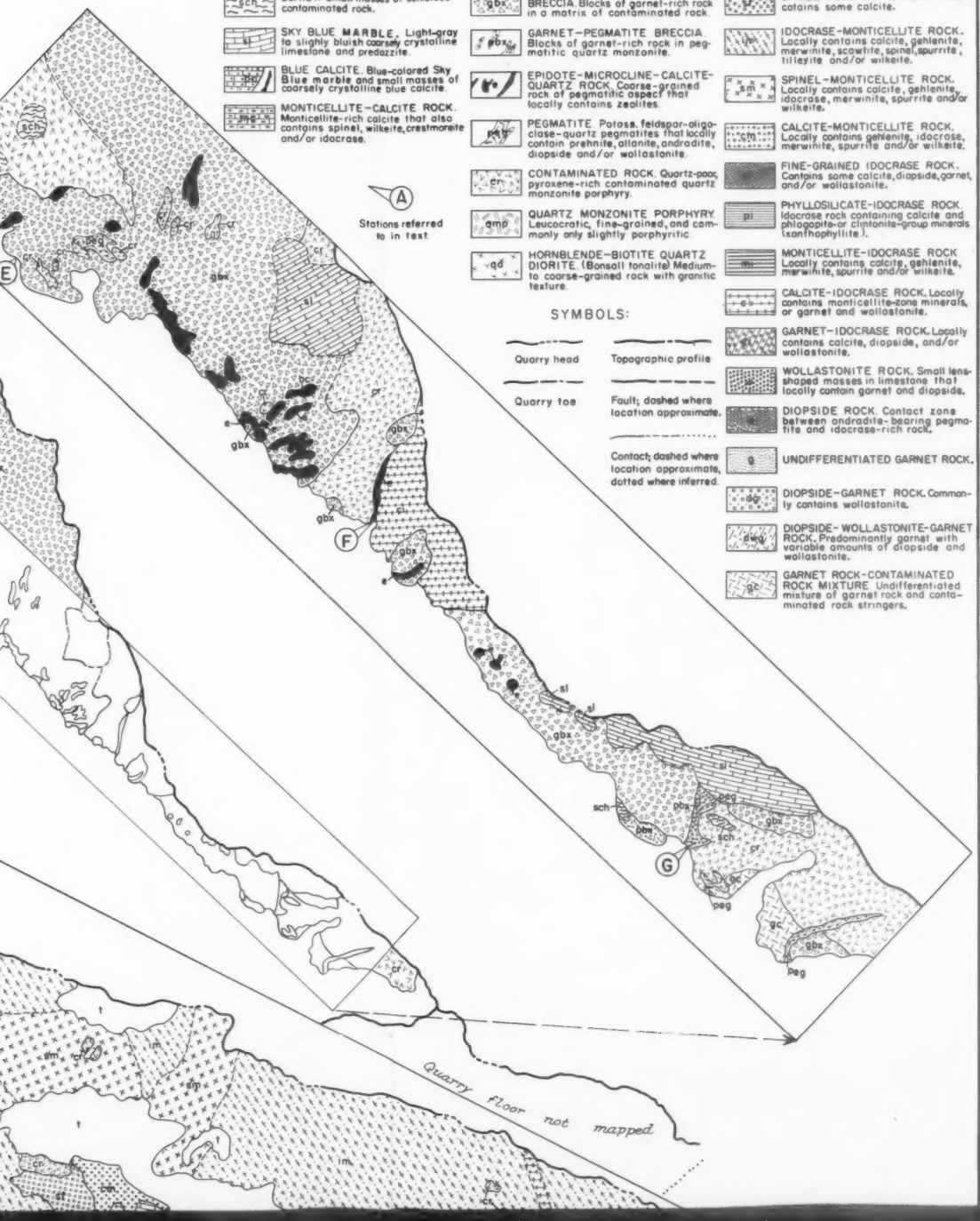
GNEISS, HORNFELS AND SCHIST. Mainly hornblende-biotite-quartz gneiss and schist. Pyroxene in thin calcareous members.
SCHIST. Small masses of schistose contaminated rock.
SKY BLUE MARBLE. Light-gray to slighly bluish coarsely crystalline limestone and predazzite.
BLUE CALCITE. Blue-colored Sky Blue marble and small masses of coarsely crystalline blue calcite.
MONTICELLITE-CALCITE ROCK. Monticellite-rich calcite that also contains spinel, wilkeite, crestmoreite and/or idocrase.
TALUS, EXCAVATION DEBRIS, & UNDIFFERENTIATED ALLUVIAL DEPOSITS
GARNET-CONTAMINATED ROCK BRECCIA. Blocks of garnet-rich rock in a matrix of contaminated rock.
GARNET-PEGMATITE BRECCIA. Blocks of garnet-rich rock in pegmatitic quartz monzonite.
EPIDOTE-MICROCLINE-CALCITE-QUARTZ ROCK. Coarse-grained rock of pegmatitic aspect that locally contains zeolites.
PEGMATITE. Potass. feldspar-oligoclase-quartz pegmatites that locally contain prehnite, allanite, andradite, diopside and/or wollastonite.
CONTAMINATED ROCK. Quartz-poor, pyroxene-rich contaminated quartz monzonite porphyry.
QUARTZ MONZONITE PORPHYRY. Leucocratic, fine-grained, and commonly only slightly porphyritic.
HORNBLENDE-BIOTITE QUARTZ DIORITE. (Bonsall tonalite) Medium- to coarse-grained rock with granitic texture.
UNDIFFERENTIATED MONTICELLITE ROCK. Small masses of monticellite-rich rock.
SPINEL-FORSTERITE ROCK. Also cotains some calcite.
IDOCRASE-MONTICELLITE ROCK. Locally contains calcite, gehlenite, merwinite, scawtite, spinel, spurrite, tilleyite and/or wilkeite.
SPINEL-MONTICELLITE ROCK. Locally contains calcite, gehlenite, idocrase, merwinite, spurrite and/or wilkeite.
CALCITE-MONTICELLITE ROCK. Locally contains gehlenite, idocrase, merwinite, spurrite and/or wilkeite.
FINE-GRAINED IDOCRASE ROCK. Contains some calcite, diopside, garnet, and/or wollastonite.
PHYLLOSILICATE-IDOCRASE ROCK. Idocrase rock containing calcite and phlogopite-or clintonite-group minerals (xanthophyllite).
MONTICELLITE-IDOCRASE ROCK. Locally contains calcite, gehlenite, merwinite, spurrite and/or wilkeite.
CALCITE-IDOCRASE ROCK. Locally contains monticellite-zone minerals, or garnet and wollastonite.
GARNET-IDOCRASE ROCK. Locally contains calcite, diopside, and/or wollastonite.
WOLLASTONITE ROCK. Small lens-shaped masses in limestone that locally contain garnet and diopside.
DIOPSIDE ROCK. Contact zone between andradite-bearing pegmatite and idocrase-rich rock.
UNDIFFERENTIATED GARNET ROCK.
DIOPSIDE-GARNET ROCK. Commonly contains wollastonite.
DIOPSIDE-WOLLASTONITE-GARNET ROCK. Predominantly garnet with variable amounts of diopside and wollastonite.
GARNET ROCK-CONTAMINATED ROCK MIXTURE. Undifferentiated mixture of garnet rock and contaminated rock stringers.
A
Stations referred to in text.
SYMBOLS:
Quarry head
Quarry toe
Topographic profile
Fault; dashed where location approximate.
Contact; dashed where location approximate, dotted where inferred.
Quarry floor not mapped
E
F
G

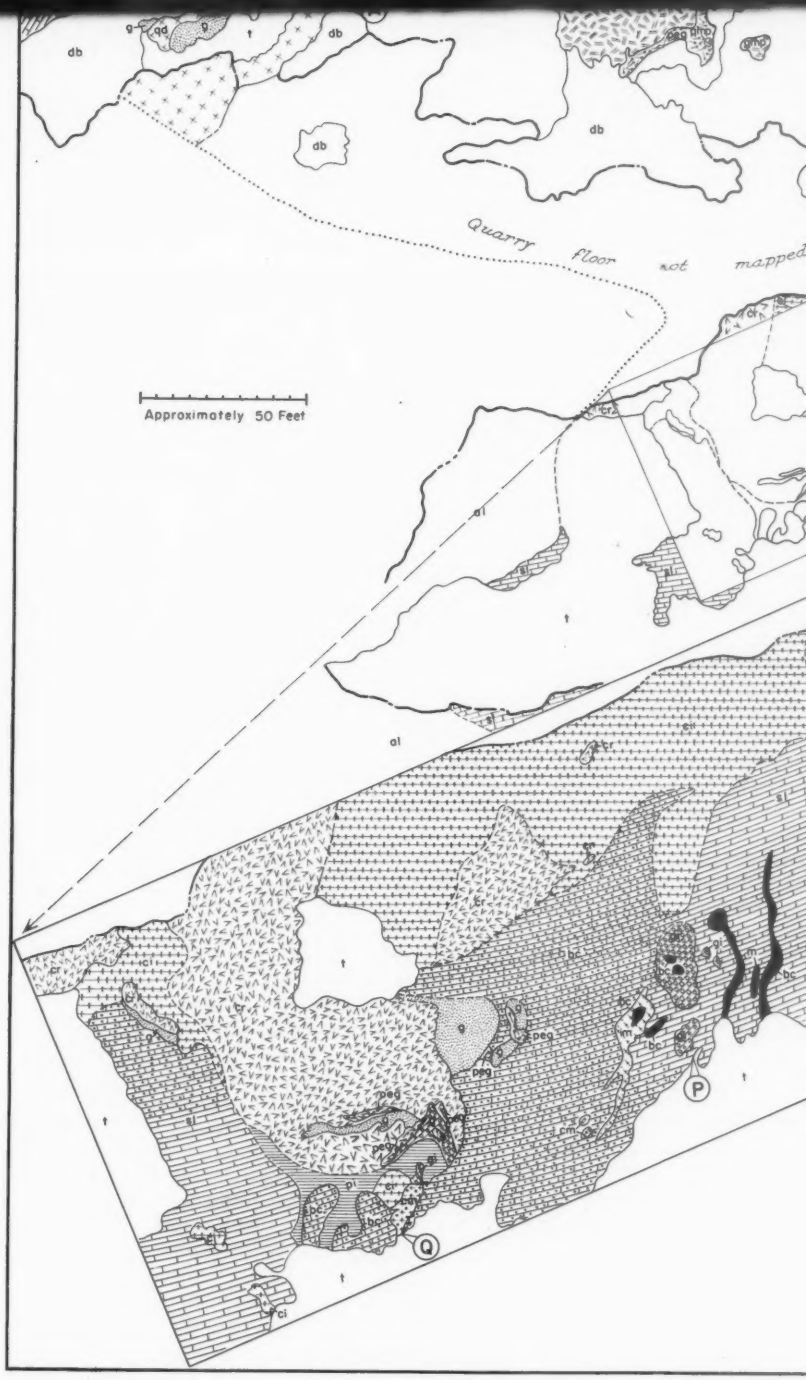
Quarry floor not mapped
Approximately 50 Feet
db
qd
g
t
al
cr
bc
peg
P
Q

GEO

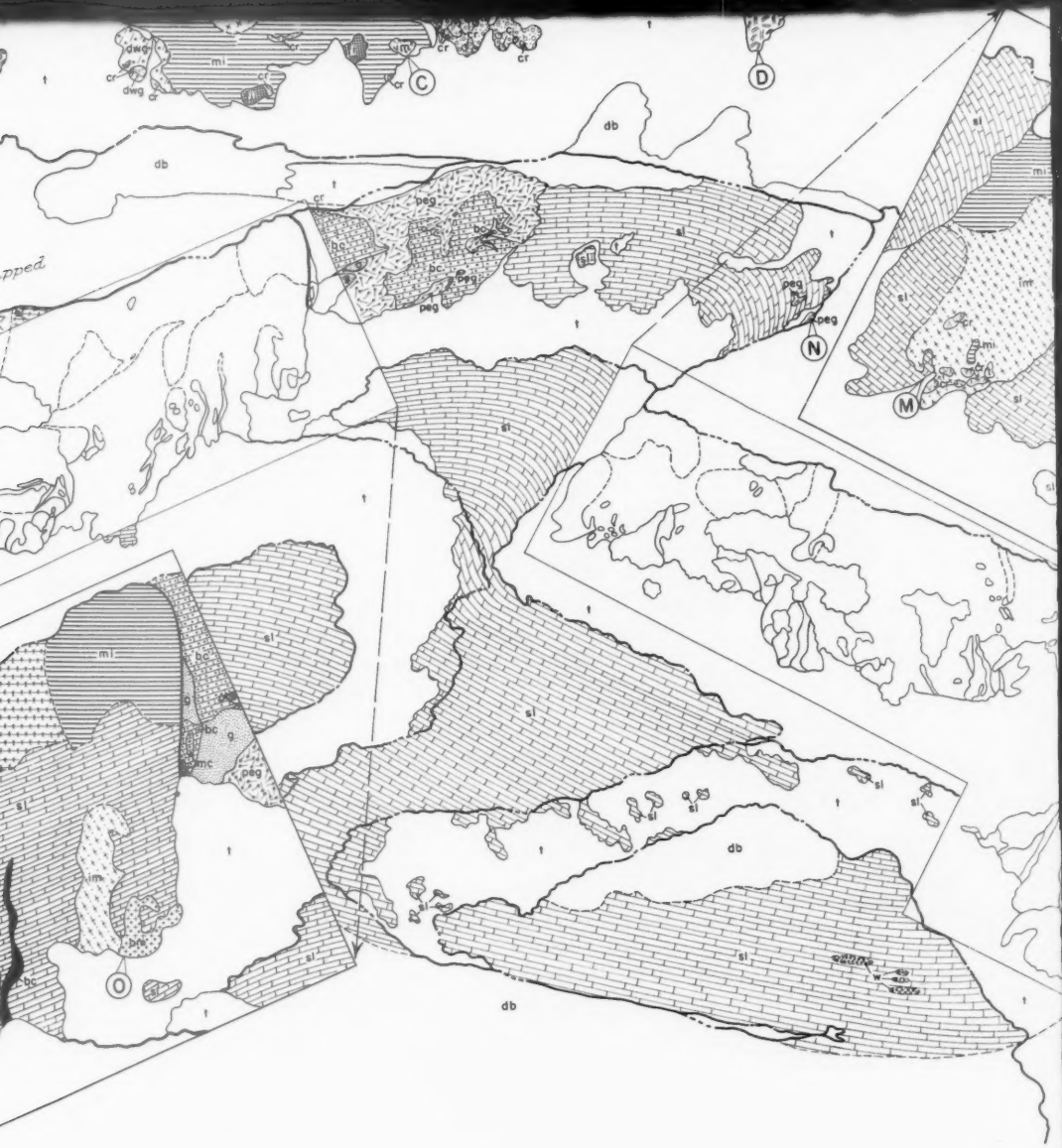

GEOLOGIC MAP OF FACES OF THE COMMERCIAL QUARRY.

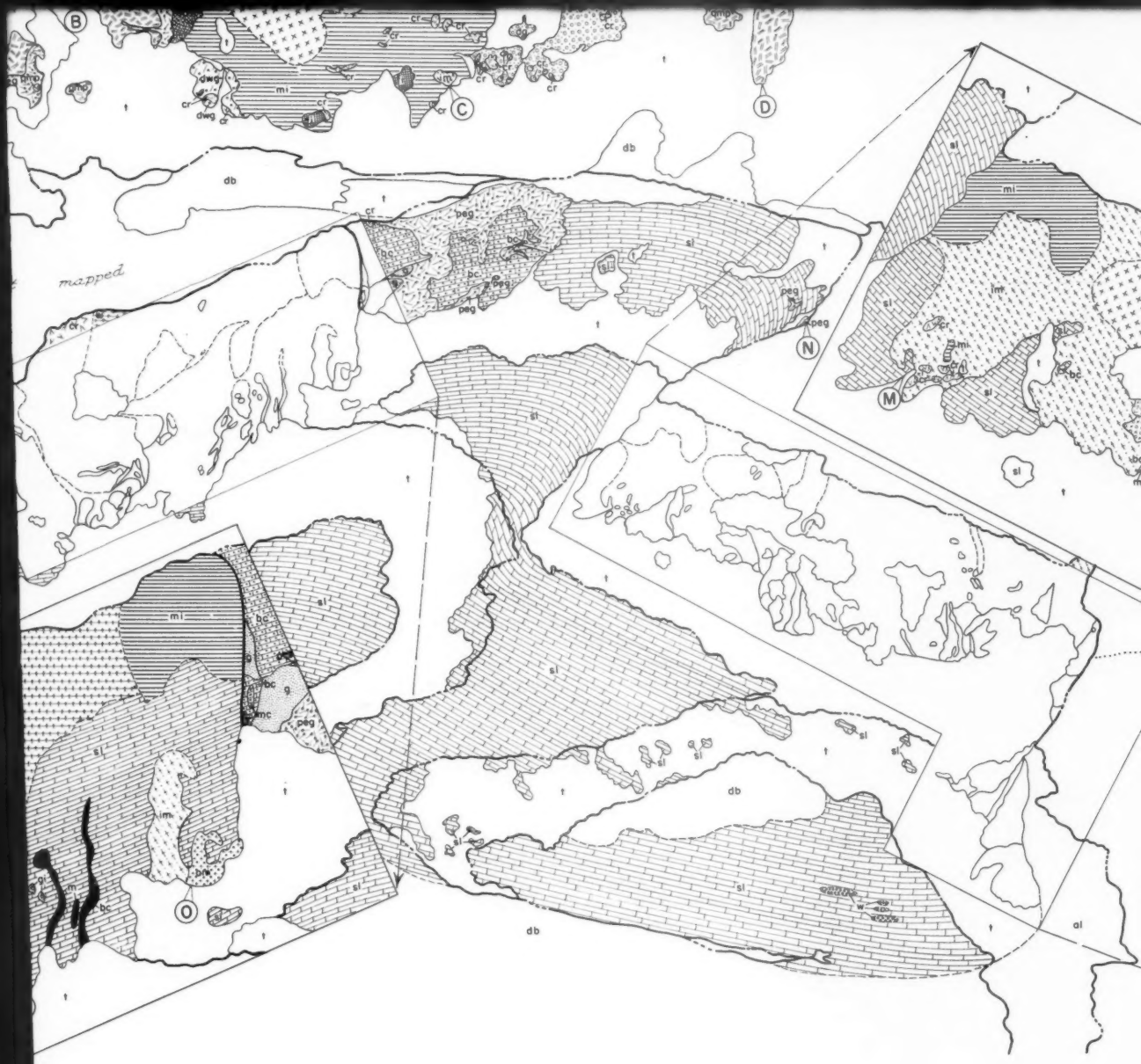

GEOLOGIC MAP OF FACES OF THE COMMERCIAL QUARRY, CREST

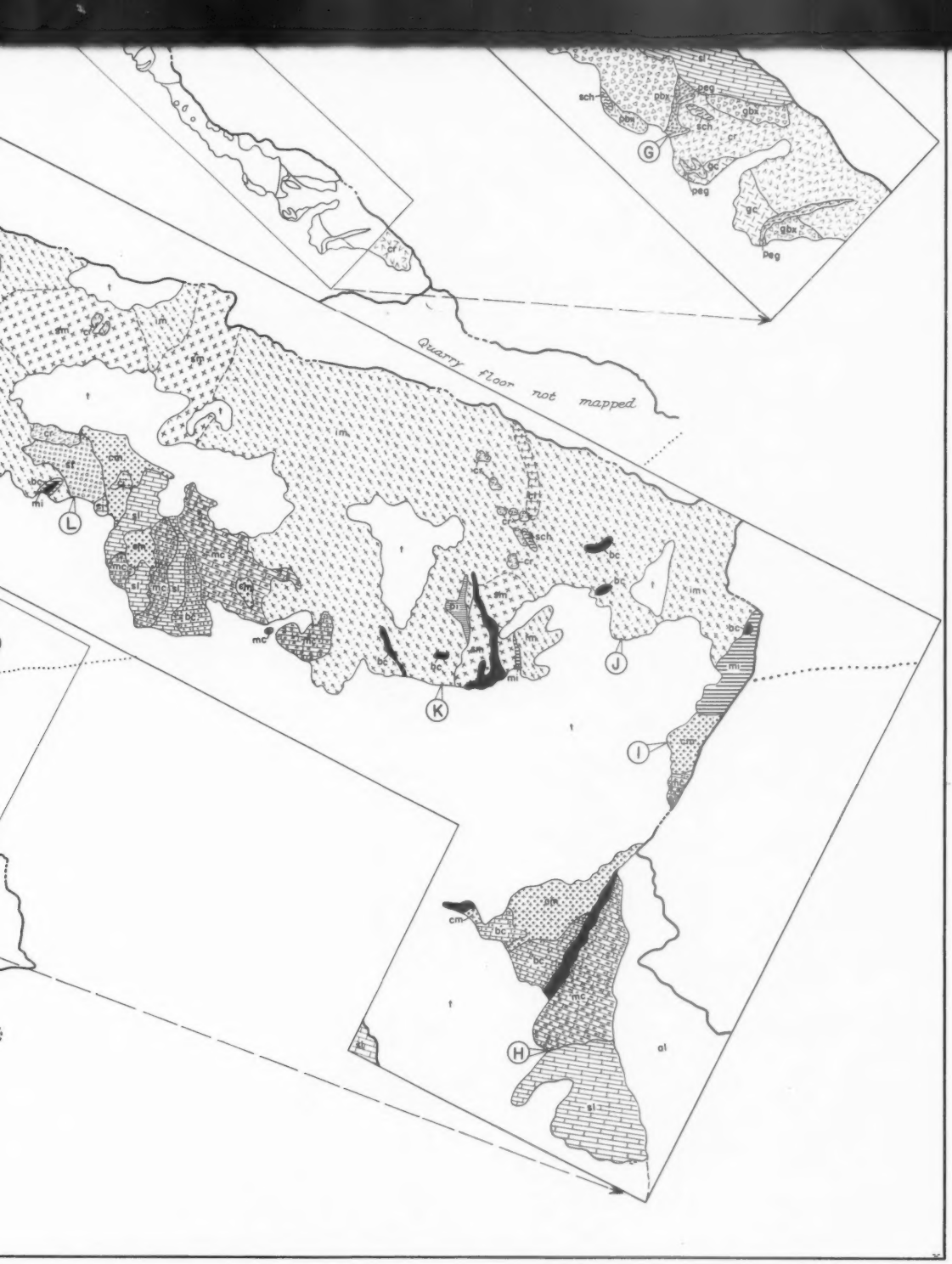

STMORE, CALIFORNIA

L

Z
out
serv
and
are
a fe
eral
rese
brov
in g
Sc
leac
be r
exte
corr
leach
been
of le
Sidn
bin,
Roc
Fors
that

"The
is de
pre-V
tive
drift
ering
on dr

Du
cene
India
sider
leach
neath
nant
prese
overl
impli

In
tinui

Short Notes

BULLETIN OF THE GEOLOGICAL SOCIETY OF AMERICA
VOL. 70, PP. 921–926, 3 FIGS. JULY 1959

LEACHED, CLAY-ENRICHED ZONES IN POST-SANGAMONIAN DRIFT IN SOUTHWESTERN OHIO AND SOUTHEASTERN INDIANA

BY ANSEL M. GOODING, JAMES THORP, AND ERLING GAMBLE

Zones of leaching and clay accumulation in outwash beneath calcareous till have been observed at many places in southwestern Ohio and southeastern Indiana. Most of these zones are a few inches to a foot or more thick, and in a few places tongues extend as much as several feet down into the sand and gravel. They resemble the *B* horizons of present-day gray-brown podzolic soils of the Fox series developed in glaciofluvial terrace materials.

Several workers have considered these leached zones that contain accumulated clay to be remnants of a Fox-like paleosol of regional extent and have used them as a key horizon for correlations in southwestern Ohio. These leached, clay-enriched zones in outwash have been supposed to be of the same age as a zone of leaching in till exposed in a railroad cut at Sidney, Ohio (Goldthwait, 1955; Flint and Rubin, 1955; Forsyth and La Rocque, 1956; La Rocque and Forsyth, 1957; Flint, 1957; and Forsyth, 1957). Flint and Rubin (1955) state that

> "The soil, as well as the till and gravel in which it is developed, is believed to be post-Sangamon and pre-Wisconsin of existing terminology. The alternative possibility, that the soil is Sangamon and the drift beneath it Illinoian, is unlikely because weathering of the till is not comparable to that developed on drift of known Illinoian age."

During several years of study of the Pleistocene in the Whitewater valley of southeastern Indiana and surrounding areas, we found considerable evidence to suggest that the zones of leaching and clay accumulation in outwash beneath calcareous till in this area are not remnants of a paleosol but are extensions of the present surface soils through joints in the thin overlying till. This evidence and some of the implications are presented below.

In the area considered, a distinct soil discontinuity between the Miami and Russell silt loams marks the boundary between two till sheets (tentatively "Champaign" and "Shelbyville" respectively). (*See* Gooding, 1957, p. 19–23, Figs. 4, 5, Pl. I.) The Miami soils to the north are developed in till that overlies the presumed paleosol; the Russell soils to the south are developed in till that, according to the published interpretations of the workers previously mentioned, must be of the same age as the stratified drift in which the suggested paleosol is developed. The greater depth of leaching of the Russell soils might seem to support the interpretation of a soil-forming interval between these two till sheets. However, the nature of the parent material, especially the thickness of loess mantles, is important in evaluating depths of leaching.

Gooding (1957) found that the depth of leaching on glaciofluvial terrace surfaces of the same level, and of the same age, varied directly with the thickness of the loess mantle. This relationship was found also on the till uplands in the area of Miami soils. The depth of leaching of the Russell soils averages about 1½ times that of the Miami soils; this corresponds to differences in the thickness of the loess mantle on Russell and Miami soils. Miami-like soils occur at places in the area of Russell soils and, to a lesser extent, a few patches of Russell-like soils occur in the area of Miami soils, depending on the thickness of the loess mantle. Thus, we think that variations in the thickness of relatively fast-leaching loess is more responsible than is the time factor for the difference in depth of leaching between the areas of Miami and Russell silt loam soils.

Evidence from terrace studies in the Whitewater basin (Gooding, 1957) suggests that the time intervals between the post-Sangamonian glaciations in the basin were probably short and cool. Ice blocks up to three quarters of a mile across, believed to have been vestiges of the ice sheet that deposited the drift on which the

Russell soils are developed, were buried in the valley train associated with the advance of the ice that deposited the drift on which the Miami soils are developed. These ice blocks remained frozen while the ice melted back a short distance and then readvanced to Leverett and Taylor's (1915) "Bloomington" moraine position at the head of the basin. A scour surface formed by meltwater from the "Bloomington" ice partially exhumed some of the blocks of ice buried earlier. Their subsequent melting produced kettles, some of which lie on the escarpment between the valley-train terrace level, and the "Bloomington" scour terrace level. Thus, buried ice blocks apparently existed in valleys during the assumed interval of paleosol formation.

If the time interval between the glaciations that deposited the drift on which the Russell and Miami soils are formed was warm and long enough—estimated at 16,000 years by Flint and Rubin (1955, p. 4)—to permit the development of Fox soils similar to those found at the surface in the area today, then certain gravel-terrace soils beyond the Miami-Russell soil boundary should have very deeply leached profiles. No such deeply leached gravel-terrace soils of post-Sangamonian age exist in the Whitewater basin. Deep leaching on Whitewater terraces is confined to deep "backwater" silt deposits.

The detailed stratigraphic studies in the Whitewater basin so far indicate that there are at least three (the first may consist of two) post-Sangamonian tills regionally in the basin (Gamble, 1955, M. S. Thesis, Earlham College, 44 p.; Gooding, in preparation). The upper till does not extend south of the Miami-Russell soil discontinuity, but the other two extend well to the south of this line. Thin zones of leaching and clay accumulation, with a few more deeply penetrating leached tongues, have been observed at many places in outwash beneath post-Sangamonian till far south of the Miami-Russell soil discontinuity, as well as beneath the uppermost post-Sangamonian till in the area of Miami soils. In addition, similar leached, clay-enriched zones in outwash sand and gravel lie beneath thin till at Winchester, Indiana, on a terrace of the White River. This till is more clayey than the till south of Leverett and Taylor's (1915) "Bloomington" moraine in the Whitewater basin and surely is younger. Thus, the authors believe that these leached, clay-enriched zones in outwash beneath till are related to the existing landscape and surface soils and occur at various stratigraphic horizons.

In all places where the authors have observed the leached, clay-enriched zones in outwash, the overlying calcareous till is thin, thoroughly oxidized, and well jointed. This has also been noted by Dr. Guy D. Smith (Oral communication). Figures 1 and 2 illustrate two exposures that show some interesting features bearing on

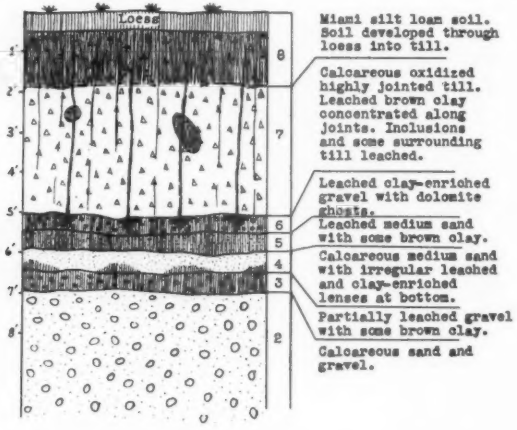

FIGURE 1.—SECTION SHOWING THE RELATIONSHIP OF LEACHED, CLAY-ENRICHED ZONE IN OUTWASH TO SURFACE SOIL AND JOINTS IN OVERLYING TILL
Section exposed along creek bank in NE ¼, SW ¼, Sec. 15, T.14 N., R.1 W., Wayne County, Indiana.

the origin of the leached, clay-enriched zones in outwash beneath calcareous till.

At the locality shown by Figure 1, the following features are important:

Evidence leading to this same interpretation is seen at the location shown by Figure 2:

(1) The thin till (2) in this exposure is thoroughly oxidized and well jointed. Clay is

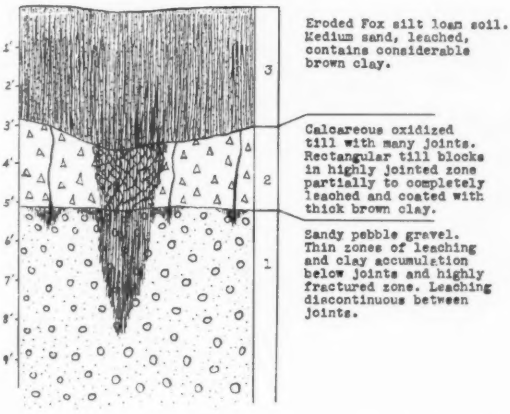
1'
2'
3'
4'
5'
6'
7'
8'
9'
3
2
1
Eroded Fox silt loam soil. Medium sand, leached, contains considerable brown clay.
Calcareous oxidized till with many joints. Rectangular till blocks in highly jointed zone partially to completely leached and coated with thick brown clay.
Sandy pebble gravel. Thin zones of leaching and clay accumulation below joints and highly fractured zone. Leaching discontinuous between joints.

FIGURE 2.—SECTION SHOWING THE RELATIONSHIP OF LEACHED, CLAY-ENRICHED ZONE IN OUTWASH TO SURFACE SOIL AND JOINTS IN OVERLYING TILL

Section exposed in gravel pit north of Cambridge City, Indiana, in the SW corner, Sec. 23, T.16 N., R.12 E.

(1) Stratification is well preserved in the leached, clay-enriched zones, especially in the sand units. Also, the leaching and clay accumulation is variable from one unit to another. The sand unit (4) is only partially leached at the bottom; the overlying and underlying units (5 and 3) are more thoroughly leached and are richer in clay. These features are not normal characteristics of the *B* horizon of a Fox soil.

(2) The joints in the thin oxidized till (7) are lined with dark-brown, noncalcareous clay, and they extend visibly into the underlying leached gravel (6). Leaching is most nearly complete, and there is more clay, adjacent to the joints than away from the joints in unit 6.

(3) Two leached sand inclusions were found in the overlying till (7), but both were bisected by joints, and some of the till around one of the inclusions was leached.

The evidence at the location shown in Figure 1 seems to indicate clearly that leaching of the outwash (units 3 through 6) beneath, and the sand inclusions within, the till (7) occurred after the deposition of till (7), not before. Thus, the leaching and clay accumulation beneath till is an extension of the present surface soil and not a remnant of a buried paleosol.

rich along these joints in the till (2) and in the leached sand gravel (1) immediately beneath them. Leaching in the outwash is discontinuous laterally between joints.

(2) At one place the thin till is strongly jointed into rectangular blocks. These blocks of till are partially to completely leached and covered with heavy dark-brown clay coatings. A leached, clay-enriched tongue extends from the overlying leached sand (3), through the highly jointed area in the thin till (2), and 3 feet down into the underlying outwash (1).

At the locality shown in Figure 2, the leached, clay-enriched zone in outwash beneath calcareous till cannot be a remnant of a paleosol but is an extension of the *B* horizon of the present surface soil through joints in the thin till (2).

Another point believed to be significant is that, to our knowledge, a complete Fox-like soil profile has never been found beneath till in the area considered.

We believe it significant also that no buried zone of leaching and clay accumulation has been found in till considered to be of post-Sangamonian age anywhere in the area, except at the Sidney, Ohio, cut.

We have visited and studied the Sidney,

Ohio, cut on two occasions. We believe that the paleosol developed in till at this section (*see* La Rocque and Forsyth, 1957, Fig. 2) is only the lower part of a truncated soil whose total pre-cut. Figure 3 is our modification of, and addition to, La Rocque and Forsyth's (1957, Fig. 2) descriptions of this section. We discovered a zone of leaching and clay accumulation 6 inches

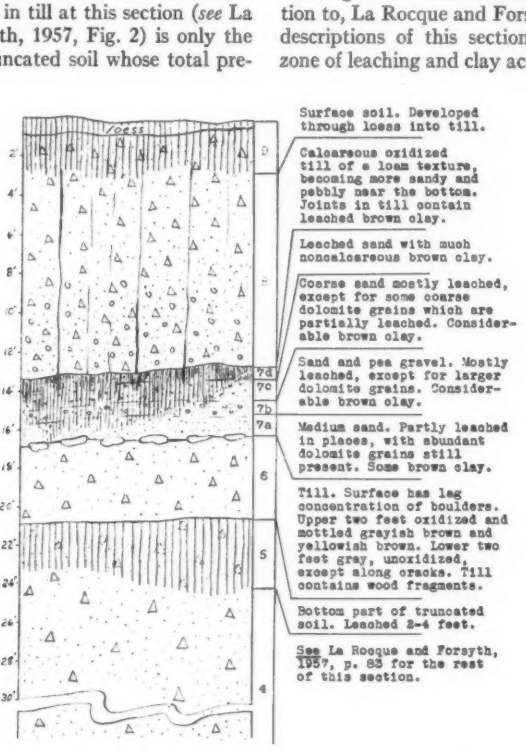
loess
2'
4'
6'
8'
10'
12'
14'
16'
18'
20'
22'
24'
26'
28'
30'
D
C
7d
7c
7b
7a
6
5
4
Surface soil. Developed through loess into till.
Calcareous oxidized till of a loam texture, becoming more sandy and pebbly near the bottom. Joints in till contain leached brown clay.
Leached sand with much noncalcareous brown clay.
Coarse sand mostly leached, except for some coarse dolomite grains which are partially leached. Considerable brown clay.
Sand and pea gravel. Mostly leached, except for larger dolomite grains. Considerable brown clay.
Medium sand. Partly leached in places, with abundant dolomite grains still present. Some brown clay.
Till. Surface has leg concentration of boulders. Upper two feet oxidized and mottled grayish brown and yellowish brown. Lower two feet gray, unoxidized, except along cracks. Till contains wood fragments.
Bottom part of truncated soil. Leached 2-4 feet.
See La Rocque and Forsyth, 1957, p. 83 for the rest of this section.

FIGURE 3.—THE AUTHOR'S MODIFICATION OF, AND ADDITION TO, LA ROCQUE AND FORSYTH'S (1957, FIG. 2) DESCRIPTION OF THE SIDNEY, OHIO, CUT

truncation depth of development may have been more than twice the thickness of the present zone of leaching, which is locally as much as 3–4 feet. We believe that the soil-forming interval was considerably longer than the 16,000 years suggested by Flint and Rubin (1955, p. 4). Therefore, if the widely occurring zones of leaching and clay accumulation in outwash beneath till are remnants of a Fox-like paleosol correlating stratigraphically with the zone of leaching in till at the Sidney, Ohio, cut (as suggested by Goldthwait, 1955; Flint and Rubin, 1955; Forsyth and La Rocque, 1956; La Rocque and Forsyth, 1957; Flint, 1957; Forsyth, 1957), they would be much more weathered and deeply developed than is the case.

There is a more serious basis for questioning the interpretations which the previously mentioned workers have given to the Sidney, Ohio, to 2 feet thick at the top of the sand and gravel (7) beneath the oxidized and jointed "pebbly till" (8). This leached, clay-enriched zone in units 7a through 7d is identical with others found regionally in the area that are correlated by the previously mentioned workers with the truncated paleosol developed in till 5 but is here separated from till 5 by another till (6).

Conclusions

We believe that the post-Sangamonian leached, clay-enriched zones in outwash beneath calcareous till in southwestern Ohio and southeastern Indiana are related to the present landscape and are extensions of the present surface soils. The sands and gravels have been leached and illuviated by water that has passed through present surface soils and joints in the thin overlying calcareous till. They occur at

several stratigraphic horizons in this area and can be expected wherever the necessary conditions of good drainage through jointed surface till on outwash exist. The interpretation of these leached, clay-enriched zones in outwash beneath calcareous till as paleosols will inevitably lead to erroneous conclusions.

Acknowledgments

This paper developed out of Pleistocene geology and soil-genesis studies being carried out in the Whitewater basin of southeastern Indiana and surrounding areas, under the support of National Science Foundation Grants No. 997 and No. 3484, the Charles F. Kettering Foundation, and the Soil Conservation Service, U. S. Department of Agriculture.

References Cited

Flint, R. F., 1957, Glacial and Pleistocene geology: N. Y., John Wiley & Sons, Inc., 553 p.

Flint, R. F., and Rubin, Meyer, 1955, Radiocarbon dates of pre-Mankato events in eastern and central North America: Science, v. 121, no. 3149, p. 649–658

Forsyth, Jane, 1957, "Early" Wisconsin drift in Ohio (Abstract): Geol. Soc. America Bull., v. 68, p. 1728

Forsyth, Jane and La Rocque, Aurèle, 1956, Age of the buried soil at Sidney, Ohio (Abstract): Geol. Soc. America Bull., v. 67, p. 1696

Goldthwait, R. P. (*Leader*), 1955, Pleistocene chronology of southwestern Ohio: 5th Bienn. Pleistocene Field Conf. Guidebook, Pt. 2, 72 p.

Gooding, A. M., 1957, Pleistocene terraces in the upper Whitewater drainage basin, southeastern Indiana: Earlham Coll. Sci. Bull. No. 2, 65 p.

La Rocque, Aurèle, and Forsyth, Jane, 1957, Pleistocene molluscan faunules of the Sidney Cut, Shelby Co., Ohio: Ohio Jour. Sci., v. 57, no. 2, p. 81

Leverett, Frank, and Taylor, Frank, 1915, The Pleistocene of Indiana and Michigan and the history of the Great Lakes: U. S. Geol. Survey Mon. 53, 529 p.

Department of Geology and Soil Science, Earlham College, Richmond, Ind.

Manuscript Received by the Secretary of the Society, January 6, 1958

BULLETIN OF THE GEOLOGICAL SOCIETY OF AMERICA
VOL. 70, PP. 927–928 JULY 1959

LEACHED, CLAY-ENRICHED ZONES IN POST-SANGAMONIAN DRIFT IN SOUTHWESTERN OHIO AND SOUTHEASTERN INDIANA: A REPLY

BY RICHARD P. GOLDTHWAIT

Gooding, Thorp, and Gamble (1959) challenge a paleosol hypothesis, which has been under study and test in southwestern Ohio by several geologists and pedologists for 10 years. We have withheld full publication pending further proof either for or against this hypothesis. Observations now embrace more than 50 sections. Unfortunately many of these sections come and go with the power shovel. At first we were loath to believe that buried leached clay-enriched zones could be paleosols. Some clay-lined joints were observed in the till above. Little by little we swung toward the paleosol hypothesis, because of (1) horizontal continuity for 100-200 feet and depth to 4 or 5 feet of this leached clay-enriched zone in a few places and (2) the significant thickness of blue unoxidized till seen over a few of those "paleosols". In some places we are unable to find vertical cracks, or those present have no clay skin, yet the clay-enriched zone below is widespread. Is till 8 or 9 feet deep too thick for surface development of clays?

The Ohio stratigraphy is no longer tied to a simple Russell-Miami soil line, as implied by Gooding *et al.* Full-time professional soil workers (Stout, Petro, Holowaychuck, Dotson) have found a deep Russell soil in small areas along the outer Wisconsin moraines of the Scioto lobe in Ohio, and these may be "early Wisconsin", *i.e.*, equivalent to the "paleosol" in question. Elsewhere, in both the Miami and Scioto lobes, C^{14} dates show only one ice sheet advancing to the outer moraine (Goldthwait and Burns, 1958) culminating 17,000–19,000 years ago. The new soils distinctions, shallow Russell (67s), deep Miami (60), or shallow Miami (6B), all relate to halts, minor readvances, and varying loess cover long after formation of the "paleosol" in question. This is irrelevant to the preclassical Wisconsin-post-Sangamon stratigraphy as we now in interpret it.

Ohio workers have admitted for a long time that the lack of any one good buried *A* horizon and the occurrence of leached clay-enriched zones solely in stratified deposits cast question on the paleosol hypothesis. We believe, however, that in some places in Ohio the "paleosol" does have a typical B2 horizon like present Fox soils. At many places we see good sand-gravel stratification going into and through the leached clay-enriched pendants both in modern Fox soil, as at Scippio Creek (Goldthwait, 1955, Stop 17A), and in the "paleosol." It is difficult for us to see how "these features are not normal characteristics of the B horizon of a Fox soil," as Gooding *et al.* state.

At Sidney, Ohio, several years ago we found leached gray sand masses at the top of the buried soil; these seemed to be a disturbed macerated *A* zone. As already published (Forsyth and La Rocque, 1956) and soon to be published in more detail the rest of this paleosol more closely resembles classical Wisconsin profiles known in central Ohio. The fossil zone below seems to indicate a Wisconsin interstadial date. Therefore, we disagree with the analysis of the Sidney cut. The discovery of a leached clay-enriched zone at Sidney by Gooding *et al.* is a new contribution. Compared to some other possible paleosols in Ohio this one has few soil-like characteristics (horizontal extent, pendants, vertical zonation); we suggest that it probably developed from the surface downward. However, several other cool-climate peats resting on weathered zones in till near by must represent long-exposed surfaces (Goldthwait and Burns, 1958). We believe that these peats and the main Sidney paleosol may indicate a post-Sangamon preconventional-Wisconsin interval, regardless of the origin of leached clay-enriched zones. The evidence that convinces us of a mid-Wisconsin interval of retreat (pre-27,000 B.P.) is in till cuts at Sidney, Brush Creek, and Hamilton, not in these Fox-like "paleosols".

Scioto Valley in Ohio, like the Whitewater Valley in Indiana, does not exhibit any terraces that contain soil intermediate between Wisconsin (Fox) and Illinoian (Park); however, Paint Creek tributary and Hocking Valley, Ohio, do have some terraces intermediate in depth of leaching and intensity of B-zone clay accumulation (Kempton and Goldthwait, in press). European glacial workers, analysts of

sea-floor sediments, and recent students of Southwestern Lakes now tell us that the last long glacial stage began at least 50,000 or 60,000 years ago, not 30,000. We believe that these Hocking Valley terraces may record the early (Wurm I) part of this period.

This reply is not a denial of the probable surface origin of phenomena in Figures 1 and 2 of Gooding *et al.* but an appeal to keep an open mind on similar phenomena. We believe further distinction is needed. Misinterpretation in either direction will lead to very erroneous conclusions!

References Cited

Forsyth, J. L., and La Rocque, Aurèle, 1956, Age of the buried soil at Sidney, Ohio (Abstract): Geol. Soc. America Bull., v. 67, p. 1696

Goldthwait, R. P., 1955, (*Leader*) Pleistocene chronology of southwestern Ohio 5th Bienn. Pleistocene Field Conf. Guidebook Pt. 2, 72 p.

Goldthwait, R. P., and Burns, G. W., 1958, Wisconsin age forests in western Ohio: Ohio Jour. Sci., v. 58, p. 209–230

Gooding, A. M., Thorp, James, and Gamble, Erling, 1959, Leached, clay-enriched zones in Post-Sangamonian drift in southwestern Ohio and southeastern Indiana: Geol. Soc. America Bull., v. 70, p. 921–926

Kempton, J. P., and Goldthwait, R. P., in press, Glacial outwash terraces of the Hocking and Scioto River valleys, Ohio: Ohio Jour. Sci., v. 59

Department of Geology, Ohio State University, Columbus, Ohio

Manuscript Received by the Secretary of the Society, March 20, 1958

BULLETIN OF THE GEOLOGICAL SOCIETY OF AMERICA
VOL. 70, PP. 929–934, 4 FIGS. JULY 1959

GRAVITY ANOMALIES OFF THE WEST COAST OF NORTH AMERICA. 1: SEAMOUNT JASPER

BY J. C. HARRISON AND W. C. BRISBIN

Seamount Jasper is an approximately conical peak rising 1900 fathoms from an irregular ocean bottom of about 2200 fathoms average depth. It lies about 320 nautical miles southwest of San Diego, California, and was chosen for the present study because the return trip from San Diego and the survey could be made within the 5-day period for which a submarine could be made available. It is the only seamount for which this is true and which had been previously dredged and surveyed topographically (Menard, 1955, p. 1159–1160; Fig. 8), with the exception of the San Juan Seamount which may not be typical because of its proximity to the continental slope. Menard's (1955, pl. 1) chart of the bathymetry in the vicinity of the Murray fracture zone shows the position of Seamount Jasper in relation to the regional bathymetry.

The gravity measurements used in this study were taken on board the USS BAYA in 1954 and have been described and the anomalies published by Harrison, Brown, and Spiess (1957). A marker buoy was anchored near the summit of the seamount before the start of the survey, and the station positions are known relative to this buoy with considerably greater accuracy than are their latitudes and longitudes. Unfortunately no very accurate fixes were obtained while the submarine was in the close vicinity of the buoy, and the published station co-ordinates depend on the position of the summit determined during the earlier topographic surveys by the Scripps Institution of Oceanography and the Naval Electronics Laboratory. The interpretation, however, depends mainly on the relative accuracy of the measurements, which may be as high as ± 2 mgal for the free-air anomalies. The positions of stations used in this interpretation are shown in Figure 1.

A profile of free-air anomalies (Fig. 2) shows a large increase in anomaly over the seamount. This is to be expected as the seamount is a mass on the sea floor much nearer the observing submarine than any possible associated masses. The direct effect of the seamount can be removed by using the Bouguer anomaly in which a topographic correction is added to the free-air anomalies, equal to the increase in gravity that would result if the sea water were replaced by rock of an assumed density. The value of the Bouguer anomaly would be independent of the presence of the seamount if the true density were used and if there were no anomalous masses beneath the seamount. Systematic variations in the anomalies over the seamount can mean either that the incorrect density has been used in computing the topographic corrections or that there is an anomalous mass associated with the seamount. The Bouguer anomaly used in this investigation is the modified anomaly in which the topographic correction is made for the assumed density out to a distance of 100 miles from the station. More distant topography is assumed to be of density 2.67 gm/cc and to be compensated according to Airy's hypothesis for a crustal thickness of 30 km. The attraction of this topography and its compensation amount to about 30 mgal in the neighborhood of the seamount, but it changes by only 4 mgal along the profile AB. The profiles in Figure 2, computed for assumed densities of 2.67 and 2.5 gm/cc, show a mimimum over the seamount; when a density of 2.1 gm/cc is assumed the profiles show a maximum over the seamount. For a density of 2.3 gm/cc the anomaly is not influenced by the presence of the seamount, indicating that the gravitational effect of the seamount can be explained entirely if it has this density.

The method of least squares can be used to find the density for which the value of the Bouguer anomaly varies least and to estimate the uncertainty of this determination. If the topographic correction for Hayford's zones A to O is T when computed for a density of 2.67 gm/cc, the correction for any other density, d, is $(d - 1.03)/(2.67 - 1.03) \times T = KT$, where K is a function of d. The attraction of topography outside zone O, and of its compensation, was added to the free-air anomalies to give a modified free-air anomaly, A. If the Bouguer anomaly does not vary over the seamount then $A + KT$ = constant. The data for stations 11–28 were solved by the method of least squares to determine the best value for K. This proved to be 0.7484, corresponding to a density

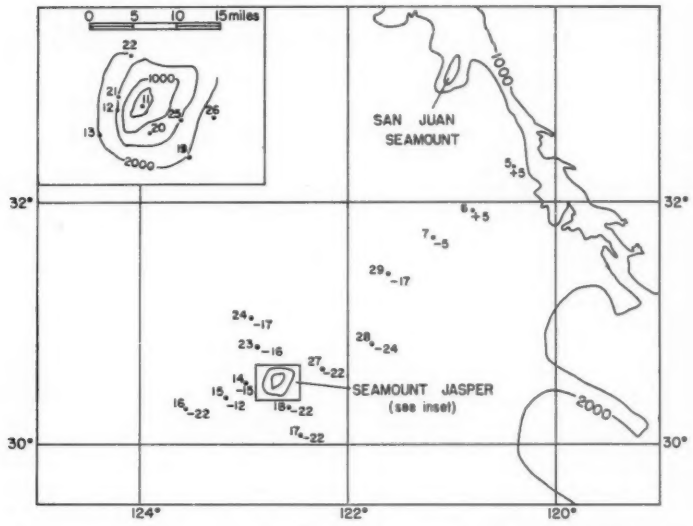

FIGURE 1.—POSITIONS OF GRAVITY STATIONS IN THE VICINITY OF SEAMOUNT JASPER
Upper left-hand figure: station number
Lower right-hand figure: Airy Heiskanen isostatic anomaly for $T = 30$ km
Contour interval 1000 fathoms on main chart, 500 fathoms in inset

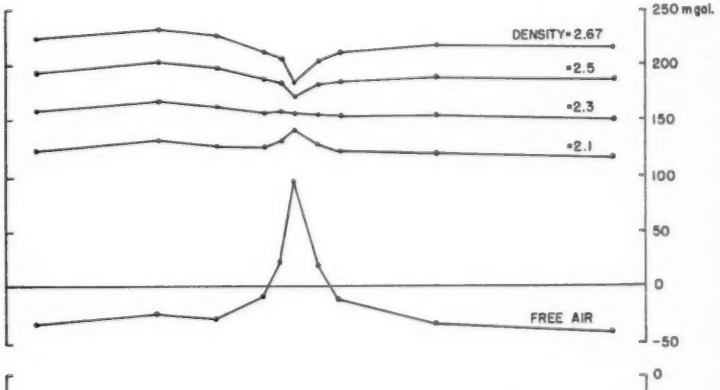

FIGURE 2.—TOPOGRAPHIC AND GRAVITY PROFILES ACROSS SEAMOUNT JASPER
See Figure 3 for line of profile

of 2.28 gm/cc. The calculated standard deviation is 0.04 gm/cc.

The differences between the modified Bouguer anomalies for a density of 2.3 gm/cc and of 2.3 gm/cc for the rock composing the seamount appears very reasonable, although this density is much less than could be assumed for a nonvesicular rock of the same type.

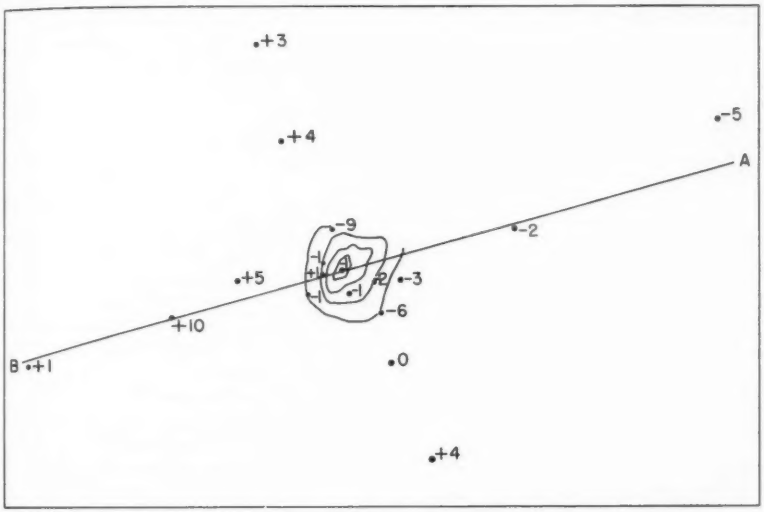

FIGURE 3.—DIFFERENCES BETWEEN MODIFIED BOUGUER ANOMALIES FOR 2.3 GM/CC DENSITY AND THE MEAN ANOMALY AT STATIONS 11–28

their mean value at stations 11–28 are shown in Figure 3. These are generally quite small. The only two worthy of note are at stations 15 (+10 mgal) and 22 (−9 mgal). The root mean square value of the other anomalies is 3.1 mgal, and they can be readily accounted for by errors in the determination of the free-air anomalies and the topographic reductions. The anomalies at stations 15 and 22 are probably real but remain unexplained.

The single assumption that the seamount is made of rock of average density 2.3 gm/cc is sufficient to give a very good account of the observed gravity field. This value is in good agreement with Woollard's (1951) conclusions concerning the density of the island block beneath Oahu. The samples dredged from the seamount are vesicular basalts consisting of plagioclase laths in a glassy groundmass which has been replaced in part by goethite and a little hematite. The density of these samples is 2.05 gm/cc, and the seismic P wave velocity, kindly determined by Leon Knopoff, is 3.7 km/sec. These densities and velocity are somewhat lower than that to be expected for the entire seamount as the available samples are highly vesicular and physically altered. A mean density

Many other solutions of the gravity problem are possible. If one assumes that the seamount is of density 2.67, the pattern of modified Bouguer anomalies shows a circularly symmetrical minimum centered over the seamount. This is consistent with an anomalous body beneath the seamount. The modified Bouguer anomalies for a density of 2.67 gm/cc are plotted as a function of distance from the center of symmetry of the seamount (which is slightly to the east of its shoalest point) in Figure 4, and the solid curve shows the anomaly produced by a sphere which has its center at a depth of 13 km below sea level and which has a mass deficiency of 1.1×10^{18} gm. The root mean square scatter of the anomalies from this curve is about the same as the root mean square scatter of the anomalies calculated for a density of 2.3 gm/cc, so the two solutions fit the gravity data equally well. Whatever value is assumed for the density of the seamount, within the range of geologically plausible values (2.1–2.9 gm/cc), it will be possible to find a mass beneath the seamount to explain the Bouguer anomaly field. For a density of 2.3 gm/cc there is no need to assume any anomalous mass beneath the seamount. The interpretation of the anomalies

which indicates a density of 2.3 gm/cc for the seamount is in good accord with Woollard's result for Oahu and with the vesicular character of the dredged samples, but it is not unique. The mass and shape of the additional body that must be assumed if the seamount does not have this density are not readily specified, as many mass distributions can be found to fit the data well enough.

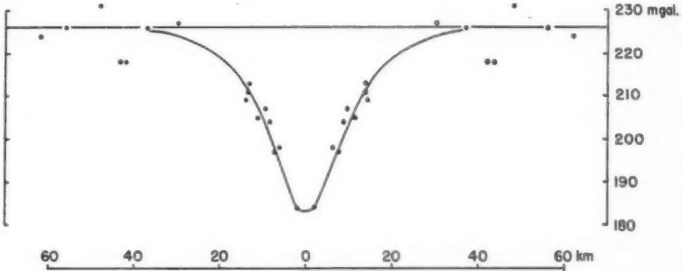

FIGURE 4.—MODIFIED BOUGUER ANOMALIES FOR 2.67 GM/CC DENSITY PLOTTED AS A FUNCTION OF DISTANCE FROM CENTER OF SYMMETRY OF SEAMOUNT JASPER
Radius of sphere producing solid anomaly curve is calculated for a density deficit of 0.33 gm/cc

The volume of the seamount above the 2200-fathom line is 7.8×10^{17} cc, and thus the load, calculated for a body of density 2.3 gm/cc immersed in sea water, is about 10^{18} gm. For a density of 2.67 gm/cc the load is 1.3×10^{18} gm, but this is almost exactly balanced by the mass deficit below (1.1×10^{18} gm), and the seamount is in a sense compensated. However, none of the mass distributions assumed on any of Airy's or Hayford's hypotheses for which tables exist fit the data as well as the spherical mass. The maximum stress differences required to support the seamount, if it is a load of density 2.3 gm/cc, are about 4×10^8 dynes/sq cm, and, because of its small radius, stress differences of this order of magnitude need not extend to a depth of more than a few tens of kilometers. These stress differences are less than the usually accepted strengths of crustal rocks near the surface, so there is no reason for thinking that the seamount must be compensated.

The free-air and isostatic anomalies at the stations around the seamount are uniformly negative, with a mean value of about −20 mgal relative to the International Gravity Formula. The mean free-air anomaly at stations 11–28, leaving out those stations on, or at the foot of, the seamount, is −29 mgal, the mean Airy-Heiskanen isostatic anomaly for $T = 20$ km is −24 mgal and for $T = 30$ km is −19 mgal. Undoubtedly there is a regional mass deficit equivalent to about 20 mgal attraction in an area surrounding Seamount Jasper extending as far as the present survey.

This deficit may, or may not, be associated with the large number of seamounts in the area. Suppose that material of 3.3 gm/cc density be withdrawn uniformly from beneath an area 60 miles in radius, the sea floor subsiding a distance equal to the thickness of the layer of material removed. Some 2.7×10^{19} gms of material, equivalent to a layer 210 m thick, must be removed in order to produce a regional anomaly of −20 mgal, which may be compared with the mass of volcanic rock in the four seamounts and a probably volcanic ridge within a 60-mile radius of the summit of Seamount Jasper. The estimated volume of these features is 2.6×10^{18} cc, and the mass of volcanic rock calculated from this figure lies between 5 and 6×10^{18} gm. A range of values is possible because it is not known whether the vesicles in the rock contain sea water. In either case the mass of rock is only about one-fifth of the 2.7×10^{19} gm needed, according to the hypothesis described above, to explain the widespread negative gravity anomalies.

It is not possible to explain more than a fraction of the regional negative anomaly in terms of the mass deficit produced by material extruded as seamounts. The observation that the

regional depth of the Baja California seamount province is about 500 m less than that of the Deep Plain to the north, where seamounts are very much less common (Menard, 1955, p. 1158), also contradicts the hypothesis that the sea floor subsides as material is removed at depth and extruded as volcanic rock. However, the hypothesis that lighter material, which is still in large part present, was formed at depth beneath the Baja California seamount province prior to the extrusion of the seamounts can explain both the regional negative anomaly and the decrease in depth of the province. The expansion of the material at depth, which may have been caused by partial melting, would have caused the ocean floor to rise. The displacement of sea water by the upward movement of the sea floor would have produced a regional mass deficit—a rise of 500 m would have displaced 500 m of sea water and produced a regional negative anomaly of about 20 mgal. Extrusion of magma would cause the sea floor to subside once more, but, if only a small proportion of the lighter material were extruded during the period of volcanic activity, the net effect would still have been a raising of the sea floor.

The problem of the negative anomalies surrounding seamount Jasper is not an isolated one. J. L. Worzel (1957) reports that, in the Atlantic Ocean, the free air anomaly over the area between the United States, Bermuda and the Caribbean Islands averages about −40 mgal, and that (personal communication) unpublished data in the Pacific Ocean shows that large areas here also are characterised by negative free air anomalies.

Raitt (1956) finds that the thickness of the crustal layers in the central Pacific does not vary systematically with the depth of water. He concludes (p. 1637) that "this indicates that isostatic compensation is not accomplished in these areas by a simple increase in the thickness of the first three layers". The idea, that, over the oceans, the regional variations in bathymetry and gravity field are related to density changes at depth possibly associated with the formation of magma is an interesting one for further consideration when more gravity and seismic data become available.

References Cited

Harrison, J. C., Brown, G. L., and Spiess, F. N., 1957, Gravity measurements in the northeastern Pacific Ocean: Am. Geophys. Union Trans., v. 38, p. 835–840

Menard, H. W., 1955, Deformation of the northeastern Pacific Basin and the west coast of North America: Geol. Soc. America Bull., v. 66, p. 1149–1198

Raitt, R. W., 1956, Seismic refraction studies of the Pacific Ocean Basin. Part I: Crustal thickness of the central equatorial Pacific: Geol. Soc. America Bull., v. 67, p. 1623–1639

Woollard, G. P., 1951, A gravity reconnaissance of the island of Oahu: Am. Geophys. Union Tran., v. 32, p. 358–368

Worzel, J. L., 1957, Gravity at sea, Columbus, Ohio: Inst. Geodesy, Photogrammetry and Cartography Pub. 7, p. 65–67

Institute of Geophysics, University of California, Los Angeles, Calif.; Dept. Geology, University of Manitoba, Winnipeg, Manitoba, Canada

Manuscript Received by the Secretary of the Society, April 7, 1958

Publication No. 94, Inst. of Geophysics, University of California

Work Supported by Office of Naval Research Contract Nonr 233(19)

BULLETIN OF THE GEOLOGICAL SOCIETY OF AMERICA
VOL. 70, PP. 935–938 JULY 1959

LOWER PRECAMBRIAN ROCKS OF THE TIMISKAMING REGION, QUEBEC AND ONTARIO, CANADA

By W. G. Q. Johnston

In his summary of the geology of Western Quebec and adjacent parts of Ontario, Wilson (1956) discusses, among other things, the Timiskaming–Grenville relations east of Lake Temagami, Ontario. He made a few field observations in this area, which had been previously studied and reported on (Johnston, 1954a). Apparently, because of lack of time and the arduous trips to reach them, Wilson did not visit the critical outcrops found and described by the writer, and hence limited field observations in this area have influenced his summary of Todd's and the writer's work to a point of making it a somewhat distorted account.

Wilson is in complete disagreement with the writer's observation that a complex zone of thrust faults of major tectonic significance forms the boundary of the Timiskaming and Grenville subprovinces in this area.

Part of Wilson's discussion considers linear valleys. He states (p. 1421): "The occurrence of linear valleys on or near this boundary Timiskaming–Grenville contact], therefore, is not so important as Johnston believed".

There is no mention of linear valleys in this paper, much less any conclusions based on them as Wilson states. It would appear Wilson has confused linear valleys, a superficial geomorphic form, with lineation, an important structure within the rocks.

In the area in question there are a great many linear valleys as there are practically everywhere in the Canadian Shield. However, in this area, as the writer has pointed out (Johnston, 1954a, p. 1052), there is commonly continuous outcrop across these valleys, and faults are readily discernible in the northeast-trending set. They are not drift-filled as Wilson (1956, p. 1419) implies.

As Wilson points out, linear valleys have the same general trend great distances from the Timiskaming–Grenville contact; so do the fracture patterns of the rocks, as the writer emphasized (Johnston, 1954a, p. 1049; 1954b, p. 8). The uniformity and similarities of fractures and joint patterns over a large portion of the Timiskaming subprovince (which controlled the subsequently uniform linear valley pattern) is not due to coincidence as Wilson advocates but is probably due to some relationship of these fractures to the deformation (faults) at the contact of the Timiskaming and Grenville subprovinces.

As opposed to the conclusion that the faults at contact of the subprovinces are major thrust faults, a conclusion arrived at after 7 months of field work involving observations on and measurement of more than 3000 structures and the later analysis of these structures, Wilson from a few observations west of the main zone of faulting explains these faults as relatively minor and of little significance, and the result of intrusions of diabase and gabbro. He makes the statement (p. 1422) that: "The preponderance of evidence favors the conclusion that most of them [faults] are related to movements that accompanied the intrusion of the Nipissing and olivine diabase gabbro."

What the preponderance of evidence is Wilson does not mention. To the writer there is convincing evidence that the intrusion of the diabase, or movements associated with its intrusion, which there undoubtedly were, was not the cause of these faults for the following reasons:

(1) Practically all the movement on these faults in the Timiskaming subprovince took place long before the intrusion of the diabase as has been pointed out (table of events, Pl. 2, Johnston, 1954a, and in a section devoted to the age of the structures). This conclusion is based on the regional distribution and intensity of deformation in rocks of various ages in the Timiskaming subprovince. However, in the portion of the Grenville subprovince concerned there are few rocks of definitely established age with which to date movement, and even the late olivine diabase dikes have been deformed, and the Nipissing diabase, if present, has been transformed to amphibolite by deformation (Johnston, 1954a, p. 1064). Observations in the area indicate that all deformations, regardless of age, produced the same fracture pattern and associated structures, as can be best seen from statistical equal-area plots of these structures (Johnston, 1954a, Pl. 4). These fracture pat-

terns, lineations, other structures, and the mineral fabric itself are the same in Proterozoic and Archean rocks, and their origins are intimately connected with the problem of the age relation of the Timiskaming and Grenville subprovinces and at present must all be considered a part of this problem whether Archean, Proterozoic, pre-Cobalt, pre-, or post-Nipissing diabase. At and near the boundary of the Timiskaming and Grenville subprovince there has been Proterozoic movement on faults, in the area in question and elsewhere; however at the present state of our knowledge it is wrong to assign all movement on these faults to the Proterozoic. In the area in question these faults are major structures and consequently would be expected to have had a long and complex history. The writer believes the major movement is pre-Cobalt and could well be Archean (Johnston, 1954a, Pl. 2). The Cobalt series was deposited on highly schistose Archean rocks and in valleys along these faults which later became active.

The Nipissing and olivine diabase are the least deformed rocks in the area, and undeformed chilled contacts of these rocks are found in contact with strongly deformed country rocks (Johnston, 1954a, p. 1064). Todd's map, which covers part of the area in question, illustrates that the intrusion of the diabase was controlled by earlier northeast-striking faults (Todd, 1925, p. 28). In fact much of the deformation was pre-Nipissing diabase, and pre-Cobalt. Wilson's statement (p. 1421) that: . . . "the close association of the more intense deformation in the region with intrusions of diabase described by Todd and Johnston" . . . is not a fair abstract from either Todd's work or the writer's.

(2) More abundant and much larger intrusions of Nipissing diabase occur northwest of the area in question, yet here deformation in the Cobalt series is practically lacking in contrast to the intense deformation found along the eastern limit of the Cobalt series where it occurs nearest the Timiskaming–Grenville contact.

(3) Northeast-striking faults adjacent to the diabase can be traced along strike to localities miles from known outcrops of diabase. Conversely in the area mentioned in (2) above northeast-striking faults and associated structures are not nearly so abundant or strongly developed, yet diabase is much more abundant.

(4) If movements accompanying intrusion of the Nipissing diabase produced the northeast-trending faults as Wilson concludes then all other secondary structures in the area that analysis indicates are intimately related (Johnston, 1954a, p. 1063) must be of the same origin. The intrusion of rock such as the Nipissing diabase is generally considered associated with quiescence and tension which is the direct opposite of the writer's observations that a shortening along a northwest-southeast axis took place as indicated by northeast-trending fold axes, flattening of pebbles and mineral grains, boudinage, and a well-developed southeast-plunging lineation parallel to tectonic transport in a northwest direction. Wilson does not explain the lineations and other structural features of the area or why massive granite of low-grade metamorphism and a highly contorted gneiss in the amphibolite facies lie on either side of faults termed minor and local by him.

Regarding the deformation in the Cobalt series Wilson states: . . ."and most of the deformation in the Cobalt sediments occurs adjacent to or near the contact of this diabase". This statement is incorrect as can be seen from examination of the outcrops of Cobalt along its eastern extremity as at Ross Lake, east of Southwest Bay, Rabbit Lake, and at Rankin Lake. The deformation in the Cobalt series is not related to bodies of Nipissing diabase but increases to the southeast and is most intense at its eastern limit—*i.e.*, at outcrops nearest the Timiskaming–Grenville contact where in many cases it has been overturned to the west and dips under the older granite at faults marking its southeastern limit. To casual examination the Cobalt series may appear as scattered erosional remnants, in this locality, but these scattered erosional remnants are not due to absence of faulting, but to the fact that the basal member of the Cobalt series was deposited on a surface of mountainous topography. To quote Todd (1925, p. 29) it is probably fairer to quote too long a passage than too short a one as Wilson (p. 1420) appears to have done with this same quotation.

> "The contact between the sediments and the granite is parallel to the northeast-southwest lines of regional disturbance. This fact, taken in conjunction with the abundant evidence of movement in the region of the contact, suggests that the junction of the two rocks lies in a fault zone in which the movement has been intense. The upthrown side is to the south, and the sediments originally resting on the granite have been removed by erosion in the process of base levelling. Since the Cobalt series has been almost entirely eroded away to the south of this fault zone, it is probable that the displacement was very great".

Wilson emphasizes that the deformation is minor and local, whereas any information the writer obtained indicated it was regional. Examination of the map or statistical diagrams of structures (Johnston, 1954a, Pls. 2, 4) indicates that the results of deformation are uniform throughout the area. From very limited observations outside the area studied, lineation has much the same attitude from Sudbury at least as far north as Fabre township in Quebec a few miles north of the area in question where Pierre Mauffette (1953) concluded from detailed mapping that a fault forms the contact of the Timiskaming and Grenville subprovinces. Wilson did not comment on Mauffette's findings. Still farther afield Wahl and Osborne found that structures 100 miles to the east have strong similarities to those in the area studied by the writer (Johnston, 1954a, No. 30, Pl. 4).

Regarding delineation of the Timiskaming–Grenville contact Wilson states (p. 1421): "But this contact has been almost obliterated by the intrusion of the granodiorite and the successive phases of the potassic granite, and it cannot be fixed so definitely as Johnston has indicated".

There is truth in the above statement as has been pointed out (Johnston, 1954a, p. 1057, 1067); however, because faulting is post granite and the contact is a major fault there are localities such as Hangingstone Lake where the contact can be established within a few feet. Detailed mapping and petrographic study could very accurately define the contact, as the increase in the degree of recrystallization (metamorphism) southeastward is, in reality, the difference and the fine point of distinction between the two subprovinces at the contact in this area.

One of Wilson's arguments in refuting the presence of faults mapped by others at the Timiskaming–Grenville boundary is the discordance of strike of these faults which is more westerly than the strike of the boundary. This apparent discrepancy is due to the common nonparallelism of faults and associated schistosity with the strike of the zone of dislocation to which they belong. This is evident from sections of this boundary which have been studied; faults actually transect the boundary and have been traced from one subprovince into the other (Johnston, 1954a, Pl. 2).

To continue this reply further here or elsewhere can serve no useful purpose. The writer prefers to confine any further discussion to a verbal one at the critical outcrops in question with anyone so interested.

References Cited

Johnston, W. G. Q., 1954a, Geology of the Temiskaming-Grenville contact Southeast of Lake Temagami, Northern Ontario, Canada: Geol. Soc. America Bull., v. 65, p. 1047–1074

—— 1954b, Geology of the northeast quarter of Dasserat township, Temiscamingue County, Quebec: Geol. Survey Canada Paper 53–8, 17 p.

Mauffette, Pierre, 1953, Preliminary report on part of Fabre Township: Quebec Dept. Mines Prog. Rept. no. 274, 6 p.

Todd, E. W., 1925, The Matabitchuan area: Ont. Dept. Mines Annual Rept. XXXIV, pt. 111, 38 p.

Wahl, W. G., and Osborne, F. F., 1950, Cawatose map-area: Quebec Dept. Mines Geol. Rept. 44, 37 p.

Wilson, M. E., 1956, Early Precambrian rocks of the Timiskaming region, Quebec and Ontario, Canada; Geol. Soc. America Bull., v. 67, p. 1397–1430

Elk Lake, Ontario, Canada

Manuscript received by the Secretary of the Society, January 21, 1957

BULLETIN OF THE GEOLOGICAL SOCIETY OF AMERICA
VOL. 70, PP. 939-940 JULY 1959

HAVE THE SEDIMENTS OF THE COBALT SERIES NEAR THE SOUTH END OF LAKE TIMISKAMING BEEN DEFORMED INTO MOUNTAINS?

BY M. E. WILSON

Before considering the items in the writer's paper discussed by Johnston, it will be helpful to review briefly the geological background for the hypothesis that a continuous fault or fault zone of late Precambrain age extends from Lake Huron northeastward for more than 700 miles to Lake Mistassini in Quebec. In 1936 G. W. H. Norman suggested that northeasterly trending faults that intersect the Proterozoic Chibougamau and Mistassini series in the Lake Chibougamau–Lake Mistassini area were related to a fault extending from Killarney on the north shore of Lake Huron northeast for 24 miles to timber berth 48, which Quirke (Quirke and Collins, 1930, p. 38–39) had postulated doubtfully to explain the straight course of the boundary of the intrusion of Killarney granite in that region. In 1947 Norman also indicated a fault (with broken symbols) beneath glacial drift covering the contact between Early Precambrian altered volcanic rocks on the north and banded gneisses to the south, in the Grand Lake Victoria area, Quebec, about midway between Lake Mistassini and the north shore of Lake Huron. In its western part, this assumed fault is shown to bend south 55° to join a northerly trending fault underlying the north arm of Grand Lake Victoria. In 1946 H. C. Cooke described exposures of deformed chert and quartzite indicating a fault, in a creek valley southwest of South Coniston station in the Sudbury district, Ontario. In 1947 (p. 20) Cooke in a figure illustrating a description of the geology of the Canadian Shield, without additional supporting field investigation, extended this fault southwest to Lake Huron and northeast to Labrador. In 1950 Derry and associates on the tectonic map of Canada, also without further field work, showed the fault to extend from Lake Huron to Lake Mistassini. Up to the time of Johnston's investigation, the existence of this major structure had been reported for only four localities, at two of which the evidence is inconclusive, but, even if it be assumed that the fault exists in these two places, more than 350 miles of the indicated length of 700 miles remained in which the fault was not known.

The writer examined the district east and west of the south end of Lake Timiskaming in 1954, following Johnston's study in that area, but prior to the publication of his paper, to determine (1) whether the sediments of the Cobalt series were cut off abruptly on the south by a Lake Huron–Lake Mistassini fault as indicated (with broken symbols) on the tectonic map of Canada, and (2) to review earlier observations in that general region. The district examined by Johnston lies within the heavily wooded Timagami Forest Reserve, where good rock exposures are restricted mainly to (1) the shores of lakes, (2) the rock cuts along the Ontario Northland Railway, and (3) the Ontario provincial highways and subsidiary roads. The writer saw the exposures of groups (2) and (3) but saw those of group (1) only where accessible from roads. The rocks adjacent to Rabbit Lake were not examined. These, however, had been described by Barlow (1897, p. 222–224) and Todd (1925, p. 29–30). Johnston underestimates the extent of the writer's observation in his map area and overlooks the fact that the writer's earliest geological mapping was on the east side of Lake Timiskaming where the relationships of the Cobalt series can also be seen.

At the beginning of his paper, Johnston includes a map (Pl. 1) showing the places where faulting has been reported or suggested to occur along the course of the assumed Lake Huron–Lake Mistassini fault. It could be inferred, therefore, that he undertook the examination of his map area with only post-Cobalt series deformation in mind. On the other hand, the statement in the abstract of his paper that "movement has taken place many times, the latest in late Precambrian" indicates that, despite the great structural unconformity that separates the Cobalt sediments from the deeply eroded granite on which they rest, he combined the post-Cobalt series (Proterozoic) faulting with the Archean Ottawa Mountains uplift, as if they were parts of a single orogeny. The writer in 1913 (p. 110) and 1918 (p. 56) pointed out that the belt of banded gneisses lying along

the northwest border of the Grenville subprovince "originally formed the core of a Precambrian mountain chain", but the so-called Grenville front is assumed to be a Late Precambrian thrust movement. The writer's consideration of the Lake Huron–Lake Mistassini fault problem was, therefore, concerned mainly with Proterozoic deformation.

The original Huron of Logan on Lake Timiskaming, now known as Cobalt series, although extensively intruded by sills and dikes of diabase or gabbro, except where adjacent to faults dips at low angles or is horizontal, and this condition persists to its southernmost exposure both east (Wilson, 1910, map) and west of Lake Timiskaming. It has not been deformed by folding or faulting into mountains. Furthermore, the basal conglomerate member of the series rests unconformably on granite that intrudes the banded gneisses of the Ottawa Mountains belt to the south.

The Cobalt series, not only in the areas examined by Todd and Johnston, but throughout the Lake Timiskaming region, is intersected by faults in many places. Most of these are normal faults; some are overthrusts. Because the Cobalt sediments have not been mountain-built and the gabbro-diabase is the only rock intruding them, the thrust faulting is possibly related to these intrusions. Some observations favoring this hypothesis are:

(1) Todd (1925, p. 30) states that the "intense earth movements" in the Rabbit Lake area (also examined by Johnston) occurred both before and after the intrusion of the Nipissing diabase.

(2) Barlow (1897, p. 231) notes that the deformation in (Cobalt) conglomerate on Rabbit Lake increases "as the mass of diabase or gabbro is approached".

(3) In the Cobalt area, where a sill of diabase 1000 feet thick has been intruded, thrust faults up to a maximum displacement of 550 feet occur (Knight, 1922, pt. 2, p. 12–16).

(4) The intrusions of diabase or gabbro on Rabbit Lake continue southwest into the northwestern part of Johnston's map area where he shows faults intersecting the Cobalt series.

Johnston's comments refer to relatively minor details, but he overlooks the main problem—the age of mountain building. Because the Cobalt series rests with great unconformity on granite that intrudes the banded gneisses of the Ottawa Moutain belt, and because most of the southernmost exposures of the Cobalt sediments have been neither recrystallized nor deformed, it must be concluded that all the mountain building in the area occurred before the Cobalt series was deposited and is of Archean age. The Early Precambrian mountain building and the local faulting in the Cobalt series are entirely dissimilar structural features separated in time by many millions of years of erosion and are almost certainly different in origin.

References Cited

Barlow, A. E., 1897, Report on the geology and natural resources of the area included by the Nipissing and Timiskaming map-sheets, comprising portions of the district of Nipissing, Ontario, and of Pontiac County, Quebec: Geol. Survey Canada Ann. Rept., v. 10, pt. i, p. 302

Cooke, H. C., 1946, Problems of Sudbury geology, Ontario: Geol. Survey Canada Bull. 3, p. 77

—— 1947, Geology and economic minerals of Canada 3d edition: Geol. Survey Canada Econ. Geology ser., no. 1, p. 11–97

Derry, Duncan A., *et al.*, 1950, Tectonic map of Canada: New York, Geol. Soc. America

Johnston, W. G. Q., Geology of the Timiskaming-Grenville contact southeast of Lake Timagami, northern Ontario, Canada: Geol. Soc. America Bull., v. 65, p. 1047–1073

Knight, C. W., 1922, Cobalt and South Lorrain silver areas: Ontario Dept. Mines 31st Ann. Rept., pt. 2, p. 358

Norman, G. W. H., 1936, The northeast trend of Late Precambrian tectonic features in the Chibougamau district, Quebec: Royal Soc. Canada Trans., 3d ser., v. 30, sec. 4, p. 119–128

—— 1947, Vaquelin, Pershing, and Haig townships, Abitibi County, Quebec: Geol. Survey Canada Paper 47-12, p. 16

Quirke, T. T., and Collins, W. H., 1930, The disappearance of the Huronian; Geol. Survey Canada Mem. 160, p. 129

Todd, E. W., 1925, The Matabitchuan area: Ontario Dept. Mines 34th Ann. Rept., pt. 3, p. 38

Wilson, M. E., 1910, Geology of an area adjoining the east side of Lake Timiskaming: Geol. Survey Canada, p. 46

—— 1913, The banded gneisses of the Laurentian highlands of Canada: Am. Jour. Sci., 4th ser. v. 36, p. 109–122

—— 1918, Timiskaming County, Quebec: Geol. Survey Canada Mem. 103, p. 197

GEOLOGICAL SURVEY OF CANADA, OTTAWA, CANADA
MANUSCRIPT RECEIVED BY THE SECRETARY OF THE SOCIETY, MARCH 9, 1957

BULLETIN OF THE GEOLOGICAL SOCIETY OF AMERICA
VOL. 70, PP. 941-946, 2 FIGS. JULY 1959

PALEOZOIC AND MESOZOIC FOSSILS IN A THICK STRATIGRAPHIC SECTION IN THE EASTERN SIERRA NEVADA, CALIFORNIA

BY C. DEAN RINEHART, DONALD C. ROSS, AND N. KING HUBER

Introduction

A thick section of metamorphosed Paleozoic and Mesozoic rocks is exposed in two roof pendants, one each in the Mount Morrison and Devils Postpile quadrangles in the eastern Sierra Nevada near Mammoth Lakes, California (Fig. 1). In the course of geologic mapping in these quadrangles by the U. S. Geological Survey in co-operation with the California Division of Mines, fossils of Ordovician, Pennsylvanian, Permian(?), and Early Jurassic ages were collected from weakly metamorphosed parts of the pendants. Detailed mapping in the Mount Morrison quadrangle has been completed by Rinehart and Ross, and a report on this area is in preparation. Similar mapping in the Devils Postpile quadrangle by Rinehart and Huber is in progress. In the part of the Devils Postpile quadrangle not yet covered in the present study, the contacts shown on the map (Fig. 1) are after Erwin (1934).

Because diagnostic fossils are extremely rare in the metamorphic rocks of the Sierra Nevada, these fossils are considered important enough to merit this short note prior to completion of the detailed mapping in the Devils Postpile quadrangle and the publication of more comprehensive reports on the two quadrangles.

Geologic Setting

The metamorphic rocks crop out in two essentially discrete masses: a pendant in the Mount Morrison quadrangle called the Mount Morrison pendant, and another in the Devils Postpile quadrangle called the Ritter Range pendant (Fig. 1). The metamorphic rocks constitute a stratigraphic section more than 60,000 feet thick. Although the rocks are folded, faulted, and metamorphosed, they form an essentially homoclinal sequence that strikes northwest and dips steeply southwest; primary sedimentary structures such as graded bedding and cross bedding as well as the relative stratigraphic position of fossil-bearing beds indicate that the bedding tops are consistently to the west as far west as the North Fork of the San Joaquin River. A major synclincal axis lies just west of the North Fork, and west of this axis the section is reversed with tops to the east. The oldest rocks, which constitute the easternmost parts of both pendants, consist wholly of metasedimentary rocks of Paleozoic age and are overlain by a thick sequence of metavolcanic rocks of Mesozoic age that crops out in the western part of the Mount Morrison pendant and in most of the Ritter Range pendant.

Paleozoic stratigraphy in the Mount Morrison pendant.—The Paleozoic sequence is best preserved in the Mount Morrison pendant and can be divided into three groups of formations approximately 14,750, 10,500, and 7250 feet thick, respectively, from the base to the top. The bottom group is apparently conformable with the middle group, and the middle and top groups are in fault contact. These thicknesses are somewhat in excess of those originally reported by Rinehart and Ross (1954, p. 1297) prior to completion of a study of the Mount Morrison pendant.

The lowest (easternmost) group of strata consists of alternating thin-bedded pelitic hornfels, slate, marble, and calcareous quartz sandstone with about 1500 feet of marble at the base. This group locally contains graptolites of Ordovician age; Early Ordovician (Arenig) forms occur east of Middle to Late Ordovician (Caradoc) forms.

The middle group is dominantly composed of alternating pelitic hornfels and calcareous quartz sandstone. No diagnostic fossils have been found within this group.

The upper (westernmost) group consists dominantly of pelitic hornfels with a distinctive marble formation 500 feet thick and 2000 feet above the base. Fossils of Pennsylvanian age occur in this marble, and fossils of Permian(?) age occur in hornfels stratigraphically above the marble.

The distribution of the lithologic types and the relative stratigraphic positions of the fossil-bearing zones, which have been used for dating the Paleozoic sequence, are indicated in Figure 2.

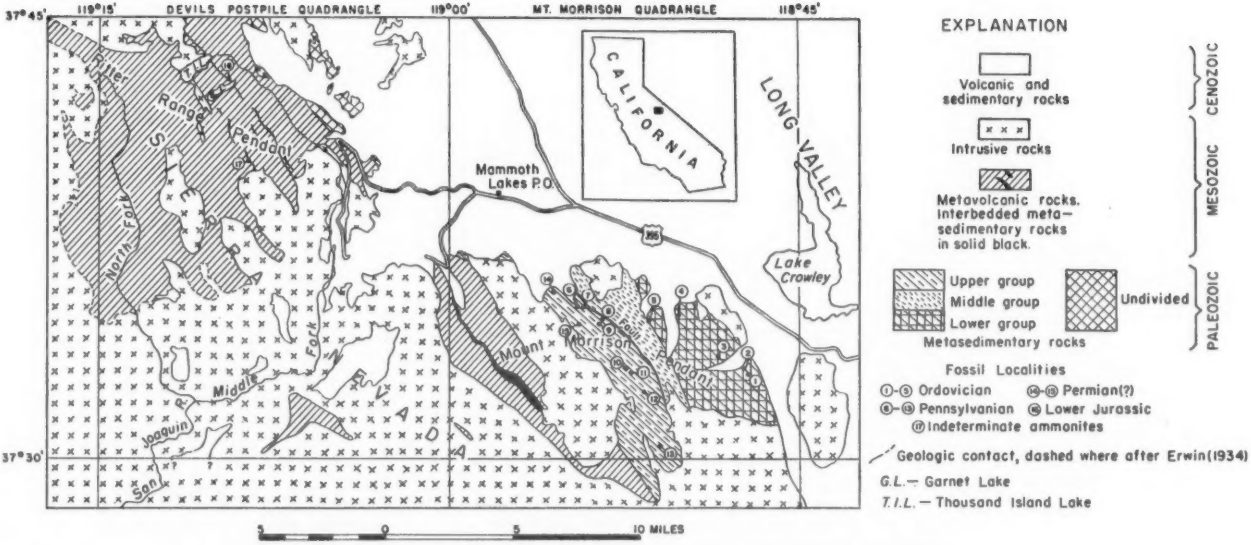

FIGURE 1.—GENERALIZED GEOLOGIC MAP OF MAMMOTH LAKES REGION, CALIFORNIA

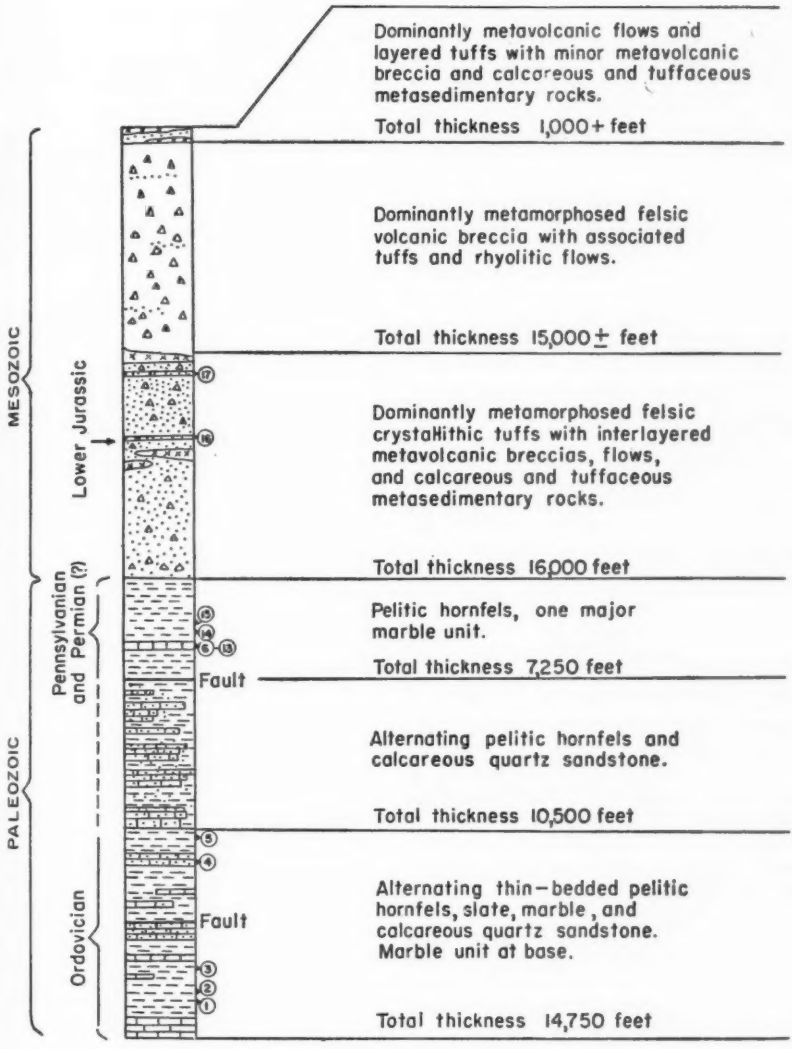

FIGURE 2.—GENERALIZED COLUMNAR SECTION OF PALEOZOIC AND MESOZOIC METAMORPHIC ROCKS IN THE MAMMOTH LAKES REGION, CALIFORNIA

Mesozoic stratigraphy in the Ritter Range pendant.—The contact between the Paleozoic and Mesozoic strata appears to be conformable in the Devils Postpile quadrangle where it is best exposed. In the Mount Morrison quadrangle faulting obscures the nature of the contact. The Mesozoic sequence is best preserved in the Ritter Range pendant and consists chiefly of felsic metavolcanic tuffs and flows with minor interbedded calcareous and tuffaceous metasedimentary rocks. Some shearing and minor folding occurs, but there appears to be little likelihood of major repetition by folding or faulting east of the North Fork of the San Joaquin River. The total Mesozoic sequence exceeds 30,000 feet in thickness.

The Early Jurassic fossils described in this note occur in a narrow belt of calcareous metasedimentary rocks which is interbedded with the metavolcanic rocks and which lies approximately 10,000 feet stratigraphically above the base of the Mesozoic sequence. The rocks below the fossil-bearing beds consist of relatively uniform crystallithic tuffs and a few minor flows (Fig. 2).

Paleozoic Fossils

Fossils ranging in age from Early Ordovician to Permian(?) were collected from more than 20 localities in metasedimentary formations in the Mount Morrison pendant. The localities that yielded the best preserved and most significant fossils are indicated on Figure 1.

Ordovician fossils.—Graptolites collected from the lower part of the stratigraphic section (localities 1–5) were examined by R. J. Ross, Jr., of the U. S. Geological Survey, and noted to have a possible range in age of Early Ordovician to Early Silurian. According to Ross (written communication, 1958), material from locality 1 contains *Tetragraptus* cf. *T. fruticosus* (Hall) and is of Arenig age. Material from locality 5 "shows surprisingly good preservation" and contains *Orthograptus* sp., *Climacograptus bicornis* (Hall), *Climacograptus* cf. *C. bicornis* var. *tridentatus* (Lapworth), and *Dicranograptus* sp. Ross regards this collection as Caradoc, possibly Middle Caradoc. Material from localities 2, 3, and 4 is less well preserved but is possibly Caradoc to Early Silurian in age, probably Ordovician. According to R. J. Ross, Jr. (written communication, 1958), "this graptolite fauna is correlative with those reported from the Vinini, Valmy, and Palmetto formations of Nevada, from the Phi Kappa formation and Ramshorn slate of Idaho, and from the Ledbetter slate of Washington."

Pennsylvanian fossils.—Brachiopods, together with some fragmental horn corals and bryozoans, were collected from several localities in a marble unit in the upper part of the Paleozoic sequence (localities 6–13). These collections were examined by Mackenzie Gordon, Jr., of the U. S. Geological Survey, and he regards them as being of probable Early Pennsylvanian age (Written communication, 1958). He states:

"The best preserved lot of fossils is that from locality M152 [6 on map] where a typical *Linoproductus* which appears to be the one most common in the Early Pennsylvanian of the western United States, is associated with a dictyoclostid with fine costae of almost equal weight and spacing as those of the *Linoproductus*. This productid probably is *Dictyoclostus coloradoensis* (Girty), but none of the specimens are well enough preserved to show other features, such as the *Antiquatonia*-like spines on the lateral slopes found typically in this species. The single productid in collection M150 [9 on map] which we have compared with *Dictyoclostus inflatus* (McChesney) represents a form that is common in the Late Mississippian (Chester equivalents) in the western United States and ranges up into Lower Pennsylvanian rocks of this region. The total assemblage, therefore, contains elements that are typical of such rocks as the lower part of the Ely limestone and the stratigraphically equivalent lower part of the Oquirrh formation both of the Great Basin region."

Similar material, although less well preserved, was found at localities 7, 8, 10, 11, 12, and 13 (Fig. 1).

Mayo (1931, p. 515) described a crinoid stem and a brachiopod "thought to be near *Leiorhynchus sp.* (?)" collected from marble "a few hundred yards east of Laurel Creek, in southwestern Mono County." He noted that "they somewhat resemble mid-Devonian forms." This locality is almost certainly within the same marble unit from which the suite of Pennsylvanian fossils described here was collected.

Permian(?) fossils.—Additional fossil material collected from pelitic hornfels in the uppermost part of the Paleozoic sequence was also examined by Mackenzie Gordon, Jr. (Written communication, 1958). He states:

"The only collection that contains enough fossils to be termed an assemblage is that of the conglomeratic hornfels at locality M158 [15 on map] with bryozoans and brachiopods. The chonetid in this assemblage is of a type with deep, moderately wide sinus, which occurs commonly in Permian rocks of the western United States, and its occurrence together with small productids with a heavy platform inside the ventral valve suggests a possible

Permian age for the beds. The single fragment of a Neospirifer found at locality M160 [14 on map] has rather weak fasciculation and prominent subangular margins bordering on the sinus in the ventral valve. This is much like *N. bakeri* (King) of the Middle Permian of west Texas. In summary, although no well-preserved fossils are present in this stratigraphic unit, its fauna suggests possible Permian age. The genera involved, however, are rather long-ranging ones found also in Pennsylvanian and Mississippian rocks."

Mesozoic Fossils

In 1941 fossil pectens were reported from metasedimentary rocks on the north side of Garnet Lake (Loc. 16 on Fig. 1) in the Devils Postpile quadrangle. Specimens collected at this time by a group of Sierra Club campers were deposited with the California Academy of Sciences where they were regarded as being of Early Jurassic or Late Triassic age (Sierra Club, 1941, p. 19). This identification was made by L. G. Hertlein of the Academy (Written communication, March 1958).

During the present mapping additional material was collected from this locality and was examined by N. J. Silberling of the U. S. Geological Survey (written communication, 1958) who states that:

"Most of the fossils obtained are the distorted and fragmentary impressions of large pectenoid pelecypods. Based on the nature of their ribbing, some of these can be assigned to the genus *Weyla*, which is known only from the Lower Jurassic. Unfortunately, none of the available specimens are sufficiently well preserved for specific identification. Professor S. W. Muller of Stanford University, who is currently preparing a monograph on the genus *Weyla*, has been kind enough to examine the material and is in agreement with the generic determination. Other pectenoid forms in the collection with more numerous and more nearly equal ribs and interspaces are provisionally assigned to *Aequipecten*, the first occurrence of which is in the Lower Jurassic.

"In addition to these pelecypods the only other recognizable fossils in the collection are solitary corals, crinoid columnals, and an indeterminate concentrically-ribbed pelecypod. The corals superficially resemble the stylophyllid corals associated with *Weyla* in the Sunrise formation of Early Jurassic age (Muller and Ferguson, 1939, p. 1611–1612) that outcrops in western Nevada about 75 miles northeast of the Garnet Lake locality."

A few specimens of indeterminate ammonites were collected from near the Minaret mine in the Devils Postpile quadrangle (Loc. 17 on Fig. 1). They occurred in a calcareous tuff approximately 5000 feet stratigraphically above the Garnet Lake locality. Although too poorly preserved for identification the fossils indicate a marine environment, and the forms they most closely resemble are not incompatible with the Early Jurassic age indicated by the pectens.

Significance of Fossils

The fossils collected from the metamorphic rocks in the two pendants are of particular importance as they permit for the first time the recognition of Ordovician rocks in the Sierra Nevada, Permian and Carboniferous rocks in the Sierra outside of the western Sierra foothill belt, and Lower Jurassic rocks in the Sierra south of the American River drainage basin. In addition they represent the only diagnostic fossils reported from a 200-mile segment of the belt of discontinuous roof pendants in the High Sierra.

References Cited

Erwin, H. D., 1934, Geology and mineral resources of northeastern Madera County, California: Calif. Jour. Mines and Geology, v. 30, p. 7–78

Mayo, E. B., 1931, Fossils from the eastern flank of the Sierra Nevada, California: Science, v. 74, p. 514–515

Muller, S. W., and Ferguson, H. G., 1939, Mesozoic stratigraphy of the Hawthorne and Tonopah quadrangles, Nevada: Geol. Soc. America Bull., v. 50, p. 1573–1624

Rinehart, C. D., and Ross, D. C., 1954, Paleozoic section in the eastern Sierra Nevada, Mono County, California (Abstract): Geol. Soc. America Bull., v. 65, p. 1297

Sierra Club, 1941, Second Sierra Club base camp outing, July 26–August 9, 1941: San Francisco, Sierra Club, mimeographed, 22 p.

U. S. Geological Survey, Menlo Park, Calif.
Manuscript Received by the Secretary of the Society, December 16, 1958
Publication Authorized by the Director, U. S. Geological Survey
Prepared in Co-operation with the State of California, Dept. Nat. Resources, Div. Mines

BULLETIN OF THE GEOLOGICAL SOCIETY OF AMERICA
VOL. 70, PP. 947-950 JULY 1959

MINIMUM AGE OF THE LOWER DEVONIAN SLATE NEAR JACKMAN, MAINE

BY P. M. HURLEY, A. J. BOUCOT, A. L. ALBEE, HENRY FAUL, W. H. PINSON, H. W. FAIRBAIRN

In the immediate vicinity of Jackman, northwestern Maine, a quartz monzonite stock about 2 miles in diameter intrudes Lower Devonian slate, Upper Silurian conglomerate and calcareous sandstone, and pre-Upper Silurian porphyritic quartz monzonite. Although most of the stock lies beneath Wood Pond, the younger quartz monzonite is well exposed on Hog Island, and the contact is exposed on the slope of Sally Mountain on the west side of Wood Pond. The contact effects around the stock include the development of cordierite hornfels in the slate, of calc-silicate minerals in the calcareous sandstone, and recrystallization of biotite in the porphyritic quartz monzonite. Cordierite has been observed in rock containing fossils that establish the geologic age of the sediments. The stratigraphic section and important fossils are listed in Table 1.

TABLE 1.—STRATIGRAPHIC SECTION AND IMPORTANT FOSSILS NEAR JACKMAN, MAINE

Post-Oriskany	Biotite quartz monzonite and bordering contact-metamorphic rocks	
Lower Devonian (Oriskany)	Seboomook slate of Perkins (1925)	*Leptoceolia flabellites*, about ¾ mile north of the contact with the stock. Spiriferoids of Oriskany type in the cordierite hornfels
Upper Silurian	Calcareous slate, argillaceous and sandy limestone, conglomerate, and calcareous sandstone	Brachiopods *Protathyris* sp. and *Choneles jerseyensis*, near Fox's Camp, about 4 miles west-northwest of the contact with the stock. Less diagnostic brachiopods of Silurian age, near Mud Pond, about 0.9 mile west of contact with stock.
Pre-Upper Silurian	Porphyritic quartz monzonite with coarse megacrysts of K feldspar. Hornblende and biotite are extensively altered to chlorite, clinozoisite, etc.; plagioclase somewhat altered to white mica and clinozoisite	

Boucot identified and dated the brachiopods. Geological mapping of the contact and surrounding area is by Albee and E. L. Boudette. Earlier more general investigations of the geology of the area were reported by Boucot (1953, Ph.D. Thesis, Harvard University) and by Hurley and Thompson (1950).

Age measurements have been made on biotite from the post-Oriskany quartz monzonite and from the pre-Upper Silurian quartz monzonite, on the cordierite hornfels containing fossils, and on three samples of Seboomook slate (Perkins, 1925) from the surrounding area (Table 2).

The ages are calculated on the basis of $\lambda_e = .585 \times 10^{-10}$ yr.$^{-1}$; $\lambda = 5.30 \times 10^{-10}$ yr.$^{-1}$; for potassium 40 $K^{40} = 1.22 \times 10^{-4}$ g/g K; and $\lambda_\beta = 1.39 \times 10^{-11}$ yr.$^{-1}$ for rubidium 87. Potassium analyses were by Perkin-Elmer flame photometer using Li internal standard. Argon analyses were by isotope dilution, using Ar^{36} as a measure of air contamination. Reproducibility of argon analysis has been found to be normally better than 2 per cent and in potassium analysis, between separate solutions, better than 2 per cent if more than one photometric measurement is made on each solution.[1] Because the whole-rock samples are probably less homogeneous, the reproducibility for total-age measurements on whole rocks is estimated to have an upper limit of 5 per cent. Interlaboratory analyses of a standard sample compared to the argon content of air lead us to believe

[1] A report on analytical procedures and tests of precision and accuracy is in preparation

TABLE 2.—K-AR AND RB-SR AGES SHOWING MINIMUM AGE OF LOWER DEVONIAN IN SECTION NEAR JACKMAN, MAINE

Samples with prefix R are whole rocks analyzed at Massachusetts Institute of Technology, those with prefix B are biotites analyzed at Massachusetts Institute of Technology, and those with prefix Me. are biotites analyzed by the U. S. Geological Survey.

Sample No.	Locality	K (per cent)	Ar^{40}/K^{40}	Air Correction (per cent)	Age (m.y.)
B-3609	Quartz monzonite, southwest corner of Hog Island, Wood Pond, Attean quad., Me. 45° 37.45′N., 70° 16.85′W.	5.49	.0231	16.0	360 ± 17
		5.59	.0239	5.5	370 ± 17
		5.56	.0233	0	362 ± 15
		5.49			
		Av. 5.53			Av. 364 ± 10
Me-10	Same as B-3609	7.01	.0226	4.3	353 ± 10
R-3883	Cordierite hornfels containing spiriferoids of Oriskany age, edge of Wood Pond, Jackman, Me.	2.84	.0243	0	365 ± 10
		2.86			
		Av. 2.85			
R-3447	Seboomook slate,* 4.5 miles northwest of Jackman on Rte. 201, Attean quad., 45° 41.48′N., 70° 16.95′W.	2.61	.0244	3.0	377 ± 18
		2.71			
		Av. 2.66			
R-3444	Seboomook slate, Rte. 201 at Jackman Field, 2 miles north of Parlin Pond, Long Pond quad., 45° 33.18′N., 70° 7.56′W.	3.29	.0238	1.8	368 ± 15
		3.26			
		Av. 3.27			
R-3448	Gray Seboomook slate, Rte. 15, 5 miles east of Jackman, west end of Long Pond, Long Pond quad., 45° 37.58′N., 70° 9.63′W.	2.57	.0224	12	350 ± 15
		2.57			
		Av. 2.57			
B-3593	Porphyritic quartz monzonite, much chloritized, small island in Attean Pond, Attean quad., 45° 33.85′N., 70° 18.60′W.	3.74	.0229	3.2	356 ± 15
Me-9	Two separate biotite concentrates from same location as B-3593	4.47	.0236	17	366 ± 10
		4.01	.0236	32	366 ± 10

Sample No.	Locality	Sr ppm	Rb ppm	†Sr^{87} ppm	†Sr^{87}/Rb^{87}	Rb-Sr Age
B-3609A	Same as B-3609, except purer bictite concentrate	46.1	472	.720	.00538	360 ± 28

* Of Perkins (1925)

† Radiogenic

that absolute errors of the argon analyses are not over 2 per cent.

Age measurements by Lyons *et al.* (1957, Table 5) using the Pb-alpha method on zircons from granitic rocks in this area gave somewhat younger values. Two of these measurements (320 m.y., 316 m.y.) were on the Katahdin granite which is also post-Oriskany in age (Boucot, 1954). Three of the measurements (330 m.y., 302 m.y., 322 m.y.) were made on samples thought to be from the post-Oriskany quartz monzonite near Jackman, but which are now known to be from an area within the pre-Upper Silurian quartz monzonite. This suggests that the zircons from the pre-Upper Silurian quartz monzonite have been recrystallized by the later metamorphism and will not give a "true" age. It would be desirable to confirm by lead-isotope age measurements this metamorphic recrystallization of zircon, inasmuch as zircon commonly retains the "true" age of metamorphosed rocks (Tilton *et al.*, 1958).

Petrographic and X-ray study by Albee shows that metamorphic recrystallization was extensive, and detrital and authigenic potassium-bearing minerals almost certainly do not remain in the slates in sufficient quantity to affect the measurements of the age of the metamorphic minerals. The muscovite and chlorite are relatively coarse-grained and commonly oriented in a systematic relationship to the slaty cleavage. Potassium feldspar was not observed, and plagioclase feldspar is not abundant; hence essentially all the potassium in the slate seems to be in muscovite. X-ray-diffraction study, including heat and glycol treatment, indicates that the character of the muscovite and chlorite is unlike that of the authigenic mica and chlorite normally found in sedimentary rocks. Moreover, montmorillonite, kaolinite, and mixed-layer minerals, which are abundant in argillaceous sediments, are absent.

From these measurements it is concluded that the age of the quartz monzonite and the time of metamorphism of the slates is at least 360 m.y. Therefore, the Oriskany sedimentation took place prior to this time. This is in agreement with the findings of Fairbairn *et al.* (in press), in Nova Scotia, where sediments of similar age have been intruded by granitic rocks near Nictaux. Similar ages ranging from 320 to 380 m.y. have been reported for the latest major metamorphic event all along the Appalachians (Wasserburg *et al.*, 1957; Carr and Kulp, 1957; Kulp *et al.*, 1957; Long and Kulp, 1958; Tilton *et al.*, 1958). This age has tentatively been correlated with the Late Ordovician, Taconic orogeny (Long and Kulp, 1958, p. 603), but our results indicate that this major metamorphic event was post-Early Devonian.

Acknowledgments

We are very much indebted to S. H. Hart, P. L. D. Elmore, and W. W. Brannock for assistance and potassium analyses, and to the Division of Research of the U.S. Atomic Energy Commission, for support of the project under which part of this research was carried out.

References Cited

Aldrich, L. T., Wetherill, G. W., Davis, G. L., and Tilton, G. R., 1958, Radioactive ages of micas from granitic rocks by Rb-Sr and K-A methods: Am. Geophys. Union Trans., v. 39, p. 1124–1134

Boucot, A. J., 1954, Age of the Katahdin granite: Am. Jour. Sci., v. 252, p. 144–148

Carr, D. R., and Kulp, J. L., 1957, Potassium-argon method of geochronometry: Geol. Soc. Am. Bull., v. 68, p. 763–784

Fairbairn, H. W., Hurley, P. M., Pinson, W. H., and Cormier, R. F. (in press), Age of the granitic rocks of Nova Scotia: Geol. Soc. Am. Bull.

Hurley, P. M., and Thompson, J. B., 1950, Airborne magneto-meter and geological reconnaissance survey in northwestern Maine: Geol. Soc. Am. Bull., v. 61, p. 835–841

Kulp, J. L., Long, L. E., and Eckelmann, F. D., 1957, Age of the Piedmont and Southern Appalachians (Abstract): Geol. Soc. Am. Bull., v. 68, p. 1758

Long, L. E., and Kulp, J. L., 1958, Age of the metamorphism of the rocks of the Manhattan Prong: Geol. Soc. Am. Bull., v. 69, p. 603–606

Lyons, J. B., Jaffe, H. W., Gottfried, D., and Waring, C. L., 1957, Lead-alpha ages of some New Hampshire granites: Am. Jour. Sci., v. 255, p. 527–546

Perkins, E. H., 1925, Contributions to the geology of Maine, No. 2; Part 1, The Moose River sandstone and its associated formations: Am. Jour. Sci., 5th ser., v. 10, p. 368–375

Tilton, G. R., Wetherill, G. W., Davis, G. L. and Hopson, C. A., 1958, Ages of minerals from the Baltimore gneiss near Baltimore, Maryland: Geol. Soc. Am. Bull., v. 69, p. 1469–1474

Wasserburg, G. J., Pettijohn, F. J., and Lipson, J., 1957, A^{40}/K^{40} ages of micas and feldspars from the Glenarm series near Baltimore, Maryland: Science, v. 126, p. 355–357

Massachusetts Institute of Technology, Cambridge, Mass. (Hurley, Boucot, Pinson, Fairbairn); U. S. Geological Survey, Washington, D. C. (Albee, Faul)

Manuscript Received by the Secretary of the Society, March 6, 1959

M.I.T. Age Studies Contribution No. 5